GHENT UNIVERSITY

FACULTEIT GENEESKUNDE EN GEZONDHEIDSWETENSCHAPPEN

Ghent University, Faculty of Medicine and Health Sciences

The FOXM1/BRIP1 axis in replicative stress induced DNA damage response in neuroblastoma:

functional exploration and zebrafish modeling

This thesis is submitted as fulfillment of the requirements for the degree of Doctor in Health Sciences by Suzanne Vanhauwaert, 2017

Promoter:
Prof. dr. Frank Speleman

Co-promoter:
Prof. dr. Katleen De Preter

Thesis submitted to fulfill the requirements for the degree of Doctor of Health Sciences

Promoter

Prof. dr. Frank Speleman

Department of Pediatrics and Medical Genetics, Ghent University, Ghent, Belgium

Co-promoter

Prof. dr. Katleen De Preter

Department of Pediatrics and Medical Genetics, Ghent University, Ghent, Belgium

Members of the examination committee

Shizhen Zhu MD, PhD

Mayo Clinic, 200 First St. SW Rochester, MN 55905 Rochester, Minnesota, USA

Anna Sablina, PhD

VIB-KU Leuven Center for Cancer Biology O&N 4, Leuven, Belgium

Kathleen Claes, PhD

Department of Pediatrics and Medical Genetics, Ghent University, Ghent, Belgium

Tom Van Maerken, MD, PhD

Department of Pediatrics and Medical Genetics, Ghent University, Ghent, Belgium

Steven Goossens, PhD

Department of Pediatrics and Medical Genetics, Ghent University, Ghent, Belgium

Joni Van der Meulen, PhD

Department of Pediatrics and Medical Genetics, Ghent University, Ghent, Belgium

The research described here was conducted at the Center for Medical Genetics (Ghent University, Ghent, Belgium) and Dana Farber Cancer Institute (Harvard Medical School, Boston, USA) and funded by grants from the Research Foundation Flanders (FWO), the Flemish League against Cancer (VLK) and Villa Joep.

Table of content

List of abbreviations:

ALK	Anaplastic lymphoma kinase receptor tyrosine kinase
AML	Acute myeloid leukemia
BACH1	Brca1-Associated C-terminal Helicase
BARD1	BRCA1-associated RING domain-1
BRCA1	Breast cancer 1
BRCA2	Breast cancer 2
BRIP1	BRCA1 Interacting Protein C-Terminal Helicase 1
CHR	Cell cycle genes homology region elements
CI	Combination index
CldU	chloro-deoxyuridine
DHODH	Dihydroorate dehydrogenase
DPC	Days post coitus
DREAM	RB-like, E2F and multi-vulval class B
DSB	DNA double strand break
dβh	Dopamine beta hydroxylase
ERE	Expressed repeat element
ESC	Embryonic stem cells
FA	Fanconi anemia
FANCJ	Fanconi anemia complementation group J
FOXM1	Forkhead box protein M
GO	Gene Ontology
GWAS	Genome wide association study
HPF	Hours post fertilization
HR	Homologous recombination pathway
HU	Hydroxy-urea
IdU	Iodo-deoxyuridine
IAP	Inhibitor of apoptosis
IP-MS	Immunoprecipitation mass spectrometry
IRG	interrenal gland
LMO1	LIM domain only 1
MEF	Mouse embryonic fibroblasts
MYCN	V-Myc Avian Myelocytomatosis Viral Oncogene Neuroblastoma Derived Homolog
MPNST	Malignant peripheral nerve sheet tumor
MRN	Mre11/Rad50/Nijmegen breakage syndrome gene 1
NB	Neuroblastoma
NER	Nucleotide excision repair
NHEJ	Non homologous end joining
NGS	Next generation sequencing
NRC	Neuroblastoma Research Consoritium
PHOX2B	Paired like homeobox 2B
PI	Propidium Iodide

RAG2	Recombinase activating gene 2
RPA	Replication protein A
RT-qPCR	Reverse transcription quantitative PCR
ssDNA	Single stranded DNA
SNPs	Single nucleotide polymorphisms
SRO	Smallest region of overlap
T-ALL	T-cell acute lymphoblastic leukemia
TLS	Translesion synthesis
TMS	Telomestatin
TSG	Tumor suppressor
WRN	Werner helicase
XRCC1	X-ray repair cross-complementing protein 1
ZFN	Zinc finger nuclease

PART I: introduction

There is a can in cancer,

because we can beat it

Introduction:

Neuroblastoma

A little bit of history…

Neuroblastoma (NB) was first described in 1864 by the German physicist Rudolf Virchow who observed an abdominal tumor mass in a child and called it, unaware of the origin of the tumor, a glioma[1]. About three decades later, in 1891, the German pathologist Felix Marchand reported that the tumor develops from the sympathetic nervous and the adrenal medulla. In 1910 James Homer Wright understood that the adrenal tumors were mainly composed of an identical cell type and realized that the tumor originates from the primitive neural cells -the neuroblasts-, and therefore named it neuroblastoma[2].

While tremendous progress has been made in treatment of childhood leukemia, success rates for high risk NB remain disappointing. It is a very complex and heterogeneous disease, on the one hand, NB accounts for disproportionate morbidity and mortality among the cancer of childhood while on the other hand, it is associated with one of the highest proportions of spontaneous and complete regression of all human cancers[3]. Typically, NB is subdivided in four stages based on the International NB Risk Group (INRG) Staging System. While stage L1 and L2 are localized or locoregional tumors with a favorable prognosis, patients with stage M have a metastatic disease and poor clinical outcome[4]. A specific subgroup of patients are those with stage MS, marked by metastases and the unusual capacity of spontaneous differentiation and regression and favorable outcome.

NB: when development goes wrong

NB is the most common extracranial pediatric solid tumor in children, accounting for approximately 7-10% of pediatric cancers and nearly 15% of all pediatric cancer deaths in patients younger than 15 years old[3]. Tumors develop from precursor cells of the sympatho-adrenal lineage that arise from the neural crest, a transient component of the ectoderm that gives rise to diverse cell types, including the peripheral nervous system, the craniofacial skeleton and pigment cells[5]. Only progenitors from the sympathetic lineage acquire the genetic events that lead to neuroblastoma development, resulting in tumors that can arise anywhere along the sympathetic nervous system[5].

At the end of the third week and in the beginning of the fourth week of embryonal development, sympathoadrenal cells from the neural crest in the trunk region of the embryo follow a ventral migratory path from the neural crest and neural tube to give rise to various structures, including the sympathetic nervous system that develops from the fate-restricted sympatho-adrenal progenitor cells, the so-called neuroblasts[5-7]. Upon migration, these neuroblasts start to express a series of factors that further allow their differentiation into either the ganglionic or the chromaffin lineage. Together, these cells form the differentiated cells that populate the sympathetic ganglia, paraspinal ganglia and adrenal medulla. Interestingly, during normal sympathoadrenal development, expression of MYCN is high in the early post-migratory neural crest, where it regulates the ventral migration and expansion of the neural crest cells. Later on, MYCN protein levels gradually reduce during differentiation of the sympathetic neurons[6].

NB: an embryonal precancer

Several clinical and experimental features link neuroblastoma development to defective embryogenesis and pathological neuroblast precancer. The idea of an embryonal origin was first supported by a study of De Preter *et al*[8], They showed that gene expression profiles of human fetal adrenal neuroblasts are remarkably similar to those of NB tumors. Interestingly, in some NB patients, new tumors form at different places and at different times early in the

life of the child, suggesting the existence of premalignant lesions and linking tumorigenesis to deregulated development[6].

The NB genomic landscape

DNA copy number alterations

The NB genomic landscape is marked predominantly by structural variants leading to amplifications, gains and losses while mutational burden is low. Therefore, NB can be considered as a so-called copy number driven cancer disease. The most frequent amplification is observed in more than 20% of the cases and encompasses the *MYCN* oncogene (V-Myc Avian Myelocytomatosis Viral Oncogene NB Derived Homolog)[9,10]. In addition to these amplicons which typically consist of 50 to 100 MYCN copies, large gains of the distal 2p-arm encompassing the *MYCN* locus are also frequently observed[11]. MYCN amplification was amongst the first identified prognostic genetic markers being associated with rapid disease progression and poor prognosis and was rapidly adopted into clinical practice[12].

MYCN is a member of the *MYC* proto-oncogene family that also includes *MYC* and *MYCL*. In addition to NB, *MYCN* amplification has been observed in a variety of other cancers with an embryonic and or a neuroendocrine origin like rhabdomyosarcoma, Wilms tumor and medulloblastoma[13]. MYCN protein functions through binding to the E-box sequences (CACGTG) in a heterodimeric complex with Max acting as a transcription factor that controls the expression of many target genes, which in turn regulate fundamental cellular processes including proliferation, cell growth, protein synthesis, metabolism, apoptosis and differentiation (Figure 1.1)[14]. Similar to MYC, MYCN plays an important role during embryonic development. Mutations in the human *MYCN* gene have been linked to birth defects, mouse embryos lacking *MYCN* die around E11.5[15] with MYCN being implicated in the early differentiation of the nervous system amongst others[16].

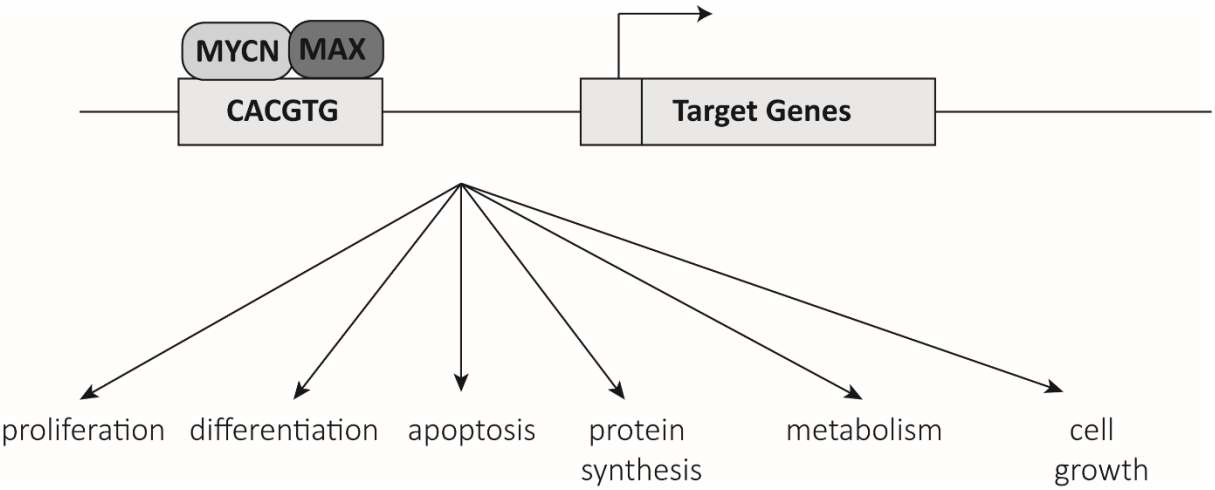

Figure 1.1: MYCN protein functions

In addition to the frequently observed *MYCN* amplification, other loci have also been reported to be present in high copy numbers, however, with much lower incidence. Often, such rare amplifications occur together with *MYCN* amplifications and a recent study from Depuydt et al indicated that this marks a group of ultra-high risk patient with extremely poor outcome (Depuydt *et al.* in preparation). *LIN28B* amplification and consequent elevated *LIN28B* expression levels cause down regulation of the *let-7* family of miRNAs resulting in further increase of MYCN protein levels[17]. Additional amplifications occurring in NB have been reported including in *ALK*, *MDM2*, *CDK4*,…[18-20]

Furthermore, typical patterns of large chromosomal gains and losses are observed in NB. First, numerical chromosomal imbalances in the absence of structural defects occur in localized L1 and L2 and special metastatic MS prognostic favorable cases, while structural imbalances including loss of 1p, loss of 11q and gain of 17q are confined to metastatic M cases with poor outcome[21]. Partial gain of chromosome arm 17q (gain of segment 17q23-qter) is the most frequent abnormality of NB cells, present in more than 50% of cases and exclusively associated with poor prognosis. The principal mechanism underlying this partial gain is an unbalanced translocation with a variety of partner chromosomes, the most common translocation partner being chromosome 1p, resulting in the loss of 1p[22]. By cloning the translocation breakpoint our team could identify a new gene, NB breakpoint family member 1 (NBPF1), which is destroyed by the translocation. The translocation truncates

NBPF1 and gives rise to two chimeric transcripts of *NBPF1* sequences fused to sequences derived from chromosome 17. On chromosome 17, the translocation disrupts one of the isoforms of *ACCN1*, a potential glioma tumor suppressor gene[23].

Chromosome 17q driver genes in NB

Partial gain of chromosome 17q is the most commonly observed genetic aberration in NB[22,24]. Because of its high frequency and its correlation with survival, it has long been assumed that one or several genes on 17q contribute to NB pathogenesis in a dosage dependent way. The specific genes and the molecular mechanisms responsible for development and progression of NB remain, however poorly understood. In a first attempt to gain better insights into the tumor process, several research groups tried to delineate the smallest region (SRO) of 17q gain[24,25]. This SRO which encompasses 17q23 till 17qter is still quite large and contains around 600 genes. Therefore other strategies to identify the culprit candidate genes had to be pursued. Interestingly, by performing DNA copy number analysis on 25 NB cell lines using comparative genomic hybridization, Saito-Ohara *et al*. identified a minimal region of gain at 17q23[26] in one cell line. This region contains only 15 genes including *BRIP1* and *PPM1D,* which encodes the phosphates WIP1, a negative regulator of p53 activity[27]. Downregulation of *PPM1D* using antisense oligonucleotides was shown to have a drastic effect on the growth of several NB cell lines[26].

BIRC5 or *survivin*, a member of the inhibitor of apoptosis (IAP) family, is a well-recognized oncogene in a variety of cancers and located on 17q25.3. Because of its well established role as an oncogene and its chromosomal location, one wondered if *BIRC5* could function as an oncogene in NB as well. Indeed, BIRC5 is strongly overexpressed in human neuroblastoma tumors and correlates with poor survival outcome independent of 17q gain[28]. Likewise, silencing of *BIRC5* in several NB cell lines resulted in mitotic catastrophy[28]. Another gene that has been put forward as a potential important NB 17q gene is *NM23-H1* or *NME1*[29,30]. Higher expression levels of NM23-H1 are correlated with a worse outcome in NB patients without *MYCN* amplification and in patients younger than 12 months of age[30]. It is postulated that NME1 together with its binding partner h-Prune acts as a pro-metastatic gene in NB[29].

Mutations/single base pair variants

The most frequently recurring mutation in NB has been reported in *ALK* (anaplastic lymphoma kinase receptor tyrosine kinase) occurring in 8% of the cases and slightly more frequent in metastatic cases[18,31]. These activating mutations are mostly confined to the ATPase activating domain with two major hotspot mutations at positions R1275 and F1174 and leading to constitutive activation of the receptor[32]. The discovery of these *ALK* mutations was a landmark for the development of precision oncology for NB patients and clinical trials with *ALK* inhibitors were initiated to evaluate their benefit for treating NB patients[33,34]. Further, studies investigated how ALK activation contributes to the tumor phenotype and unraveled downstream signaling offering further opportunities for drugging[33]. While *ALK* mutations where discovered through the study of familial cases[35] (see below) and standard candidate gene sequencing[18], more recently a comprehensive picture was achieved through whole exome and genome sequencing of primary tumors. In addition to the previously reported *ALK* mutations, this provided further insight into the mutational landscape of NB. Analysis of 87 whole NB genomes by the Versteeg team uncovered recurrent involvement of genes implicated in neuritogenesis and also identified a subset of cases showing genomic features of chromothripsis[17]. Further studies also revealed recurrent involvement of loss of function events in *ARID1A* and *ARID1B*, either through inactivating mutations or focal deletions in 9% of the NB cases[36]. *ARID1A* and *ARID1B* are members of the SWI/SNF transcriptional complex that is thought to regulate chromatin structure and gene expression. Of interest, mutations in the *ARID1* genes are also correlated with a more aggressive NB phenotype[36]. Sequencing efforts also shed further light onto the genetic and clinical heterogeneity of NB. Indeed, inactivating *ATRX* mutations (both base pair substitutions and deletions) were observed in a significant portion of older children (> 5years) and young adolescents[37]. *ATRX* mutations were mainly found in the minimal overlapping region of deletions involving exon 5 up to exon 10, which encodes a predicted nuclear-localization signal. Of particular interest, *ATRX* mutations were also associated with longer telomeres and activation of the ALT pathway in keeping with the finding that ATRX functions as a direct repressor of ALT promoting telomere lengthening[38]. This also fits with the mutually exclusive occurrence of *ATRX* defects with *MYCN* amplification as MYCN drives hTERT overexpression thus excluding the need for alternative mechanisms for telomere

lengthening. In line with these observations, yet another sequencing study completed this picture showing that non *MYCN* amplified cases without *ATRX* mutations showed hTERT upregulation due to structural variants near the *hTERT* locus affecting *hTERT* expression levels[39,40].

Genetic predisposition to NB

Familial NB is rare and only observed in 1% of the NB patients. They differ from sporadic tumors by the fact that they are diagnosed at earlier age[41,42] and are frequently associated with other neural crest-derived developmental disorders such as Hirschsprung disease, congenital central hypoventilation syndrome and neurofibromatosis type I[43]. Due to the link of NB tumors with Hirschsprung disease and congenital central hypoventilation syndrome, *PHOX2B* was the first gene for which mutations were described that predispose the NB and was subsequently shown to be rarely targeted by somatic mutations. *PHOX2B* is a homeobox containing gene, which plays a crucial role during specification of noradrenergic cells[44,45].

Besides germline mutations, it has been shown that also single nucleotide polymorphisms (SNPs) can influence NB development. The Maris team conducted extensive genome wide association studies (GWAS) to identify particular SNPs predisposing to a higher risk of NB development. Through the Illumina HumanHap550 BeadChip assay, analysis of 1032 NB patients and 2043 controls gave a significant association between NB and the common minor alleles of three consecutive SNPs at chromosome 6p22 and containing the predicted genes *FLJ22536* and *FLJ44180* [46]. In a follow up study their analysis was restricted to 397 high-risk cases and 2043 controls and detected a new significant association of six SNPs at 2q35 within the BRCA1-associated RING domain-1 (BARD1) locus correlated with high-risk (Rs367816 OR= 1,82 $p=5xE^{-14}$ and Rs643582 OR= 1,82 $p= 2xE^{-15}$)[47]. The disease associated SNP correlates with the increase of an oncogenetically activated isoform of *BARD1*, *BARD1β*. BARD1β stabilizes Aurora kinase, which in turn will stabilize MYCN, resulting in a higher expression of MYCN.[48]. In a more comprehensive GWAS study using 2251 patients and 6097 control samples a significant association in the LIM domain only 1 (*LMO1*) at 11p15.4 was identified. The signal was enriched in the subset of patients with the most aggressive form of disease. By analyzing DNA copy number alterations in 701 primary tumors they could also show that *LMO1* was aberrant in 12,4% of the cases through a duplication event[49]. The

common causal SNP rs2168101 disrupts a GATA transcription factor binding site within a tissue specific super-enhancer element[50].

Zebrafish

Zebrafish as a model organism

Zebrafish, a tropical fish native to Southeast Asia, came in to the fore as a model organism in the early sixties for the study of developmental genetics. Its advantages for genetic studies are its high fecundity, the generation of transparent embryos that develop outside of the mother and the conservation of vertebrate organs, which allows comparison with humans[51]. Importantly, many cellular processes and developmental programs are conserved in vertebrates. The true usefulness of the model, however, was recognized as a result of several large forward genetic screens[52,53] which identified mutants in almost every organ or cell, with most of them shared with mammals. This demonstrated for the first time that fish could be used to identify genetic mutants for almost any phenotype.

However, like every model organism, zebrafish also possess some disadvantages. This species has undergone a partial genome duplication, so some genes present as two copies (approximately 20% of the genome). Next to that, their last shared ancestor with humans was 445 million years ago, so they are far more remote from humans than other animals such as rodents. Finally, not all genes are conserved in their genome, amongst others *BRCA1,* they are ectothermic (cold-blooded) and they have some anatomical differences compared to humans (lack of heart septation, limbs, lungs…)[54].

In the early years the fish were mainly used to study developmental processes and regeneration, though, in the beginning of this millennium it was noted that zebrafish can also be used to study cancer[51,55].

Zebrafish and its cancer models

In the past it was already observed that zebrafish can develop cancer after mutagenic exposure or even spontaneously. In 2003, David Langenau proved for the first time that zebrafish also can develop cancer upon ectopic overexpression of a transgene[56]. He demonstrated that overexpression of *m-MYC* under the control of the recombinase activating gene 2 (RAG2) promotor resulted in the rapid onset of adult T-cell acute

lymphoblastic leukemia (T-ALL). Leukemia initiated in the thymuses but quickly spread throughout the complete body of the fish, which was clearly visualized since *m-MYC* was GFP tagged. Interestingly, it could be shown that these tumors resemble human cancers both on the histological and genomic levels[57]. Since then, zebrafish models have been described for a variety of cancers like melanoma, pancreatic cancer, malignant peripheral nerve sheath tumors (MPNST), Ewing sarcoma and also NB (Table 1.1)[58]. Upon overexpression of *MYCN* under the control of the dβh (dopamine β hydroxylase) promotor NB tumors could be observed at 9 weeks of age[59] . In human cells, NB can be diagnosed by the presence of neurosecretory granules within the cytoplasm of the tumors cells. These neurosecretory granules were evident in the fish tumors, showing the relevance of NB zebrafish models in cancer research. Although the first results were pretty spectacular, the tumor penetrance stayed rather low. Only 22% of the MYCN transgenic fish developed tumors within half a year. In the past, it was already proven that activated ALK can collaborate in NB pathogenesis[60] and therefore one wondered if overexpression of *ALK* in the *MYCN* background fish would accelerate NB development. This turned out to be true, coexpression of ALK^{F1174L} with *MYCN* tripled the penetrance of NB and markedly accelerated tumor onset, with tumors starting to develop at 5 weeks of age[59,61]. Similar processes were observed for *NF1* (neurofibromatosis type 1), loss of *NF1* in *tg(dβh:*EGFP-MYCN) zebrafish resulted in an acceleration of NB onset. Moreover, it was shown that loss of *NF1* results in aberrant expression of the RAS-MAPK pathway and this could be therapeutically inhibited using the MEK inhibitor trametinib[62].

Zebrafish, more than a cancer model…

Besides the development of several cancer models in zebrafish, several technical revolutions took place in zebrafish. Because of its small size and its similarity to humans, 71% of the zebrafish proteins have a human orthologue, zebrafish are more and more used as a tool for drug discovery. Zebrafish are typically used to screen large compound libraries. Researchers will then specifically look for compounds that introduce a phenotype of their interest[63]. For example, in a phenotypic screen to identify FDA-approved drugs with activity against T-ALL, perphenazine was identified. Perphenazine, an antipsychotic drug, had a drastic effect on MYC-overexpressing thymocytes in zebrafish. Moreover, human T-ALLs treated with

perphenazine exhibited suppressed cell growth[64]. For melanoma, transgenic mitf-BRAF^{V600E}; p53$^{-/-}$ embryos were used to identify small molecule suppressors of the neural crest lineage. One class of compounds, inhibitors of dihydroorate dehydrogenase (DHODH), such as leflunomide, led to an almost complete retraction of neural crest development in zebrafish and a reduction in self-renewal of mammalian neural crest stem cells[65]. Recently, with the discovery of CRISPR-CAS a complete new revolution took place in the genome engineering field. In zebrafish, zinc finger nuclease (ZFN) technology and TALENs were already established techniques (Table 1.1), but because of its relative ease also CRISPR CAS was quickly introduced[66]. Moreover, also tissue specific CRISPR CAS quickly found his way into the zebrafish field[67] . What's more is that also our lab contributed to the integration of the CRISPR CAS technology in zebrafish. BATCH-GE, an easy to use bioinformatics tool for batch analysis of next generation sequencing (NGS) data was introduced[68]. BATCH-GE identifies and reports indel mutations and other precise genome editing events and calculates the corresponding mutagenesis efficiencies for a large number of samples in parallel.

Table 1.1: Transgenic models of cancers in zebrafish. Updated from[58]

Cancer	Oncogene	Tumor suppressor gene	refs
melanoma	*mitfa-BRAF^{V600E}* *mitfa:*EGFP:*NRAS^{Q61K}* *kita*:Gal4 x *uas*:*HRAS*	*Tp53$^{-/-}$* *Tp53$^{-/-}$*	69 70 71
Pancreatic cancer	*ptf1a-KRAS^{G12V}-GFP* *ptfa1:Gal4-VP16 x uas:KRAS^{G12V}-GFP*		72 73
T cell lymphoma or leukemia	*rag2:myc* *rag2:lox-dsRED2-lox-EGFP-mMYC* x *hsp70*-cre *rag2:NOTCH1* *rag2:myc x rag2:bcl2*		56,74 75 76,77 78
B cell Leukemia	*TEL-AML1* (ETV6-RUNX1)		79
Rhabdomyosarcoma	*rag2-KRAS^{G12D}*		80
Neuroblastoma	*dβh:EGFP-MYCN* *dβh:EGFP and dβh:ALK^{F1174L}* *dβh:EGFP-MYCN*	 *nfa1$^{+/-}$; nf1b$^{-/-}$*	59 59 81
AML	*pu1:MYST3/NCOA2-EGFP*		82
MPNST	 *sox10:PDGFRA;* *sox10:mCherry*	*Tp53$^{-/-}$* *nfa1$^{+/-}$; nf1b$^{-/-}$Tp53$^{-/-}$* *Tp53$^{+/-}$; BRCA2$^{-/-}$*	83 84 85
Lipoma	*krt4:Hsa.myrAkt1*		86
Ewing's sarcoma	*hsp70* or *β-actin*:*EWSR1-FL1*		87
Liver	*fabp10:Lex1:EGFP x cryB:mCherry: LexA:EGFP-kras^{G12V}* *fabp10*:TA; *TRE*: *xmrk;* *krt4*:GFP		88 89
Pancreatic neuroendocrine	*zmyod:MYCN*		90
Myeloproliferative neoplasms	*spi:NUP98-HOXA9*		91
Corticotrophin adenoma and neoplasm	*Pomc:pttg*		92
Testicular germ cell tumor	*Flck:tag* *flck:scl* *flck:lmo1*		93
Myelodysplastic syndrome		*Tet2$^{-/-}$*	94

Replicative stress and cancer

DNA replication stress

DNA replication is a vital process of the living cell that guarantees precise duplication of the genetic information and subsequent transfer to the daughter cells. Although DNA replication is a highly controlled process, various perturbations originating from exogenous and endogenous sources can interfere with this process and can eventually lead to a slowing or a stalling replication fork, a phenomenon that is called replication stress[95-97]. There are multiple reasons why replicative stress can occur: 1) depletion of nucleotides required for replication or DNA repair; 2) interstrand lesions, 3) strongly bound proteins and complex stable DNA structures (e.g. G4 structures, see further) hampering progress of the replisome, 4) RNA-DNA hybrids (R-loops) causing replication-transcription conflict etc… (Figure 1.2). Upon replication fork stalling, dormant origins of replications are activated to permit activation of replication. However, if two converging forks stall in regions lacking dormant regions, cells must restart at least one of these forks to ensure full genome duplication. Single strand DNA at the stalled replication forks will be coated by the ssDNA binding replication protein A (RPA). RPA-coated ssDNA stimulates the activation of the DNA damage-checkpoint kinases ATR (and its obligatory partner ATRIP) and CHK1. Once activated, the ATR-CHK1 checkpoint response recruits accessory proteins, which will stabilize the halted fork and guarantees rapid resumption of DNA synthesis (Figure 1.3). When the amount of ssDNA surpasses the total of available RPA, the fork may collapse (defined as unloading of the replisome from the fork) leading to the generation of DNA double strand breaks (DSBs)[98].

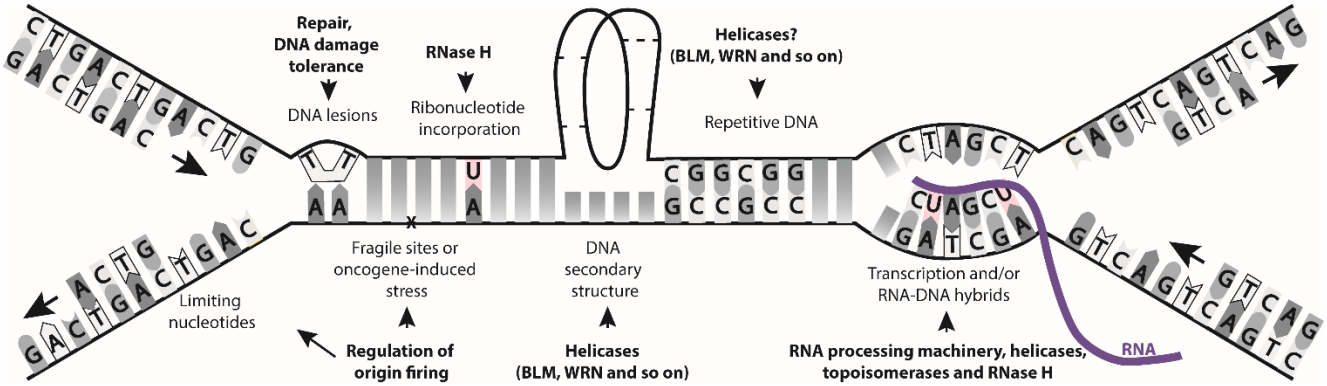

Figure 1.2: Mechanisms that can result in DNA replication stress. There are a number of mechanisms that can slow or stall DNA replication, including limiting nucleotides, DNA lesions, ribonucleotide incorporation, repetitive DNA elements, transcription complex and/or DNA hybrids, DNA secondary structures and fragile sites. Figure adapted from[95]

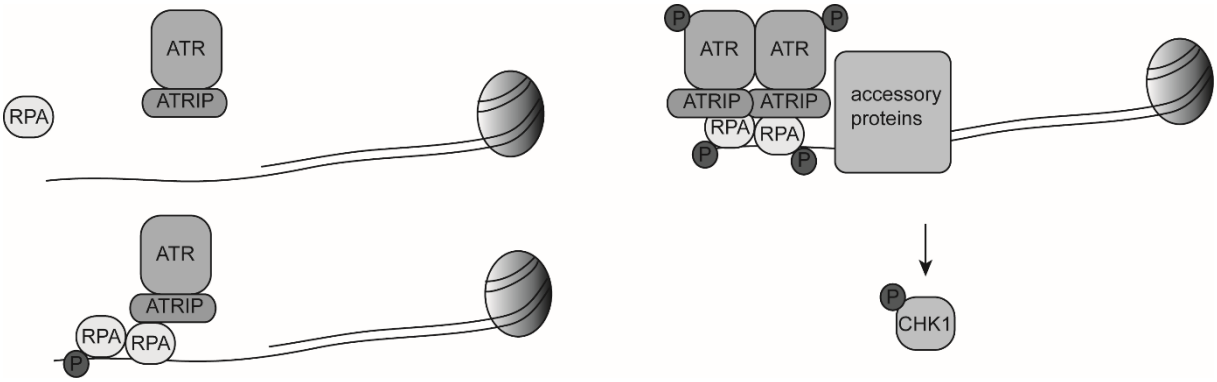

Figure 1.3: The ATR-CHK1 pathway. Figure adapted from[99]

Replication stress and cancer: the story of Jekyll and Hide

Replicative stress drives tumor initiation: Cancer is the result of uncontrolled cell growth, and the accumulation of genomic alternations during cell division is a driving force for tumorigenesis. Subsequently, it is not surprising that replicative stress can contribute to tumorigenesis, given that excessive replication stress can result in DSB causing genomic instability (chromosomal rearrangements, deletions and chromosomal loss). In fact, replicative stress is a double edged sword, while on the one hand replicative stress can lead to genomic instability and in that way promote tumorigenesis, on the other hand replicative stress also represents an Achilles heel of the cancer cell where too much replicative stress can be fatal and may force the cell to go into apoptosis. For example, several oncogenes are known to cause replicative stress. MYC not only promotes cell growth by positively regulating the expression of many genes controlling the cell cycle (amongst others), it also represses anti-proliferative genes[100,101]. In addition to the transcriptional regulation, MYC also stimulates cell cycle progression by directly controlling replication initiation. It binds with the pre-replicative complex and will bind to DNA replication origins. Overexpression of *MYC* causes increased replication origin activity with subsequent DNA damage and checkpoint activation[102,103]. *In vitro* and *in vivo* experiments in *MYC* transgenic mice originally showed that transient *MYC* expression results in increased genomic instability and chromosomal aberrations that are typically observed in *MYC*-dependent human tumors and can contribute to cancer initiation and progression[104].

Cancer cells may become addicted to a replicative stress induced DNA damage response phenotype: It has been shown that excessive chronic replicative stress can hamper tumor growth and in embryonic stem cells accelerate aging[105]. In keeping with this finding, a mouse model overexpressing CHK1 through an extra copy was shown to be more prone to tumor development[106]. Furthermore, in T-ALL the Barrata team demonstrated the upregulation of *CHK1*, indicating that (hyper)activation of the ATR/CHK1 signaling pathway is required for survival and growth of these leukemic blast cells. Indeed, pharmacological inhibition or silencing of *CHK1* using shRNAs impaired T-ALL proliferation and viability[107,108]. In NB, similar mechanisms have been observed. The MRN complex, a major sensor of DNA double stranded breaks, is induced by MYCN and is essential to restrain MYCN-dependent

replication stress[109,110]. In glioblastoma, it has been shown that TOP2β, an ATP dependent enzyme that catalyzes topological changes of DNA, is highly expressed in glioblastoma stem cells[111]. A recent paper showed that *NEAT1* paraspeckle formation prevents accumulation of excessive DNA damage in cells undergoing replication stress. *NEAT1* will preserve the genomic integrity of the tumor cell by modulating ATR signaling[112]. Interestingly, in mice, reduced levels of ATR found in a mouse model of the ATR-Seckel syndrome completely prevented the development of Myc-induced lymphomas or pancreatic tumors, both of which show abundant levels of replicative stress[113]. These examples show that replicative stress is a difficult balance for the cancer cell: replicative stress may act as initial initiator of the malignant process[114], but sustained high levels of replication stress will impair the tumor cell's viability. The fact that replication stress is less observed in normal cells but is a common feature of most cancer cells opens new possibilities for therapeutical interventions. For example, it has been shown that tumors deficient in *BRCA2* like ovarian and breast cancer, can be specifically targeted using PARP inhibitors[115]. Since PARP1 is involved in the repair of single-strand breaks, upon inhibition, cells are forced to repair the break using the homologous recombination (HR) pathway. Nevertheless, tumors that are *BRCA2*$^{-/-}$ deficient cannot engage in the HR pathway so their only option will be to undergo apoptosis[115]. More recently, it was shown that cancer cells can be forced to go in apoptosis by incorporation of damaged dNTPs into the cancer cell. This can be reached by targeting MTH1, a protein that prevents the misincorporation of oxidized dNTPs during replication, using *s-crizotinib*. *MTH1* is dispensable in normal cells but since cancer usually move faster through the cell cycle, they often heavily rely on this protein[116,117]. Also molecular targeting of CHK1 has shown to be effective in different tumor types including NB[107,108,118,119]

Replication stress as a new cancer hallmark

In 2000, Hanahan and Weinberg described in their seminal paper, the hallmarks of cancer. They proposed that in general, cancer cells acquire six different hallmarks during their development. Typically, cancer cells will have a self-sufficiency in growth signals, they will be insensitive to growth inhibition signals, they will evade programmed cell death (apoptosis), limit their replication potential, sustain their angiogenesis and will invade tissues and metastasize[120]. About one decade later, several new breakthroughs in the cancer field and

subsequently an update of the hallmarks of cancer was warranted. In this update, four new cancer hallmarks were introduced and one of them was genomic instability[121]. While increased genomic instability in cancer is now a very well established concept as best exemplified by the rare cancer predisposition syndromes caused by germline loss of function mutations in DNA repair genes[122], hyperactivation of the DNA repair machinery has thus far received much less attention, despite accumulating evidence that this phenotype indeed is present in various cancer types[123]. This is also illustrated and supported by this thesis in which we convincingly show that cancer cells are dependent for growth on high BRIP1 levels and also show that BRIP1 overexpression leads to accelerated tumor formation (Chapter 3). Moreover, in this thesis we also demonstrate that MYCN drives a FOXM1 activated DNA damage repair network that protects the tumor cells from excessive replicative stress induced DNA damage (Chapter 4).

BRIP1 (alias FANCJ or BACH1)

BRIP1: the BRCA1 binding protein

BRIP1, also known as *FANCJ* or *BACH1*, was first described by Cantor *et al*, as an interaction partner of *BRCA1* (Breast Cancer Gene 1)[124]. The BRCA1 protein is a very large protein with only a few recognizable domains of which the RING domain and the BRCT domain are the most studied. Earlier, it was already shown that the RING domain of BRCA1 dimerizes with BARD1[125]. Since several clinical relevant point mutations were identified in the BRCT domain, it was important to identify the protein(s) that could bind to this domain. A GST fusion protein containing the BRCT motifs was used for a far western blot, and a 130kDa protein, BRIP1, was identified that binds to this tag. One mutation in BRIP1 (P1749R) led to greatly reduced binding, while the mutation M1775R completely abolished BRCA1 binding through the BRCT domain[124]. Radiation experiments in U20S osteosarcoma cells further showed a role for BRIP1 in DNA double strand break repair through BRCA1 binding, where BRCA1 binding defective BRIP1 mutants showed a remarkable delay in DNA repair 6 hours after radiation[124]. In a follow-up study it was shown that the interaction between BRCA1 and BRIP1 depends on the phosphorylation status of BRIP1 and that this phosphorylation-dependent interaction is required for DNA damage induced checkpoint control during the G2/M phase of the cell cycle[126]. Further *in silico* structural analysis revealed that BRIP1 also consists of 7 helicase domains, and that only the 3' part of the BRIP1 protein binds to the BRCT domain (Figure 1.4). The helicase domains shows strong homology to the catalytic and nucleotide binding domains of known members of the DEAH helicases and it was shown that BRIP1 is a member of the DEAH helicase family[124].

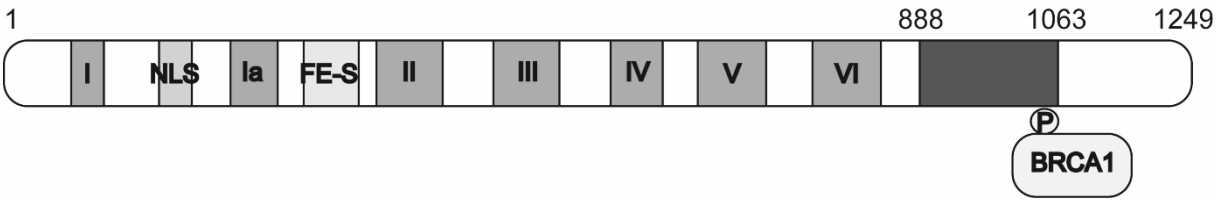

Figure 1.4: The BRIP1 protein. BRIP1 consists of 7 helicase domains, a nuclear localization signal (NLS), a FE-S domain and a BRCA1 binding domain located at its 3'end.

BRIP1 is a Fanconi anemia gene

Fanconi anemia (FA) is an autosomal recessive disorder characterized by increased cancer susceptibility, congenital abnormalities, short stature and bone marrow failure causing anemia. FA patients are strongly predisposed to several types of cancer but are particularly prone to acute myeloid leukemia (AML)[127]. The FA cells show marked chromosomal instability and enhanced sensitivity to bifunctional alkylating agents that cross-link DNA (like mitomycin c, cisplatin) which is therefore used as diagnostic test. FA is a multigenic disorder, with at least twenty-one distinct complementation groups[128,129] .The main function of the FA pathway seems to be the coordination of several distinct DNA repair pathways like, nucleotide excision repair (NER), translesion synthesis (TLS) and the homologous recombination pathway (HR).Originally thought to be involved in removing DNA crosslinks, more recent data have shown that the FA pathway also has an important role in the protection of stalled and repair of collapsed replication forks and resolving replication-transcription conflicts[130,131].

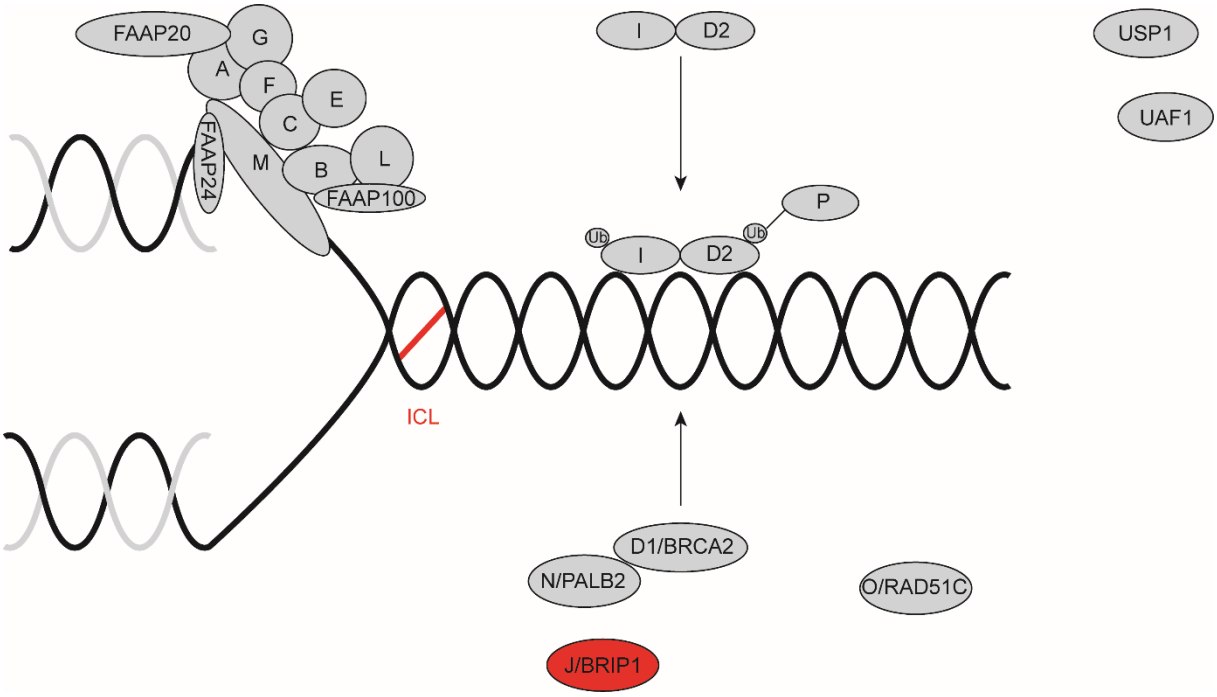

Figure 1.5: The FA complex. The pathway is activated when a replication fork stalls at an interstrand crosslink (ICL). The FA core complex binds to the stalled fork, leading to monoubiquitination and recruitment of the I and D2 proteins. The downstream FA proteins are recruited to DNA repair complexes. Figure adapted from[132]

The FA proteins can typically be divided in two groups, whereby the majority of proteins belong to the core complex, which is a large multi-subunit ubiquitin ligase, the remainder of the proteins act downstream of this core complex. Upon DNA damage, the core complex will be recruited to the nucleus and bind to the stalled DNA replication fork. Subsequently, the core complex will then ubiquitinate FANCD2 and FANCI (Figure 1.5). Downstream of FANCD2, act FANCD1, FANCJ and FANCN. These proteins will then repair the DNA damage[128] (Figure 1.5). Interestingly, in 2005, BRIP1 and FANCJ were shown to be the same protein [133-135]. Moreover, in a following study it was shown that the BRCT-binding domain of BRIP1 is not required for its role in DNA crosslink repair or cell cycle arrest, showing that the BRIP1 helicase acts independently of BRCA1 in Fanconi anemia for repairing DNA crosslink [136].

BRIP1 as a potential tumor suppressor gene

FA is a penetrant cancer susceptibility syndrome and several members of the complex are well known tumor suppressors (TSG), amongst others, *BRCA2* and *FANCN*. Since *BRIP1* is a member of the FA complex, researchers studied if germline *BRIP1* mutations have an effect on tumor incidence. Indeed, heterozygous *BRIP1* germline sequence variants were identified in familial breast, ovarian and prostate cancer[124,137-139]. However, a recent large scale case-control study found no evidence of an association with breast cancer for 10 truncating variants of BRIP1. The upper 95% confidence limit excludes a twofold risk of breast cancer, often taken as the lower threshold for a moderate risk allele[140].

BRIP1 and interstrand crosslink (ICL) repair

Interstrand DNA crosslinks can be formed as a natural product of metabolism or through induction of chemotherapeutic agents. In *E. coli* ICLs are repaired via a two-cycle repair mechanism. In the first round, incisions will be made on one strand on either side of the ICL, producing a gapped intermediate with the incised oligonucleotide attached to the intact strand. This gap is then filled by recombination repair or lesion bypass synthesis. In a final step, the remaining monoadduct is removed by the Nucleotide Excision Repair (NER) pathway[141]. Despite intensive research, the exact mechanism in mammals remains unclear.

In the paper that described BRIP1 for the first time, it was shown that BRIP1 deficient cells are more sensitive for agents that introduce ICLs[124]. Since this acts independent of BRCA1[136], Peng and colleagues used a two-step immunoaffinity strategy to identify new interaction partners of BRIP1. BRIP1 was found to exist in a protein complex with MutLα, a mismatch repair complex consisting of MLH1 and PMS1. Like BRIP1, MutLα was found to act downstream of FANCD2 monoubiquitination. BRIP1 interacts directly with MLH1 and independent of BRCA1. The interaction was mapped to the helicase domain of BRIP1, more specifically to lysine 141 and 142. Interestingly, disruption of the native MLH1/BRIP1 interaction generates sensitivity to ICLs[142]. Although PMS1 does not directly associate with BRIP1, it stabilizes the BRIP1/MLH1 interaction. The functional role of BRIP1 in ICL processing remains largely unclear and controversial, in part, due to differences between experimental systems[143]. For instance, in DT40 chicken cells, loss of BRIP1 did not affect homologous recombination. This is probably due to the binding sites for MLH1 and BRCA1 that are not conserved in chicken BRIP1[143].

BRCA1 and its binding partner BRIP1

BRCA1 is located on chromosome 17q21 and is best known for its tumor suppressor function in breast and ovarian cancer. Several functions have been attributed to *BRCA1*, but its role in dsDNA break repair is the most studied. One of the earliest indications that *BRCA1* is involved in DNA repair was the observation that BRCA1 associates and co-localizes with RAD51 in nuclear foci in mitotic cells[144]. Co-localization with RAD51 has shown to be required for the strand invasion during HR (Figure 1.6)[145]. BRCA1 is also found to be associated with another DNA damage response protein, RAD50, which forms a tight complex with Mre11 and Nijmegen breakage syndrome gene 1. This complex of Mre11/Rad50/Nijmegen breakage syndrome gene 1 (MRN) is implicated in both homologous recombination and non-homologous end joining[145] (NHEJ).

BRIP1 binds to BRCA1 during HR and interestingly, when BRIP1 is uncoupled from BRCA1, the DNA damage response is altered. Specifically cells that express BRIP1^{S990A}, a variant that cannot bind to BRCA1, are sensitive to dsDNA breaks and have a reduced RAD51-based HR[146]. Therefore, BRIP1 likely has a complex role in HR, it contributes to HR when bound to

BRCA1 and inhibits HR when unbound to BRCA1[146], however, the exact role of BRIP1 in HR is not clear. Possibly, BRIP1 has an indirect role in HR as a 'place-holder' to prevent other proteins from disrupting HR, such as the anti-recombination helicases BLM or RTEL[146].

Although the mutation burden in NB patients is very low, an extremely rare homozygous nonsense germline mutation in *BRCA1* (c.1151T>G/ p. Leu384Stop) has been described. The affected girl was five years of age and diagnosed with stage IV NB and FA[147].

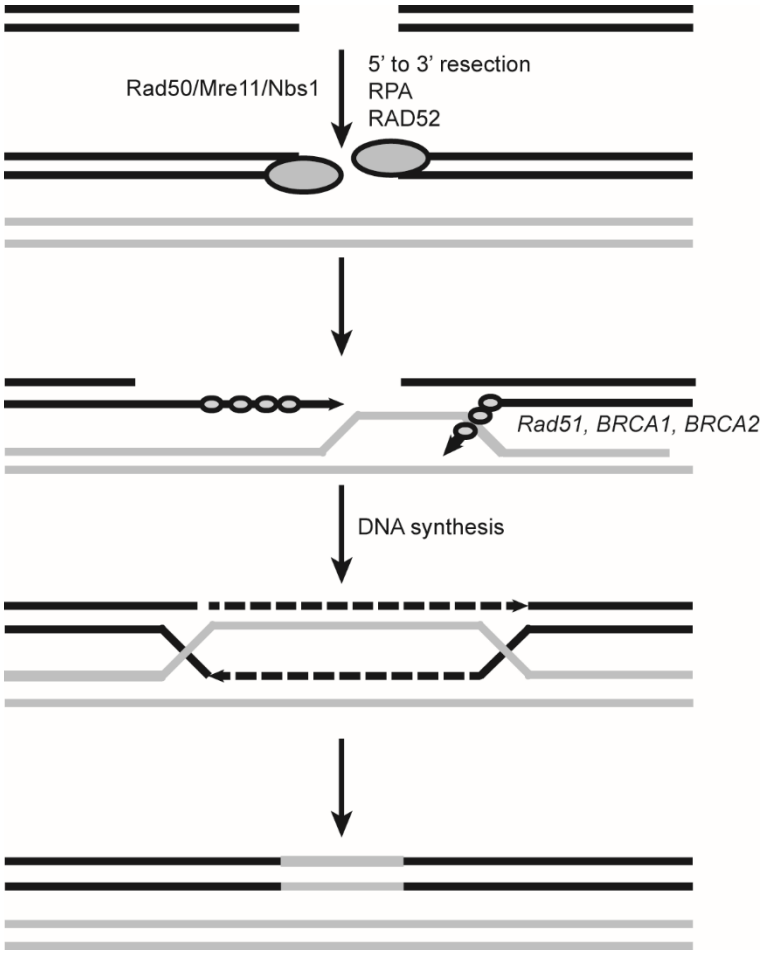

Figure 1.6: Key steps of dsDNA break repair by HR. Figure adapted from[145]

The helicase function of BRIP1

The first germline mutations found in *BRIP1*, were located in the helicase domains indicating that these sequence changes disrupt its protein function. Later, it was shown that *BRIP1* is both a DNA dependent ATPase and a 5' to 3' DNA helicase[148] . A biochemical study showed that the dimeric form of BRIP1 displays maximal catalytic ATPase and DNA helicase activity

on relatively short forked duplex substrates of 20 base pairs long[149]. BRIP1 is limited in its processivity, poorly unwinding substrates with duplexes of fifty base pairs or greater. Interestingly, BRIP1 is able to unravel forked duplex substrates of 47bp, but only in the presence of high concentrations of RPA[150] .Next to that, a DNA junction is also required for BRIP1 to initiate unwinding of the adjacent duplex. BRIP1 is even able to unravel DNA-RNA hybrids (R-loops), however it fails on RNA-RNA hybrids. In *C. elegans* it was shown that *dog-1,* the worm homologue of BRIP1, is required to maintain genetic stability of guanine rich DNA[151]. Mutations in *dog-1* resulted in a mutant phenotype characterized by deletions throughout genomic DNA that was initiated at tracts of consecutive cG/dG bases. Here it was shown for the very first time that in addition of unwinding conventional duplex DNA substrates, BRIP1 also resolves alternate DNA structures like DNA G- quadruplexes. In this thesis we have explored the role of BRIP1 in NB through functional *in vitro* assays and in vivo modeling. Interestingly, in a parallel study, I observed a MYCN driven FOXM1 pathway activation as a dominant transcriptional perturbed signature during tumor formation (Chapter 4). FOXM1 is a well-known transcription factor controlling cell cycle and DNA damage repair and amongst others also regulates BRIP1 levels together with many other DNA repair genes.

FOXM1: a central regulator of cell cycle and DNA damage

FOXM1 in normal development and disease

The forkhead box protein M1 (*FOXM1*), located on chromosome 12p33, belongs to the large family of the forkhead transcription factors. This forkhead family consists of more than 50 members, and all of them have a central role during normal development and organogenesis. Three isoforms of FOXM1 protein have been previously described, FOXM1b and FOXM1c function as transcriptional activators while FOXM1a is transcriptionally inactive[152]. Several studies used in situ hybridization and immunohistochemistry to show that FOXM1 is expressed in many cell types during embryogenesis. These include precursor cells for liver and heart, smooth muscle and endothelial cells, pancreatic cells, thymocytes, precursors of granule neurons as well as epithelium and mesenchyme of the embryonic lung and intestine[152-154]. Because of its essential role in the embryogenesis, it is no surprise that knock out of *FOXM1* in mouse is embryonic lethal[155]. Complete FOXM1 null mice die in utero 18.5 days post coitus (dpc) due to multiple abnormalities in various organs including liver, lungs, blood vessels and heart. The other cell types in FOXM1$^{-/-}$ mice show no visible changes in either size or proliferation rates raising the possibility that FOXM1 has different functions according to the cell type[156].

FOXM1 functions as a transcription factor and mainly acts as a regulator of the cell cycle and DNA damage. FOXM1 preferentially binds to promotor regions with a consensus sequence "TAAACA", although with lower affinity then his other family members of the forkhead proteins[157]. Its expression is restricted to proliferating cells and is both at the mRNA and protein level regulated by the cell cycle. The expression increases during the entry of the S-phase, peaks during G2 and M and is diminished during mitotic exit[158]. Likewise, its transcriptional activity is tightly regulated throughout the cell cycle by multisite phosphorylation by different kinases, sumo proteins and its counteracting phosphatases, reaching its maximum activity in the G2 phase of the cell cycle[159-161]. More recently, it was shown that FOXM1 not only binds to "TAAACA" repeats but also to cell cycle genes homology region elements (CHR). In mammalian cells, these repeats control the transcription of a cluster of genes at the G2/M transition. Previously, it was already shown

that the dimerization partner of the DREAM complex (RB-like, E2F and multi-vulval class B) binds to these CHR sequences[162-164]. The DREAM complex is a protein complex responsible for the regulation of cell cycle dependent gene expression, its main function is to repress gene expression during quiescence (G0). One of the genes repressed by the complex is the proto-oncogene *MYC*[162,165]. In G0 p130 will prevent E2F4/5 from binding to its gene promotors, while entry into G1 will cause dissociation of p130 of the complex (Figure 1.7). During the G0 phase there is no expression of BMYB (MYBL2), however, during G1 BMYB will be expressed and will bind to MuvB during S phase to promote the expression of the key G2/M phase genes (CDK1, CCNB1). During G2 phase FOXM1 will then be recruited to further promote gene expression (Figure 1.8)[162].

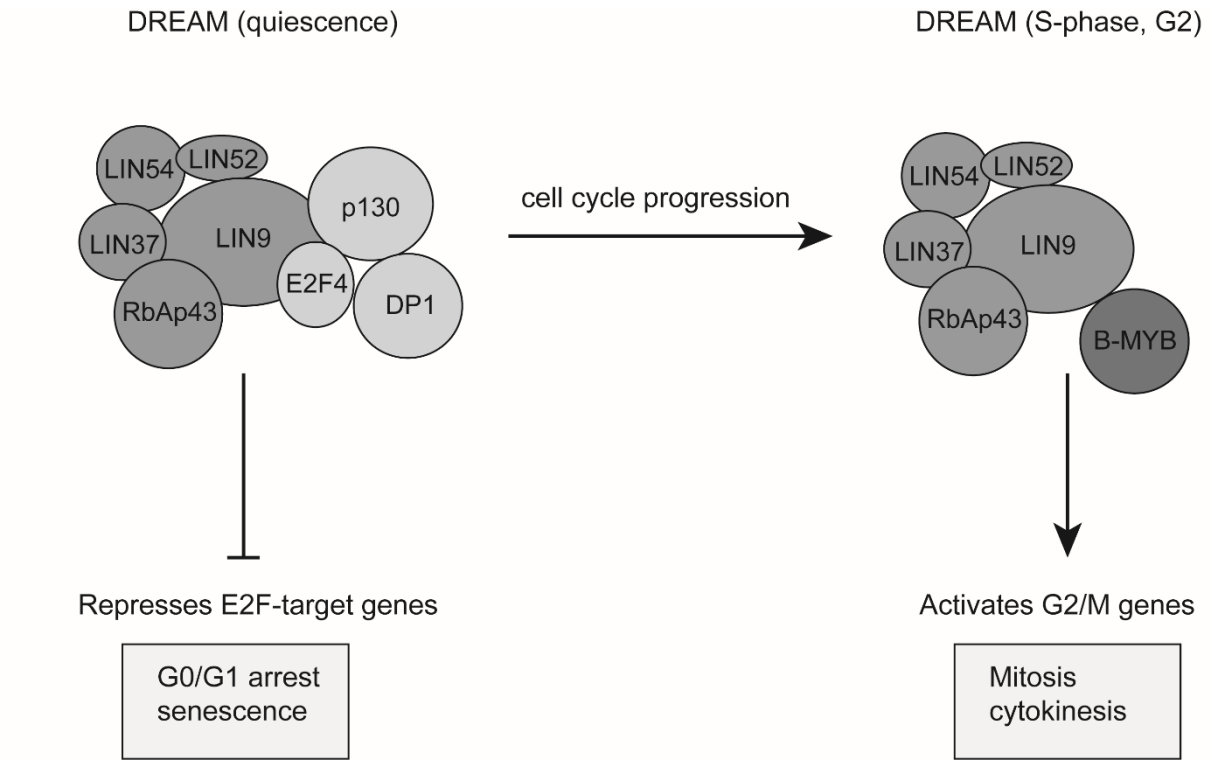

Figure 1.7 DREAM complex in quiescence and mitosis. Figure adapted from[166]

Since FOXM1 has such an important role in cell proliferation and cell cycle progression, it is not surprising that increased expression of FOXM1 was detected in numerous cancer cell lines and human cancers[167]. One of the first studies detected upregulation of FOXM1 in basal cell carcinoma compared to normal skin samples[168]. Interestingly, in a meta-analysis of expression signatures of over 18,000 human tumors, FOXM1 was identified as a major

predictor of adverse patient outcome[169]. Up until today, overexpression of FOXM1 has been observed in more than 25 different tumor entities, including lung cancer, AML and NB[170]. In NB, FOXM1 serves as a critical activator of the tumorigenic properties of the aggressive forms of the NB cells. Next to that, FOXM1 has a direct connection with the pluripotency-associated gene SOX2 in mediating the anchorage independent growth of the cells. NB cells with diminished FOXM1 expression undergo spontaneous differentiation with reduced levels of SOX2[171].

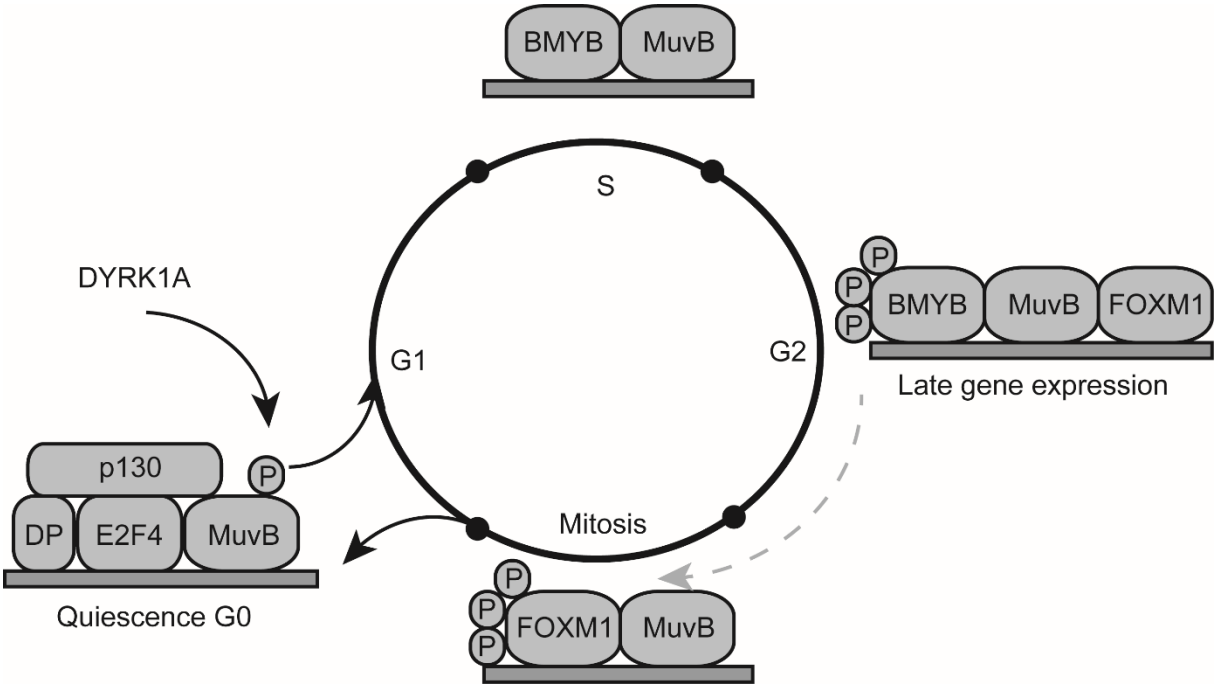

Figure 1.8: cell cycle control by the DREAM complex. Figure adapted from[162]

Molecular targeting of FOXM1

Because of its involvement in cancer biology, FOXM1 was awarded the title "molecule of the year" in 2010. Since then several research groups tried to develop molecules that target FOXM1. Since FOXM1 is a transcription factor and therefore the compounds needs to translocate to the nucleus and bind to FOXM1 at the membrane, targeting is challenging. Despite this hurdle, several compounds that target FOXM1 have already been described, although most of them are assumed to affect FOXM1 indirectly. Siomycin A, thiostreptin and in general all proteasome inhibitors can be used to inhibit the expression of FOXM1[170].

Gartel et al, hypothesized that proteasome inhibitors stabilize NRFM, which is a negative regulator of FOXM1. NRFM binds to FOXM1 and hence will inhibit the transcriptional activity of FOXM1. Since FOXM1 has a positive effect on its own expression through an autoregulation loop, expression of *FOXM1* will decrease[172,173]. In addition to that, Balasubramanian *et al*. proposed an alternative mechanism, where thiostreptin binds to FOXM1 and consequently causes a blockage of the binding to the promoters of its target genes[174] . Although proteasome inhibitors can be useful, such drugs act very broadly and unspecific thus requiring more specific compounds to target FOXM1.

To achieve this goal, using an assay based on fluorescence polarization, a small molecule (FDI6) that disrupts the FOXM1-DNA interaction could be identified from a library consisting of 54211 molecules[175]. By using mass spectrometry, it was confirmed that FDI6 specifically binds to FOXM1. Treatment of MCF7 cells with FDI6 showed already after 3h a clear transcriptional effect of the known downstream targets of FOXM1 (like CDKN3, CENPA…)[175]. While these results are promising, recent data indicate that thus far, despite these reports and their validation, the effective " on target" effects of these drugs on FOXM1 are seriously questioned thus hampering reliable drugging studies to study e.g. dependency of tumor cells to FOXM1 and assess cancer types as possible targets for clinical FOXM1 drugging (Bollen, personal communication).

The role of FOXM1 in the DNA damage response

The first indications of a role for *FOXM1* in DNA damage response came from an observation that *FOXM1* deficient cells have an increased level of DNA damage[176]. Mouse embryonic fibroblasts (MEFs) derived from FOXM1 knockout mice showed high levels of γH2AX (a biomarker for DNA double stranded breaks) compared to wild type MEFs[176]. Those cells also had an increased number of TUNEL foci, suggesting a defect in DNA repair.

When performing *FOXM1* knock down experiments using siRNAs in osteosarcoma U2OS cells, high levels of spontaneous γH2AX foci were detected. This increase also correlated with decreased levels of the X-ray repair cross-complementing protein 1 (XRCC1) and decreased levels of the breast cancer-associated gene 2 (BRCA2), two genes involved in DNA repair. Remarkably, however, this observation could not be confirmed in breast cancer cells[176].

In a cisplatin resistant breast cancer cell line, upregulation of FOXM1, BRCA2 and XRCC1 was observed upon cisplatin treatment, while downregulation of BRCA2 and XRCC1 was not observed prior to FOXM1 downregulation, suggesting that FOXM1 might regulate the expression of other genes involved in the DNA damage repair pathway[177]. In a follow up study, it was shown that double stranded breaks (through yH2AX staining) accumulate in breast cancer cells sensitive for epirubicin compared to breast cancer epirubicin resistant cells. Moreover, it was proven that FOXM1 overexpression was responsible for obtaining epirubicin resistance and it was demonstrated for the first time that FOXM1 is required for DNA double strand break (DSB) repair by homologous recombination (HR). In respect to that, BRIP1 (BRCA1 associated C-terminal helicase) was identified as a direct transcriptional target of FOXM1. Interestingly, ectopic overexpression of BRIP1 was able to partially rescue the increased DNA damage and repair in FOXM1 null cells[160,178].

The G4 genome

G_4-DNA

G-quadruplex structures (also known as G_4–DNA) are tertiary structures formed in nucleic acids by guanine rich sequences. Four guanine bases can associate through Hoogsteen hydrogen bonding to from a square planar structure called a guanine tetrad, and two or more guanine tetrads can stack on top of each other to form a G-quadruplex (Figure 1.9)[179].

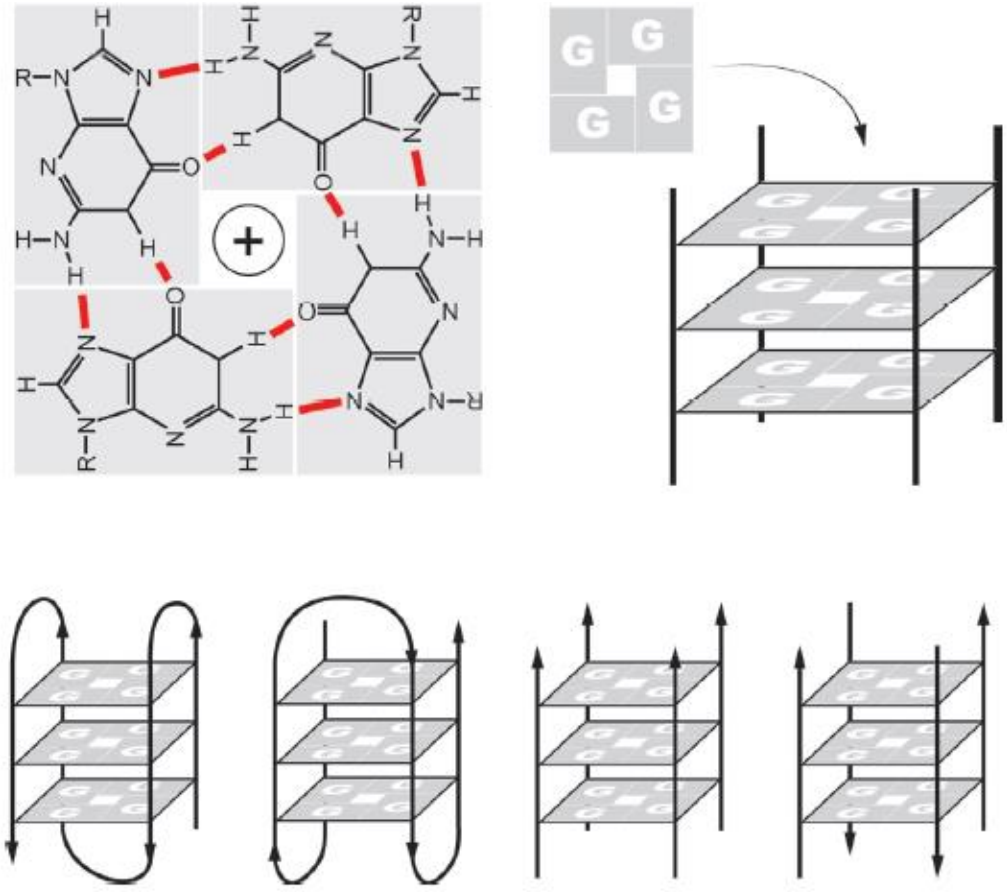

Figure 1.9: Structures of G-quadruplexes. G-quadruplexes contain tracts of three to four guanines and can be formed in DNA or RNA. The building blocks of G4 DNA are G-quartets that arise from the association of four guanines into a cyclic arrangement stabilized by Hoogsteen hydrogen bonding. The planar G-quartets pack on top of each other, forming four stranded helical structures. Figure adapted from[180].

Quadruplexes can be formed from one, two or four separate strands of DNA (or RNA) and can present a wide variety of topologies, which are in part a consequence of various possible combinations of strand directions, as well as variations in loop size and sequence[179] (Figure 1.9). Typically, the length of the nucleic acid sequences involved in the tetrad formation will determine how the quadruplex will fold[180].

In the early 1950's it was already discovered that guanine-rich nucleic acids can self-associate but their scientific value was at that moment neglected. Only after realizing that these G_4-structures can be formed at the end of telomere regions and in this way will decrease the activity of the telomerase enzyme, researchers started to study these functions in depth. By using computational analysis of the human genome it was revealed that the human genome contains over 300 000 sequences that have the potential to form G-quadruplexes, which further strengthens their possible important role in the human genome[181]. Next to that, it was found that the localization of G_4-structures is not ad random, G_4-DNA colocalizes with functional regions in the genome and furthermore are highly conserved between different species pinpointing to a selection pressure to maintain such sequences at specific genomic areas. Moreover, G_4-DNA is also present in bacteria and in viruses[180,182-185].

The highest abundance of G_4-structures is still in the telomeres, where it was shown that stabilization of the G_4-structures using a G_4 stabilizing compounds impairs proper telomerase activity and telomere shortening. It has been hypothesized that G-quadruplexes can sequester the 3' end of the telomere. Indeed, *in vivo* data have indicated that parallel G-quadruplexes can form at human telomeres, and that telomeres containing a G-quadruplex are a site of localization for human telomerase[186].

G4 structures regulate transcription and translation

The finding that about 50% of the human genes contain a G_4-structure near their promotor regions suggests a role for quadruplex structures in regulating gene expression. Fascinatingly, G_4-structures are more frequently observed in oncogenes than in housekeeping or tumor suppressor genes[181] . The first oncogene described with a G_4-structure in the promotor was *cMYC*, where it was shown that stabilizing the G_4-structure in

its promotor resulted in aberrant transcription. Next to transcription, it has also been described that G-quadruplex structures are important to control translation. Andrew Wolfe and colleagues from our lab could show that genes dependent on transcription of eIF4A contain a 12-nucleotide pG4 signature that can form RNA G-quadruplex structures. eIF4A helps by the translation of mRNAs with long and complex UTRs, like MYC, NOTCH, BCL2, known oncogenes in T-ALL. Consequently, this paper showed for the first time that RNA G-quadruplex structures are important for proper translation[187]. Blocking these RNA G-quadruplex structures using silvestrol resulted in cell death in T-ALL cell lines and primary T-ALL patient samples.

G4 structures in replication and genome instability and the role of BRIP1

Since single stranded DNA (ssDNA) is formed during DNA replication and G_4-structures have the tendency to form during DNA replication, G_4-structures can have a great impact on DNA replication. Upon creation, they have to be resolved as fast as possible, since otherwise this can lead to replication stress and eventually genome instability. By using Xenopus egg extracts to replicate exogenous G4 sequence on single-stranded DNA plasmids, it could be shown for the first time that DNA replication forks stall at G4 structures[188]. Mapping of the nascent strands at nucleotide resolution demonstrated that replication proceeded to within a few nucleotides from the G4. Furthermore, it has been shown that when cells face stable G-quadruplex structures, cells will activate dormant origins of DNA replication, in order to further control DNA replication[189]. If cells are unable to maintain processive DNA replication this will lead to the uncoupling of the DNA synthesis and recycling of the histones. In the original *C. Elegans* paper, mutations in *dog-1*, the homologue of BRIP1, resulted in a mutant phenotype characterized by deletions throughout genomic DNA that was initiated at tracts of consecutive cG/dG bases[151]. Since that report, several other observations were made confirming that BRIP1 has a role in unraveling G_4-DNA structures. In Fanconi anemia patients with mutations in *BRIP1*, the loss of BRIP1 G4 unwinding function, correlates with the accumulation of large genomic deletions in the neighborhood of G4 sequences[190]. Furthermore, in human cells, BRIP1 deficiency resulted in a hypersensitivity to the G4 stabilizing ligand Telomestatin (TMS), neither FANCA or FANCD2 mutant human cell lines

were sensitive to TMS, suggesting that BRIP1 functions in G4 DNA metabolism independently from the classical FA pathway[191]. Finally, BRIP1 also has a G4 recognition site. Interestingly, the two lysine residues (K141/142) that are involved in G-quadruplex recognition also interact with MLH1 for repairing interstrand crosslinks[192].

So far, two different mechanisms for the unraveling of G4 DNA have been described. In *C. Elegans* loss of the BLM orthologue resulted in a massive increase in G-tract deletions, suggesting that BRIP1 and BLM may have an overlapping function in resolving G4 secondary structures[193]. Next to that, it was also observed that BRIP1 can interact with BLM helicase, further alluding that both of them function together in facilitating efficient DNA synthesis past the leading or lagging strand of G4 structures during replication[194]. In another *in vitro* study it was demonstrated that also WRN (Werner Helicase) smoothens DNA synthesis past a G4 structure in a DNA template[195]. Therefore, it was hypothesized that BLM and WRN would translocate on the opposite strand as BRIP1, and together these helicases collaborate to efficiently resolve the G4 structure so the unfolded G-rich sequence can be copied[196] (Figure 1.10). Another mechanism for the unraveling of G4 structures requires the involvement of REV-1 helicase. In this situation, REV1 will bind to the opposite strand of BRIP1 and together they will unwind the G4 structure[197] (Figure 1.10). Up till today, it is largely unknown how BLM/WRN or REV1 exactly collaborate with BRIP1 for the unwinding of G4 structures[196] .

Targeting G4 structures

The specific geometry of the G4 structure, with four grooves of unequal width coupled with an unusual electrostatic potential, is predicted to allow specific recognition by small compounds that bind within the grooves or intercalate with the DNA triple-helix. Indeed, several compounds, including porphyrins and anthraquinones, target G4 DNA and inhibit telomerase *in vitro*[198]. Up till today, several compounds have been described, each with their advantages and disadvantages. TMPYP4 tosylate has a strong affinity for G4 structures but turns out to be toxic for mice[199]. Similar effects were observed for pyridostatin[200]. BRACO-19 on the other side, has a less strong affinity for G4 DNA but is tolerated pretty well by mice.

Moreover, BRACO-19 was highly active on a broad range of tumors and reduced tumor size in average with 96% compared with untreated controls[201] .

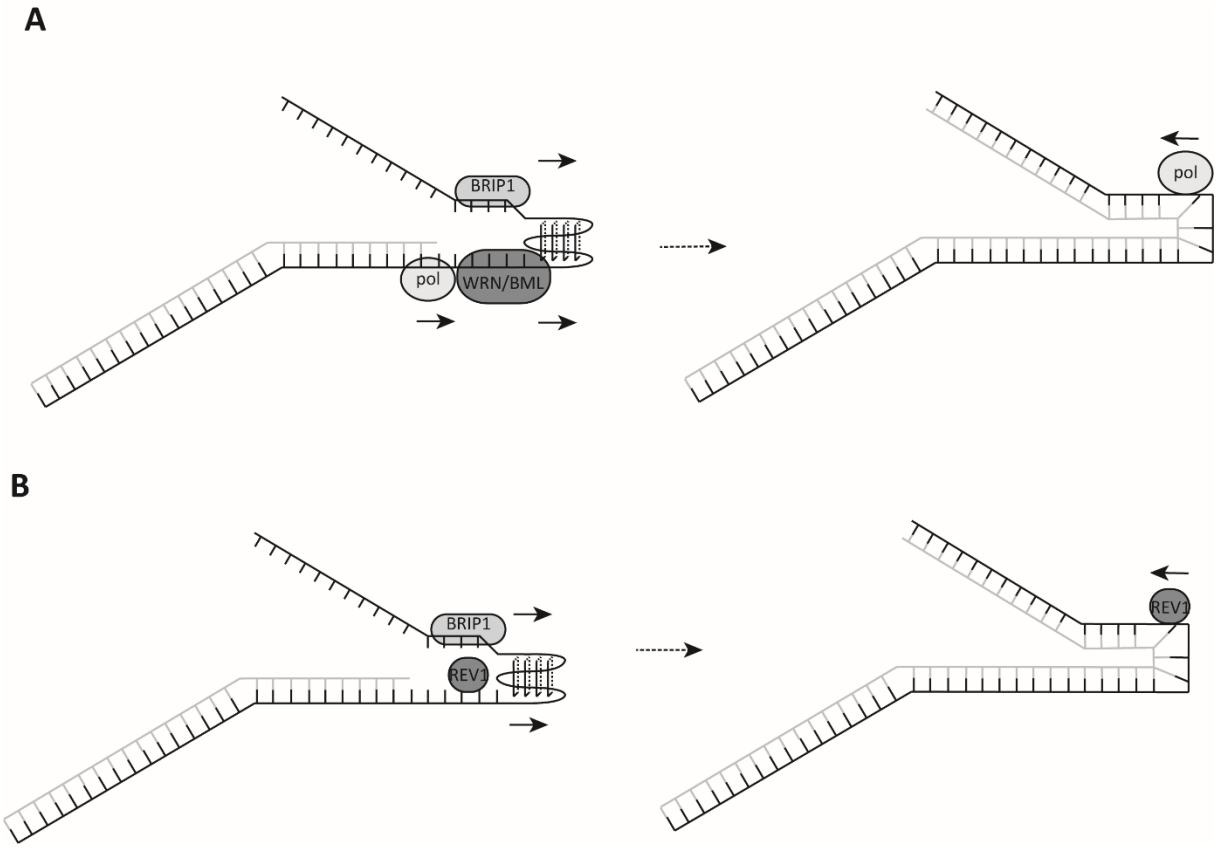

Figure 1.10: Proposed model how BRIP1 resolves G4 structures. (A) BRIP1 acts together with BLM (or WRN) helicase to resolve the G quadruplex structure (B) BRIP1 interacts with REV1 at the site of the G4 structure, allowing it the catalyze DNA synthesis past the G4 structure. Figure adapted from[196]

References:

1. R V: Hyperplasie der Zirbel und der Nebennieren. Die krankhaften Geschwulste 2, 1864-1865
2. Cushing H, Wolbach SB: The Transformation of a Malignant Paravertebral Sympathicoblastoma into a Benign Ganglioneuroma. Am J Pathol 3:203-216 7, 1927
3. Maris JM: Recent advances in neuroblastoma. N Engl J Med 362:2202-11, 2010
4. Monclair T, Brodeur GM, Ambros PF, et al: The International Neuroblastoma Risk Group (INRG) staging system: an INRG Task Force report. J Clin Oncol 27:298-303, 2009
5. Jiang MR, Stanke J, Lahti JM: The Connections between Neural Crest Development and Neuroblastoma. Cancer and Development 94:77-127, 2011
6. Marshall GM, Carter DR, Cheung BB, et al: The prenatal origins of cancer. Nature Reviews Cancer 14:277-289, 2014
7. Louis CU, Shohet JM: Neuroblastoma: Molecular Pathogenesis and Therapy. Annual Review of Medicine, Vol 66 66:49-63, 2015
8. De Preter K, Vandesompele J, Heimann P, et al: Human fetal neuroblast and neuroblastoma transcriptome analysis confirms neuroblast origin and highlights neuroblastoma candidate genes. Genome Biology 7, 2006
9. Kohl NE, Gee CE, Alt FW: Activated expression of the N-myc gene in human neuroblastomas and related tumors. Science 226:1335-7, 1984
10. Kohl NE, Kanda N, Schreck RR, et al: Transposition and amplification of oncogene-related sequences in human neuroblastomas. Cell 35:359-67, 1983
11. Van Roy N, Van Limbergen H, Vandesompele J, et al: Chromosome 2 short arm translocations revealed by M-FISH analysis of neuroblastoma cell lines. Medical and Pediatric Oncology 35:538-540, 2000
12. Huang M, Weiss WA: Neuroblastoma and MYCN. Cold Spring Harbor Perspectives in Medicine 3, 2013
13. Marshall GM, Carter DR, Cheung BB, et al: The prenatal origins of cancer. Nat Rev Cancer 14:277-89, 2014
14. Eilers M, Eisenman RN: Myc's broad reach. Genes Dev 22:2755-66, 2008
15. Hurlin PJ: N-Myc functions in transcription and development. Birth Defects Res C Embryo Today 75:340-52, 2005
16. Hirning U, Schmid P, Schulz WA, et al: A comparative analysis of N-myc and c-myc expression and cellular proliferation in mouse organogenesis. Mech Dev 33:119-25, 1991
17. Molenaar JJ, Koster J, Zwijnenburg DA, et al: Sequencing of neuroblastoma identifies chromothripsis and defects in neuritogenesis genes. Nature 483:589-93, 2012
18. George RE, Sanda T, Hanna M, et al: Activating mutations in ALK provide a therapeutic target in neuroblastoma. Nature 455:975-8, 2008
19. Corvi R, Savelyeva L, Amler L, et al: Cytogenetic evolution of MYCN and MDM2 amplification in the neuroblastoma LS tumour and its cell line. Eur J Cancer 31A:520-3, 1995
20. Van Roy N, Forus A, Myklebost O, et al: Identification of two distinct chromosome 12-derived amplification units in neuroblastoma cell line NGP. Cancer Genet Cytogenet 82:151-4, 1995

21. Bown N: Neuroblastoma tumour genetics: clinical and biological aspects. J Clin Pathol 54:897-910, 2001

22. Bown N, Cotterill S, Lastowska M, et al: Gain of chromosome arm 17q and adverse outcome in patients with neuroblastoma. N Engl J Med 340:1954-61, 1999

23. Vandepoele K, Andries V, Van Roy N, et al: A constitutional translocation t(1;17)(p36.2;q11.2) in a neuroblastoma patient disrupts the human NBPF1 and ACCN1 genes. PLoS One 3:e2207, 2008

24. Janoueix-Lerosey I, Penther D, Thioux M, et al: Molecular analysis of chromosome arm 17q gain in neuroblastoma. Genes Chromosomes Cancer 28:276-84, 2000

25. Vandesompele J, Van Roy N, Van Gele M, et al: Genetic heterogeneity of neuroblastoma studied by comparative genomic hybridization. Genes Chromosomes Cancer 23:141-52, 1998

26. Saito-Ohara F, Imoto I, Inoue J, et al: PPM1D is a potential target for 17q gain in neuroblastoma. Cancer Research 63:1876-1883, 2003

27. Kleiblova P, Shaltiel IA, Benada J, et al: Gain-of-function mutations of PPM1D/Wip1 impair the p53-dependent G1 checkpoint. Journal of Cell Biology 201:511-521, 2013

28. Lamers F, van der Ploeg I, Schild L, et al: Knockdown of survivin (BIRC5) causes apoptosis in neuroblastoma via mitotic catastrophe. Endocrine-Related Cancer 18:657-668, 2011

29. Carotenuto M, Pedone E, Diana D, et al: Neuroblastoma tumorigenesis is regulated through the Nm23-H1/h-Prune C-terminal interaction. Scientific Reports 3, 2013

30. Okabe-Kado J, Kasukabe T, Honma Y, et al: Clinical significance of serum NM23-H1 protein in neuroblastoma. Cancer Sci 96:653-60, 2005

31. Chen Y, Takita J, Choi YL, et al: Oncogenic mutations of ALK kinase in neuroblastoma. Nature 455:971-4, 2008

32. Hallberg B, Palmer RH: The role of the ALK receptor in cancer biology. Ann Oncol 27 Suppl 3:iii4-iii15, 2016

33. Carpenter EL, Mosse YP: Targeting ALK in neuroblastoma--preclinical and clinical advancements. Nat Rev Clin Oncol 9:391-9, 2012

34. Barone G, Anderson J, Pearson AD, et al: New strategies in neuroblastoma: Therapeutic targeting of MYCN and ALK. Clin Cancer Res 19:5814-21, 2013

35. Mosse YP, Laudenslager M, Longo L, et al: Identification of ALK as a major familial neuroblastoma predisposition gene. Nature 455:930-U22, 2008

36. Sausen M, Leary RJ, Jones S, et al: Integrated genomic analyses identify ARID1A and ARID1B alterations in the childhood cancer neuroblastoma. Nat Genet 45:12-7, 2013

37. Cheung NK, Zhang J, Lu C, et al: Association of age at diagnosis and genetic mutations in patients with neuroblastoma. JAMA 307:1062-71, 2012

38. Napier CE, Huschtscha LI, Harvey A, et al: ATRX represses alternative lengthening of telomeres. Oncotarget 6:16543-58, 2015

39. Valentijn LJ, Koster J, Zwijnenburg DA, et al: TERT rearrangements are frequent in neuroblastoma and identify aggressive tumors. Nat Genet 47:1411-4, 2015

40. Peifer M, Hertwig F, Roels F, et al: Telomerase activation by genomic rearrangements in high-risk neuroblastoma. Nature 526:700-4, 2015

41. Knudson AG, Strong LC: Mutation and Cancer - Neuroblastoma and Pheochromocytoma. American Journal of Human Genetics 24:514-&, 1972

42. Kushner BH, Gilbert F, Helson L: Familial Neuroblastoma - Case-Reports, Literature-Review, and Etiologic Considerations. Cancer 57:1887-1893, 1986

43. Rohrer T, Trachsel D, Engelcke G, et al: Congenital central hypoventilation syndrome associated with Hirschsprung's disease and neuroblastoma: Case of multiple neurocristopathies. Pediatric Pulmonology 33:71-76, 2002

44. Trochet D, Bourdeaut F, Janoueix-Lerosey I, et al: Germline mutations of the paired-like homeobox 2B (PHOX2B) gene in neuroblastoma. Am J Hum Genet 74:761-4, 2004

45. Mosse YP, Laudenslager M, Khazi D, et al: Germline PHOX2B mutation in hereditary neuroblastoma. Am J Hum Genet 75:727-30, 2004

46. Maris JM, Mosse YP, Bradfield JP, et al: Chromosome 6p22 locus associated with clinically aggressive neuroblastoma. N Engl J Med 358:2585-93, 2008

47. Capasso M, Devoto M, Hou C, et al: Common variations in BARD1 influence susceptibility to high-risk neuroblastoma. Nat Genet 41:718-23, 2009

48. Bosse KR, Diskin SJ, Cole KA, et al: Common Variation at BARD1 Results in the Expression of an Oncogenic Isoform That Influences Neuroblastoma Susceptibility and Oncogenicity. Cancer Research 72:2068-2078, 2012

49. Wang K, Diskin SJ, Zhang HT, et al: Integrative genomics identifies LMO1 as a neuroblastoma oncogene. Nature 469:216-220, 2011

50. Oldridge DA, Wood AC, Weichert-Leahey N, et al: Genetic predisposition to neuroblastoma mediated by a LMO1 super-enhancer polymorphism. Nature 528:418-+, 2015

51. Lieschke GJ, Currie PD: Animal models of human disease: zebrafish swim into view. Nature Reviews Genetics 8:353-367, 2007

52. Driever W, Solnica-Krezel L, Schier AF, et al: A genetic screen for mutations affecting embryogenesis in zebrafish. Development 123:37-46, 1996

53. Haffter P, Granato M, Brand M, et al: The identification of genes with unique and essential functions in the development of the zebrafish, Danio rerio. Development 123:1-36, 1996

54. Seth A, Stemple DL, Barroso I: The emerging use of zebrafish to model metabolic disease. Disease Models & Mechanisms 6:1080-1088, 2013

55. Dooley K, Zon LI: Zebrafish: a model system for the study of human disease. Current Opinion in Genetics & Development 10:252-256, 2000

56. Langenau DM, Traver D, Ferrando AA, et al: Myc-induced T cell leukemia in transgenic zebrafish. Science 299:887-890, 2003

57. Rudner LA, Brown KH, Dobrinski KP, et al: Shared acquired genomic changes in zebrafish and human T-ALL. Oncogene 30:4289-4296, 2011

58. White R, Rose K, Zon L: Zebrafish cancer: the state of the art and the path forward. Nature Reviews Cancer 13:624-636, 2013

59. Zhu S, Lee JS, Guo F, et al: Activated ALK collaborates with MYCN in neuroblastoma pathogenesis. Cancer Cell 21:362-73, 2012

60. De Brouwer S, De Preter K, Kumps C, et al: Meta-analysis of Neuroblastomas Reveals a Skewed ALK Mutation Spectrum in Tumors with MYCN Amplification. Clinical Cancer Research 16:4353-4362, 2010

61. Zhu S, Thomas Look A: Neuroblastoma and Its Zebrafish Model. Adv Exp Med Biol 916:451-78, 2016

62. He SN, Mansour MR, Zimmerman MW, et al: Synergy between loss of NF1 and overexpression of MYCN in neuroblastoma is mediated by the GAP-related domain. Elife 5, 2016

63. MacRae CA, Peterson RT: Zebrafish as tools for drug discovery. Nature Reviews Drug Discovery 14:721-731, 2015

64. Gutierrez A, Pan L, Groen RWJ, et al: Phenothiazines induce PP2A-mediated apoptosis in T cell acute lymphoblastic leukemia. Journal of Clinical Investigation 124:644-655, 2014

65. White RM, Cech J, Ratanasirintrawoot S, et al: DHODH modulates transcriptional elongation in the neural crest and melanoma. Nature 471:518-522, 2011

66. Hwang WY, Fu YF, Reyon D, et al: Efficient genome editing in zebrafish using a CRISPR-Cas system. Nature Biotechnology 31:227-229, 2013

67. Ablain J, Durand EM, Yang S, et al: A CRISPR/Cas9 Vector System for Tissue-Specific Gene Disruption in Zebrafish. Developmental Cell 32:756-764, 2015

68. Boel A, Steyaert W, De Rocker N, et al: BATCH-GE: Batch analysis of Next-Generation Sequencing data for genome editing assessment. Scientific Reports 6, 2016

69. Dovey M, White RM, Zon LI: Oncogenic NRAS cooperates with p53 loss to generate melanoma in zebrafish. Zebrafish 6:397-404, 2009

70. Santoriello C, Gennaro E, Anelli V, et al: Kita driven expression of oncogenic HRAS leads to early onset and highly penetrant melanoma in zebrafish. PLoS One 5:e15170, 2010

71. Patton EE, Widlund HR, Kutok JL, et al: BRAF mutations are sufficient to promote nevi formation and cooperate with p53 in the genesis of melanoma. Curr Biol 15:249-54, 2005

72. Liu S, Leach SD: Screening Pancreatic Oncogenes in Zebrafish Using the Gal4/UAS System. Zebrafish: Disease Models and Chemical Screens, 3rd Edition 105:367-381, 2011

73. Park SW, Davison JM, Rhee J, et al: Oncogenic KRAS induces progenitor cell expansion and malignant transformation in zebrafish exocrine pancreas. Gastroenterology 134:2080-90, 2008

74. Langenau DM, Feng H, Berghmans S, et al: Cre/lox-regulated transgenic zebrafish model with conditional myc-induced T cell acute lymphoblastic leukemia. Proc Natl Acad Sci U S A 102:6068-73, 2005

75. Feng H, Langenau DM, Madge JA, et al: Heat-shock induction of T-cell lymphoma/leukaemia in conditional Cre/lox-regulated transgenic zebrafish. Br J Haematol 138:169-75, 2007

76. Chen J, Jette C, Kanki JP, et al: NOTCH1-induced T-cell leukemia in transgenic zebrafish. Leukemia 21:462-71, 2007

77. Blackburn JS, Liu S, Raiser DM, et al: Notch signaling expands a pre-malignant pool of T-cell acute lymphoblastic leukemia clones without affecting leukemia-propagating cell frequency. Leukemia 26:2069-78, 2012

78. Feng H, Stachura DL, White RM, et al: T-lymphoblastic lymphoma cells express high levels of BCL2, S1P1, and ICAM1, leading to a blockade of tumor cell intravasation. Cancer Cell 18:353-66, 2010

79. Sabaawy HE, Azuma M, Embree LJ, et al: TEL-AML1 transgenic zebrafish model of precursor B cell acute lymphoblastic leukemia. Proc Natl Acad Sci U S A 103:15166-71, 2006

80. Langenau DM, Keefe MD, Storer NY, et al: Effects of RAS on the genesis of embryonal rhabdomyosarcoma. Genes Dev 21:1382-95, 2007

81. He SN, Mansour MR, Zimmerman MW, et al: Synergy between loss of NF1 and overexpression of MYCN in neuroblastoma is mediated by the GAP -related domain. Cancer Research 76, 2016

82. Zhuravleva J, Paggetti J, Martin L, et al: MOZ/TIF2-induced acute myeloid leukaemia in transgenic fish. Br J Haematol 143:378-82, 2008

83. Berghmans S, Murphey RD, Wienholds E, et al: tp53 mutant zebrafish develop malignant peripheral nerve sheath tumors. Proc Natl Acad Sci U S A 102:407-12, 2005

84. Ki DH, He S, Rodig S, et al: Overexpression of PDGFRA cooperates with loss of NF1 and p53 to accelerate the molecular pathogenesis of malignant peripheral nerve sheath tumors. Oncogene, 2016

85. Shive HR, West RR, Embree LJ, et al: BRCA2 and TP53 collaborate in tumorigenesis in zebrafish. PLoS One 9:e87177, 2014

86. Chu CY, Chen CF, Rajendran RS, et al: Overexpression of Akt1 enhances adipogenesis and leads to lipoma formation in zebrafish. PLoS One 7:e36474, 2012

87. Leacock SW, Basse AN, Chandler GL, et al: A zebrafish transgenic model of Ewing's sarcoma reveals conserved mediators of EWS-FLI1 tumorigenesis. Dis Model Mech 5:95-106, 2012

88. Nguyen AT, Emelyanov A, Koh CH, et al: An inducible kras(V12) transgenic zebrafish model for liver tumorigenesis and chemical drug screening. Dis Model Mech 5:63-72, 2012

89. Li Z, Huang X, Zhan H, et al: Inducible and repressable oncogene-addicted hepatocellular carcinoma in Tet-on xmrk transgenic zebrafish. J Hepatol 56:419-25, 2012

90. Yang HW, Kutok JL, Lee NH, et al: Targeted expression of human MYCN selectively causes pancreatic neuroendocrine tumors in transgenic zebrafish. Cancer Res 64:7256-62, 2004

91. Forrester AM, Grabher C, McBride ER, et al: NUP98-HOXA9-transgenic zebrafish develop a myeloproliferative neoplasm and provide new insight into mechanisms of myeloid leukaemogenesis. Br J Haematol 155:167-81, 2011

92. Liu NA, Jiang H, Ben-Shlomo A, et al: Targeting zebrafish and murine pituitary corticotroph tumors with a cyclin-dependent kinase (CDK) inhibitor. Proc Natl Acad Sci U S A 108:8414-9, 2011

93. Gill JA, Lowe L, Nguyen J, et al: Enforced expression of Simian virus 40 large T-antigen leads to testicular germ cell tumors in zebrafish. Zebrafish 7:333-41, 2010

94. Gjini E, Mansour MARC, He S, et al: A Zebrafish Model of Myelodysplastic Syndrome Produced through Tet2 Genomic Editing. Leukemia Research 39:S11-S11, 2015

95. Zeman MK, Cimprich KA: Causes and consequences of replication stress. Nat Cell Biol 16:2-9, 2014

96. Mazouzi A, Velimezi G, Loizou JI: DNA replication stress: causes, resolution and disease. Exp Cell Res 329:85-93, 2014

97. Hamperl S, Cimprich KA: Conflict Resolution in the Genome: How Transcription and Replication Make It Work. Cell 167:1455-1467, 2016

98. Berti M, Vindigni A: Replication stress: getting back on track. Nat Struct Mol Biol 23:103-9, 2016

99. Marechal A, Zou L: RPA-coated single-stranded DNA as a platform for post-translational modifications in the DNA damage response. Cell Research 25:9-23, 2015

100. Bouchard C, Dittrich O, Kiermaier A, et al: Regulation of cyclin D2 gene expression by the Myc/Max/Mad network: Myc-dependent TRRAP recruitment and histone acetylation at the cyclin D2 promoter. Genes Dev 15:2042-7, 2001

101. Dominguez-Sola D, Gautier J: MYC and the control of DNA replication. Cold Spring Harb Perspect Med 4, 2014

102. Dominguez-Sola D, Ying CY, Grandori C, et al: Non-transcriptional control of DNA replication by c-Myc. Nature 448:445-51, 2007

103. Gaillard H, Garcia-Muse T, Aguilera A: Replication stress and cancer. Nat Rev Cancer 15:276-89, 2015

104. Felsher DW, Zetterberg A, Zhu J, et al: Overexpression of MYC causes p53-dependent G2 arrest of normal fibroblasts. Proc Natl Acad Sci U S A 97:10544-8, 2000

105. Ruzankina Y, Asare A, Brown EJ: Replicative stress, stem cells and aging. Mech Ageing Dev 129:460-6, 2008

106. Lopez-Contreras AJ, Gutierrez-Martinez P, Specks J, et al: An extra allele of Chk1 limits oncogene-induced replicative stress and promotes transformation. J Exp Med 209:455-61, 2012

107. Sarmento LM, Barata JT: CHK1 and replicative stress in T-cell leukemia: Can an irreverent tumor suppressor end up playing the oncogene? Adv Biol Regul 60:115-21, 2016

108. Sarmento LM, Povoa V, Nascimento R, et al: CHK1 overexpression in T-cell acute lymphoblastic leukemia is essential for proliferation and survival by preventing excessive replication stress. Oncogene 34:2978-90, 2015

109. Petroni M, Giannini G: A MYCN-MRN complex axis controls replication stress for the safe expansion of neuroprogenitor cells. Mol Cell Oncol 3:e1079673, 2016

110. Petroni M, Sardina F, Heil C, et al: The MRN complex is transcriptionally regulated by MYCN during neural cell proliferation to control replication stress. Cell Death Differ 23:197-206, 2016

111. Kenig S, Faoro V, Bourkoula E, et al: Topoisomerase IIbeta mediates the resistance of glioblastoma stem cells to replication stress-inducing drugs. Cancer Cell Int 16:58, 2016

112. Adriaens C, Standaert L, Barra J, et al: p53 induces formation of NEAT1 lncRNA-containing paraspeckles that modulate replication stress response and chemosensitivity. Nat Med 22:861-8, 2016

113. Murga M, Campaner S, Lopez-Contreras AJ, et al: Exploiting oncogene-induced replicative stress for the selective killing of Myc-driven tumors. Nat Struct Mol Biol 18:1331-5, 2011

114. Bartkova J, Horejsi Z, Koed K, et al: DNA damage response as a candidate anti-cancer barrier in early human tumorigenesis. Nature 434:864-870, 2005

115. Bryant HE, Schultz N, Thomas HD, et al: Specific killing of BRCA2-deficient tumours with inhibitors of poly(ADP-ribose) polymerase. Nature 434:913-917, 2005

116. Gad H, Koolmeister T, Jemth AS, et al: MTH1 inhibition eradicates cancer by preventing sanitation of the dNTP pool. Nature 508:215-+, 2014

117. Huber KVM, Salah E, Radic B, et al: Stereospecific targeting of MTH1 by (S)-crizotinib as an anticancer strategy. Nature 508:222-+, 2014

118. Cole KA, Huggins J, Laquaglia M, et al: RNAi screen of the protein kinome identifies checkpoint kinase 1 (CHK1) as a therapeutic target in neuroblastoma. Proceedings of the National Academy of Sciences of the United States of America 108:3336-3341, 2011

119. Sakurikar N, Eastman A: Will Targeting Chk1 Have a Role in the Future of Cancer Therapy? Journal of Clinical Oncology 33:1075-+, 2015

120. Hanahan D, Weinberg RA: The hallmarks of cancer. Cell 100:57-70, 2000

121. Hanahan D, Weinberg RA: Hallmarks of Cancer: The Next Generation. Cell 144:646-674, 2011

122. Spry M, Scott T, Pierce H, et al: DNA repair pathways and hereditary cancer susceptibility syndromes. Front Biosci 12:4191-207, 2007

123. Macheret M, Halazonetis TD: DNA Replication Stress as a Hallmark of Cancer. Annual Review of Pathology: Mechanisms of Disease, Vol 10 10:425-448, 2015

124. Cantor SB, Bell DW, Ganesan S, et al: BACH1, a novel helicase-like protein, interacts directly with BRCA1 and contributes to its DNA repair function. Cell 105:149-160, 2001

125. Hashizume R, Fukuda M, Maeda I, et al: The RING heterodimer BRCA1-BARD1 is a ubiquitin ligase inactivated by a breast cancer-derived mutation. Journal of Biological Chemistry 276:14537-14540, 2001

126. Yu XC, Chini CCS, He M, et al: The BRCT domain is a phospho-protein binding domain. Science 302:639-642, 2003

127. Mathew CG: Fanconi anaemia genes and susceptibility to cancer. Oncogene 25:5875-5884, 2006

128. Moldovan GL, D'Andrea AD: How the Fanconi Anemia Pathway Guards the Genome. Annual Review of Genetics 43:223-249, 2009

129. Palovcak A, Liu WJ, Yuan FH, et al: Maintenance of genome stability by Fanconi anemia proteins. Cell and Bioscience 7, 2017

130. Yeo JE, Lee EH, Hendrickson EA, et al: CtIP mediates replication fork recovery in a FANCD2-regulated manner. Human Molecular Genetics 23:3695-3705, 2014

131. Kais Z, Rondinelli B, Holmes A, et al: FANCD2 Maintains Fork Stability in BRCA1/2-Deficient Tumors and Promotes Alternative End-Joining DNA Repair. Cell Rep 15:2488-99, 2016

132. D'Andrea AD: BRCA1: a missing link in the Fanconi anemia/BRCA pathway. Cancer Discov 3:376-8, 2013

133. Levitus M, Waisfisz Q, Godthelp BC, et al: The DNA helicase BRIP1 is defective in Fanconi anemia complementation group J. Nature Genetics 37:934-935, 2005

134. Litman R, Peng M, Jin Z, et al: BACH1 is critical for homologous recombination and appears to be the Fanconi anemia gene product FANCJ. Cancer Cell 8:255-265, 2005

135. Levran O, Attwooll C, Henry RT, et al: The BRCA1-interacting helicase BRIP1 is deficient in Fanconi anemia. Nature Genetics 37:931-933, 2005

136. Bridge WL, Vandenberg CJ, Franklin RJ, et al: The BRIP1 helicase functions independently of BRCA1 in the Fanconi anemia pathway for DNA crosslink repair. Nature Genetics 37:953-957, 2005

137. Seal S, Thompson D, Renwick A, et al: Truncating mutations in the Fanconi anemia J gene BRIP1 are low-penetrance breast cancer susceptibility alleles. Nature Genetics 38:1239-1241, 2006

138. Kote-Jarai Z, Jugurnauth S, Mulholland S, et al: A recurrent truncating germline mutation in the BRIP1/FANCJ gene and susceptibility to prostate cancer. British Journal of Cancer 100:426-430, 2009

139. Rafnar T, Gudbjartsson DF, Sulem P, et al: Mutations in BRIP1 confer high risk of ovarian cancer. Nature Genetics 43:1104-U91, 2011

140. Easton DF, Lesueur F, Decker B, et al: No evidence that protein truncating variants in BRIP1 are associated with breast cancer risk: implications for gene panel testing. Journal of Medical Genetics 53:298-309, 2016

141. Muniandy PA, Liu J, Majumdar A, et al: DNA interstrand crosslink repair in mammalian cells: step by step. Critical Reviews in Biochemistry and Molecular Biology 45:23-49, 2010

142. Peng M, Litman R, Xie J, et al: The FANCJ/MutL alpha interaction is required for correction of the cross-link response in FA-J cells. Embo Journal 26:3238-3249, 2007

143. Cantor SB, Xie J: Assessing the link between BACH1/FANCJ and MLH1 in DNA crosslink repair. Environ Mol Mutagen 51:500-7, 2010

144. Scully R, Chen J, Plug A, et al: Association of BRCA1 with Rad51 in mitotic and meiotic cells. Cell 88:265-75, 1997

145. Zhang J, Powell SN: The role of the BRCA1 tumor suppressor in DNA double-strand break repair. Mol Cancer Res 3:531-9, 2005

146. Xie J, Litman R, Wang S, et al: Targeting the FANCJ-BRCA1 interaction promotes a switch from recombination to poleta-dependent bypass. Oncogene 29:2499-508, 2010

147. Mehmet D, Unal S, Gumruk F, et al: A Homozygous Germ Line Nonsense Mutation in BRCA1 Leading Fanconi Anemia and Neuroblastoma. Blood 128, 2016

148. Cantor S, Drapkin R, Zhang F, et al: The BRCA1-associated protein BACH1 is a DNA helicase targeted by clinically relevant inactivating mutations. Proc Natl Acad Sci U S A 101:2357-62, 2004

149. Wu Y, Sommers JA, Loiland JA, et al: The Q motif of Fanconi anemia group J protein (FANCJ) DNA helicase regulates its dimerization, DNA binding, and DNA repair function. J Biol Chem 287:21699-716, 2012

150. Gupta R, Sharma S, Sommers JA, et al: FANCJ (BACH1) helicase forms DNA damage inducible foci with replication protein A and interacts physically and functionally with the single-stranded DNA-binding protein. Blood 110:2390-8, 2007

151. Cheung I, Schertzer M, Rose A, et al: Disruption of dog-1 in Caenorhabditis elegans triggers deletions upstream of guanine-rich DNA. Nat Genet 31:405-9, 2002

152. Ye HG, Kelly TF, Samadani U, et al: Hepatocyte nuclear factor 3/fork head homolog 11 is expressed in proliferating epithelial and mesenchymal cells of embryonic and adult tissues. Molecular and Cellular Biology 17:1626-1641, 1997

153. Kalin TV, Ustiyan V, Kalinichenko VV: Multiple faces of FoxM1 transcription factor Lessons from transgenic mouse models. Cell Cycle 10:396-405, 2011

154. Kalin TV, Wang IC, Meliton L, et al: Forkhead Box m1 transcription factor is required for perinatal lung function. Proceedings of the National Academy of Sciences of the United States of America 105:19330-19335, 2008

155. Krupczak-Hollis K, Wang XH, Kalinichenko VV, et al: The mouse Forkhead Box m1 transcription factor is essential for hepatoblast mitosis and development of intrahepatic bile ducts and vessels during liver morphogenesis. Developmental Biology 276:74-88, 2004

156. Kalin TV, Ustiyan V, Kalinichenko VV: Multiple faces of FoxM1 transcription factor: lessons from transgenic mouse models. Cell Cycle 10:396-405, 2011

157. Littler DR, Alvarez-Fernandez M, Stein A, et al: Structure of the FoxM1 DNA-recognition domain bound to a promoter sequence. Nucleic Acids Research 38:4527-4538, 2010

158. Laoukili J, Alvarez M, Meijer LA, et al: Activation of FoxM1 during G2 requires cyclin A/Cdk-dependent relief of autorepression by the FoxM1 N-terminal domain. Mol Cell Biol 28:3076-87, 2008

159. Fu Z, Malureanu L, Huang J, et al: Plk1-dependent phosphorylation of FoxM1 regulates a transcriptional programme required for mitotic progression. Nature Cell Biology 10:1076-1082, 2008

160. Alvarez-Fernandez M, Medema RH: Novel functions of FoxM1: from molecular mechanisms to cancer therapy. Front Oncol 3:30, 2013

161. Schimmel J, Eifler K, Sigurethsson JO, et al: Uncovering SUMOylation dynamics during cell-cycle progression reveals FoxM1 as a key mitotic SUMO target protein. Mol Cell 53:1053-66, 2014

162. Sadasivam S, DeCaprio JA: The DREAM complex: master coordinator of cell cycle-dependent gene expression. Nature Reviews Cancer 13:585-595, 2013

163. Sadasivam S, Duan S, DeCaprio JA: The MuvB complex sequentially recruits B-Myb and FoxM1 to promote mitotic gene expression. Genes Dev 26:474-89, 2012

164. Carroll MW, Matthews DA, Hiscox JA, et al: Temporal and spatial analysis of the 2014-2015 Ebola virus outbreak in West Africa. Nature 524:97-101, 2015

165. Lee H, Ragusano L, Martinez A, et al: A dual role for the dREAM/MMB complex in the regulation of differentiation-specific E2F/RB target genes. Mol Cell Biol 32:2110-20, 2012

166. Esterlechner J, Reichert N, Iltzsche F, et al: LIN9, a subunit of the DREAM complex, regulates mitotic gene expression and proliferation of embryonic stem cells. PLoS One 8:e62882, 2013

167. Benayoun BA, Caburet S, Veitia RA: Forkhead transcription factors: key players in health and disease. Trends Genet 27:224-32, 2011

168. Teh MT, Wong ST, Neill GW, et al: FOXM1 is a downstream target of Gli1 in basal cell carcinomas. Cancer Research 62:4773-4780, 2002

169. Gentles AJ, Newman AM, Liu CL, et al: The prognostic landscape of genes and infiltrating immune cells across human cancers. Nat Med 21:938-45, 2015

170. Halasi M, Gartel AL: Targeting FOXM1 in cancer. Biochemical Pharmacology 85:644-652, 2013

171. Wang ZB, Park HJ, Carr JR, et al: FoxM1 in Tumorigenicity of the Neuroblastoma Cells and Renewal of the Neural Progenitors. Cancer Research 71:4292-4302, 2011

172. Gartel AL: A new target for proteasome inhibitors: FoxM1. Expert Opinion on Investigational Drugs 19:235-242, 2010

173. Gartel AL: Thiostrepton, proteasome inhibitors and FOXM1. Cell Cycle 10:4341-4342, 2011

174. Hegde NS, Sanders DA, Rodriguez R, et al: The transcription factor FOXM1 is a cellular target of the natural product thiostrepton. Nature Chemistry 3:725-731, 2011

175. Gormally MV, Dexheimer TS, Marsico G, et al: Suppression of the FOXM1 transcriptional programme via novel small molecule inhibition. Nature Communications 5, 2014

176. Tan YJ, Raychaudhuri P, Costa RH: Chk2 mediates stabilization of the FoxM1 transcription factor to stimulate expression of DNA repair genes. Molecular and Cellular Biology 27:1007-1016, 2007

177. Kwok JMM, Peck B, Monteiro LJ, et al: FOXM1 Confers Acquired Cisplatin Resistance in Breast Cancer Cells. Molecular Cancer Research 8:24-34, 2010

178. Monteiro LJ, Khongkow P, Kongsema M, et al: The Forkhead Box M1 protein regulates BRIP1 expression and DNA damage repair in epirubicin treatment. Oncogene 32:4634-45, 2013

179. Burge S, Parkinson GN, Hazel P, et al: Quadruplex DNA: sequence, topology and structure. Nucleic Acids Res 34:5402-15, 2006

180. Rhodes D, Lipps HJ: G-quadruplexes and their regulatory roles in biology. Nucleic Acids Research 43:8627-8637, 2015

181. Huppert JL, Balasubramanian S: Prevalence of quadruplexes in the human genome. Nucleic Acids Research 33:2908-2916, 2005

182. Konig SL, Evans AC, Huppert JL: Seven essential questions on G-quadruplexes. Biomol Concepts 1:197-213, 2010

183. Maizels N, Gray LT: The G4 genome. PLoS Genet 9:e1003468, 2013

184. Frees S, Menendez C, Crum M, et al: QGRS-Conserve: a computational method for discovering evolutionarily conserved G-quadruplex motifs. Hum Genomics 8:8, 2014

185. Beaume N, Pathak R, Yadav VK, et al: Genome-wide study predicts promoter-G4 DNA motifs regulate selective functions in bacteria: radioresistance of D. radiodurans involves G4 DNA-mediated regulation. Nucleic Acids Res 41:76-89, 2013

186. Moye AL, Porter KC, Cohen SB, et al: Telomeric G-quadruplexes are a substrate and site of localization for human telomerase. Nat Commun 6:7643, 2015

187. Wolfe AL, Singh K, Zhong Y, et al: RNA G-quadruplexes cause eIF4A-dependent oncogene translation in cancer. Nature 513:65-70, 2014

188. Castillo Bosch P, Segura-Bayona S, Koole W, et al: FANCJ promotes DNA synthesis through G-quadruplex structures. EMBO J 33:2521-33, 2014

189. Madireddy A, Purushothaman P, Loosbroock CP, et al: G-quadruplex-interacting compounds alter latent DNA replication and episomal persistence of KSHV. Nucleic Acids Res 44:3675-94, 2016

190. London TBC, Barber LJ, Mosedale G, et al: FANCJ Is a Structure-specific DNA Helicase Associated with the Maintenance of Genomic G/C Tracts. Journal of Biological Chemistry 283:36132-36139, 2008

191. Wu YL, Shin-ya K, Brosh RM: FANCJ helicase defective in Fanconia anemia and breast cancer unwinds G-quadruplex DNA to defend genomic stability. Molecular and Cellular Biology 28:4116-4128, 2008

192. Wu CG, Spies M: G-quadruplex recognition and remodeling by the FANCJ helicase. Nucleic Acids Research 44:8742-8753, 2016

193. Youds JL, O'Neil NJ, Rose AM: Homologous recombination is required for genome stability in the absence of DOG-1 in Caenorhabditis elegans. Genetics 173:697-708, 2006

194. Suhasini AN, Rawtani NA, Wu YL, et al: Interaction between the helicases genetically linked to Fanconi anemia group J and Bloom's syndrome. Embo Journal 30:692-705, 2011

195. Kamath-Loeb AS, Loeb LA, Johansson E, et al: Interactions between the Werner syndrome helicase and DNA polymerase delta specifically facilitate copying of tetraplex and hairpin structures of the d(CGG)(n) trinucleotide repeat sequence. Journal of Biological Chemistry 276:16439-16446, 2001

196. Bharti SK, Awate S, Banerjee T, et al: Getting Ready for the Dance: FANCJ Irons Out DNA Wrinkles. Genes 7, 2016

197. Sarkies P, Murat P, Phillips LG, et al: FANCJ coordinates two pathways that maintain epigenetic stability at G-quadruplex DNA. Nucleic Acids Research 40:1485-1498, 2012

198. Mergny JL, Helene C: G-quadruplex DNA: A target for drug design. Nature Medicine 4:1366-1367, 1998

199. Zheng XH, Nie X, Liu HY, et al: TMPyP4 promotes cancer cell migration at low doses, but induces cell death at high doses. Scientific Reports 6, 2016

200. Rodriguez R, Miller KM, Forment JV, et al: Small-molecule-induced DNA damage identifies alternative DNA structures in human genes. Nat Chem Biol 8:301-10, 2012

201. Burger AM, Dai FP, Schultes CM, et al: The G-quadruplex-interactive molecule BRACO-19 inhibits tumor growth, consistent with telomere targeting and interference with telomerase function. Cancer Research 65:1489-1496, 2005

PART II: Research Objectives

DNA is like a computer program, but far far more

advanced than any software ever created

~Bill Gates~

Research objectives:

After decades of intensive research, the cancer entity NB remains an enigmatic disease and advances in unraveling the genome biology have been slow and challenging. This is reflected in the little amount of personalized therapeutic options and the slow progress in the survival changes of patients with aggressive disease. This, however, can partly be explained by the unique features of NBs. While in most other tumors several mutations can be identified, the mutational burden in NBs is low. Instead, several genomic aberrations are often identified, and this is why NB is typically regarded as a copy number disease. One of the irregularities that is typically observed is the gain of chromosome 17q, which is correlated with poor patient outcome. Despite thorough research, up till today, it is still unclear which genes on chromosome 17q contribute to the development of NB.

Aim1: Unraveling the role of BRIP1 in NB development

The first aim of my thesis was to follow up on a previous bio-informatics approach intended to identify candidate oncogenes on chromosome 17q (**paper 1**). This strategy identified *BRIP1* as a potential driver gene in NB oncogenesis. *BRIP1* is a member of the Fanconi anemia pathway and therefore in general considered as a tumor suppressor. To study its oncogenic capacities in NB, knock down experiments were performed in NB cell lines and a transgenic zebrafish model that overexpresses *BRIP1* was developed.

Aim2: Establishing a miRNA ESC signature score for the stratification of NB patients

NB has been regarded as a developmental disorder, hence in this study, we wanted to deeper explore whether an ESC derived expression signature could capture a stemness phenotype in NB cells that is associated with therapy resistance **(paper 2)**. FOXM1 was identified as a major driver and several compounds that target FOXM1 were therefore evaluated for use in NB in a follow-up study **(paper 3).**

Aim3: Identification of expressed repeat elements (EREs) in zebrafish to use for normalization in RT-qPCR.

RT-qPCR is an elegant technique for performing gene expression analyses. Because of its relative ease and simplicity it is frequently applied. To correct for technically induced variation and thus measure true biological variation in samples, it is important to apply a good normalization strategy. Since in zebrafish, many commonly used reference genes are not always applicable because of their variability in expression levels, we evaluated a new normalization strategy using EREs.

PART III: Results

The important thing is not to stop questioning.

Curiosity has its own reason for existing.

~Albert Einstein~

Chapter 3: BRIP1 overexpression accelerates MYCN driven neuroblastoma formation and is part of a FOXM1 driven gene signature providing protection to excessive replicative stress

Authors: Suzanne Vanhauwaert, Christophe Vanneste, Carina Leonelli, Kaat Durinck, Bieke Decaesteker, Annelies Fieuw, Givani Dewyn, Els Janssens, Siebe Loontiens, Shuning He, Sharon Cantor, Kevin Freeman, Nadine Van Roy, Geertrui Denecker, Winnok De Vos, A. Thomas Look, Katleen De Preter, Frank Speleman

In preparation

BRIP1 overexpression accelerates MYCN driven neuroblastoma formation and is part of a FOXM1 driven gene signature providing protection to excessive replicative stress

Authors: Suzanne Vanhauwaert[1,2], Christophe Vanneste[1,2], Carina Leonelli[1,2], Kaat Durinck[1,2], Bieke Decaesteker[1,2], ,Annelies Fieuw[1,2], Givani Dewyn[1,2], Els Janssens[1,2], Siebe Loontiens[1,2], Shuning He[3,4], Sharon Cantor[5], Kevin Freeman[6], Nadine Van Roy[1,2], Geertrui Denecker[1,2], Winnok De Vos[7,8], A. Thomas Look[3], Katleen De Preter[1,2], Frank Speleman[1,2]

Affiliations:

1)Cancer for Medical Genetics (CMGG), Ghent University, Ghent, Belgium

2)Cancer Research Institute Ghent (CRIG), Ghent University, Ghent, Belgium

3)Department of Pediatric Oncology, Dana-Farber Cancer Institute, Harvard Medical School, Boston, MA, 02215, USA

4)Division of Pediatric Hematology/Oncology, Boston Children's Hospital, Boston, MA, 02215, USA

5)Division of Hematology-Oncology, University of Massachusetts Medical School, Worcester, MA, USA

6)Oncology Department, St Jude Children's Research Hospital, 262 Danny Thomas Place, Memphis, TN38105

7) Faculty of Bioscience Engineering, Department of Molecular Biotechnology, Laboratory of Cell Systems and Imaging, Ghent University, Ghent, Belgium

8) Faculty of Pharmaceutical Biomedical and Veterinary Sciences, Department of Veterinary Sciences, Laboratory of Cell Biology and Histology, Antwerp University, Antwerp, Belgium.

Abstract:

Neuroblastoma is the most common extracranial tumor in children and despite multimodal therapies the survival rates for children with aggressive neuroblastoma are still disappointingly low. Chromosome 17q gain is by far the most common DNA copy number alteration in high stage neuroblastoma. Due to the large size of the recurrently involved chromosome segments, the causal 17q drivers still remain to be identified.

In this study, using an integrated bio-informatics approach, we identified the DNA helicase *BRIP1* as top ranked candidate 17q driver gene. High expression of *BRIP1* correlates with poor patient outcome. In neuroblastoma cell lines, we show that BRIP1 knock down significantly reduced cell viability and colony forming capacity. Next, overexpression of BRIP1 in *tg(dβh-MYCN-eGFP)* transgenic zebrafish caused accelerated tumor formation. Given *BRIP1*'s roles in preserving genome integrity, we show that knock down results in increased pRPA32 protein indicative for replication stress and that BRIP1 creates a cellular state what we call "replicative stress resistance". BRIP1 is a downstream target of FOXM1 and moreover our data strongly suggest that FOXM1, a known important mediator of the MYCN driven oncogenic transformation of fetal neuroblasts controls the expression of several dosage sensitive 17q genes.

In conclusion, we identified a new cooperative oncogene, BRIP1, involved in neuroblastoma oncogenesis opening perspectives for new therapeutic approaches.

Introduction:

Neuroblastoma is the most common extracranial tumor in children and is characterized by a variable clinical course and genetic heterogeneity[1]. Tumors are subdivided in four subclasses, stage L1 and L2 cases present with localized or locoregional disease with favorable prognosis, while patients with stage M have metastatic disease and poor clinical outcome. Stage MS cases have an unusual presentation with tumor spread to only the skin, liver, and/or bone marrow (less than 10% bone marrow involvement) in patients younger than 18 months and the majority of patients remarkably show regression with little or no treatment[2].

Recent sequencing efforts in neuroblastoma established a mutational landscape with a low mutational burden in comparison to other cancer types. In addition to the previously noted *ALK* activating mutations in only 10% of cases[3,4], further rare mutations were noted in *RAS*-pathway genes, epigenetic regulators and genes implicated in neuritogenesis[5-8]. Given these overall low mutation frequencies, selecting patients for precision treatment for molecular targets is challenging at present. In contrast to mutations, large copy number alterations (CNAs) in neuroblastoma are frequent and show remarkable recurrent patterns[9,10]. The metastatic tumor subtype almost invariably presents with partial 17q gain (often in combination with 1p loss, *MYCN* amplification and 2p-gains) which is also highly correlated with poor survival outcome[10]. Since gain of 17q is so frequently observed, it is assumed that one or several genes on 17q contribute to the development of the disease in a dosage dependent way.

CNAs are a hallmark of cancer and can drive the expression of oncogenes or delete tumor suppressor genes and thus represent a source for therapeutic gene target discovery[11]. However, such CNAs typically harbor many genes hampering classical candidate gene approaches and require *in vitro* or *in vivo* screens or bio-informatics approaches to identify the culprit candidates. Of further note, using an *in vivo* screening approach, Mohankumar *et al*. identified eight new ependymoma oncogenes and 10 ependymoma tumor suppressor genes remarkably converging on a small number of cell functions contributing to the cellular state of the transformed cell[12]. Considering neuroblastoma as a CNA driven cancer, we decided to apply an integrated bio-informatics approach using CNA and gene expression

data from primary human neuroblastomas in combination with transcriptome data from dynamic regulation of gene expression in Th-MYCN driven tumor formation.

Using this approach, we identified *BRIP1* (previously also called *FANCJ* or *BACH1*), located on 17q23 within the commonly gained region on chromosome 17q, as top candidate cooperative driver. Subsequently we showed that forced overexpression in sympathetic progenitor cells caused accelerated MYCN driven tumor formation in a zebrafish model. BRIP1 is a downstream target of FOXM1, a transcription factor with key roles in cell cycle and the DNA damage pathway. Interestingly, also BRCA1, another FOXM1 downstream target, and many member of the Fanconi anemia pathway are highly upregulated during neuroblastoma development. We therefore propose that BRIP1 is a key play together with other FOXM1 targets in protecting neuroblastoma cells from excessive levels of replicative stress thus allowing smooth DNA replication and avoiding replication-transcription conflicts in these highly proliferative cancer cell.

Material and methods:

Neuroblastoma 17q gene ranking

A subset of 356 patients with a 17q gain was selected from a large neuroblastoma cohort with aCGH data available (Depuydt *et al*, in preparation). Each gene presenting at least once in one of these 17q gains was ranked according to the sum logarithmic of the following ranked criteria: 1) percentile of 17q gains the gene is part of; 2) impact of high median gene expression on survival in the Fischer cohort[7]; and 3) the linear regression coefficient of the gene in our prior TH-MYCN model, indicating genes having a potential driving role in early neuroblastoma development[14].

17q dosage impact on BRIP1

In order to validate an overall impact of 17q gain on BRIP1 expression, copy number data and paired expression data was retrieved from the NRC cohort for BRIP1. Copy number fold changes above 0.3 were considered as a BRIP1 gain. High and low expression were considered in respect to median expression in the cohort.

Survival analysis

Kaplan Meier analysis and Log Rank analysis was performed on the NRC neuroblastoma dataset (283 neuroblastoma patients) and the Fisher dataset[7].

Th-MYCN

Experiments were performed as described by Beckers et al[14]. In brief, we sacrificed Th-MYCN+/+ mice at one (n = 4) and two weeks (n = 4) after birth to harvest superior cervical and celiac ganglia containing foci of neuroblast hyperplasia, and 6-week old (n = 4) Th-MYCN+/+ mice to dissect advanced neuroblastoma tumors, arisen from the neuroblast hyperplasia. Additionally, we dissected the superior cervical and celiac ganglia from Th-MYCN-/- mice at one (n = 4), two (n = 4) and six weeks (n = 4) after birth to control for gene

expression changes during normal postnatal development of the sympathetic ganglia. We assayed each individual harvested sample with a murine-specific gene expression microarray.

Cell Culture

Neuroblastoma cell lines were grown as monolayer cultures at 37°C and 5% CO2 as in a humid atmosphere. The culture medium was RPMI 1640 (GIBCO, Life Technologies) containing 10% Fetal Calf Serum (FCS), 2mmol/l glutamine and the following antibiotics: Penicillin (1%), Kanamycin (1%) and Streptomycin (1%). Used cell lines were SH-SY5Y (MYCN non amplified, ALK^{F1174L} mutant, partial 17q gain, high expression of BRIP1, FOXM1 and BRCA1) and IMR-32 (MYCN amplified, partial ALK amplification, partial 17q gain, high expression of BRIP1, FOXM1 and BRCA1).

Lentiviral transduction BRIP1

shRNA knock down for BRIP1 was achieved using MISSION shRNA clones TRCN0000049916 and TRCN0000049917 (Sigma-Aldrich, St Louis, USA). Virus production was performed with 15µg of plasmid in $3*10^6$ HEK293TN cells using a calcium phosphate trans lentiviral packaging system, according to the protocol provided by the company (Thermofisher Scientific). Virus was harvested and concentrated with the PEG-it virus precipitation protocol (system Bioscience) and subsequently used for lentiviral transduction of IMR-32 and SH-SY5Y neuroblastoma cell lines.

shRNA knock down for FOXM1 was achieved using MISSION shRNA clones (TRCN0000015544) in IMR-32 cells and was performed as described above.

RT-qPCR, Caspase glo, colony forming assays and cell cycle analysis

Knock down after puromycin selection (0.5µg/ml for IMR-32 and 1µg/ml for SH-SY5Y) was confirmed using RT-qPCR. RNA isolation was performed using the protocol provided by the company (miRNEASY catalogue number 217004, Qiagen) followed with DNAse on column

treatment (RNAse-free DNAse set catalogue number 79254, Qiagen). cDNA synthesis was executed with 500ng RNA input according to the protocol of the company (iScript catalogue number 170-8891, Bioké). RT-qPCR reactions were carried out in duplicate with a total volume of 5µl, including 2µl of cDNA, 2.5µl SsoAdvanced (172-5204, Bio-rad) and 0.25µl per primer pair (0.5µM). Following RT-qPCR primers were used for BRIP1 (TGCTGTTTAATCCTCTGAGAATAG; CATGTTTAATCTGTTAGGAATCTGA), FOXM1 (AGACACCCATTAAGGAAACG, TTTGTACTGGGCTGAAATCC) and reference genes HPRT1(TGACACTGGCAAAACAATGCA ,GGTCCTTTTCACCAGCAAGCT), YWHAZ(ACTTTTGGTACATTGTGGCTTCAA, CCGCCAGGACAAACCAGTAT). Cycling conditions were: 95°C (15s) – 60°C (15s) – 72°C (60s) with in total 44 cycli. Data were analyzed via qBasePlus software (Biogazelle).

Caspase 3/7 was measured 24, 48 and 72h after seeding, using the caspase-glo 3/7 assay (Promega) according to the guidelines of the company. In brief, cells were seeded in a 96-well plate with a density of 10 000 cells per well. Experiments were performed in triplicates (technical and biological) and GloMax luminometer was used for luminescence measurements.

For the colony forming assays, cells were seeded, 2000 cells in a 6 cm dish, 72h upon lentiviral transduction to see the immediate effects upon BRIP1 knock down. 14 days after seeding cells were fixed with 0.5ml formaldehyde and subsequently stained with 0.005% crystal violet. Colonies were counted using the Image J software.

Cell cycle analysis with PI Staining was performed according to the guidelines of the company (ab14083, Abcam). Cells were trypsinized and resuspended in 70% ice cold ethanol. Following several washing steps, cells were resuspended in PBS and RNAseA was added (final concentration 0.2mg/ml). After addition of PI the cells were immediately analyzed on the flow sorter (S3 cell sorter, Biorad).

DNA combing assay

DNA fiber combing analysis was conducted using logarithmically growing IMR-32 and SH-SY5Y cells as described by Schwab et al[15]. Cells were pulsed with iodo-deoxyuridine (IdU), and then pulsed with 5-chloro-2'-deoxyuridine thymidine (CldU) combined with hydroxyurea (HU). The cells were harvested and washed. A portion of the cells was lysed on a glass slide and the DNA fibers were straightened (combed) and fixed. Cells were subjected to immunofluorescence staining with mouse anti-bromodeoxyuridine (BrdU) (1/100, mouse anti-BrdU clone 44, 347580, BD Bioscience) or rat anti-BrdU (1/100, Rat monoclonal Anti-BrdU antibody [BU1/75 5(ICR1)], ab6326, Abcam). The cells were washed with cold PBS, and incubated with Alexa 546-labeled anti-mouse (1/500, A21123, life technologies) and Alexa 488 labeled anti-rat (1/1000, A21470, life technologies) at room temperature in the dark for 1h.

Western blotting and immunofluorescence

Protein extraction was done via RIPA buffer and protein concentration was measured using the Lowry protein assay. Protein extracts were separated with SDS-PAGE, blotted on a nitrocellulose membrane and probed with antibodies against BRIP1 (1/1000 ; 4578S cell signaling), RPA32 (1/500, 14170S; cell signaling), pCHK1 (1/750, 2348S, cell signaling) and vinculin (1/10000, V9131, Sigma-Aldrich). Proteins were detected with HRP-conjugated goat anti mouse/rabbit IgG antibody (1/15000, sc2005, Bio-connect; 1/15000 A27036 thermo fisher scientific) and developed with ChemiDoc-it imaging system (UVP).

For immunofluorescence, the cells were fixed in 4% paraformaldehyde and stained with anti-γ-H2AX (1/500) antibodies.

RNA sequencing

Poly-A captured RNA library preparation was done on biological triplicates of BRIP1 knockdown in IMR-32 and SH-SY5Y and control samples, using the TruSeq stranded mRNA kit LT. Concentration was measured via qPCR using the Kapa Library Quantification Kit (Illumina) and 1.4pM was loaded on a NextSeq 500. The NextSeq 500 High Output V2 75 cycles kit was used for single end sequencing to obtain approximately 20 million reads for every sample.
Sample and read quality was checked with FastQC (v0.11.3). Reads were subsequently aligned to the human genome GRCh38 with STAR aligner (v2.5.2b). Final gene count values were obtained with RSEM (v1.2.31), which takes read mapping uncertainty into account.
Counts were quantile normalized, followed by voom transformation and differential expression analysis with limma (R-package limma). Gene Set Enrichment Analysis (GSEA)[16] was performed on the list ordered according to differential expression statistic value (t) with limma functions *romer* and *barcodeplot*.

Zebrafish experiments

Experiments were performed as described by Zhu et al[17]. Human *BRIP1* was cloned behind the dβh-promotor and subsequently injected into the one cell stage of *tg(dβh:EGFP-MYCN)* offspring. These fish were screened every 2 weeks starting at 5 weeks post fertilization (wpf) for fluorescent EGFP expressing cell masses indicative of tumors. All experiments were approved by the Ghent University ethical committee (ECD 14/86).

Results

Integrated bio-informatics analysis identifies BRIP1 as top dosage sensitive candidate cooperative driver oncogene in neuroblastoma

In a first step of our analysis, we used CONEXIC, a computational framework that integrates CNAs and gene expression data to identify dosage sensitive driver genes[18]. Using this approach, the expected *MYCN* oncogene was amongst the top ranked drivers, validating the tool (Table 3.1). Next, we established a further ranking, which we will call ICON, for 17q genes based on (1) Percentile of 17q gains the gene is part of (2) gene expression profiles for each of the identified candidate drivers in different stages of tumor development in the Th-MYCN mouse model[14] (Figure 3.1A) and (3) impact of high median gene expression on survival in the Fischer cohort[7] (Table 3.2) (Figure 3.1B-C). In the CONEXIC analysis *BRIP1* was identified as the second highest gene, while in the ICON analysis *BRIP1* was the top-ranked candidate. Highly elevated *BRIP1* expression levels were correlated with poor prognosis in several data sets in keeping with the presumed oncogenic (cooperative) driver role for BRIP1 (Figure 3.1B). Importantly, also in high risk patients for which often prognostic signatures poorly perform to discriminate survivors from children that died of disease, high *BRIP1* expression correlates with poor patient outcome (Figure 3.1C). Finally, further suggesting the oncogenic effect of *BRIP1* overexpression in neuroblastoma cells, *BRIP1* levels were amongst the highest in neuroblastoma only preceded by T-ALL (Figure 3.1D).

Table 3.1: Top 10 dosage sensitive driver genes identified by CONEXIC

gene	Chromosomal location	Deletion/gain
MYCN	2p24.3	Amplification
BRIP1	17q23.2	Gain
DDX1	2p24.3	Gain
EXO1	1q43	Gain
VSP13D	1p36.22	Deletion
MLL	11q23.3	Deletion
EIF2C4 (AGO4)	1p34.3	Deletion
HNRNPN	1q44	Gain
DNAJC16	1p36.21	Deletion
LCK	1p35.1	Deletion

Table 3.2: Top 10 genes identified through ICON looking at % 17q gain, expression in the Th-MYCN mice and survival.

Gene	%gain	survival	Th-MCYN	Combined
BRIP1	78	0.28	1.019	21.668
INTS2	78	0.09	0.53	21.56
KPNA2	78	0.12	0.33	21.56
BIRC5	77	0.35	1.24	21.53
TK1	77	0.23	1.07	21.51
PTRH2	78	0.23	0.25	21.5
SMARCD2	78	0.02	0.44	21.48
LIMD2	78	0.03	0.35	21.47
PYCR1	77	0.21	0.57	21.46
TSEN54	77	0.21	0.26	21.42

BRIP1 knock down affects proliferation, apoptosis and cell cycle in neuroblastoma cells

To understand the role of BRIP1 in the development of neuroblastoma, we first performed a series of functional tests. Knock down experiments with 2 different hairpins targeting BRIP1 in neuroblastoma cell lines IMR-32 (*MYCN* amplified) and SH-SY5Y (*MYCN* non-amplified) were performed. For both shRNAs around 70% knock down was achieved (Figure 3.2A-B, Supplemental Figure 3.1A-B). Using the caspase-Glo assay we demonstrated increased apoptotic rates for the transduced cell lines versus controls after 72h (Figure 3.2C, Supplemental Figure 3.1C). Colony forming capacity of the BRIP1 depleted cells was dramatically reduced after BRIP1 knock down after 2 weeks (Figure 3.2D, Supplemental Figure 3.1D). Finally, cell cycle analysis showed a perturbed pattern with increased G1 phase arrested cells upon BRIP1 knock down as compared to the controls (Figure 3.2E, Supplemental Figure 3.1E). Collectively, these data indicate that neuroblastoma cells are dependent on high BRIP1 levels.

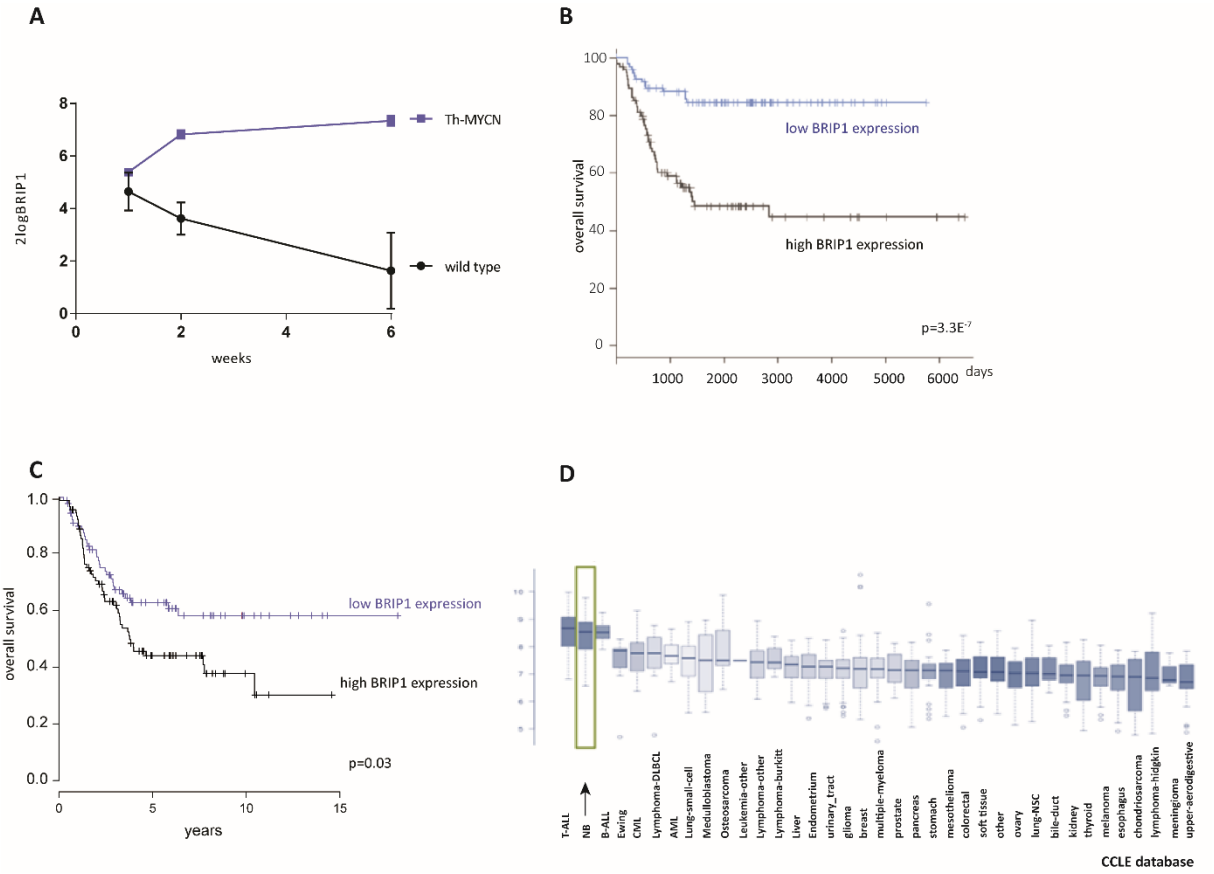

Figure 3.1:BRIP1 as a new cooperative oncogene in neuroblastoma development. (A) Dynamic upregulation of *Brip1* during tumor formation. Expression of *Brip1* is upregulated during tumor formation as is seen in hyperplastic ganglia of Th-MYCN mice, starting to develop tumors from 6 weeks after birth. In contrast, *Brip1* is downregulated in wild type mice. Error bars represent the standard deviation of 4 biological replicates. (B) Kaplan-Meier survival plot of *BRIP1* expression in 283 neuroblastoma patients. Low expression of *BRIP1* is significantly associated with better survival ($p=3.3E^{-7}$). (C) Kaplan-Meier curve within the subset of neuroblastoma stage 4 tumors. Low expression of *BRIP1* is correlated with better survival (p=0.03). (D) Expression of *BRIP1* in the cancer cell line encyclopedia database. *BRIP1* expression is the second highest in neurobastoma cell lines, highest expression is observed in T-ALL cell lines.

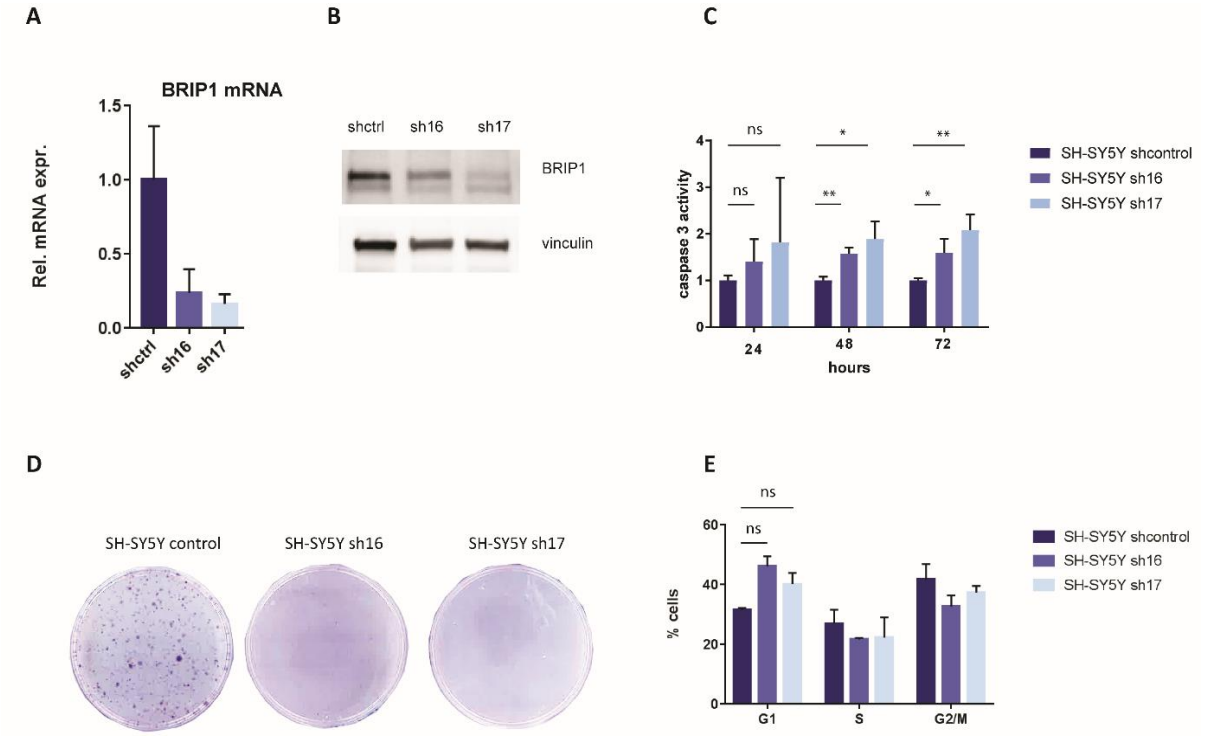

Figure 3.2: BRIP1 knock down affects apoptosis, colony forming capacity and cell cycle in neuroblastoma cells. (A) SH-SY5Y cells were transduced with shRNA targeting *BRIP1*, followed by quantitative RT-PCR assessment of *BRIP1* mRNA levels shown relative to the level in cells transduced with a scrambled shRNA. Error bars represent the standard error of mean (technical duplicates) (B) Corresponding western blot analysis of BRIP1 protein levels upon BRIP1 knock down. (C) Caspase glo assay in SH-SY5Y cells measuring caspase 3 activity upon BRIP1 knock down, error bars represent standard deviation of 3 biological replicates (D) Colony formation assays using SH-SY5Y cells depleted for BRIP1 compared to controls. Representative images of 3 independent experiments. (E) Cell cycle analysis in control cells and cells reduced for *BRIP1* .Error bar represent standard deviation of 2 biological replicates.

High BRIP1 expression accelerates neuroblastoma development in zebrafish

To corroborate our initial findings, we sought *in vivo* evidence for the oncogenic role of BRIP1 in MYCN driven neuroblastoma formation. To this end, we did forced overexpression of BRIP1 in MYCN overexpressing sympathetic progenitor cells in a stable *tg(dβh:EGFP-MYCN)* zebrafish line. First, we performed mosaic injection of *dβh-BRIP1* into stable

conditional *tg(dβh:EGFP-MYCN)* overexpressing zebrafish embryos and subsequently monitored tumor formation in two independent cohorts (10 and 8 *tg(dβh:BRIP1)* zebrafish, 52 and 38 *tg(dβh:EGFP-MYCN)* zebrafish and 33 and 30 *tg(dβh:EGFP-MYCN; dβh:BRIP1)* zebrafish). While *tg(dβh:EGFP-MYCN)* transgenic fish develop tumors as of week eleven on[17] reaching a penetrance of 22%, double transgenic *tg(dβh:EGFP-MYCN; dβh-BRIP1)* fish develop the first tumors earlier at week 9 and reach a higher penetrance of 60% (Figure 3.3A).The histopathology of the tumors was analyzed using H&E staining, and showed the expected large blue round cell typically observed in embryonal undifferentiated tumors (Figure 3.3B).

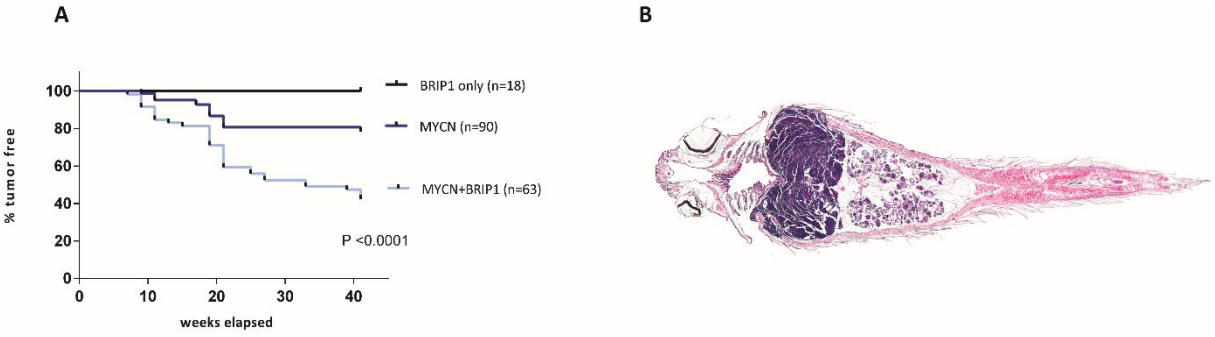

Figure 3.3: Overexpression of *dβh-BRIP1* into *tg(dβh:EGFP-MYCN)* results in the acceleration of neuroblastoma tumor formation and increases tumor penetrance. (A) Tumor free survival of *tg(dβh:EGFP-MYCN), tg(dβh:BRIP1)* and *tg(dβh:EGFP-MYCN; dβh:BRIP1)* zebrafish. (B) immunohistochemistry of *tg(dβh:EGFP-MYCN; dβh:BRIP1)* zebrafish.

BRIP1 controls replication stress to maintain tumor genome integrity

BRIP1 is one of the many Fanconi anemia genes acting in concert with other binding partners, including BRCA1[20]. BRIP1 has been reported to be implicated in multiple functions related to replicative stress control including control of both CHK1 signaling and homologous DNA repair versus translesion DNA synthesis, promoting replication fork stability, recovery and restart, unwinding of stable G-quadruplex DNA structures and dissociation of RNA:DNA (R-loops) hybrids ahead of replication[21].

In order to confirm the need for elevated BRIP1 levels to control elevated replicative stress levels in rapidly dividing neuroblastoma cells, we evaluated the effect of reduced BRIP1 levels on phosphorylated RPA (pRPA, S33) on western blot. RPA decorates ssDNA and pRPA

is typically induced upon replicative stress as part of the activation of the DNA damage response ATR/CHK1 pathway and therefore considered as reliable marker for replicative stress induction. As expected, strongly upregulated levels of pRPA were observed following BRIP1 knock down in neuroblastoma cells on both western blots (Figure 3.4A). A second assay to monitor increased replicative stress is based on DNA combing and allows to visualize several aspects of DNA replication and fork dynamics. To explore this, DNA combing assays were performed in the presence and absence of hydroxy urea (HU), a well-known compound that induces replicative stress through blocking ribonucleotide reductase activity causing depletion of the nucleotide pool. Combined BRIP1 knock down and exposure to HU significantly increased replication fork stalling in keeping with the role of BRIP1 in control of replicative stress and dependency of neuroblastoma cells to high BRIP1 levels (Figure 3.4B-C, Supplementary Figure 3.2). Interestingly, reduced BRIP1 levels also induced increased pCHK1 levels, suggesting that CHK1 signaling is still intact and elevated upon BRIP1 knock down (Figure 3.4A).

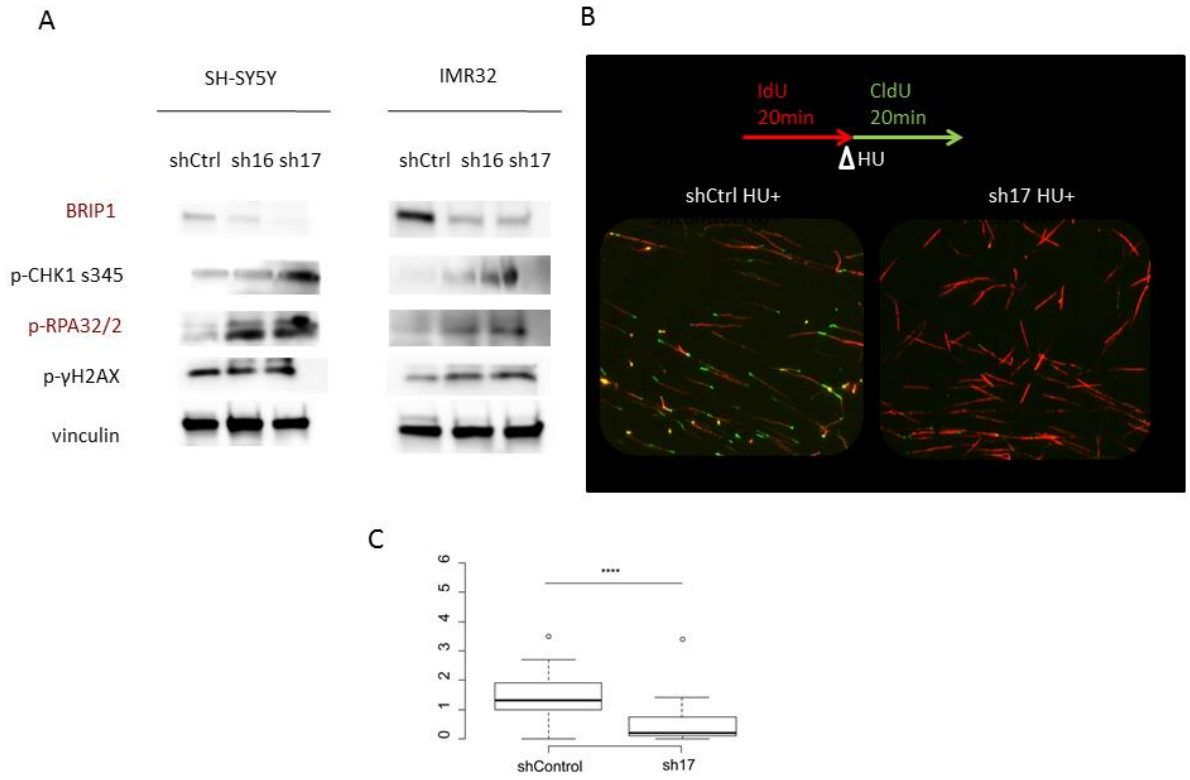

Figure 3.4: BRIP1 controls replicative stress in the neuroblastoma tumor genome. (A) western blot analysis of phospho CHK1 (s345), phospho RPA32/RPA2 (S33), and γH2AX in SH-SY5Y and IMR-32 cells upon BRIP1 knock down. (B) DNA combing analysis in IMR-32 cells with HU treatment. (C) Analysis of replication fork stalling in IMR-32 cells upon treatment of HU and BRIP1 knock down, p-values were calculated using paired t-test. For each group, the median (horizontal line), the interquartile range (box), and the upper and lower range of the data (whiskers) are shown.

BRIP1 promotes maintenance of genomic stability

In cells undergoing high chronic increased levels of replicative stress stalled replication forks, the replisome dissociates from the fork leading to fork collapse. Collapsed forks with longer stretches of single strand DNA are prone to double strand breaks and causing genomic instability. While this might initially contribute to the tumor initiation process, chronic replicative stress may become detrimental for rapidly dividing cancer cells. To avoid this, cancer cells can become addicted to hyperactivated DNA damage response for their survival.

In order to better understand the functional role of BRIP1 in neuroblastoma cells, we first tested yH2AX levels in IMR-32 cells undergoing increased replicative stress levels upon

exposure to HU and indeed could demonstrate elevated levels of DNA damage (Figure 3.5A-B). Next, we also performed RNA sequencing upon BRIP1 knock down in neuroblastoma cell lines IMR-32 and SH-SY5Y and observed cell cycle and DNA damage repair as major GO term for gene functions affected upon BRIP1 downregulation, in keeping with its presumed function in DNA repair (Figure 3.5C).

Several recent studies have explored the protein interaction network at the DNA replication fork under normal conditions or replicative stress. From this, it became evident that a large number of proteins are implicated. In a comparison of proteins binding to nascent DNA at normal, stalled or collapsed forks, increased BRIP1 activity and interaction was detected at collapsed forks[22]. In a first step to explore the BRIP1 interactome in more detail in the context of neuroblastoma cells, IP-MS is currently ongoing.

BRCA1 and other members of the FA- pathway are highly upregulated and possibly co-regulated with BRIP1

BRIP1 is known to interact with BRCA1 to execute several of the above mentioned functions. Correlation analysis using R2 for a large neuroblastoma tumor set (283 samples) showed very high level of correlation in expression levels for BRIP1 and BRCA1 (Figure 3.6A). In keeping with this finding, like BRIP1, BRCA1 is as expected also very high expressed in neuroblastoma (CCLE, R2, ..) and also linked to poor survival (Figure 3.6 B-C). In view of this observation, the important role of BRIP1 in replication fork protection and repair and the recently emerging role for the activated Fanconi anemia (FA) pathway in stabilizing replication forks and protection from collapse, we further investigated the expression levels of the FA-pathway in different stages of the neuroblastoma development. Overall, for all/most FA-genes, significant elevated to very high levels of expression were observed (Supplemental Figure 3.3) and almost all of them, except PALB2, correlated with poor survival (Supplemental Figure 3.4), suggesting an overall activation of the FA-pathway in neuroblastoma.

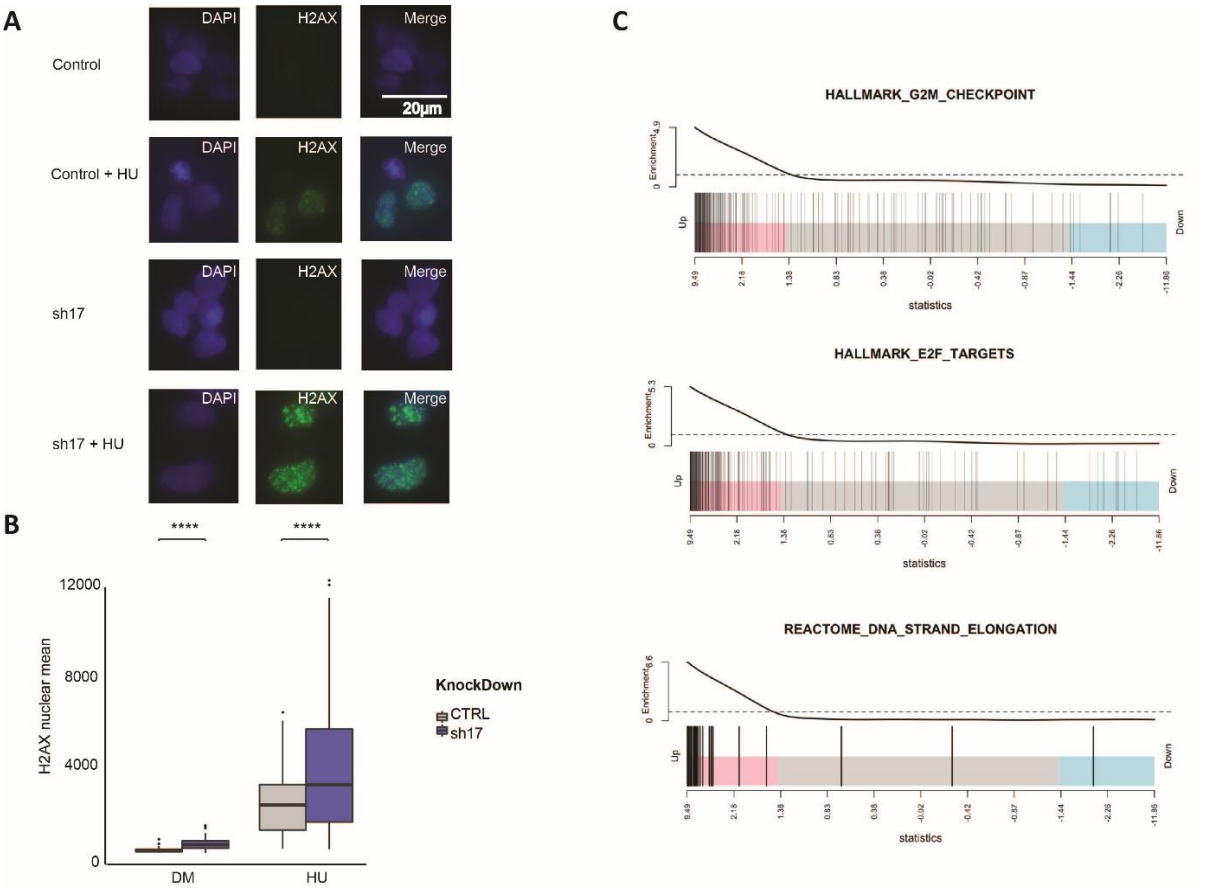

Figure 3.5 BRIP1 maintains genome integrity. (A) Immunofluorescence of γH2AX in control IMR-32 neuroblastoma cells with and without HU treatment and IMR-32 cells depleted for BRIP1 with and without treatment with HU. (B) Quantification of γH2AX spots described in (A), γH2AX is significantly increased in BRIP1 knock down cells treated with HU. The median (horizontal line), the interquartile range (box) and the upper and lower range of the data (whiskers) are shown (n= 2 biological replicates). (C) Important genesets to be found enriched upon knock down of BRIP1 in IMR-32 and SH-SY5Y cells. .

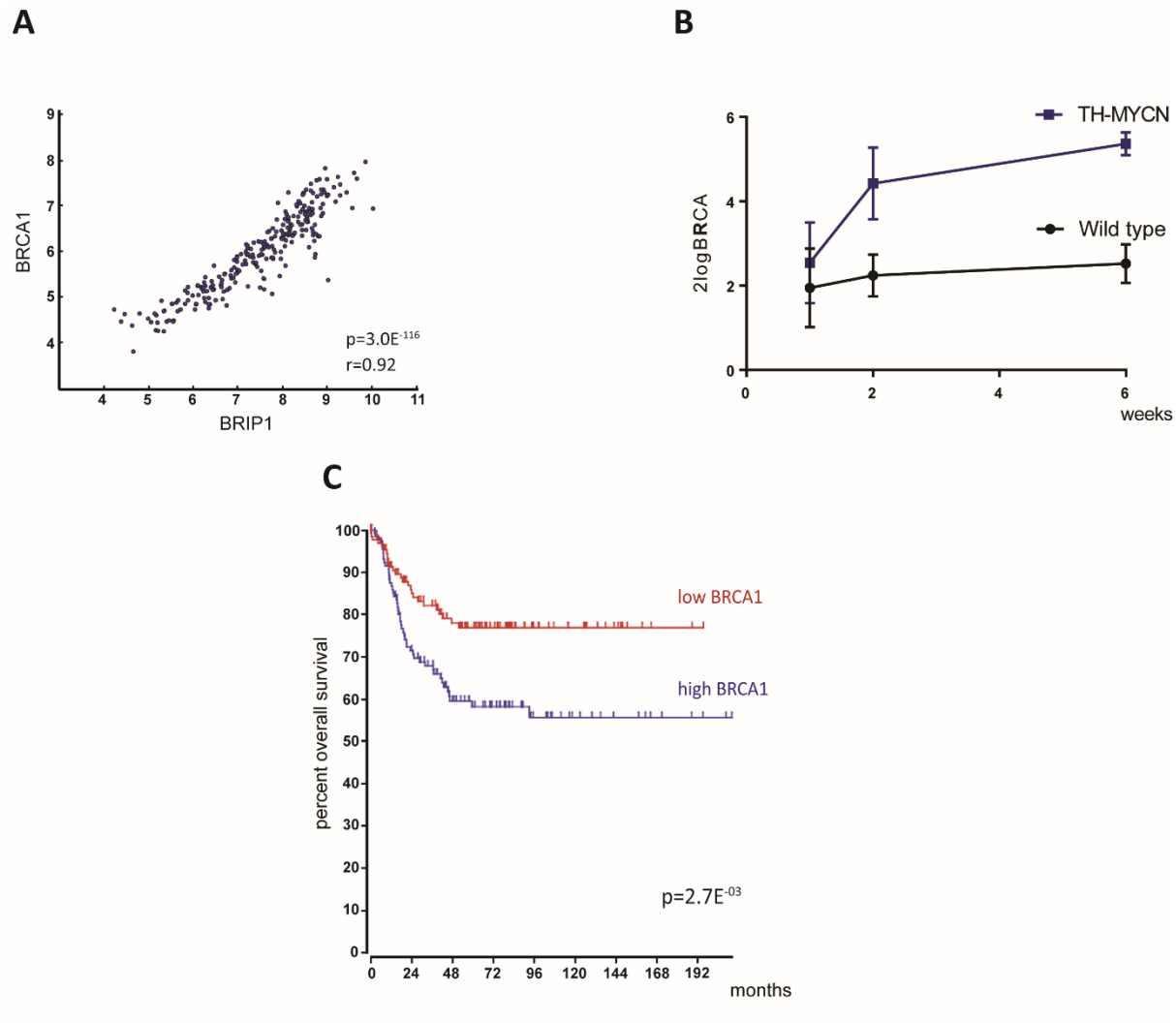

Figure 3.6: BRCA1 is highly upregulated in neuroblastoma and is correlated with BRIP1. (A) correlation plot of *BRCA1* and *BRIP1*. R-value= 0.92, P=value= $3E^{-116}$. (B) Dynamic upregulation of *Brca1* during tumor formation. Expression of *Brca1* is upregulated during tumor formation as is seen in hyperplastic ganglia of Th-MYCN mice, starting to develop tumors from 6 weeks after birth. In contrast, *BRCA1* is downregulated in wild type mice. Error bars represent standard deviation of 4 biological replicates. (C) Kaplan-Meier survival plot of 283 NB patients of *BRCA1* expression. High expression of *BRCA1* is significantly associated with poor survival

CNAs act as transcriptional amplifiers for FOXM1 target genes including BRIP1

While copy number changes have been shown to collectively install an oncogenic cellular state driving a hallmark phenotype in ependymoma, to what extent transcription factors controlling expression of these genes has not been addressed so far. First, we investigated whether BRIP1 was regulated by FOXM1 in neuroblastoma as BRIP1 was previously shown to be a *bona fide* target of this transcription factor[23]. To explore this we performed lentiviral knock down of FOXM1 in the neuroblastoma cell line IMR-32 and could indeed observe downregulation of BRIP1 upon FOXM1 depletion (Figure 3.7A-B).

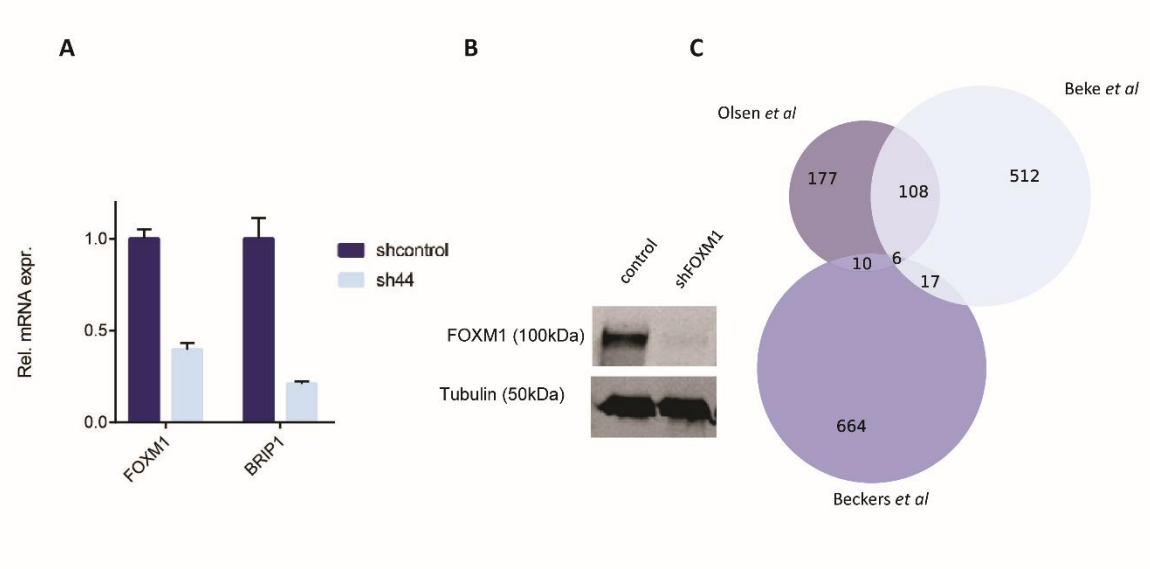

Figure 3.7: BRIP1 is a downstream target of FOXM1. (A) IMR-32 cells were transduced with shRNA targeting *FOXM1*, followed by quantitative RT-PCR assessment of *FOXM1* and *BRIP1* mRNA levels shown relative to the level in cells transduced with a scrambled shRNA. Error bars represent the standard error of mean (technical duplicates) (B) Corresponding western blot analysis of FOXM1 levels (C) Venn diagram showing the overlap on 17q genes in the study of Olsen *et al*, Beke *et al*[24], and Beckers *et al*[14]. genes included in triple overlap are *BRCA1*, *TOP2A*, *BRIP1*, *BIRC5*, *SPAG5* and *PRR11*

Next, we looked whether previously identified FOXM1 target genes were located on 17q and also generated a list of human 17q genes that were upregulated during Th-MYCN tumor formation in mice, either through an established mouse model[14] or based on a novel neural crest derived model system (Olsen *et al.* Oncogene, accepted) and downregulated upon inhibition of FOXM1[24]. Remarkably, several of the top regulated FOXM1 target genes

including TOP2A, BIRC5 and BRCA1 were identified (Figure 3.7C). Further testing of dosage sensitivity for these genes is ongoing as well as their regulation through FOXM1 in neuroblastoma cells. Taken together, these data strongly suggest that FOXM1, a known important mediator of the MYCN driven oncogenic transformation of fetal neuroblasts (Olsen et *al.* Oncogene, accepted), controls the expression of several dosage sensitive 17q genes which are canonical target genes implicated in DNA repair (or more specifically replicative stress resistance) and G2/M transition located. In other words, one can envision a mechanism through which 17q gain acts as a genomic amplifier for FOXM1 target genes implicated in the MYCN/FOXM1 controlled process of neuroblastoma formation. Therefore, we propose FOXM1 as a major novel drug target for children with high risk neuroblastoma.

Discussion:

Chromosome 17q gain is the most frequent genetic alteration occurring in neuroblastoma while, except for *ALK*, mutations are rare in this tumor thus offering limited targets for precision oncology. Recent work in ependymoma has shown that large chromosomal imbalances can impact on gene expression levels of multiple oncogenes and tumor suppressor genes and that these broad genomic driven multiple gene dosage effects can impact on a given cellular state contributing to the tumor phenotype.

Using a data mining driven approach, employing copy number and gene expression data from human neuroblastomas in combination with transcriptome data from dynamic regulation of gene expression in mouse neuroblastomas, we identified *BRIP1*, located on chromosome 17q23, as a cooperative oncogene in neuroblastoma oncogenesis. The gain-of function role for *BRIP1* is unexpected given its well established tumor suppressor role as member of the Fanconi anemia complex and partner of the well-known *BRCA1* tumor suppressor gene[13,20,25,26]. BRIP1 therefore joins the growing list of genes that can act both as oncogene and tumor suppressor depending on timing and cellular context, such as *NOTCH1* and *EZH2* [27,28]. Reduction of BRIP1 levels in neuroblastoma cells drastically impacted on proliferation, increased apoptosis and blocked cell cycle progression. Forced overexpression of *dβh-BRIP1* into the *tg(dβh:EGFP-MYCN)* zebrafish resulted in acceleration of tumor onset and an increase of tumor penetrance confirming its proposed role as an oncogene.

The BRIP1 protein can interact with BRCA1[20] and, either in combination with BRCA1, or independently, acts to preserve the integrity of the genome. BRIP1 is required for homologous recombination-mediated double strand break repair, the execution of the G2/M cell cycle checkpoint[29] and for normal progression through S phase by assisting in the resolution of stalled replication forks[30], a phenomenon called replicative stress. Given that increased replicative stress can result in DNA damage and genome instability[31], we wondered whether upregulation of *BRIP1* is required to protect neuroblastoma genome integrity. Knock down of *BRIP1* in neuroblastoma cells resulted in the upregulation of the ATR-CHK1 pathway, indicative for replicative stress. While contradictory at first sight, it has been shown that excessive replicative stress can be fatal for cancer cells. In fact, replicative stress is a double edged sword: on the one hand it can lead to genomic instability and

promote tumorigenesis, while on the other hand replicative stress also represents an Achilles heel of the cancer cell since excessive replicative stress levels can be fatal to the cancer cell forcing it into apoptosis. In keeping with this latter aspect it is of interest that in mice an extra copy of *CHK1* can predispose to cancer, which was shown to be associated with a reduction in the level of replicative stress induced by oncogenes[32]. By performing RNA sequencing upon BRIP1 knock down we observed enrichment for cell cycle and DNA replication, further strengthening our hypothesis that overexpression of BRIP1 is necessary to restrain replication stress observed by the tumor genome.

In conclusion, we could show for the first time that BRIP1 is an important cooperative oncogene for the development of neuroblastoma. Moreover, we show that BRIP1 creates a replicative resistance stress cell state necessary for maintaining the neuroblastoma tumor genome.

References:

1. Maris JM: Recent advances in neuroblastoma. N Engl J Med 362:2202-11, 2010
2. Monclair T, Brodeur GM, Ambros PF, et al: The International Neuroblastoma Risk Group (INRG) staging system: an INRG Task Force report. J Clin Oncol 27:298-303, 2009
3. George RE, Sanda T, Hanna M, et al: Activating mutations in ALK provide a therapeutic target in neuroblastoma. Nature 455:975-8, 2008
4. Chen Y, Takita J, Choi YL, et al: Oncogenic mutations of ALK kinase in neuroblastoma. Nature 455:971-4, 2008
5. Molenaar JJ, Koster J, Zwijnenburg DA, et al: Sequencing of neuroblastoma identifies chromothripsis and defects in neuritogenesis genes. Nature 483:589-93, 2012
6. Valentijn LJ, Koster J, Zwijnenburg DA, et al: TERT rearrangements are frequent in neuroblastoma and identify aggressive tumors. Nat Genet 47:1411-4, 2015
7. Peifer M, Hertwig F, Roels F, et al: Telomerase activation by genomic rearrangements in high-risk neuroblastoma. Nature 526:700-4, 2015
8. Cheung NK, Zhang J, Lu C, et al: Association of age at diagnosis and genetic mutations in patients with neuroblastoma. JAMA 307:1062-71, 2012
9. Bown N: Neuroblastoma tumour genetics: clinical and biological aspects. J Clin Pathol 54:897-910, 2001
10. Bown N, Cotterill S, Lastowska M, et al: Gain of chromosome arm 17q and adverse outcome in patients with neuroblastoma. N Engl J Med 340:1954-61, 1999
11. Beroukhim R, Mermel CH, Porter D, et al: The landscape of somatic copy-number alteration across human cancers. Nature 463:899-905, 2010
12. Mohankumar KM, Currle DS, White E, et al: An in vivo screen identifies ependymoma oncogenes and tumor-suppressor genes. Nature Genetics 47:878-+, 2015
13. Levitus M, Waisfisz Q, Godthelp BC, et al: The DNA helicase BRIP1 is defective in Fanconi anemia complementation group J. Nature Genetics 37:934-935, 2005
14. Beckers A, Van Peer G, Carter DR, et al: MYCN-targeting miRNAs are predominantly downregulated during MYCN-driven neuroblastoma tumor formation. Oncotarget 6:5204-5216, 2015
15. Schwab RAV, Niedzwiedz W: Visualization of DNA Replication in the Vertebrate Model System DT40 using the DNA Fiber Technique. Jove-Journal of Visualized Experiments, 2011
16. Subramanian A, Tamayo P, Mootha VK, et al: Gene set enrichment analysis: A knowledge-based approach for interpreting genome-wide expression profiles. Proceedings of the National Academy of Sciences of the United States of America 102:15545-15550, 2005
17. Zhu S, Lee JS, Guo F, et al: Activated ALK collaborates with MYCN in neuroblastoma pathogenesis. Cancer Cell 21:362-73, 2012
18. Akavia UD, Litvin O, Kim J, et al: An integrated approach to uncover drivers of cancer. Cell 143:1005-17, 2010
19. Barretina J, Caponigro G, Stransky N, et al: The Cancer Cell Line Encyclopedia enables predictive modelling of anticancer drug sensitivity. Nature 483:603-607, 2012
20. Cantor SB, Bell DW, Ganesan S, et al: BACH1, a novel helicase-like protein, interacts directly with BRCA1 and contributes to its DNA repair function. Cell 105:149-160, 2001

21. Brosh RM, Jr., Cantor SB: Molecular and cellular functions of the FANCJ DNA helicase defective in cancer and in Fanconi anemia. Front Genet 5:372, 2014

22. Sirbu BM, McDonald WH, Dungrawala H, et al: Identification of Proteins at Active, Stalled, and Collapsed Replication Forks Using Isolation of Proteins on Nascent DNA (iPOND) Coupled with Mass Spectrometry. Journal of Biological Chemistry 288:31458-31467, 2013

23. Monteiro LJ, Khongkow P, Kongsema M, et al: The Forkhead Box M1 protein regulates BRIP1 expression and DNA damage repair in epirubicin treatment. Oncogene 32:4634-4645, 2013

24. Beke L, Kig C, Linders JTM, et al: MELK-T1, a small-molecule inhibitor of protein kinase MELK, decreases DNA-damage tolerance in proliferating cancer cells. Bioscience Reports 35, 2015

25. Bridge WL, Vandenberg CJ, Franklin RJ, et al: The BRIP1 helicase functions independently of BRCA1 in the Fanconi anemia pathway for DNA crosslink repair. Nature Genetics 37:953-957, 2005

26. Levran O, Attwooll C, Henry RT, et al: The BRCA1-interacting helicase BRIP1 is deficient in Fanconi anemia. Nature Genetics 37:931-933, 2005

27. Radtke F, Raj K: The role of Notch in tumorigenesis: Oncogene or tumour suppressor? Nature Reviews Cancer 3:756-767, 2003

28. Hock H: A complex Polycomb issue: the two faces of EZH2 in cancer. Genes Dev 26:751-5, 2012

29. Yu XC, Chini CCS, He M, et al: The BRCT domain is a phospho-protein binding domain. Science 302:639-642, 2003

30. Kumaraswamy E, Shiekhattar R: Activation of BRCA1/BRCA2-Associated helicase BACH1 is required for timely progression through S phase. Molecular and Cellular Biology 27:6733-6741, 2007

31. Zeman MK, Cimprich KA: Causes and consequences of replication stress. Nat Cell Biol 16:2-9, 2014

32. Lopez-Contreras AJ, Gutierrez-Martinez P, Specks J, et al: An extra allele of Chk1 limits oncogene-induced replicative stress and promotes transformation. J Exp Med 209:455-61, 2012

Supplementary Figures:

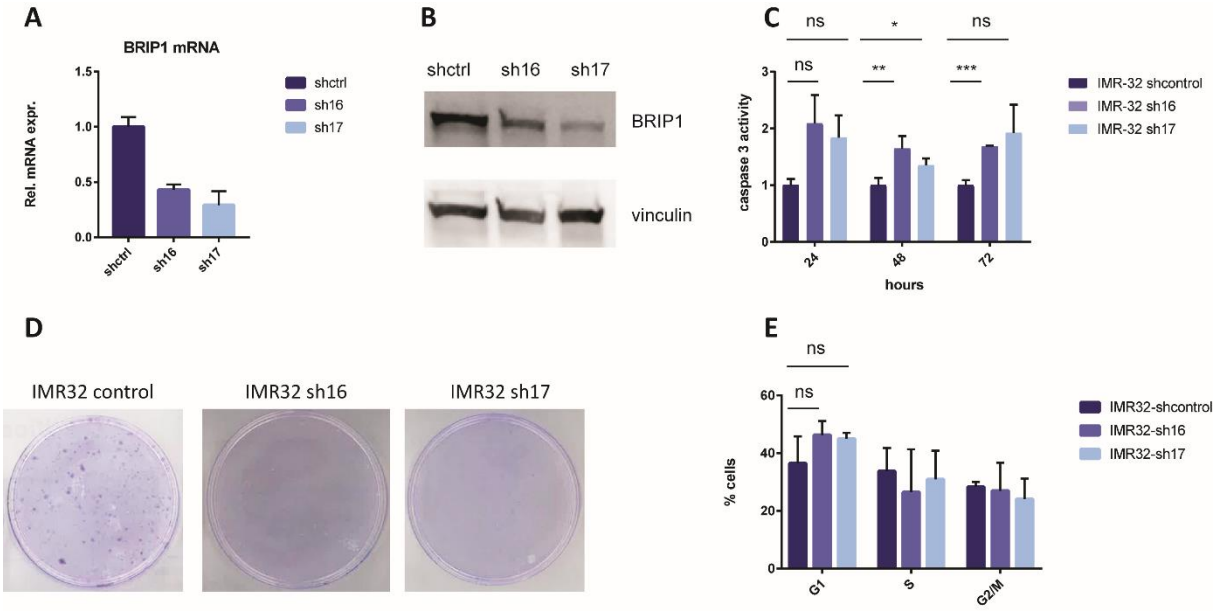

Supplementary Figure 3.1: *BRIP1* knock down affects apoptosis, colony forming capacity and cell cycle in neuroblastoma cells. (A) IMR-32 cells were transduced with shRNA targeting *BRIP1*, followed by quantitative RT-PCR assessment of *BRIP1* mRNA levels shown relative to the level in cells transduced with a scrambled shRNA. Error bars represent the standard error of mean (technical duplicates) (B) Western blot analysis of BRIP1 protein levels upon *BRIP1* knock down. (C) Caspase glo assay in IMR-32 cells measuring caspase 3 activity upon *BRIP1* knock down, error bars represent standard deviation of 3 biological replicates (D) Colony formation assays using IMR-32 cells depleted for *BRIP1* compared to controls. Representative images of 3 independent experiments. (E) Cell cycle analysis in control cells and cells reduced for *BRIP1* .Error bar represent standard deviation of 3 biological replicates.

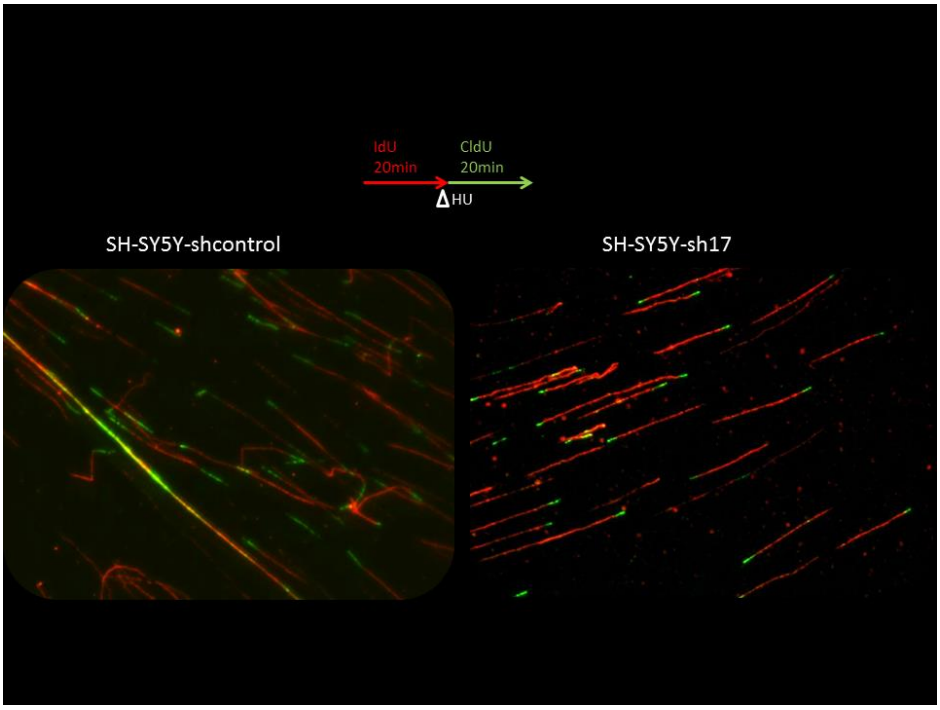

Supplementary Figure 3.2: DNA combing analysis in SH-SY5Y cells with HU treatment

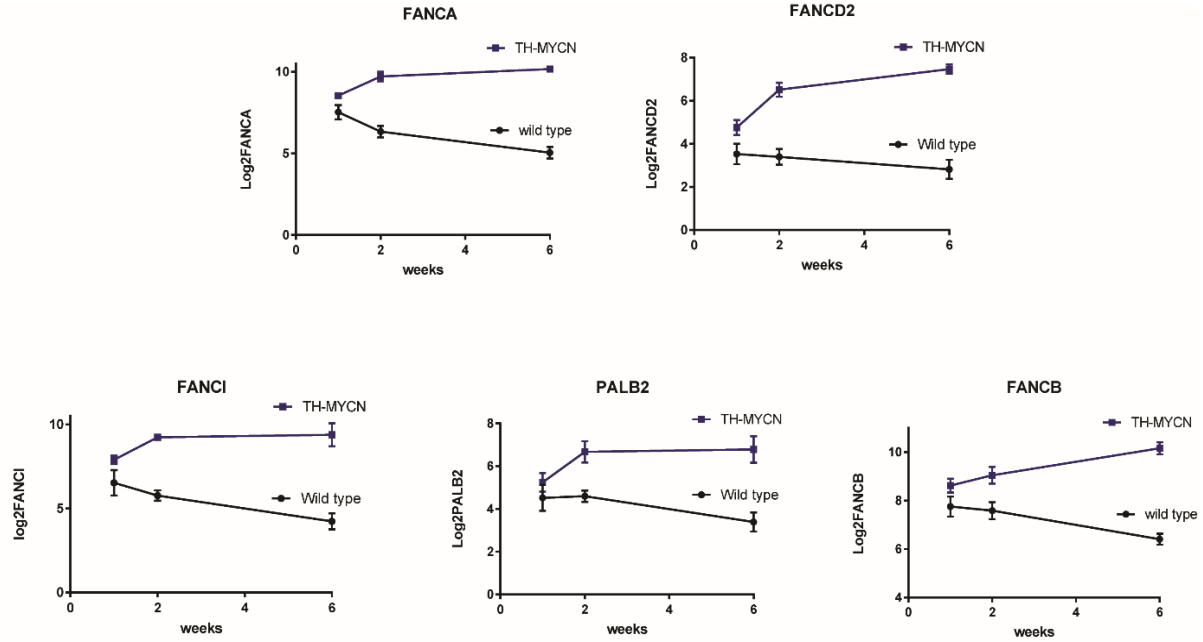

Supplementary Figure 3.3: Expression of FA genes during neuroblastoma development in mice.

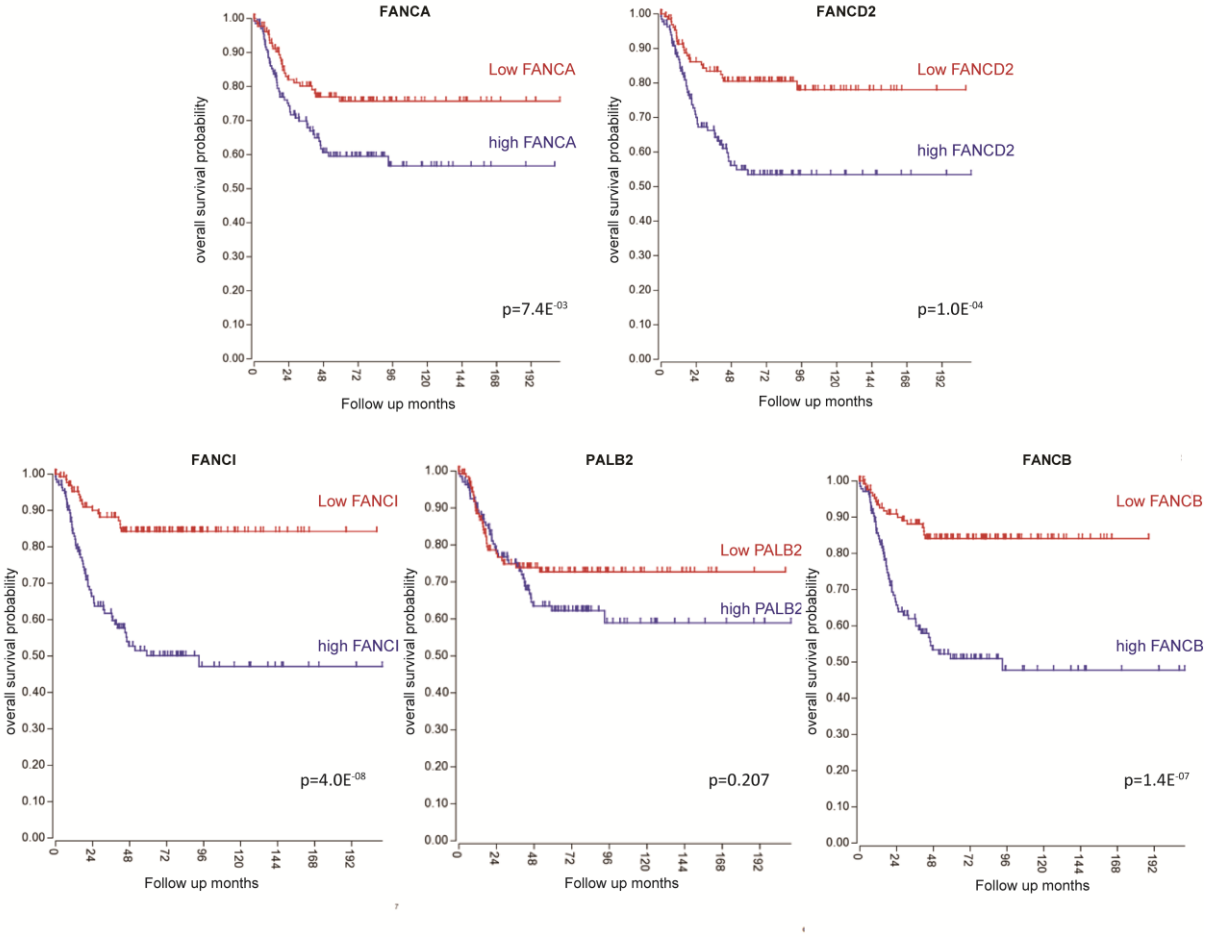

Supplementary Figure 3.4: Kaplan-Meier curves of several members of the FA pathway.

Chapter 4: A MYCN activated FOXM1 driven embryonal pathway defines therapy resistant neuroblastoma patients and marks FOXM1 as target for future drug screening

Authors: Suzanne Vanhauwaert, Sara De Brouwer, Bieke Decaesteker, Carina Leonelli, Pieter Mestdagh, Jo Vandesompele, Karen Sermon, Geertrui Denecker, Christophe Vanneste, Frank Speleman, Katleen De Preter

Paper submitted to Clinical Cancer Research

A MYCN activated FOXM1 driven embryonal pathway defines therapy resistant neuroblastoma patients and marks FOXM1 as target for future drug screening

Authors: Suzanne Vanhauwaert[1,2], Sara De Brouwer[1,2], Bieke Decaesteker[1,2], Carina Leonelli[1,2], Pieter Mestdagh[1,2], Jo Vandesompele[1,2], Karen Sermon[3], Geertrui Denecker[1,2], Christophe Vanneste[1,2], Frank Speleman[1,2], Katleen De Preter[1,2]

Affiliations:

1)Center for Medical Genetics (CMGG), Ghent University, Ghent, Belgium

2)Cancer Research Institute Ghent (CRIG), Ghent University, Ghent, Belgium

3)Research Group Reproduction and Genetics, Faculty of Medicine and Pharmacy, Vrije Universiteit Brussel, Laarbeeklaan 103, 1090, Brussels, Belgium.

Statement of translational relevance:

Despite intensive multimodal therapies, survival rates for aggressive neuroblastoma patients are still disappointingly low. In this study, we wanted to deeper explore whether an ESC derived expression signature could capture a stemness phenotype in neuroblastoma cells that is associated with therapy resistance. An ESC miRNA signature could be defined that allows to discriminate patients with worse survival outcome in the global cohort of neuroblastoma patients, but most interestingly also in a subset of high-risk tumors, i.e. stage 4 tumors without *MYCN* amplification. Analysis of the protein coding genes that are correlated with the ESC miRNA signature score in neuroblastoma patients, pointed at a FOXM1 driven cell cycle and DNA repair activation in therapy resistant tumors. These findings reveal new targets for molecular therapy of tumors where current treatment regimens fail.

Abstract:

Purpose: Chemotherapy resistance is responsible for high mortality rates in high-risk neuroblastomas. *MYCN* is a major oncogenic driver in neuroblastoma controlling pluripotency genes including LIN28B. Therefore, we hypothesized that enhanced embryonic stem cell (ESC) gene regulatory programs could mark tumors with increased risk for therapy failure enabling the selection of patients for novel therapy approaches.

Material and Methods: An ESC microRNA expression signature was established based on publically available data. In addition, an ESC mRNA signature was generated including the 500 protein coding genes with the highest positive correlation with the miRNA ESC signature score in 200 neuroblastoma tumors.

Results: High ESC miRNA signature scores were significantly correlated with poor neuroblastoma patient outcome in the global patient cohort and more importantly also within the subset of stage 4 tumors without *MYCN* amplification. In addition, in neuroblastoma tumors with *MYCN* amplification the ESC mRNA signature scores were significantly increased. Further data-mining identified FOXM1, member of the DREAM complex, as the major driver of the ESC mRNA signature score, controlling a large set of genes implicated in cell cycle control and DNA damage response. In addition, re-analysis of published data showed that MYCN transcriptionally activates FOXM1 in neuroblastoma cells.

Conclusion: A novel ESC miRNA signature score stratifies neuroblastomas with poor prognosis, enabling the identification of tumors that are therapy resistant. The finding that this signature is strongly FOXM1 driven, warrants for drug screens and drug design targeted at FOXM1 or key components controlling this pathway.

Introduction

Childhood cancers have been regarded as developmental disorders and differ in many aspects from adult cancers. Typically, most childhood cancers show low mutational burden[1] and present with a very immature phenotype. It is assumed that embryonal tumors such as medulloblastoma, Wilms' tumor, embryonal rhabdomyosarcoma and neuroblastoma arise from immature progenitor cells that still have a high level of stemness characteristics[1]. In these immature cells, disruption of normal early developmental pathways can cause differentiation arrest creating pre-malignant lesions that can subsequently develop to full blown tumors.

Neuroblastomas that arise mainly in very young children with a median average age of diagnosis of 17 months[1], are believed to emerge from cells of the developing adreno-sympathetic nervous system[1]. In an earlier study, we provided support for this hypothesis through analysis of human fetal adrenal neuroblast transcriptomes which showed close similarity to malignant neuroblastoma gene expression profiles[2]. Also the few neuroblastoma driver genes that were identified so far, including *MYCN*, *ALK*, *PHOX2B* and *LIN28B*, are all involved in early stages of the sympathetic nervous system development[3-5] with both LIN28B and MYCN implicated as major drivers of stemness[6]. Novel therapies targeting these neuroblastoma driver genes such as ALK inhibitors and inhibitors of the BRD4-MYCN-promotor interaction are already emerging[7]. While these developments are promising, outcome of high-risk neuroblastoma patients is still disappointingly low and insights into therapy resistance mechanisms and new venues for targeting these resistant cells are needed. High treatment failure rates could possibly be explained by the stemness features of cancer initiating cells, including enhanced DNA repair capacity[8]. Therefore, scrutinizing in more detail the stemness features of pediatric cancers may provide new insights into therapy resistance and may also offer novel targets for therapeutic intervention.

In this study, we explored the stemness features of neuroblastoma tumor cells using an *in silico* analysis starting from a normal embryonal stem cell driven miRNA signature. This approach was based on three important concepts. First, several hallmark characteristics of stem cells, including the capacity to self-renewal and differentiation are mimicked in the highly proliferative cancer cells, suggesting that similar regulatory networks are active in

normal stem cells and cancer stem cells[9]. Secondly, miRNAs are key players in the tight control of (stem) cell fate[10]. These small non-coding RNA molecules play a crucial role in stem cell pluripotency, control of self-renewal, lineage-specific differentiation, and cell reprogramming[10]. The miRNA pathway has been shown to be crucial in embryonic development and in embryonic stem cells (ESCs), as shown by Dicer knockout analysis[11]. Specific patterns of miRNAs have been reported to be expressed only in ESCs and in early phases of embryonic development. Hence, regulatory networks tightly controlled by miRNAs can be assumed to play important roles in normal and cancer stem cell biology. Third, miRNA expression patterns can distinguish tumor types and tissue types better than mRNA expression patterns[12]. From these observations we anticipated that miRNAs could act as a proxy to capture stem cell features in neuroblastoma cells.

To this end, we used an unique *in silico* approach to investigate the stemness characteristics in neuroblastoma tumor cells and obtained three important results: (1) a 60 miRNA ESC signature could discriminate patients with poor survival within a subset of the high-risk neuroblastoma patients; (2) biological function enrichment analysis on the coding genes correlated with the miRNA ESC signature score in neuroblastoma revealed increased DNA repair mechanisms in tumors with high stem cell capabilities driven by the FOXM1 transcription factor, which was further confirmed by FOXM1 knock down experiments; (3) analysis of transcriptional changes after FOXM1 knock-down in neuroblastoma cells and re-analysis of published datasets strongly supports the contribution of FOXM1 to the MYCN driven tumor and stemness phenotype of neuroblastoma cells. In view of these findings, our data should fuel renewed efforts for identifying novel on target compounds to block FOXM1 activation in high-risk neuroblastomas.

Materials & Methods

Re-analysis of publically available datasets

In this study, we reanalyzed several published expression datasets: miRNA expression data of different embryonal stem cell lines and differentiated tissue (GSE34199)[13-17], 2) miRNA expression data of 200 neuroblastoma tumor samples[18], 3) matching mRNA expression profiling data of the same 200 samples (GEO85047), 4) RNA sequencing data of 498 neuroblastoma tumors (GSE62564, GSE49711)[19], 5) miRNA and mRNA expression data of the Th-MYCN neuroblastoma progression model (E-MTAB-2618)[20], 6) miRNA expression data of the different neuroblastoma mouse models[5,20], 7) mRNA expression data of the shMYCN knock-down system (GSE39218)[21] , 8) mRNA expression data of JQ1 and OTX015 treated neuroblastoma cell lines (GSE43392, E-MTAB-3672)[22,23], 9) mRNA expression profiling data of siFOXM1 treated breast cancer cells (GSE55204, GSE25741)[24,25] and shFOXM1 treated glioma cells (GSE63963)[26], 10) mRNA expression profiling data of glioma, prostate, and breast cancer cell lines after pharmacological inhibition of FOXM1 with siomycin A and FDI-6 (GSE50227, GSE36531, GSE58626)[27-29], 11) data of the cancer cell line encyclopedia[30] and 12) medulloblastoma mRNA expression data (GSE30530)[31]. The R-package GEOquery and ArrayExpress were used to download the publically available (normalized) data directly into the R-environment. ChIP-seq data of MYCN and H3K27ac in BE2C, Kelly, NGP and SHEP21N were downloaded from ArrayExpress (E-GEOD-80154) and converted to bigwig files to visualize the ChIP tracks in IGV.

miRNA profiling of normal neuroblasts and human embryonic stem cell lines

miRNA expression of 8 embryonal stem cell lines[32] and 7 normal neuroblast samples[2] was profiled and normalized as previously described[33] (*data will be submitted to a data repository*).

Data-mining and statistical analysis

We performed signature score analysis on both mRNA and miRNA expression data using a rank-scoring algorithm as described in[34]. In brief, for each tumor sample (mRNA or miRNA) expression values were transformed to ranks (a rank of 1 matching with the lowest

expressing gene). Next, rank scores for the signature genes were summed for each sample generating a signature score.

Correlation of the score with survival was tested using Kaplan-Meier plots and log-rank analysis by grouping the samples in 2 equal groups (score above or below the median value) (R-survival package). Comparison of signature scores or expression between groups of samples was done using the parametric t-test or non-parametric Mann-Whitney test (R-base package). Signature score and gene expression correlation analysis was performed using Pearson correlation analysis (R-base package). Gene set enrichment analysis (GSEA)[35] was performed using the version 5.2 geneset catalogue. Multivariate logistic regression analysis was performed on a subset of samples including only the patients that died of disease or survived for at least 3 years after diagnosis.

FOXM1 gene silencing through shRNA knock-down and verification of knock down by RT-qPCR and Western Blot analysis

ShRNA knock down for FOXM1 was achieved using MISSION shRNA (Sigma) TRCN0000015544. Viral production was performed with 15 µg of plasmid in 3 million HEK293TN cells using the calcium phosphate trans-lentiviral packaging system, according to the protocol provided by the manufacturer (Lifetechnologies). The viral particles were concentrated using the PEG-it virus precipitation protocol (System Biosciences) and afterwards transduced in the neuroblastoma cell line IMR-32.

24h after transduction the medium was refreshed and cells were selected with puromycin (0.5µg/ml). Cells were harvested for RNA 96h after transduction. RNA isolation was performed using the miRNeasy micro kit, according to the guidelines of the company (Qiagen, catalogue number 217084), including DNAse treatment on column (RNAse-free DNAse set, Qiagen, catalogue number 79254). cDNA synthesis was carried out using 500ng of RNA with the iScript cDNA synthesis kit (Bio-Rad, catalogue number 170-8891). RT-qPCR primers for FOXM1 (AGACACCCATTAAGGAAACG,TTTGTACTGGGCTGAAATCC) and reference genes HPRT1(TGACACTGGCAAAACAATGCA ,GGTCCTTTTCACCAGCAAGCT), YWHAZ(ACTTTTGGTACATTGTGGCTTCAA, CCGCCAGGACAAACCAGTAT), SDHA (TGGGAACAAGAGGGCATCTG, CCACCACTGCATCAAATTCATG) were designed using primerXL (www.primerXL.org). RT-qPCR reactions were performed in duplicate in a total volume of 5µl, including 2µl of cDNA and 3µl of ssAdvanced SYBR Green qPCR mastermix (Bio-Rad).

Cycling conditions were 95°C (15s) – 60°C (15s) – 72°C (60s) and 44 cycli. Data analysis was performed using the qBasePlus software (Biogazelle). Protein extraction was done via RIPA buffer and protein concentration was measured using the Lowry protein assay. Protein extracts were separated with SDS-PAGE, blotted on a nitrocellulose membrane and probed with antibodies against FOXM1 (1/1000 ; 5436S cell signaling), and β-actin (1/10000, A2228, Sigma-Aldrich). Proteins were detected with HRP-conjugated goat anti rabbit IgG antibody (1/15000, A27036, thermos fisher scientific) and developed with ChemiDoc-it imaging system (UVP).

Differential gene expression analysis by RNA sequencing of FOXM1 knock-down in neuroblastoma cells

Poly-A captured RNA library preparation was done on biological triplicates of FOXM1 knock-down and control samples, using the TruSeq stranded mRNA kit LT. Concentration was measured via qPCR using the Kapa Library Quantification Kit (Illumina) and 1.4pM was loaded on a NextSeq 500. The NextSeq 500 High Output V2 75 cycles kit was used for single end sequencing to obtain approximately 20 million reads for every sample.

Sample and read quality was checked with FastQC (v0.11.3). Reads were subsequently aligned to the human genome GRCh38 with STAR aligner (v2.5.2b). Final gene count values were obtained with RSEM (v1.2.31), which takes read mapping uncertainty into account.

Counts were normalized with the TMM method (R-package edgeR), followed by voom transformation and differential expression analysis with limma (R-package limma). Gene Set Enrichment Analysis (GSEA)[35] was performed on the list ordered according to differential expression statistic value (t).

ChIP-sequencing of MYCN and H3K27ac in neuroblastoma cell line CLB-GA

In addition to published ChIP-seq data, we also performed ChIP-seq in the non-MYCN amplified CLB-GA cell line. Chromatine immunoprecipitation for MYCN and H3K27ac was done in fifty million CLB-GA cells using 12.5 µg of MYCN-specific (Santa-Cruz, B8.4.B, sc-53993) and H3K27ac-specific (Abcam, ab4729) antibody according the ChIP-protocol described in[36]. DNA was subsequently adaptor ligated and amplified using the NebNext Ultra DNA Library Prep Kit (E7370S) and sequenced on the NextSeq500 using the NextSeq 500 High Output Kit V2, 75 cycles kit (Illumina). Raw reads were mapped to hg19 reference

genome using Bowtie2 and peakcalling was performed using MACS2. Bigwig files were generated to visualize the ChIP-seq tracks in IGV.

Information of the used neuroblastoma cell lines

The CLB-GA cell line was obtained from the lab of Valerie Combaret (Lyon, France).

The IMR-32 cell line was obtained from the lab of Rogier Versteeg (Amsterdam, The Netherlands).

All cell lines in our laboratory were screened upon arrival with the MycoAlert Detection Assay (cat nr. LT07-318, Lonza) and immediately expanded for freezing in order to assure Mycoplasma free cells as a stock. Routinely monthly random screenings were done, which were each time completely negative.

Both cell lines used in the paper (CLB-GA and IMR-32) were brought in culture, and passaged two times before starting the experiments. Cells were kept in culture for maximum 20 passages. After that: new cells were brought in culture.

All cell lines were routinely STR genotyped, to confirm the authenticity of the cell lines.

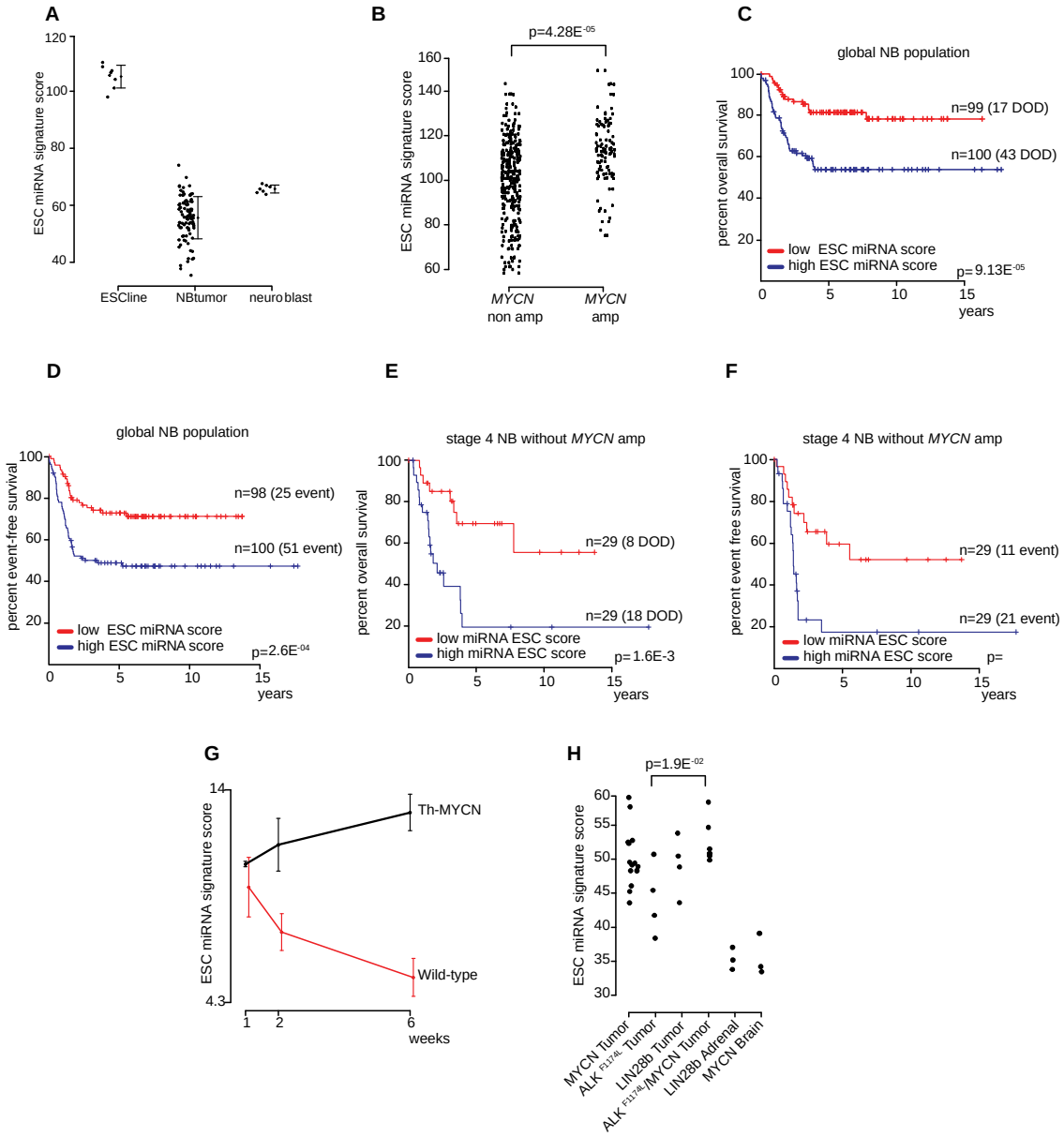

Figure 4.1: Identification of a ESC miRNA signature score that stratifies neuroblastoma patients within a subset of high-stage neuroblastoma.

(A)ESC miRNA signature scores in embryonic stem cells (ESC line)[32], neuroblastoma tumors (NB tumors)[18] and normal neuroblasts[2]. (B) ESC miRNA signature scores in MYCN non amplified neuroblastoma tumors (MNA) compared to MYCN amplified neuroblastoma tumors (MA). (C-D) Kaplan-Meier and log rank analysis of 200 neuroblastoma patients with a high or low ESC miRNA signature score (using median as cut-off). DOD, dead of disease. (E-F) Kaplan-Meier and log rank analysis within the subset of stage 4 MYCN non amplified patients. (H) ESC miRNA signature score during tumor development in Th-MYCN transgenic mice. (G) ESC miRNA signature scores for MYCN, ALK^{F1174L} and Lin28b neuroblastoma mice tumors and their normal counterparts (adrenal gland and brain tissue).

Results

Embryonic stem cell miRNA signature score analysis identifies patients with poor survival within a subset of high-risk neuroblastoma patients

In order to evaluate the stem cell features of neuroblastoma cells, we first established a robust miRNA embryonic stem cell (ESC) signature based on literature data. To this end, gene lists were retrieved from 4 published studies reporting on differential miRNA expression analysis of ESCs versus more differentiated cells (Supplemental Table 4.1)[14-17]. miRNA genes that were listed in at least 2 of the publications were included in the ESC signature (Table 4.1). A gene cluster with a well-known role in ESCs is the miR-302/367 cluster, of which all components are present in the signature. Using signature score analysis (see M&M), we could validate the signature in an independent dataset of ESCs with high miRNA signature scores for the ESC samples compared to differentiated somatic tissue (Supplemental Figure 4.1)[13] .

Next, we generated miRNA expression data of ESCs[32], normal neuroblasts and neuroblastoma tumor samples[2,18]. We confirmed high scores for the ESCs compared to those of neuroblastoma tumor samples (Figure 4.1A). The normal counterpart cells, i.e. the normal neuroblasts isolated from fetal adrenal glands, have ESC miRNA signature scores in the higher range of the scores identified in neuroblastoma tumors samples. The large dynamic range of scores in neuroblastoma tumors warranted us to evaluate whether this heterogeneous expression pattern could reflect tumor characteristics including *MYCN* status and patient survival. Indeed, tumors presenting with *MYCN* amplification have significantly higher signature scores than *MYCN* single copy tumors (t-test, p-value = 4.282e-05) (Figure 4.1B). In addition, Kaplan-Meier and log-rank analysis pointed at a significant correlation with survival, i.e. patients with higher scores have lower survival chances (Figure 4.1C and D). According to multivariate logistic regression analysis, this significant correlation is independent of the currently used risk markers, i.e. *MYCN* status, stage (stage 4 versus other stage) and age at diagnosis (below or above 1 year) (Odds' ratio 3.08, p=2.16E-2 for the signature score using median cut-off). More specifically, *MYCN* single copy stage 4 tumors with high ESC miRNA signature scores (above the median score) have extremely low survival probability, i.e. 19.6% overall survival at 5 years after diagnosis (95% confidence interval: 7.52%-51.1%) versus 69.5% (52.6%-91.9%) in tumors with low ESC miRNA signature score

(Figure 4.1E and F). This relation cannot be generalized to all other tumor types as we could not confirm this link in published miRNA expression datasets of ovarian cancer and glioblastoma (data not shown)[37,38].

Taken together, these data indicate that highly aggressive neuroblastoma cells in patients with ultra-high risk and very poor survival are enriched for a stemness ESC derived gene signature and that application of this signature could be helpful for early detection of patients for novel treatment strategies.

The ESC miRNA signature score is dynamically upregulated during MYCN driven tumor formation and is highest in the ALK^{F1174L}/MYCN double transgenic mice

In the tyrosine hydroxylase (Th)-MYCN neuroblastoma mouse model, a clear increase in the ESC miRNA signature score during tumor development from pre-neoplastic lesions in the ganglia at week 1 and 2 to full-blown tumors at week 6 after birth is observed (Figure 4.1H)[20]. Furthermore, Th-*MYCN*- and also dβh-iCre; LSL- *ALK^{F1174L}*-, and dβh-iCre; LSL-*LIN28B*-driven mice tumors are characterized by higher ESC miRNA signature scores compared to normal adrenal gland (Figure.4.1G)[5,39]. Interestingly, the ESC miRNA signature score in double transgenic mice tumors (*MYCN/ALK^{F1174L}*) is significantly higher than in *ALK^{F1174L}*-driven tumors (significant difference with p=1.905E-2), in concordance with shorter time to tumor appearance and thus more tumor aggressiveness in double transgenic mice compared to *ALK^{F1174L}*-transgenic mice.

Overall, these results generated in human and mice tumors show that a high ESC signature score is linked to higher tumor aggressiveness, in keeping with the observed poor survival in patients with tumors with high miRNA ESC score.

The ESC mRNA gene signature in neuroblastoma is highly enriched for FOXM1 driven cell cycle and DNA repair genes

In order to understand the underlying biological functions of high miRNA ESC signature scores in aggressive neuroblastoma, GSEA analysis was performed on the list of coding genes ranked according to degree of expression correlation with the ESC miRNA signature score in 200 NB tumor samples (Supplemental Table 4.2). Gene sets enriched among the positively correlated genes are involved in chromatin remodeling, response to DNA damage (double strand DNA breaks) and cell cycle (MSigDB c5-gobp) as well as embryonic stem cells (MSigDB

c2-cgp) and MYC and E2F targeting (MSigDB Hallmark genesets) (adjusted p-values < 0.001) (Figure 4.2A-F). These findings were confirmed by DAVID-gene ontology analysis on the top 500 correlated genes showing enrichment for cell cycle and DNA damage/repair genes (functional annotation clustering: first cluster with cell cycle gene sets has enrichment score of 41.93, second cluster with DNA damage/repair functional classes has enrichment score of 29.52, cut-off for significance is 1.3).

We also performed motif enrichment analysis using iRegulon[40] to identify transcription factors that drive the expression of the top 500 correlated genes, further referred to as the ESC mRNA signature (Supplemental Table 4.3)[40]. Within the top 10 most significantly enriched transcription factors, several members of the DREAM complex, which has an important role in transcriptional repression of cell cycle genes and maintaining quiescence, are present including E2F, MYBL2 and FOXM1[41]. DREAM-complex members FOXM1, MYBL2, E2F1/2/3/7/8 and LIN9 are all part of the top 500 correlated gene list. Furthermore, FOXM1 is a transcription factor known to target several genes involved in the enriched DNA repair pathway, including *EXO1*, *BRIP1*, *BRCA1*, *BRCA2*, *CHEK1*, *BUB1B*, *XRCC2* and *RAD51AP1k*, all of which are in the top 50 of the ESC mRNA signature[42]. Also part of the gene list is *CENPF* which is a known FOXM1 target that cooperates with FOXM1 as recently shown for prostate cancer[43], as well as *MELK*, *CDK6*, *PLK1* which are all described as regulators of FOXM1 phosphorylation[44]. Interestingly, the expression of 3 of these genes i.e. *MELK*, *MYBL2* and *PLK1* is remarkably highly correlated with *FOXM1* expression levels in 200 neuroblastoma tumors (correlation coefficients > 0.9) suggesting a very tight co-regulated transcriptional control.

Collectively, our findings support that the ESC mRNA gene signature in neuroblastoma is driven by the FOXM1 transcription factor.

Differentially expressed genes after FOXM1 knock-down in neuroblastoma cells are enriched for mRNA ESC signature genes

To provide more direct proof that the ESC mRNA gene signature is strongly FOXM1 driven, we next performed FOXM1 knock down and gene expression profiling in the neuroblastoma cell line IMR-32 with high ESC mRNA signature score and high *FOXM1* expression levels (Supplemental Figure 4.2A-B). Subsequent GSEA of down regulated genes after FOXM1 knock-down revealed enrichment for gene sets related to DNA repair, E2F and MYC targeting

(MSigDB Hallmark genesets) and in cell cycle and double strand break repair (MSigDB c5-gobp) (Figure 4.3A-D). Of further note, the 500 ESC geneset is also significantly enriched in the IMR-32 FOXM1 knock-down data (Figure 4.3E) (GSEA-analysis, adjusted p-values < 0.001). This is also confirmed in other cancer types where the ESC mRNA signature goes down upon chemical and pharmacological FOXM1 knock-down (Supplemental Figure 4.3)[27-29].

Taken together, this experimental analysis further supports the data-mining driven observation that the ESC mRNA gene signature in neuroblastoma cells is enriched for genes that are transcriptionally regulated by FOXM1.

The ESC mRNA signature is activated by MYCN activity in vivo and in vitro in keeping with direct binding of MYCN to the FOXM1 promotor

Previous work has provided evidence for a coordinated role of MYC and FOXM1 in controlling normal S-phase progression in mouse embryonic stem cells[45]. Furthermore, as indicated above, we observed MYC target gene enrichment in the genes downregulated upon FOXM1 knock-down. Therefore, we further investigated MYCN controlled regulation of the FOXM1 gene signature. To this end, we reanalyzed data of several *in vitro* MYCN neuroblastoma model systems. In these datasets, we observed decreased ESC mRNA signature scores and *FOXM1* expression levels upon MYCN knock-down and pharmacological MYCN activity inhibition using JQ1 and OTX015 (Figure 4.4A, B, C)[21-23]. Also in the Th-MYCN mouse model an increase in ESC mRNA signature score and *FOXM1* expression is observed upon *MYCN* driven development from hyperplastic ganglia towards full-blown neuroblastoma tumors (Figure 4.4D)[20]. Remarkably, the expression of all top 50 correlated genes from the ESC mRNA signature, including *FOXM1*, increases upon Th-MYCN driven neuroblastoma development (Figure 4.4D). In neuroblastoma tumors, the ESC mRNA signature score is significantly higher in tumors with versus without *MYCN* amplification (both in the global cohort and the subset of stage 4 tumors) (Figure 4.4E-F, Supplemental Figure 4.4I-J). Interestingly, higher ESC mRNA signature scores were also observed in other tumor cell lines with *MYCN* amplification (Supplemental Figure 4.5)[31]. Altogether, these data point to an important role of MYCN in the regulation of the ESC signature genes. Therefore, we further investigated the possible binding of MYCN to the FOXM1 promotor region using ChIP sequencing data for MYCN and subsequent analysis of binding sites at or near the

FOXM1 promotor. In these data, direct binding of MYCN on the FOXM1 promotor is clearly observed in both MYCN amplified and non-amplified cell lines. Clear peaks for H3K27ac were also observed showing open chromatin and active transcription (Figure 4.4H) (E-GEOD-80154).

Furthermore, similar as to the ESC miRNA signature, ESC mRNA signature scores are related to survival in a global cohort of neuroblastoma tumors, but also in a subgroup of stage 4 tumors without *MYCN* amplification (Supplemental Figure 4.4A-D). This observation is confirmed in an independent dataset of 498 neuroblastoma tumors (Supplemental Figure 4.4E-H)[19].

Altogether, these data point at a MYCN activated FOXM1 driven ESC signature that is prognostic in neuroblastoma tumors.

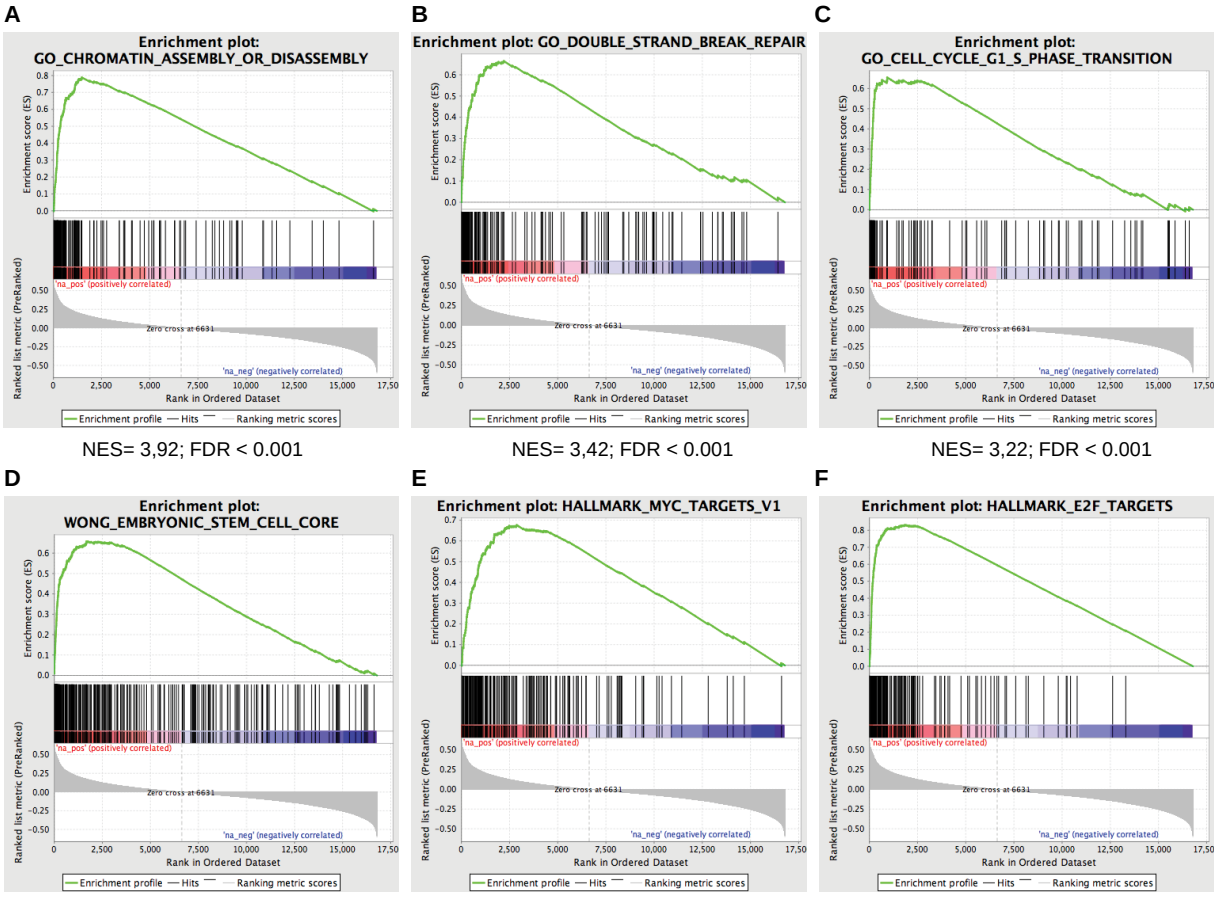

Figure 4.2: Important genesets found to be enriched using gene set enrichment analysis (GSEA) on the list of coding genes ranked according to the degree of correlation with the ESC miRNA signature score in 200 neuroblastoma patient samples. NES= normalized enrichment score, FDR= false discovery rate.

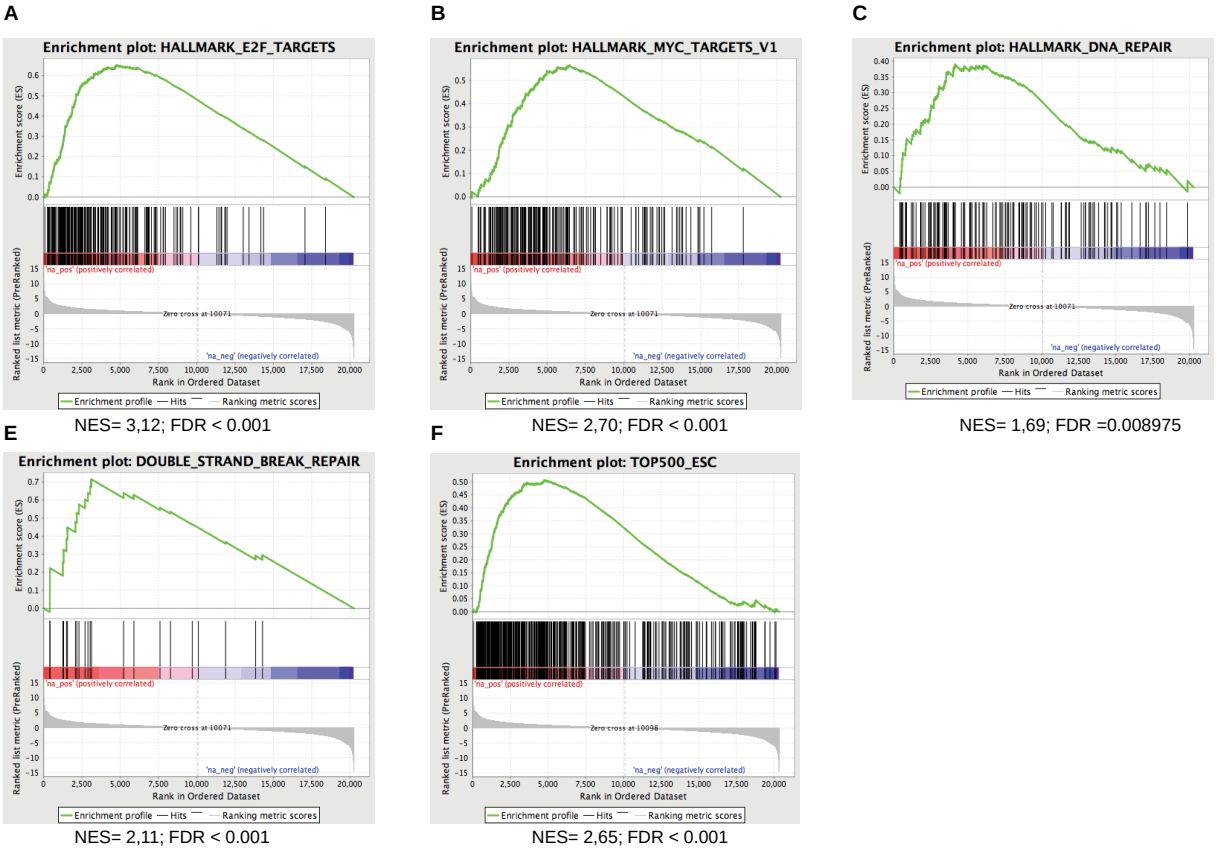

Figure 4.3: Important genesets found to be enriched using gene set enrichment analysis (GSEA) upon knock down of FOXM1 in IMR32. NES= normalized enrichment score, FDR= false discovery rate.

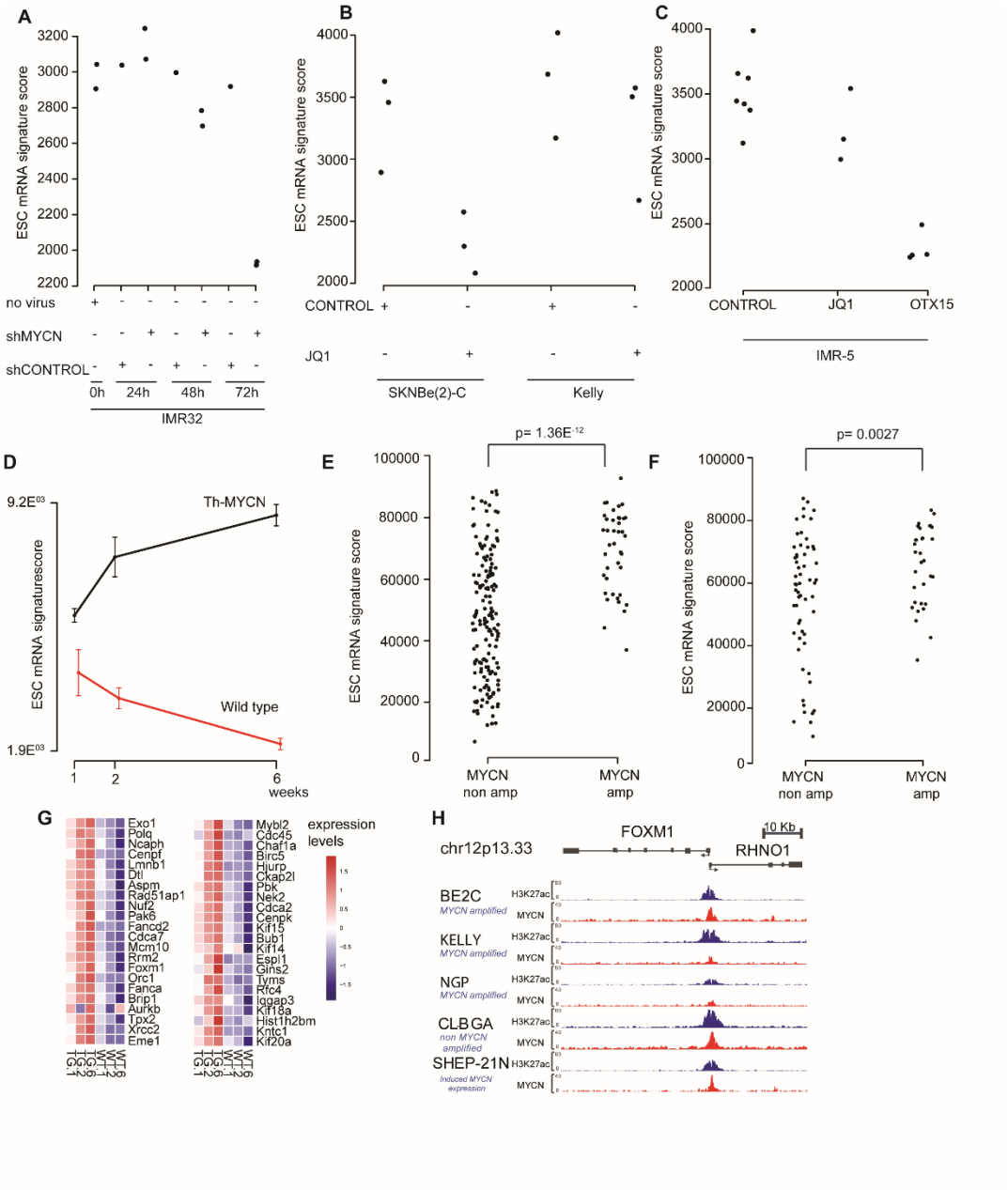

Figure 4.4: Association between MYCN and FOXM1 in the ESC mRNA signature score

(A) ESC mRNA signature score upon lentiviral knock-down of MYCN in IMR-32 neuroblastoma cells, (B) upon pharmacological inhibition of MYCN with JQ1 in SKNBE(2)-C and Kelly neuroblastoma cells, (C) after inhibition of MYCN with JQ1 and OTX015 in IMR5 neuroblastoma cells, and (D) during tumor development in Th-MYCN mouse model. (E-F) ESC mRNA signature score in neuroblastoma patient samples with and without *MYCN* amplification in a global cohort (F) and in stage 4 neuroblastoma patient samples. (G) Heatmap of expression of the top 50 correlated genes of the ESC mRNA signature in the Th-MYCN mouse model. (H) ChIP-seq profiles of H3K27ac and MYCN transcription factor binding at the FOXM1 promotor in both MYCN amplified (NGP, BE2C, KELLY) and MYCN non amplified (CLB-GA, qval=6.3x10^{-5}) cell lines as well as the SHEP21N cell line with induced MYCN expression.

Discussion

Several studies have shown that a stem cell like (stemness) gene signature may offer prognostic information in certain cancer types[9]. Given that (1) neuroblastoma is an embryonal neural crest derived tumor, (2) MYCN is critical for the maintenance of embryonic stem cell-derived neural crest stem cells[6] and (3) LIN28B, a known stem cell marker, acts as oncogene in neuroblastoma[5], we wanted to deeper explore whether an ESC derived miRNA signature could capture a stemness phenotype in neuroblastoma cells and be applied as tool to select neuroblastoma patients with therapy resistant tumors. Having established an ESC derived miRNA prognostic classifier, we could indeed show that within the subgroup of high-risk patients we were able to predict with high confidence patients that would not benefit from current treatment regimes. Indeed, neuroblastoma patients with high ESC miRNA signature score have higher chance to die of disease or relapse as illustrated in Kaplan-Meier analyses. The survival difference for tumors with different scores is most striking for high-stage neuroblastoma tumors without *MYCN* amplification, while all tumors with *MYCN* amplification have higher ESC miRNA signature scores. Such a prognostic classifier could be helpful to identify patients in a subset of high-stage cases that would be eligible for phase I trials for novel compounds in so-called basket trials[46].

To understand the key drivers of the high ESC signature scores and possible cause of therapy resistance mechanisms in ultra-high risk neuroblastomas and as a prelude to drugging the stemness phenotype in neuroblastoma, we applied a unique data mining approach. We established a mRNA signature derived from correlation analysis of the initial ESC miRNA signature score with gene expression profiling data in a large set of primary human neuroblastomas. Functional and motif enrichment analysis on the top 500 correlated genes, further referred to as the ESC mRNA signature, pointed at a central role of transcription factor FOXM1 and several other members of the DREAM complex, including MYBL2, E2F and LIN9 in controlling the stem cell characteristics of aggressive neuroblastoma cells, by keeping cell cycle and DNA repair mechanisms in check. The DREAM complex has an important role in cell cycle by coordinating the shift from quiescence to proliferation[41]. When cells exit the G0 phase, FOXM1 and MYBL2 are recruited to promote mitotic gene expression[41] thereby controlling proper DNA replication and avoiding excessive genomic damage[41]. Both genes

have been described to have a role in sustaining the self-renewal capacity of pluripotent stem cells[45], as also shown in neuroblastoma cells[47]. This regulatory axis may represent an important novel therapeutic vulnerability for neuroblastoma. These results are also in keeping with earlier findings of Wang et al[47] who reported FOXM1 regulation of Sox2 and Bmi1 expression impacting on renewal of neural progenitor cells and survival of neuroblastoma cells.

Next, we further explored the link between MYCN and stemness[6] through further analysis of several MYCN model systems, i.e. the dynamic regulated transcriptome of Th-MYCN driven mouse neuroblastomas[20], neuroblastoma cell lines upon knock-down of MYCN expression[21] and upon pharmacological inhibition of MYCN activity[22,23]. Collectively, these data demonstrate correlation of high ESC mRNA signature scores with high MYCN activity, further confirmed by high ESC mRNA signature scores in MYCN amplified human tumors compared to non-MYCN amplified cases. Not unexpectedly, a subset of high-stage neuroblastoma tumors without *MYCN* amplification also have elevated ESC signature scores, in keeping with high MYC activity in these cells. Similar as with the miRNA ESC signature, this subgroup of neuroblastoma patients is marked by very poor survival outcome.
Interestingly, our ESC mRNA gene set shows a very strong overlap with a gene set recently derived by Olsen *et al*. (Oncogene, accepted) in a novel mouse neural crest derived neuroblastoma model. In brief, this study describes how mouse neural crest cells are grown and differentiated *in vitro* to generate sympathetic progenitor cells. Subsequently, these cells were transduced with MYCN and injected into mice to generate neuroblastomas. Analysis of the MYCN upregulated genes in the resulting mouse tumors also showed a strong enrichment of FOXM1 controlled genes involved in cell cycle and DNA damage control corroborating our data in human primary tumors and the Th-MYCN mouse model.

In a huge pan-cancer dataset including ~18.000 tumors, a *FOXM1* regulatory network was identified as a major predictor of adverse outcome across different tumor entities[48], matching with the described link of FOXM1 with cancer therapy resistance[49] and its role in DNA damage control[42] as described in stem cells and tumors like neuroblastoma. In the light of the studies that pinpoint FOXM1 as an important pan-cancer gene, several labs are undertaken efforts to identify drugs that target FOXM1. The past years, several drugs

presumed to target FOXM1 activity have been reported but so far none of these drugs has been successfully applied in the clinic, possibly due to off target and or insufficient on target effects of these drugs. While our study warrants further drug screening for more potent and specific FOXM1 inhibitors[29], it is also of great interest that the FOXM1 upstream regulatory kinase MELK is also highly expressed, suggesting that this could act as a good candidate drug target for ultra-high risk neuroblastoma patients. Recently, a specific MELK inhibitor, MELK-T1 was tested, and could represent a useful novel drug for improving survival rates for children with neuroblastoma[50].

Similar as our ESC miRNA signature, Ittai Ben-Porath et al. [9] has built an ESC mRNA signature consisting of 380 genes overexpressed in ESC according to 5 or more out of 20 profiling studies and could show an associated to prognosis in breast cancer. We tested this mRNA signature in expression data of 200 neuroblastoma tumors and could show correlation of high signature score with worse outcome in the global patient cohort, but not in the subset of high-stage tumors without *MYCN* amplification (data not shown). Moreover, the signature did not contain the DREAM complex genes, FOXM1, MYBL2, LIN9 and E2F. Thus, our unique approach did not only lead to more strong and robust prognostic signatures, but also revealed some putative mechanism of therapy resistance in neuroblastoma.

In conclusion, by (re)analysis of published and unpublished expression profiling data, we could unravel a MYC(N)-FOXM1-ESC signaling axis that is active in therapy resistant neuroblastoma tumors and that unveils new vulnerable nodes for targeted therapy of tumors where current treatment regimens fail.

Acknowledgements:

S.V. is funded by the VLK (Flemish League against cancer) and Villa Joep. B.D. and C.V. are supported by the FWO (Fund for Scientific Research-Flanders). In addition, we would like to acknowledge FWO for financial support (project-numbers G053012N, G021415N and 1516313N).

References:

1. Marshall GM, Carter DR, Cheung BB, Liu T, Mateos MK, Meyerowitz JG, et al. The prenatal origins of cancer. Nat Rev Cancer. 2014;14:277-89.

2. De Preter K, Vandesompele J, Heimann P, Yigit N, Beckman S, Schramm A, et al. Human fetal neuroblast and neuroblastoma transcriptome analysis confirms neuroblast origin and highlights neuroblastoma candidate genes. Genome Biol. 2006;7:R84.

3. Kohl NE, Kanda N, Schreck RR, Bruns G, Latt SA, Gilbert F, et al. Transposition and amplification of oncogene-related sequences in human neuroblastomas. Cell. 1983;35:359-67.

4. George RE, Sanda T, Hanna M, Frohling S, Luther W, 2nd, Zhang J, et al. Activating mutations in ALK provide a therapeutic target in neuroblastoma. Nature. 2008;455:975-8.

5. Molenaar JJ, Domingo-Fernandez R, Ebus ME, Lindner S, Koster J, Drabek K, et al. LIN28B induces neuroblastoma and enhances MYCN levels via let-7 suppression. Nat Genet. 2012;44:1199-206.

6. Knoepfler PS. Why myc? An unexpected ingredient in the stem cell cocktail. Cell Stem Cell. 2008;2:18-21.

7. Barone G, Anderson J, Pearson AD, Petrie K, Chesler L. New strategies in neuroblastoma: Therapeutic targeting of MYCN and ALK. Clin Cancer Res. 2013;19:5814-21.

8. Dean M, Fojo T, Bates S. Tumour stem cells and drug resistance. Nat Rev Cancer. 2005;5:275-84.

9. Ben-Porath I, Thomson MW, Carey VJ, Ge R, Bell GW, Regev A, et al. An embryonic stem cell-like gene expression signature in poorly differentiated aggressive human tumors. Nat Genet. 2008;40:499-507.

10. Gangaraju VK, Lin H. MicroRNAs: key regulators of stem cells. Nat Rev Mol Cell Biol. 2009;10:116-25.

11. Bernstein E, Kim SY, Carmell MA, Murchison EP, Alcorn H, Li MZ, et al. Dicer is essential for mouse development. Nature Genetics. 2003;35:215-7.

12. Lu J, Getz G, Miska EA, Alvarez-Saavedra E, Lamb J, Peck D, et al. MicroRNA expression profiles classify human cancers. Nature. 2005;435:834-8.

13. Mallon BS, Chenoweth JG, Johnson KR, Hamilton RS, Tesar PJ, Yavatkar AS, et al. StemCellDB: the human pluripotent stem cell database at the National Institutes of Health. Stem Cell Res. 2013;10:57-66.

14. Wilson KD, Venkatasubrahmanyam S, Jia F, Sun N, Butte AJ, Wu JC. MicroRNA profiling of human-induced pluripotent stem cells. Stem Cells Dev. 2009;18:749-58.

15. Ren J, Jin P, Wang E, Marincola FM, Stroncek DF. MicroRNA and gene expression patterns in the differentiation of human embryonic stem cells. J Transl Med. 2009;7:20.

16. Bar M, Wyman SK, Fritz BR, Qi J, Garg KS, Parkin RK, et al. MicroRNA discovery and profiling in human embryonic stem cells by deep sequencing of small RNA libraries. Stem Cells. 2008;26:2496-505.

17. Stadler B, Ivanovska I, Mehta K, Song S, Nelson A, Tan Y, et al. Characterization of microRNAs involved in embryonic stem cell states. Stem Cells Dev. 2010;19:935-50.

18. De Preter K, Mestdagh P, Vermeulen J, Zeka F, Naranjo A, Bray I, et al. miRNA Expression Profiling Enables Risk Stratification in Archived and Fresh Neuroblastoma Tumor Samples. Clinical Cancer Research. 2011;17:7684-92.

19. Wang C, Gong BS, Bushel PR, Thierry-Mieg J, Thierry-Mieg D, Xu JS, et al. The concordance between RNA-seq and microarray data depends on chemical treatment and transcript abundance. Nature Biotechnology. 2014;32:926-32.

20. Beckers A, Van Peer G, Carter DR, Mets E, Althoff K, Cheung BB, et al. MYCN-targeting miRNAs are predominantly downregulated during MYCN-driven neuroblastoma tumor formation. Oncotarget. 2015;6:5204-16.

21. Valentijn LJ, Koster J, Haneveld F, Aissa RA, van Sluis P, Broekmans ME, et al. Functional MYCN signature predicts outcome of neuroblastoma irrespective of MYCN amplification. Proc Natl Acad Sci U S A. 2012;109:19190-5.

22. Puissant A, Frumm SM, Alexe G, Bassil CF, Qi J, Chanthery YH, et al. Targeting MYCN in neuroblastoma by BET bromodomain inhibition. Cancer Discov. 2013;3:308-23.

23. Henssen A, Althoff K, Odersky A, Beckers A, Koche R, Speleman F, et al. Targeting MYCN-Driven Transcription By BET-Bromodomain Inhibition. Clin Cancer Res. 2016;22:2470-81.

24. Park YY, Jung SY, Jennings NB, Rodriguez-Aguayo C, Peng G, Lee SR, et al. FOXM1 mediates Dox resistance in breast cancer by enhancing DNA repair. Carcinogenesis. 2012;33:1843-53.

25. Bergamaschi A, Madak-Erdogan Z, Kim YJ, Choi YL, Lu HL, Katzenellenbogen BS. The forkhead transcription factor FOXM1 promotes endocrine resistance and invasiveness in

estrogen receptor-positive breast cancer by expansion of stem-like cancer cells. Breast Cancer Res. 2014;16.

26. Kim SH, Joshi K, Ezhilarasan R, Myers TR, Siu J, Gu C, et al. EZH2 protects glioma stem cells from radiation-induced cell death in a MELK/FOXM1-dependent manner. Stem Cell Reports. 2015;4:226-38.

27. Minata M, Gu CY, Joshi K, Nakano-Okuno M, Hong C, Nguyen CH, et al. Multi-Kinase Inhibitor C1 Triggers Mitotic Catastrophe of Glioma Stem Cells Mainly through MELK Kinase Inhibition. Plos One. 2014;9.

28. Kuner R, Falth M, Pressinotti NC, Brase JC, Puig SB, Metzger J, et al. The maternal embryonic leucine zipper kinase (MELK) is upregulated in high-grade prostate cancer. J Mol Med. 2013;91:237-48.

29. Gormally MV, Dexheimer TS, Marsico G, Sanders DA, Lowe C, Matak-Vinkovic D, et al. Suppression of the FOXM1 transcriptional programme via novel small molecule inhibition. Nat Commun. 2014;5:5165.

30. Barretina J, Caponigro G, Stransky N, Venkatesan K, Margolin AA, Kim S, et al. The Cancer Cell Line Encyclopedia enables predictive modelling of anticancer drug sensitivity. Nature. 2012;483:603-7.

31. Korshunov A, Remke M, Kool M, Hielscher T, Northcott PA, Williamson D, et al. Biological and clinical heterogeneity of MYCN-amplified medulloblastoma. Acta Neuropathol. 2012;123:515-27.

32. Mateizel I, Spits C, De Rycke M, Liebaers I, Sermon K. Derivation, culture, and characterization of VUB hESC lines. In Vitro Cell Dev Biol Anim. 2010;46:300-8.

33. Mestdagh P, Feys T, Bernard N, Guenther S, Chen C, Speleman F, et al. High-throughput stem-loop RT-qPCR miRNA expression profiling using minute amounts of input RNA. Nucleic Acids Res. 2008;36.

34. Fredlund E, Ringner M, Maris JM, Pahlman S. High Myc pathway activity and low stage of neuronal differentiation associate with poor outcome in neuroblastoma. P Natl Acad Sci USA. 2008;105:14094-9.

35. Subramanian A, Tamayo P, Mootha VK, Mukherjee S, Ebert BL, Gillette MA, et al. Gene set enrichment analysis: A knowledge-based approach for interpreting genome-wide expression profiles. P Natl Acad Sci USA. 2005;102:15545-50.

36. Durinck K, Van Loocke W, Van der Meulen J, Van de Walle I, Ongenaert M, Rondou P, et al. Characterization of the genome-wide TLX1 binding profile in T-cell acute lymphoblastic leukemia. Leukemia. 2015;29:2317-27.

37. Cancer Genome Atlas Research N. Comprehensive genomic characterization defines human glioblastoma genes and core pathways. Nature. 2008;455:1061-8.

38. Shih KK, Qin LX, Tanner EJ, Zhou Q, Bisogna M, Dao F, et al. A microRNA survival signature (MiSS) for advanced ovarian cancer. Gynecol Oncol. 2011;121:444-50.

39. Heukamp LC, Thor T, Schramm A, De Preter K, Kumps C, De Wilde B, et al. Targeted expression of mutated ALK induces neuroblastoma in transgenic mice. Sci Transl Med. 2012;4:141ra91.

40. Janky R, Verfaillie A, Imrichova H, Van de Sande B, Standaert L, Christiaens V, et al. iRegulon: From a Gene List to a Gene Regulatory Network Using Large Motif and Track Collections. Plos Comput Biol. 2014;10.

41. Sadasivam S, DeCaprio JA. The DREAM complex: master coordinator of cell cycle-dependent gene expression (vol 13, pg 585, 2013). Nature Reviews Cancer. 2013;13:752-.

42. Zona S, Bella L, Burton MJ, de Moraes GN, Lam EWF. FOXM1: An emerging master regulator of DNA damage response and genotoxic agent resistance. Bba-Gene Regul Mech. 2014;1839:1316-22.

43. Aytes A, Mitrofanova A, Lefebvre C, Alvarez MJ, Castillo-Martin M, Zheng T, et al. Cross-Species Regulatory Network Analysis Identifies a Synergistic Interaction between FOXM1 and CENPF that Drives Prostate Cancer Malignancy. Cancer Cell. 2014;25:638-51.

44. Joshi K, Banasavadi-Siddegowda Y, Mo XK, Kim SH, Mao P, Kig C, et al. MELK-Dependent FOXM1 Phosphorylation is Essential for Proliferation of Glioma Stem Cells. Stem Cells. 2013;31:1051-63.

45. Lorvellec M, Dumon S, Maya-Mendoza A, Jackson D, Frampton J, Garcia P. B-Myb is Critical for Proper DNA Duplication During an Unperturbed S Phase in Mouse Embryonic Stem Cells. Stem Cells. 2010;28:1751-9.

46. Worst BC, van Tilburg CM, Balasubramanian GP, Fiesel P, Witt R, Freitag A, et al. Next-generation personalised medicine for high-risk paediatric cancer patients - The INFORM pilot study. Eur J Cancer. 2016;65:91-101.

47. Wang ZB, Park HJ, Carr JR, Chen YJ, Zheng Y, Li J, et al. FoxM1 in Tumorigenicity of the Neuroblastoma Cells and Renewal of the Neural Progenitors. Cancer Res. 2011;71:4292-302.

48. Gentles AJ, Newman AM, Liu CL, Bratman SV, Feng W, Kim D, et al. The prognostic landscape of genes and infiltrating immune cells across human cancers. Nat Med. 2015;21:938-45.

49. de Moraes GN, Bella L, Zona S, Burton MJ, Lam EWF. Insights into a Critical Role of the FOXO3a-FOXM1 Axis in DNA Damage Response and Genotoxic Drug Resistance. Current Drug Targets. 2016;17:164-77.

50. Beke L, Kig C, Linders JTM, Boens S, Boeckx A, van Heerde E, et al. MELK-T1, a small-molecule inhibitor of protein kinase MELK, decreases DNA-damage tolerance in proliferating cancer cells. Bioscience Rep. 2015;35.

Tables

Table 4.1: ESC miRNA signature

Upregulated in ESC	Downregulated in ESC
hsa-miR-141	hsa-let-7a
hsa-miR-148a	hsa-let-7e
hsa-miR-187	hsa-let-7f
hsa-miR-18a	hsa-let-7g
hsa-miR-18b	hsa-miR-100
hsa-miR-20a	hsa-miR-125a
hsa-miR-20b	hsa-miR-125b
hsa-miR-200c	hsa-miR-132
hsa-miR-19a	hsa-miR-137
hsa-miR-19b	hsa-miR-143
hsa-miR-302a	hsa-miR-145
hsa-miR-302astar	hsa-miR-152
hsa-miR-302b	hsa-miR-181a
hsa-miR-302bstar	hsa-miR-181b
hsa-miR-302c	hsa-miR-21
hsa-miR-302d	hsa-miR-22
hsa-miR-367	hsa-miR-222
hsa-miR-363	hsa-miR-23a
hsa-miR-363star	hsa-miR-23b
hsa-miR-372	hsa-miR-24
hsa-miR-498	hsa-miR-27a
hsa-miR-512-3p	hsa-miR-27b
hsa-miR-515-5p	hsa-miR-28
hsa-miR-517a	hsa-miR-29a
hsa-miR-517b	hsa-miR-376a
hsa-miR-518b	hsa-miR-495
hsa-miR-518c	hsa-miR-99a
hsa-miR-520f	

hsa-miR-520g	
hsa-miR-520h	
hsa-miR-524star	
hsa-miR-92b	
hsa-miR-96	

Supplementary data:

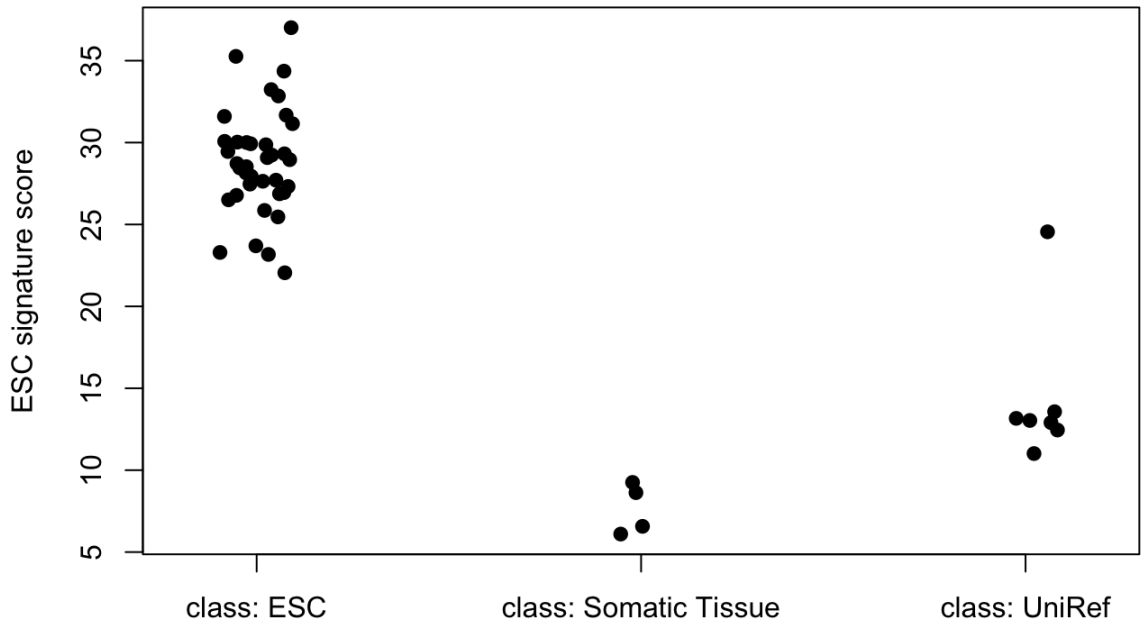

Supplemental Figure4. 1: Validation of the miRNA ESC signature in an independent dataset

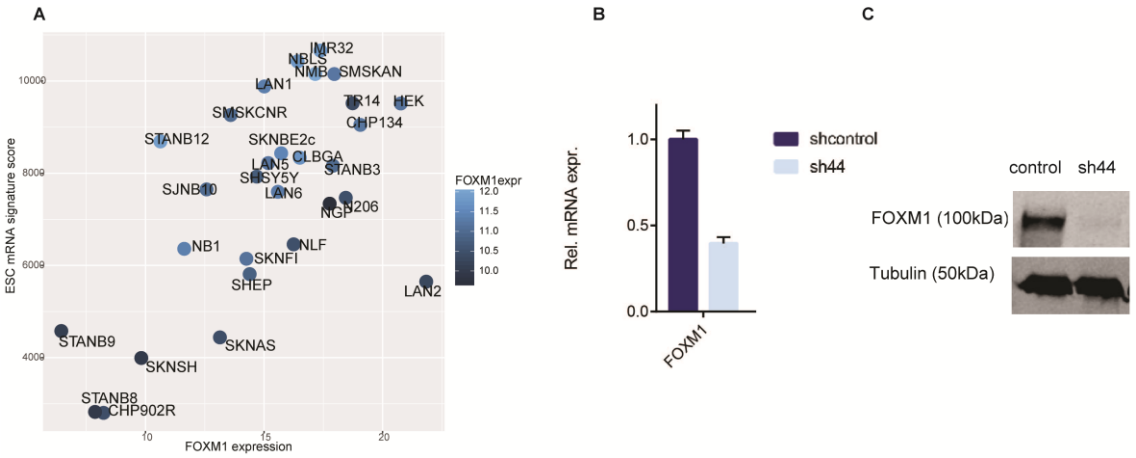

Supplemental Figure 4.2: Lentiviral transductions of FOXM1

(A) ESC mRNA signature score and FOXM1 expression levels in 29 neuroblastoma cell lines. (B) IMR-32 cells were transduced with shRNA targeting *FOXM1*, followed by quantitative RT-PCR assessment of *FOXM1.* Error bars represent the standard error of mean (technical duplicates). (C) Western Blot results for FOXM1 knock down with shRNA (loading control tubulin).

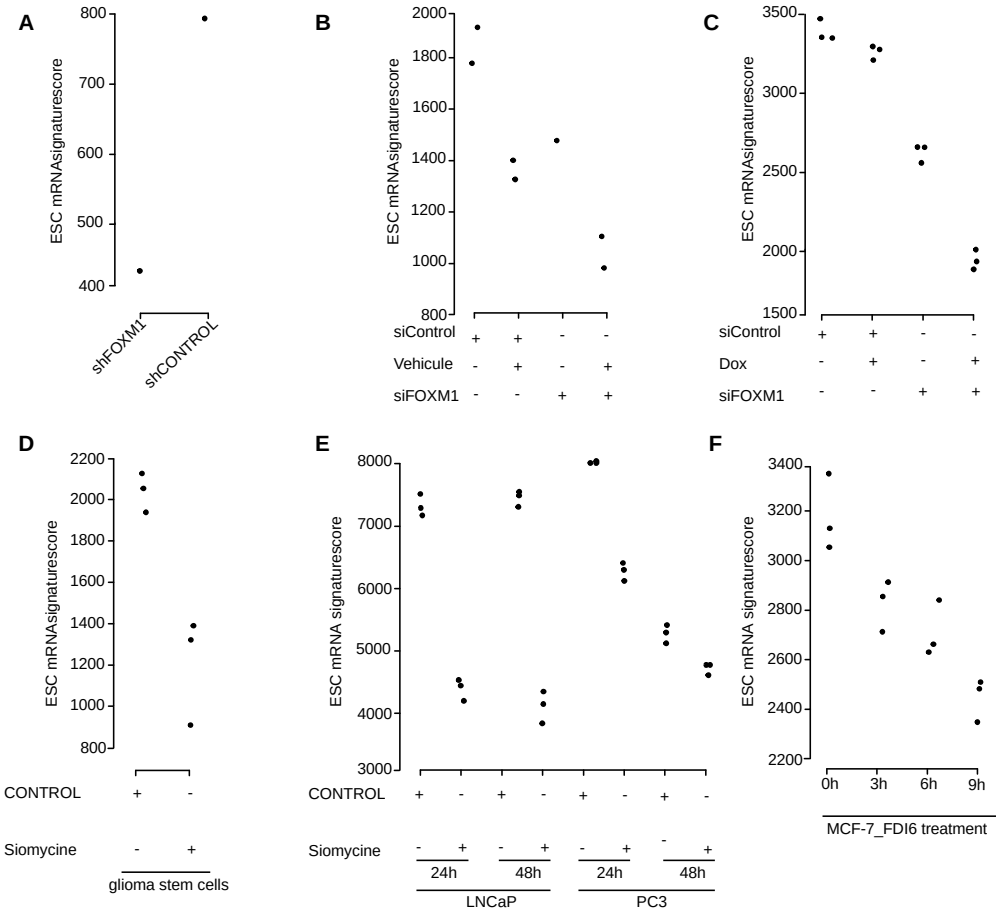

Supplemental Figure 4.3: FOXM1 also drives the ESC mRNA signature score in other cancer entities

A) ESC mRNA signature score upon lentiviral inhibition of FOXM1 in glioma cells, (B-C) upon siRNA FOXM1 inhibition in breast cancer cells, (D) upon inhibition of FOXM1 with siomycin A in glioma stem cells, (E) upon inhibition of FOXM1 with siomycin A in prostate cancer cells and (F) in breast cancer cells treated with FDI-6 to inhibit FOXM1.

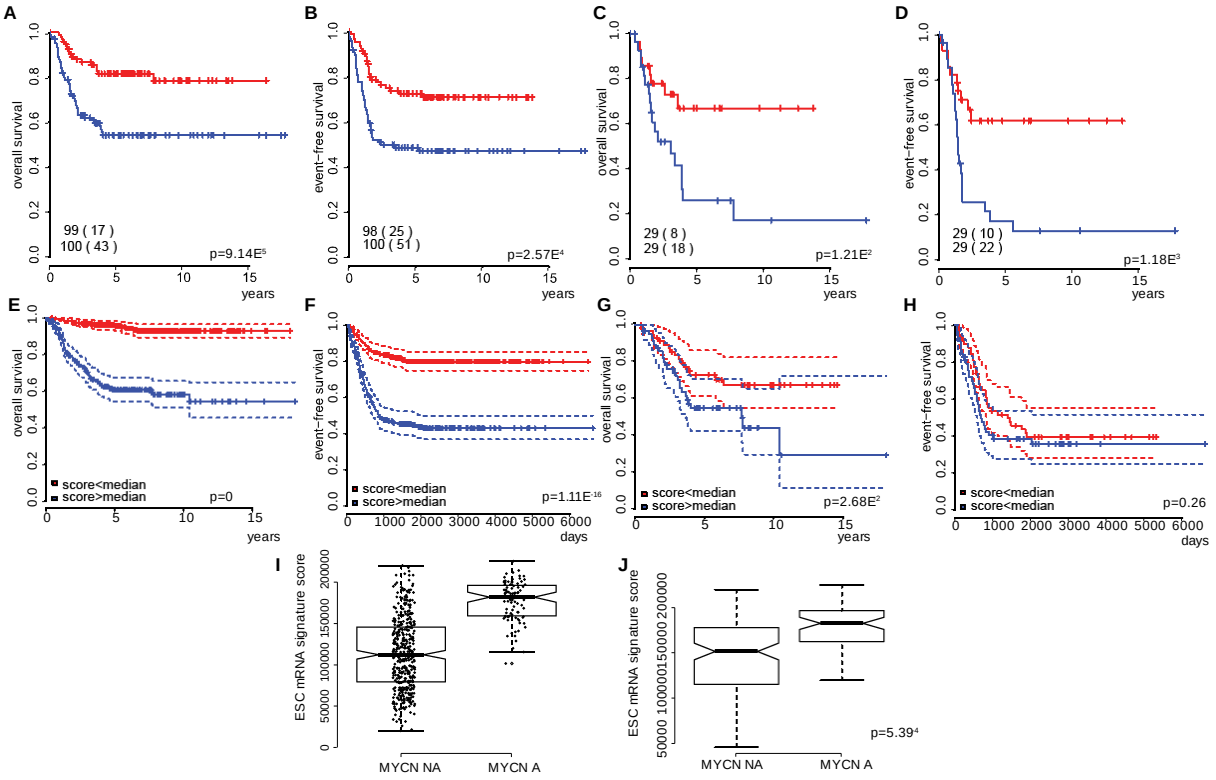

Supplemental Figure 4.4: ESC mRNA signature score is related to survival

(A-B) Kaplan-Meier and log rank analysis on 200 neuroblastoma patients with a high or low ESC mRNA signature score. (C-D) Kaplan-Meier and log rank analysis within the subset of stage 4 neuroblastoma without MYCN amplification. Kaplan-Meier and log rank analysis of 498 neuroblastoma patients with high or low ESC mRNA signature score (independent validation), in the global cohort (E-F) and with the subset of stage 4 neuroblastoma without MYCN amplification (G-H). (I-J) ESC mRNA signature score in neuroblastoma patients with or without MYCN amplification in the global cohort and stage 4 neuroblastomas only.

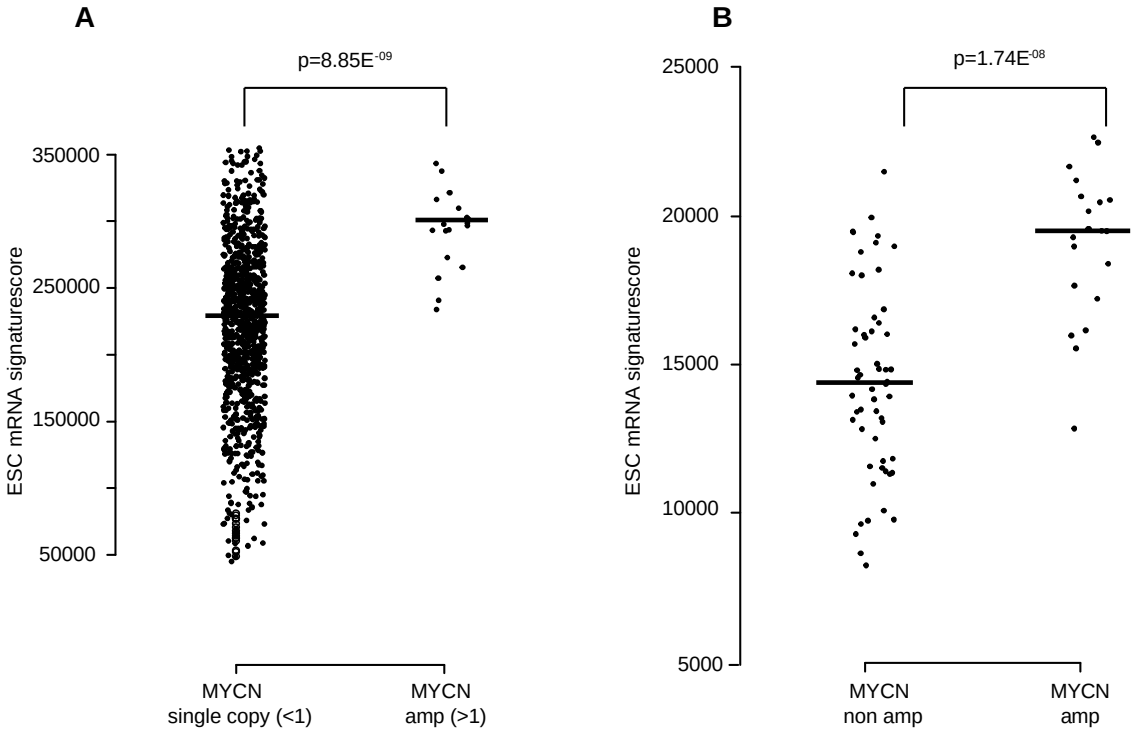

Supplemental Figure 4.5: ESC mRNA signature scores in other cancer entities with or without *MYCN* amplification

A) CCLE database analysis of the ESC mRNA signatures in *MYCN* non-amplified and *MYCN* amplified cancer cell lines. (B) ESC mRNA signature scores in medulloblastoma samples with and without *MYCN* amplification.

Supplementary Table 4.1: Genelists from 4 published studies reporting of differential miRNA expression analysis of ESC versus more differentiated cells.

Supplementary Table 4.2: list of coding genes ranked according to the degree of expression correlation with the ESC miRNA signature score in 200 neuroblastoma tumor samples.

This list is available in a digital format only and can be sent upon request.

Supplementary Table 4.3: results obtained by iRegulon.

Full list can be sent upon request

Supplementary table 4.1: Genelists from 4 published studies reporting of differential miRNA expression analysis of ESC versus more differentiated cells.

Wilson2009_up	Ren2009_up	Bar2008_up	Stadler2010_up	Wilson2009_down	Ren2009_down	Bar2008_down	Stadler2010_down
hsa-mir-486-5p	hsa-mir-127	hsa-mir-302b	hsa-mir-124a	hsa-mir-100	hsa-mir-324-3p	hsa-let-7e	hsa-mir-30a-5p
hsa-mir-30e	hsa-mir-141	hsa-mir-302c	hsa-mir-367	hsa-mir-10a	hsa-mir-29a	hsa-mir-23b	hsa-mir-24
hsa-mir-148a	hsa-mir-200b	hsa-mir-302d	hsa-mir-498	hsa-mir-125b	hsa-mir-29b	hsa-mir-27b	hsa-mir-145
hsa-mir-923	hsa-mir-200c	hsa-mir-92b	hsa-mir-19b	hsa-mir-127-3p	hsa-mir-29c	hsa-mir-152	hsa-mir-181d
hsa-mir-92a	hsa-mir-299-3p	hsa-mir-20b	hsa-mir-19a	hsa-mir-132	hsa-mir-132	hsa-mir-26a	hsa-mir-22
hsa-mir-92b	hsa-mir-302a	hsa-mir-519d	hsa-mir-18a	hsa-mir-134	hsa-mir-155	hsa-mir-23a	hsa-mir-125b
hsa-mir-363star	hsa-mir-302astar	hsa-mir-302a	hsa-mir-18b	hsa-mir-143	hsa-mir-596	hsa-mir-193a	hsa-mir-622
hsa-mir-421	hsa-mir-302b	hsa-mir-324-3p	hsa-mir-17star	hsa-mir-145	hsa-mir-495	hsa-mir-320	hsa-mir-29a
hsa-mir-489	hsa-mir-302bstar	hsa-mir-187	hsa-mir-141	hsa-mir-145star	hsa-mir-376a	hsa-mir-615	hsa-mir-125a
hsa-mir-498	hsa-mir-302c	hsa-mir-18b	hsa-mir-302bstar	hsa-mir-146b-5p	hsa-mir-368	hsa-mir-27a	hsa-mir-23a
hsa-mir-517a	hsa-mir-302d	hsa-mir-518b	hsa-mir-148a	hsa-mir-152	hsa-mir-181a	hsa-mir-218	hsa-mir-27a

hsa-mir-517b	hsa-mir-367	hsa-mir-520g	hsa-mir-302c	hsa-mir-154	hsa-mir-27a	hsa-mir-22	hsa-mir-28
hsa-mir-638	hsa-mir-369-3p	hsa-mir-524star	hsa-mir-20a	hsa-mir-181b	hsa-mir-125a	hsa-mir-196a	hsa-mir-181b
hsa-mir-182	hsa-mir-372	hsa-mir-363star	hsa-mir-302a	hsa-mir-193a-5p	hsa-mir-22	hsa-mir-10b	hsa-mir-21
hsa-mir-183	hsa-mir-515-5p	hsa-mir-154	hsa-mir-302d	hsa-mir-199a-3p	hsa-mir-143	hsa-mir-181b	hsa-mir-149
hsa-mir-663	hsa-mir-517a	hsa-mir-184	hsa-mir-101	hsa-mir-199a-5p	hsa-mir-23a	hsa-mir-542-3p	hsa-mir-500
hsa-mir-106a	hsa-mir-517b	hsa-mir-518c	hsa-mir-363	hsa-mir-214	hsa-mir-21	hsa-mir-192	hsa-mir-193b
hsa-mir-17	hsa-mir-517c	hsa-mir-512-3p	hsa-mir-20b	hsa-mir-22star	hsa-mir-125b	hsa-mir-181a	hsa-mir-486
hsa-mir-20a	hsa-mir-518b		hsa-mir-302astar	hsa-mir-23a	hsa-let-7g	hsa-mir-126	hsa-mir-503
hsa-mir-205	hsa-mir-518c		hsa-mir-302b	hsa-mir-23astar	hsa-let-7d	hsa-mir-197	hsa-mir-222
hsa-mir-302astar	hsa-mir-519b			hsa-mir-23b	hsa-let-7e	hsa-mir-30a-3p	
hsa-mir-18a	hsa-mir-519c			hsa-mir-24	hsa-let-7b	hsa-mir-188	
hsa-mir-18b	hsa-mir-519e			hsa-mir-24-2star	hsa-mir-31	hsa-mir-542-5p	
hsa-mir-302a	hsa-mir-520a			hsa-mir-27a	hsa-let-7f	hsa-mir-491	

hsa-mir-302b	hsa-mir-520b	hsa-mir-27b	hsa-let-7c	hsa-mir-28
hsa-mir-200c	hsa-mir-520c	hsa-mir-299-5p	hsa-let-7i	hsa-mir-30e-3p
hsa-mir-25	hsa-mir-520d	hsa-mir-29a	hsa-let-7a	hsa-mir-148a
hsa-mir-302c	hsa-mir-520e	hsa-mir-29b-1star	hsa-mir-221	hsa-mir-362
hsa-mir-187	hsa-mir-520f	hsa-mir-30d	hsa-mir-222	hsa-mir-625
hsa-mir-302cstar	hsa-mir-520g	hsa-mir-337-5p	hsa-mir-99a	hsa-mir-592
hsa-mir-302dstar	hsa-mir-520h	hsa-mir-34c-3p	hsa-mir-100	hsa-mir-589
hsa-mir-302bstar	hsa-mir-521	hsa-mir-370	hsa-mir-137	hsa-mir-509
hsa-mir-20b	hsa-mir-524star	hsa-mir-376a	hsa-mir-122a	hsa-mir-137
hsa-mir-363	hsa-mir-525	hsa-mir-376c	hsa-mir-206	
hsa-mir-106b	hsa-mir-526bstar	hsa-mir-379	hsa-mir-383	
hsa-mir-20bstar	hsa-mir-550	hsa-mir-382		
hsa-mir-19a	hsa-mir-612	hsa-mir-409-3p		
hsa-mir-	hsa-	hsa-mir-		

19b	mir-96	411
hsa-mir-93		hsa-mir-411star
hsa-mir-222star		hsa-mir-431
hsa-mir-519c-3p		hsa-mir-432
hsa-mir-515-5p		hsa-mir-433
hsa-mir-520g		hsa-mir-485-3p
hsa-mir-520h		hsa-mir-485-5p
hsa-mir-371-5p		hsa-mir-487a
hsa-mir-516a-5p		hsa-mir-487b
hsa-mir-518d-5p		hsa-mir-490-5p
hsa-mir-518fstar		hsa-mir-493
hsa-mir-525-5p		hsa-mir-493star
hsa-mir-516b		hsa-mir-494
hsa-mir-512-3p		hsa-mir-495
hsa-mir-373		hsa-mir-539
hsa-mir-518b		hsa-mir-543
hsa-mir-629		hsa-mir-654-3p
hsa-mir-518estar		hsa-mir-758
hsa-mir-520f		hsa-let-7a
hsa-mir-372		hsa-let-7dstar
hsa-mir-96		hsa-let-7e

	hsa-let-7f
	hsa-let-7g
	hsa-mir-886-5p
	hsa-mir-99a

Supplementary Table 4.3: results obtained by iRegulon.

# Rank	AUC	NES	Cluster code	Transcription
1	0.233221	9.52503	T1	E2F4
2	0.209607	8.43827	T2	TFDP1
3	0.169315	6.58396	T1	E2F4
4	0.166763	6.46649	T1	E2F4
5	0.156578	5.99775	T3	E2F7
6	0.149856	5.68839	T4	SIN3A
7	0.136635	5.07995	T4	SIN3A
8	0.134474	4.98049	T5	MYBL2
9	0.13371	4.94532	T6	FOXM1
10	0.131124	4.8263	T1	E2F4
11	0.128446	4.70306	T6	FOXM1
12	0.127633	4.66564	T6	FOXM1
13	0.120746	4.34869	T6	FOXM1
14	0.110909	3.89598	T4	SIN3A
15	0.108158	3.76937	T4	SIN3A
16	0.10726	3.72801	T7	E2F1
17	0.102885	3.52669	T4	SIN3A
18	0.101739	3.47394	T4	SIN3A
19	0.0987036	3.33424	T4	SIN3A
20	0.0928438	3.06456	T6	FOXM1

Chapter 5: Molecular targeting of FOXM1 in neuroblastoma cells.

Authors: Suzanne Vanhauwaert, Carina Leonelli, Katleen De Preter, Frank Speleman

In preparation

Molecular targeting of FOXM1 in neuroblastoma cells

Authors: Suzanne Vanhauwaert[1,2], Carina Leonelli[1,2], Katleen De Preter[1,2], Franki Speleman[1,2]

Affiliations:

1) Cancer for Medical Genetics (CMGG), Ghent University, Ghent, Belgium

2) Cancer Research Institute Ghent (CRIG), Ghent University, Ghent, Belgium

Abstract:

Neuroblastoma is the most common extracranial pediatric solid tumor in children, accounting for approximately 7-10% of pediatric cancers. Despite intensive multimodal therapies, survival rates for patients with aggressive forms of neuroblastoma are still disappointingly low and therefore new treatment options are warranted. The forkhead box protein M1 (FOXM1) is a transcription factor mainly involved in cell cycle and the DNA damage repair pathway and has been described as an oncogene in many cancer, including neuroblastoma. Siomycin A and FDI6 are two compounds that target FOXM1 and were evaluated for their efficacy in neuroblastoma cells. Unfortunately no convincing results could be obtained, in fact, both drugs only introduced a modest effect on FOXM1 levels and either resulted in antagonistic effects in combination experiments with frequently applied chemotherapeutics (Siomycin A) or experienced fast drug resistance (FDI6).

Short Report:

Introduction:

FOXM1 is a transcription factor and mainly acts as a regulator of the cell cycle and the DNA damage repair pathway. In normal tissues, *FOXM1* is detectable in progenitors with extensive proliferating capacity, whereas its expression is depleted in differentiated or resting cells. Because of its role in cell proliferation and DNA damage, it is not surprising that *FOXM1* has been described as an oncogene in many cancers including neuroblastoma[1] (Vanhauwaert *et al*. CCR, submitted). Interestingly, in a meta-analysis of expression signatures of over 18 000 human tumors, *FOXM1* was identified as a major predictor of adverse patient outcome[2]. In neuroblastoma, an increasing body of data is pointing at a crucial role of FOXM1 in MYCN driven oncogenesis. First, multiple highly transcriptionally upregulated genes such as BRIP1, BIRC5 and TOP2A are direct targets of FOXM1. Second, several of these genes are located on chromosome regions commonly affected by copy number alterations, most notably chromosome 17q (Vanhauwaert *et al.* this thesis). Finally, a recent study describing the transcriptional alteration in mouse neural crest derived MYCN overexpressing neuroblastomas, a strong FOXM1 signature was also noted (Olsen *et al*., Oncogene, accepted). Given the recent identification of compounds proposed to target FOXM1, we decided to evaluate their effects on neuroblastoma cell growth and survival.

Results and Discussion

Inhibition of FOXM1 using thiazole antibiotics

Siomycin A and in general all proteasome inhibitors have been described to target FOXM1, through stabilization of its negative regulator NRFM[3]. Indeed, upon administration of Siomycin A in the neuroblastoma cell line N206, a modest depletion of FOXM1 could be observed after 72h (Figure 5.1 A-B, Supplemental Figure 5.3A-B) together with evidence for reduced cell viability (Figure 5.1 C)[4]. Next, we tested Siomycin A in combination with chemotherapeutics frequently used in current neuroblastoma patient treatment protocols. Cisplatin has been described before to act synergistically with Siomycin A in gastroenteropancreatic neuroendocrine tumors[5] and was hence chosen to test in

neuroblastoma cells. Despite previous reports, no synergism could be observed in neuroblastoma cells lines N206, SK-N-SH, IMR-32 and SK-N-AS. In fact, surprisingly, in all cell lines strong antagonistic effects were seen (combination index > 1.5) (Figure 5.1D). Also other combinations with etoposide and doxorubicin resulted in strong antagonistic results (data not shown). Siomycin A is a thiazole antibiotic that targets FOXM1 indirectly via proteasome degradation and therewith also affecting the expression of several other proteins resulting in off target effects and possibly explaining our results.

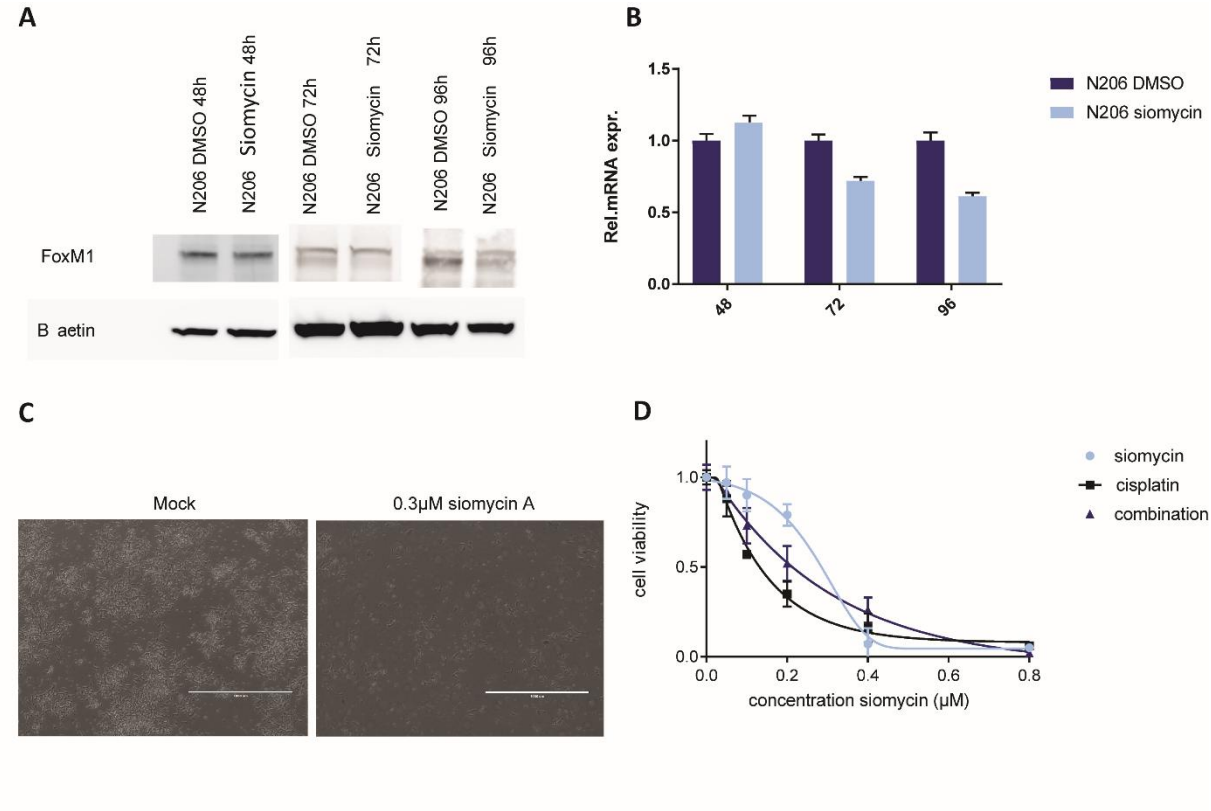

Figure 5.1: Effect of Siomycin A treatment on neuroblastoma cells. (A) Western blots of FOXM1 and the loading control β-actin upon Siomycin A treatment. (B) mRNA levels of FOXM1 after treatment with Siomycin A measured with RTqPCR. Error bars represent the standard error of mean (technical duplicates) (C) N206 neuroblastoma cells with and without Siomycin A treatment. Size of the white bar is 1000µM. (D) Dose response curves of Siomycin A, cisplatin and the combination 72h after treatment in N206 Combination index (CI) is 2.8. Error bars represent standard deviation of 2 biological replicates.

Inhibition of FOXM1 using FDI-6

FDI-6 was identified through a high-throughput library screen and was described as the first presumed "on target" FOXM1 compound[6]. The authors showed that FDI-6 binds directly to the FOXM1 protein and displaces FOXM1 from it genomic targets in MCF-7 breast cancer cells. Indeed, when tested on IMR-32 neuroblastoma cells, knock down of FOXM1 downstream targets was observed 6 hours. after addition of the drug (Figure 5.2A). However, 24h after adding FDI6, FOXM1 downstream targets were upregulated (Figure 5.2B). We tested whether this was also the case in IMR-32 cells depleted for FOXM1 by shRNAs, but in this cell system the expected knock down was still observed (Figure 5.2C). To exclude effects due to fast degradation of the FDI-6 compound, we administered the drug every 12h to the cells, however this didn't affect the outcome (data not shown). Interestingly, in the original report, the authors only showed knock down data no longer than 9h after administration, thus not allowing to compare our results for longer drug exposure.

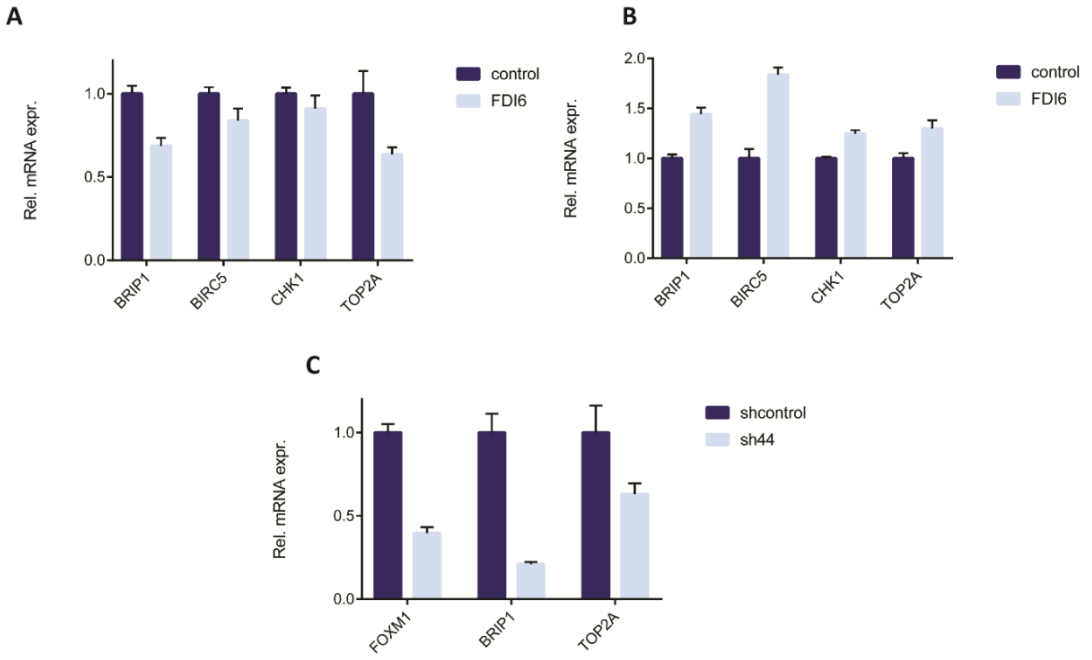

Figure 5.2: Administration of FDI6 in the neuroblastoma cell line IMR-32 (A-B) RT-qPCR results of FOXM1 downstream targets (A) 6 hours after administration of FDI6 (B) and after 24 hours. Error bars represent the standard error of mean (technical duplicates) (C). Relative mRNA expression of FOXM1 and downstream targets after FOXM1 knock down with shRNAs. Error bars represent the standard error of mean (technical duplicates)

Discussion

Because of its important roles in cell proliferation and DNA damage in cancer cells, FOXM1 has been proposed as an important putative novel drug target. So far, several approaches have been described for molecular targeting of FOXM1, amongst others, Siomycin A and FDI-6. We evaluated both Siomycin A and FDI-6 in neuroblastoma cells; however no convincing results could be obtained. In fact, both drugs only introduced a modest effect on FOXM1 levels and either resulted in antagonistic effects in combination experiments with frequently applied chemotherapeutics (siomycin A) or experienced fast drug resistance (FDI-6). Recent discussion revealed that several unpublished data are in line with our observations and support the notion that neither Siomycin A nor FDI-6 are on target compounds to inactivate FOXM1 activity. More recently, a kinase inhibitor MELK-T1, identified through a drug screen by Johnson and Johnson, shown to target the FOXM1 upstream regulator MELK, has been shown to have significant on target effects and will soon be tested extensively in the host lab. While our results were disappointing, this novel drug may hold great promise while further efforts to screen for FOXM1 targeting drugs are warranted.

Material and methods:

Compound administration

Neuroblastoma cell lines were grown as monolayer cultures at 37°C and 5% CO2 as in a humid atmosphere. The culture medium was RPMI 1640 (GIBCO, Life Technologies) containing 10% Fetal Calf Serum (FCS), 2mmol/l glutamine and the following antibiotics: Penicillin (1%), Kanamycin (1%) and Streptomycin (1%). Siomycin A (Sigma Aldrich) and FDI-6 (STK166499; Merlin Consultancy) were dissolved in DMSO and stored as 2mM (Siomycin A) and 5mM (FDI-6) stock solutions at -20°C. Keeping the final concentration of DMSO constant, cells were treated with Siomycin A with concentration ranging from 0 to 0.8µM, with Cisplatin with concentration ranging from 0µM to 48µM and for FDI-6 with a concentration of 10µM, for the time periods indicated. CI for the drugs was calculated using calcusyn.

Western blotting

Protein extraction was done via RIPA buffer and protein concentration was measured using the Lowry protein assay. Protein extracts were separated with SDS-PAGE, blotted on a nitrocellulose membrane and probed with antibodies against FOXM1 (1/1000; 5436S cell signaling), and β-actin (1/10000, A2228, Sigma-Aldrich). Proteins were detected with HRP-conjugated goat anti rabbit IgG antibody (1/15000, A27036, thermos fisher scientific) and developed with ChemiDoc-it imaging system (UVP).

RT-qPCR

RNA isolation was performed using the miRNeasy micro kit, according to the guidelines of the company (Qiagen, catalogue number 217084), including DNAse treatment on column (RNAse-free DNAse set, Qiagen, catalogue number 79254). cDNA synthesis was carried out using 500ng of RNA with the iScript cDNA synthesis kit (Bio-Rad, catalogue number 170-8891). RT-qPCR primers for FOXM1 (AGACACCCATTAAGGAAACG,TTTGTACTGGGCTGAAATCC) and reference genes HPRT1(TGACACTGGCAAAACAATGCA ,GGTCCTTTTCACCAGCAAGCT), YWHAZ(ACTTTTGGTACATTGTGGCTTCAA, CCGCCAGGACAAACCAGTAT), SDHA

(TGGGAACAAGAGGGCATCTG, CCACCACTGCATCAAATTCATG) were designed using primerXL (www.primerXL.org). RT-qPCR reactions were performed in duplicate in a total volume of 5µl, including 2µl of cDNA and 3µl of ssAdvanced SYBR Green qPCR mastermix (Bio-Rad). Cycling conditions were 95°C (15s) – 60°C (15s) – 72°C (60s) and 44 cycli. Data analysis was performed using the qBasePlus software (Biogazelle)

FOXM1 silencing through shRNAs

ShRNA knock down for FOXM1 was achieved using MISSION shRNA (Sigma) TRCN0000015544. Viral production was performed with 15 µg of plasmid in 3 million HEK293TN cells using the calcium phosphate trans-lentiviral packaging system, according to the protocol provided by the manufacturer (Life technologies). The viral particles were concentrated using the PEG-it virus precipitation protocol (System Biosciences) and afterwards transduced in the neuroblastoma cell line IMR-32.

Cell growth assessment

xCELLigence MP (Roche Diagnostics) was used to monitor cell proliferation. Background impedance was measured before seeding the cells using 40µl of RPMI 1640 containing 10% FCS and always subtracted as blank value. $1xE^4$ cells in 50µl of RPMI supplemented with 10% FCS were added. Cell proliferation was measured with a programmed signal detection every hour. Data acquisition and analysis was performed with the RTCA software (version 1.2, Roche Diagnostics).

References:

1. Wang ZB, Park HJ, Carr JR, et al: FoxM1 in Tumorigenicity of the Neuroblastoma Cells and Renewal of the Neural Progenitors. Cancer Research 71:4292-4302, 2011

2. Gentles AJ, Newman AM, Liu CL, et al: The prognostic landscape of genes and infiltrating immune cells across human cancers. Nat Med 21:938-45, 2015

3. Gartel AL: Thiazole Antibiotics Siomycin a and Thiostrepton Inhibit the Transcriptional Activity of FOXM1. Front Oncol 3:150, 2013

4. Zha Y, Xia Y, Ding J, et al: MEIS2 is essential for neuroblastoma cell survival and proliferation by transcriptional control of M-phase progression. Cell Death & Disease 5, 2014

5. Briest F, Berg E, Grass I, et al: FOXM1: A novel drug target in gastroenteropancreatic neuroendocrine tumors. Oncotarget 6:8185-8199, 2015

6. Gormally MV, Dexheimer TS, Marsico G, et al: Suppression of the FOXM1 transcriptional programme via novel small molecule inhibition. Nat Commun 5:5165, 2014

Supplementary Figure:

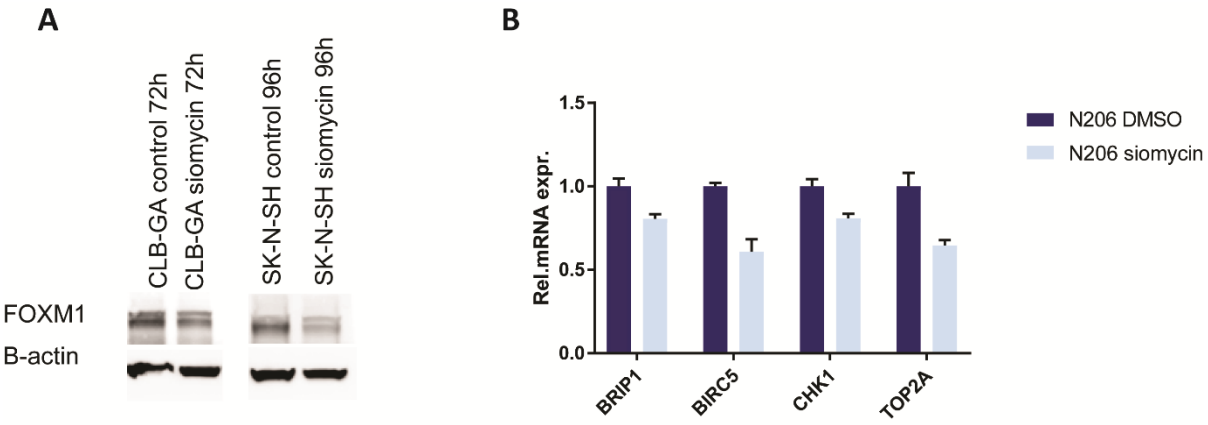

Supplemental Figure 5.3: Validation of Siomycin A efficacy in neuroblastoma cell lines. (A) Western blots of FOXM1 and the loading control β-actin upon Siomycin A treatment in CLB-GA and SK-N-SH. (B) Relative mRNA expression of FOXM1 downstream targets after FOXM1 knock down with Siomycin A. Error bars represent the standard error of mean (technical duplicates)

Chapter 6: Expressed repeat elements improve RT-qPCR normalization across a wide range of zebrafish gene expression studies

Authors: Suzanne Vanhauwaert, Gert Van Peer, Ali Rihani, Els Janssens, Pieter Rondou, Steve Lefever, Anne De Paepe, Paul J. Coucke, Frank Speleman, Jo Vandesompele, Andy Willaert

Published in Plos One, October 2014

Expressed repeat elements improve RT-qPCR normalization across a wide range of zebrafish gene expression studies

Suzanne Vanhauwaert[1], Gert Van Peer[1], Ali Rihani[1], Els Janssens[1], Pieter Rondou[1], Steve Lefever[1], Anne De Paepe[1], Paul J. Coucke[1], Frank Speleman[1], Jo Vandesompele[1,*], Andy Willaert[1,*]

[1]Center of Medical Genetics, Ghent University, Ghent 9000, Belgium

* shared last authors

To whom correspondence should be addressed at: Andy Willaert, Center of Medical Genetics, Ghent University, De Pintelaan 185, Ghent 9000, Belgium. Tel: +32 9 332 4396; Fax: +32 9 332 6549; Email: andy.willaert@ugent.be

Abstract

The selection and validation of stably expressed reference genes is a critical issue for proper RT-qPCR data normalization. In zebrafish expression studies, many commonly used reference genes are not generally applicable given their variability in expression levels under a variety of experimental conditions. Inappropriate use of these reference genes may lead to false interpretation of expression data and unreliable conclusions. In this study, we evaluated a novel normalization method in zebrafish using expressed repetitive elements (ERE) as reference targets, instead of specific protein coding mRNA targets. We assessed and compared the expression stability of a number of EREs to that of commonly used zebrafish reference genes in a diverse set of experimental conditions including a developmental time series, a set of different organs from adult fish and different treatments of zebrafish embryos including morpholino injections and administration of chemicals. Using geNorm and rank aggregation analysis we demonstrated that EREs have a higher overall expression stability compared to the commonly used reference genes. Moreover, we propose a limited set of ERE reference targets (*hatn10*, *dna15ta1* and *loopern4*), that show stable expression throughout the wide range of experiments in this study, as strong candidates for inclusion as reference targets for qPCR normalization in future zebrafish expression studies. Our applied strategy to find and evaluate candidate expressed repeat elements for RT-qPCR data normalization has high potential to be used also for other species.

Introduction

Reverse transcription quantitative PCR (RT-qPCR) is currently regarded as the gold standard for efficient measurement of mRNA gene expression, especially because of its high sensitivity, specificity, accuracy and precision, but also because of its practical simplicity and processing speed. However, variable yields of RNA extraction and reverse transcription and also variable amplification efficiencies can affect RT-qPCR results[1,2]. To correct for technically induced variation and thus measure true biological variation in samples, it is important to apply a good normalization strategy. The use of multiple reference genes as internal controls is the most frequently applied and recommended procedure for normalizing RT-qPCR data[3-7]. In this respect, specific attention should be given to the correct selection and validation of reference genes for normalization, as stated in the MIQE (Minimum Information for Publication of Quantitative Real-Time PCR Experiments) guidelines[1]. The selected reference genes should be stably expressed in the studied samples and should thus show a strong correlation with the total amount of mRNA present in the samples. Importantly, many commonly used reference genes are not generally applicable as their expression stability greatly varies under different experimental conditions[8-11]. Therefore, it is essential to determine the optimal number and choice of reference genes for the specific experimental conditions in every study. A number of studies have measured and compared the expression stability of a set of commonly used reference genes in samples derived from different species, organs, cells, developmental stages, and treatments, using one of the available tools that automatically calculate expression stability values (geNorm, BestKeeper, Normfinder)[8-11]. These studies propose the set of most stably scored reference genes as being the most suitable for normalizing gene expression data. However, the determination of stable reference genes only occurs in a comparative fashion and the detection of the 'most stably' expressed genes does not necessarily mean they are stably expressed in other conditions. Especially developmental time series and the comparison of different tissues are challenging experimental conditions to normalize[8,11,12]. Therefore, the ideal situation of using only one set of reference genes to cover all experimental conditions in a specific species has not been feasible up to now.

To tackle the aforementioned issues, we build upon a new concept, first proposed for

human samples[13-15]. This novel normalization method uses expressed repetitive elements (ERE) as reference targets, instead of protein coding mRNAs. Here, we illustrate the usefulness of this approach for zebrafish expression data. The zebrafish (*Danio rerio*), a small teleost fish, is a popular vertebrate model organism for a number of reasons, including the low maintenance cost, short reproductive cycle, external fertilization and development, production of large numbers of synchronous and rapidly developing embryos per mating and the optical transparency of zebrafish embryos. Moreover, the availability of a wide range of molecular techniques, such as overexpression/knockdown approaches, transgenesis, large-scale genome mutagenesis and lately also highly efficient targeted mutagenesis (using ZFN, TALEN and CRISPR-Cas technology) make zebrafish an excellent tool for high-throughput disease modeling. Finally, molecular genetic mechanisms and cellular physiology are highly similar between zebrafish and other vertebrates, underscoring the relevance of zebrafish for the modeling of human diseases.

We assessed and compared the expression stability of a number of EREs in the zebrafish transcriptome to a set of commonly used zebrafish reference genes in a developmental time series, in different organs from adult fish and under different treatments of zebrafish embryos including morpholino injections and administration of chemicals. Here we demonstrate that EREs outperform classically used reference genes and put forward a selection of EREs as strong candidates for inclusion as reference targets for qPCR normalization in a diverse set of zebrafish experiments. The procedure followed here for identification of zebrafish reference EREs can also easily be applied for other species.

Materials and Methods

Zebrafish maintenance and imaging

Wild-type AB zebrafish, obtained from the zebrafish international resource center (ZIRC) were maintained in 3.5 liter tanks in Zebtec semi-closed recirculation housing systems (Tecniplast, Italy) at a constant temperature of 28 °C and a 14 h light 10 h dark photoperiod. Fish were fed 4 times a day with both dry feed (SDS, UK) and brine shrimps (Ocean Nutrition, Belgium). After *in vitro* fertilization, dead embryos were removed at 8 hpf (hours post fertilization) and at 24 hpf surviving embryos were dechorionated with pronase (Sigma, St. Louis, MO, USA). At 48 hpf or 72 hpf, embryos were anesthetized with 0.016% tricaine methanesulfonate (tricaine) and mounted in 2 % methylcellulose and imaged using a Leica M165FC stereomicroscope. Approval for this study was provided by the local committee on the Ethics of Animal Experiments (Ghent University Hospital, Ghent, Belgium; Permit Number: ECD 11/37). All efforts were made to minimize pain and discomfort.

Morpholino injections

Morpholinos (MOs) are small antisense oligonucleotides that bind the mRNA of interest, resulting in a down regulation of the gene expression. In this screen, MOs targeting *chordin* and *slc2a10* were injected. A scrambled MO was also included as a negative control. *Chordin* encodes for a secreted protein that dorsalizes early vertebrate embryonic tissues and is often used as a positive control in MO experiments[16]. Chordin-MO injected embryos display abnormal u-shaped somites, an expanded blood island and an abnormal tail fin with multiple folds. *Slc2a10* encodes for GLUT10, a member of the glucose transporter family. Recessive mutations in this gene are causing the arterial tortuosity syndrome (ATS)[17]. In zebrafish embryos, knockdown of *slc2a10* using MO injection causes a wavy notochord and cardiovascular abnormalities with a reduced heart rate and blood flow, which was coupled with an incomplete and irregular vascular patterning[18]. Morpholino oligonucleotides were obtained from Gene Tools, LLC (Philomath, OR, USA). The MO against *slc2a10* (5'-CAAATAAAGTCCACTTACTTGGTCC-3') is directed against the exon 2–intron 2 donor splice site of the *slc2a10* pre-mRNA [18]. For *chordin,* the MO is directed against the start codon (5'-

ATCCACAGCAGCCCCTCCATCATCC–3′)[16]. A control MO (5'-CCTCTTACCTCAGTTACAATTTATA-3') was used as a negative control in each experiment. MOs were microinjected in 1.5 nl volume into 1- to 2-cell stage embryos at 7.5 ng for *slc2a10*, 2 ng for *chordin*, and 5 ng for the control MO. All MOs were dissolved in 0.1 % phenol red and 1x Danieu's buffer [58 mM NaCl, 0.7 mM KCl, 0.4 mM MgSO4, 0.6 mM Ca(NO3)2, 5.0 mM HEPES (pH 7.6)]. Microinjection procedures were performed using a Leica M80 stereomicroscope. At 48 hpf, embryos were dechorionated, euthanized with 0.4% tricaine, and triplicate pools of 20 embryos were collected in RNAlater (Sigma-Aldrich, St. louis, USA).

Compound treatments

Two different chemical treatments were performed: embryos were treated with 40 µM of TGFβ type 1 receptor kinase inhibitor (TGFBRI, LY-364947, #L6293, Sigma, St. Louis, USA), or 194 µM of warfarin (Coumadin, #45706 Sigma, St. Louis, USA). TGFBRI specifically targets the TGFBR1 kinase function resulting in the inhibition of phosphorylation of SMAD2 and SMAD3 and down regulation of TGFβ signaling. Treatment of early embryos with this inhibitor results in cardiovascular abnormalities including condensation of the caudal vein plexus, low heart rate and reduced blood flow[18]. Warfarin, is an oral anticoagulant drug used in treatment of thromboembolic diseases[19]. Warfarin acts as a vitamin K antagonist, and vitamin K is needed as a cofactor for the carboxylation of glutamate residues of several clotting factors. Administration of warfarin to early embryos produces teratogenic effects including developmental delay, growth retardation, eye defects, scoliosis and ear defects[20].
TGFBRI and warfarin were prepared as a 20 mM and 80 mM stock solution respectively in DMSO. Working solutions, 0 and 40 µM for TGFBRI and 0 and 194 µM for warfarin, were made in E3 chemical screening medium[21] and as previously described[18,20], embryos were incubated in the compounds starting at 8 hpf (TGFBRI) and 2.5 hpf (warfarin), dechorionated at 24 hpf, euthanized with 0.4% tricaine, and collected in triplicate pools of 20 embryos in RNAlater at 48 hpf (TGFBRI) or 72 hpf (warfarin).

Developmental time series embryos/larvae and dissection of organs from adult zebrafish

At several time points (0 hpf, 8 hpf, 24 hpf, 48 hpf, 72 hpf, 96 hpf, 6 dpf, 8 dpf, 10 dpf and 12 dpf), triplicate pools of 20 embryos/larvae were collected, euthanized with 0.4% tricaine, and stored in RNAlater. Dissection of the eye, brain, skin, testis, liver, intestines and ovaria

from two adult fish was performed as previously described [22]. After dissection, the organs were immediately snap frozen using liquid nitrogen. Subsequently they were sectioned (50 µm) using a Leica CM1900 cryotome and lysed in 700 µl of Qiazol (Qiagen, Germantown, USA).

RT-qPCR

RT-qPCR reactions were performed and reported according to MIQE guidelines[1]. If needed, RNAlater was first removed from samples with a glass Pasteur pipette and RNA isolation was performed using the miRNeasy mini kit (Qiagen) in combination with on-column DNase I treatment using the RNase-Free DNase set (Qiagen) according to the manufacturer's guidelines. RNA quality index (all RQI>8) was measured for all the samples using an Experion automated electrophoresis system (software version 3.2, Bio-Rad). As the RNA concentration of the adult tissue samples was low, whole transcriptome amplification for these samples was executed as previously described (NuGEN) [23]. cDNA was synthesized from 1µg RNA in a 20 µl reaction with the iScript kit (Bio-Rad) using a blend of oligodT and random hexamer primers. qPCR reactions were performed in a total volume of 5 µl, comprising 2.5 µl SsoAdvanced SYBR Green Supermix (Bio-Rad), 5 ng (total RNA equivalents) cDNA and 250 nM (final concentration) of each primer on a LightCycler 480 qPCR instrument (Roche) in 384-well white plates (Bio-Rad). Thermocycling conditions were as follows: 95°C for 2 min, followed by 44 cycles of 95°C for 5 s, 60°C for 30s, 72°C for 1s and finally a melting curve analysis was performed at 95°C for 5s followed by 60°C for 1 min, gradual heating to 95°C at a ramp-rate of 0.11°C/s followed by cooling to 37°C for 3 min. Primers for *bactin2*, *elfa*, *cyp19a1b*, *hprt1*, *rps18*, *tbp*, *rpl13a*, *tuba1* and *b2m* were designed using primerXL software (http://primerxl.org/). Primer sequences for *gapdh* were taken from literature[11]. Primers for the newly identified expressed repeats were designed with primer3 software (http://primer3.ut.ee/) using default settings[24]. Primer efficiencies were tested using a standard dilution series: RNA extracted from different developmental stages of zebrafish embryos (8, 24, 30, 48, 72, 96 hpf) was pooled and converted to cDNA to make a standard dilution series ranging from 16 ng to 0.0625 ng (Supplemental Figure 6.1A). Primer specificity was evaluated using melt-curve analysis (Supplemental Figure 6.1B). Primer efficiencies were also determined using LinRegPCR software[25]. For this, the raw, non-baseline-corrected qPCR data were exported from the LightCycler 480 software and imported into the LinRegPCR

software. A complete overview of all primer sequences and concomitant PCR efficiencies used in this study can be found in Table 6.1 and Supplemental Table 6.1.

Table 6.1. Reference target primer design and calculation of amplification efficiencies.

Reference target (*)	Forward primer	Reverse primer	Amplification efficiency (%)	Primer design
tc1n1	TGTCTGGGTTGGTGTTGTAT	GCTCTGTCGACTTTTGATGT	103.5	Primer3 [22]
dna11ta1	GGGACAACATGAAGGAATTGT	AAAAATGCAGGGTTCCACACA	107.6	Primer3 [22]
tdr7	GCAGCATAATTGAGTACACCC	TTGCCTATATTCACTGAGAAATGGA	102.2	Primer3 [22]
dna15ta1	TACTGTGCTCAAATTGCTTCA	AATGAGTACTGTGAACTTAATCCAT	101.1	Primer3 [22]
cr1-1	GCTCTTCAGTGTTTGAACTCTCAGT	CAATGTAGATTGTGTCAAAGCAG	101.2	Primer3 [22]
hatn8	CAATGACGGTTGGGGTTAGG	TTTAAAAAGGAGGCGTGGCA	102.4	Primer3 [22]
hatn10	TGAAGACAGCAGAAGTCAATG	CAGTAAACATGTCAGGCTAAATAA	104.3	Primer3 [22]
hatn4	ACCCTGATCAAACACACCTG	TCAAGTGCTGTTCAGGTCCTA	105.0	Primer3 [22]
loopern4	TGAGCTGAAACTTTACAGACACAT	AGACTTTGGTGTCTCCAGAATG	109.5	Primer3 [22]
sine3	GGAGACCACATGGGAAAACT	AGAGTCAGGACCTCGGTTTA	101.4	Primer3 [22]
tuba1	TCATCTTCTCCTTCCACACT	GTACGTGGGTGAGGGTAT	107.7	PrimerXL
tbp	AAGTTTACGGTGGACACAAT	CAGGCAACACACCACTTTAT	95.4	PrimerXL
b2m	ACGCTGCAGGTATATTCATC	TCTCCATTGAACTGCTGAAG	94.6	PrimerXL
elfa	GGAGACTGGTGTCCTCAA	GGTGCATCTCAACAGACTT	106.0	PrimerXL
cyp19a1b	AAGGCCATCCTAGTAACCAT	GGTTGTTGGTCTGTCTGATG	101.5	PrimerXL
bactin2	ACGATGGATGGGAAGACA	AAATTGCCGCACTGGTT	99.3	PrimerXL
rpl13α	AGGCTGAAGGTGTTTGATG	TTTCAGACGCACAATCTTGA	91.2	PrimerXL
hprt1	GAGGAGCGTTGGATACAGA	CTCGTTGTAGTCAAGTGCAT	95.7	PrimerXL
rps18	AGTTCTCCAGCCCTCTTATT	TCAACACGAACATTGATGGA	98.7	PrimerXL
gapdh	GTGGAGTCTACTGGTGTCTTC	GTGCAGGAGGCATTGCTTACA	102.5	McCurley [11]

(*)HUGO or repbase identifier.

Statistics and data analysis

The geNorm module in qbase^{+} version 2.5 (Biogazelle, http://www.qbaseplus.com) was used to compute expression stability values for all reference targets. As input for geNorm analysis, either Cq values exported directly from the LightCycler 480 software or efficiency-corrected Cq values from LinRegPCR that were calculated based on the raw, non-baseline-corrected LightCycler 480 qPCR data, were used. GeNorm calculates the gene expression stability measure M (M-value) for a reference gene as the average pairwise variation V for that gene with all other tested reference genes. Stepwise exclusion of the gene with the highest M value allows ranking of the tested genes according to their expression stability. GeNorm was also used to dertermine the optimal number of reference targets for every experiment. The geNorm algorithm determines the pairwise variation Vn/n+1, between two sequential normalization factors containing an increasing number of genes. A large variation means that the added gene has a significant effect and should preferably be included for calculation of a reliable normalization factor. Vandesompele *et al.* (2002) [7] used 0.15 as a cut-off value, below which the inclusion of an additional reference gene is not required.

Rank aggregation analysis was performed in the R statistical programming environment (version 3.0.2) using the Rankaggreg package (version 0.4-3) [26] to determine the best ranked reference genes across all experiments.

Results

Identification of candidate expressed repeat element (ERE) reference targets in the zebrafish genome

Candidate ERE reference targets in the zebrafish genome were extracted from Repbase (http://www.girinst.org/repbase), a database of repetitive DNA elements from different organisms[27] (Figure 6.1). From an initial set of 1172 repetitive elements present in the zebrafish genome, only those having more than 100 copies in the genome were retained, leaving us with 74. To identify the number of expressed loci per repetitive element, a blastn search against all RefSeq and non-RefSeq annotated transcripts known for zebrafish was carried out using the consensus repeat sequence listed in Repbase. Only repeats with a total number of combined RefSeq and non-RefSeq blast hits above 30 and with a mean conservation rate higher than 85% (indicated by Repbase) were retained, resulting in 10 candidate EREs for further analysis (*tc1n1, dna11ta1, tdr7, dna15ta1, cr1-1, hatn8, hatn10, hatn4, loopern4, sine3*). The thresholds of 30 and 85% were empirically determined in order to have a top-ranked list containing a manageable number of candidate expressed repeat elements. Next, qPCR assays were designed to target the most conserved region of the selected EREs (Table 6.1 and Supplemental Figure 6.2). Blasting of the primer sequences against the zebrafish RefSeq RNA database using primer-BLAST (http://www.ncbi.nlm.nih.gov/tools/primer-blast/) revealed that the amplified ERE fragments are exclusively located in untranslated gene regions, predominantly 3'UTR.

To investigate the potential of EREs for qPCR normalization, we aimed to compare the expression stability of the 10 candidate EREs with that of 10 commonly used reference genes in zebrafish studies. The reference genes *bactin2*, *elfa*, *cyp19a1b*, *hprt1*, *rps18*, *tbp*, *rpl13a*, *tuba1*, *b2m* and *gapdh* were selected because of their frequent use in zebrafish expression studies. The amplification efficiency of all primer pairs was assessed using a zebrafish cDNA dilution series as a template, wherein efficiencies between 90 and 110% were attained indicating sufficient reaction efficiencies (Table 6.1 and Supplemental Table 6.1).

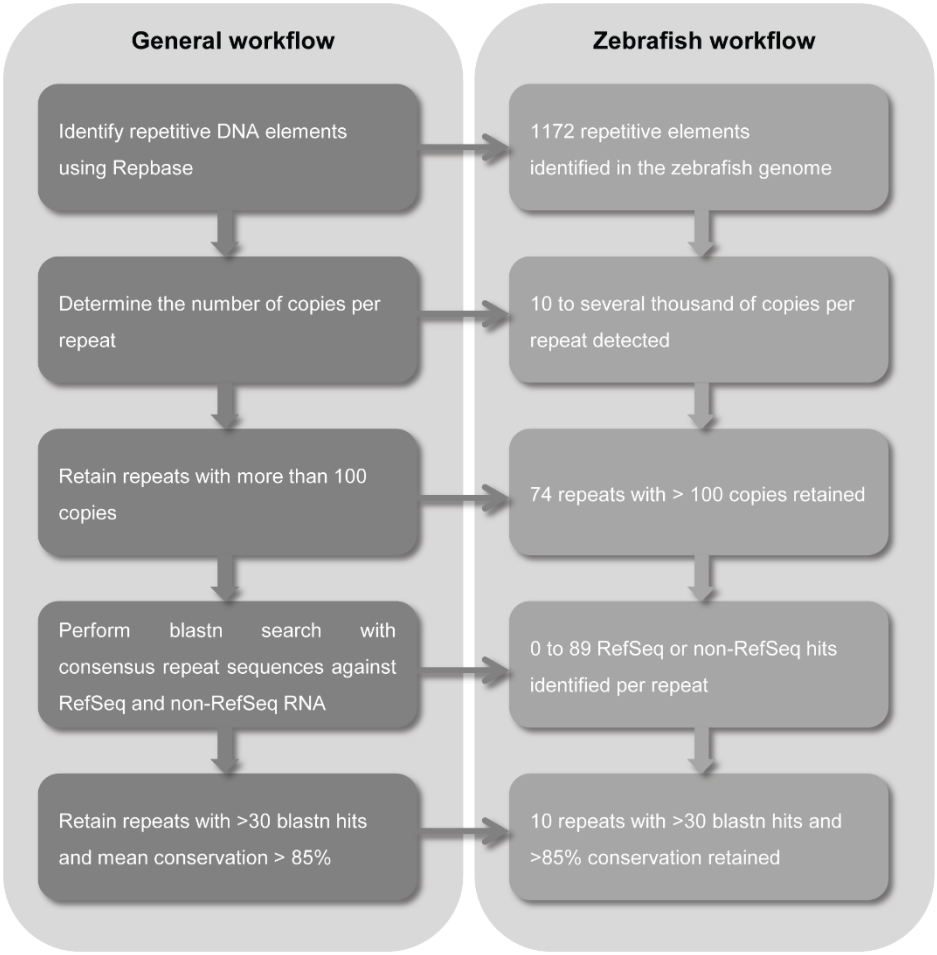

Figure 6.1. Workflow to identify candidate expressed repeat elements.

Determination of reference target expression stabilities under a wide range of conditions

For the 20 candidate reference targets (10 EREs and 10 commonly used reference genes) mRNA expression levels were measured in a wide range of experimental settings including a zebrafish developmental time series (0 hpf up to 12 dpf), a set of different organs dissected from adult fish and a set of different treatments of zebrafish embryos including the administration of chemicals and injection of morpholinos (MO) (see Methods). The average expression stability for each of the reference targets in the 4 different types of experiments was calculated using the geNorm algorithm. Reference genes are ranked according to their expression stability value (referred to as the M-value) [7]; in addition, the optimal number of genes for normalization is determined for each experiment. Reference targets with M-values below 0.5 and 0.2 are considered having a 'high' and 'very high' expression stability, respectively [12]. In the experiments where embryos were treated with compounds or injected

with MOs almost all reference targets had a 'high' expression stability and a considerable number of reference targets showed a 'very high' expression stability (Figure 6.2A-D).

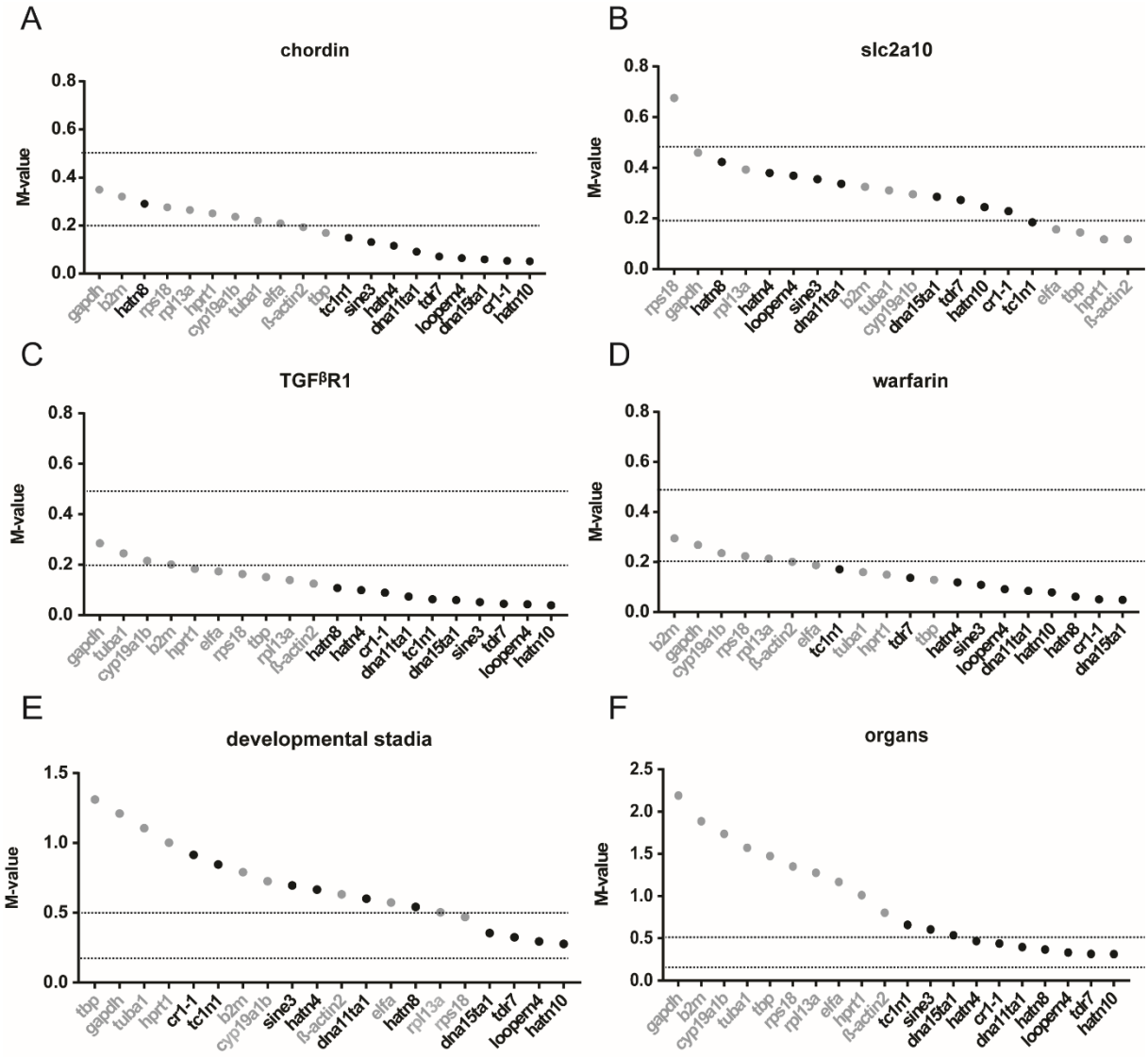

Figure 6.2. Average expression stability of common reference genes and expressed repeat elements.

Ranking of reference targets depending on their M-values calculated by geNorm. Reference targets with M-values below 0.5 and 0.2 are considered having a 'high' and 'very high' expression stability, respectively. EREs are indicated in black, commonly used reference mRNAs in grey.

In general, the EREs showed higher expression stabilities (lower M-values) compared to the reference genes, although differences in M-values are small. In the developmental time series and the comparison of the different zebrafish organs, the M-value distribution was more dispersed with relatively low expression stability (M>0.5) for the reference genes and 'high' to 'very high' expression stability for a considerable number of EREs (Figure 6.2E,F). In the time series, the ERE *hatn10,* was identified as the best reference target, with an M-value around 0.3, while the best performing mRNA reference gene was *rps18* with an M-value around 0.6 (Figure 6.2E). Of note, *gapdh*, a frequently used reference target in zebrafish, had an M-value of 1.5, which is considered as highly unstable. In the different zebrafish organs (Figure 6.2F) the best reference target is the ERE *hatn10*, with an M-value of 0.3, while the best classically used reference gene, *bactin2*, had an M-value of only 0.8. Similar results were obtained by performing a geNorm analysis for the 6 different experiments, using efficiency-corrected Cq values that were determined by linear regression analysis of qPCR fluorescence data using LinRegPCR software (Supplemental Figure 6.3)[25]. To determine the optimal number of reference targets to be used in the different experiments, the $V_{n/n+1}$ value was calculated using geNorm (see Materials and Methods). This analysis indicated that for each experimental condition the inclusion of the best two reference targets is sufficient for adequate normalization as indicated by $V_{2/3}$ values below 0.15 (Supplemental Figure 6.4, 0.15 threshold according to Vandesompele *et al.* (2002)[7]). In 5 out of 6 conditions the best two reference targets were EREs.

Finally, we aimed to identify the most stably expressed reference targets throughout the different experiments performed. A rank aggregation method based on voting theory (Borda count) was used to combine the 6 ranked lists of reference targets, generated for the 6 different experiments. This method tries to find an ordered list of reference assays as close as possible to all individual ordered lists by calculating the weighted Spearman's footrule distance, and using a cross-entropy Monte Carlo algorithm or genetic algorithm. The analysis of the 6 ordered reference target lists, clearly demonstrated that most of the EREs showed a higher overall expression stability compared to most of the commonly used reference genes, as evidenced by lower ranks and by the lower median M-value (Student's t-test; $p<0.001$) and smaller spread of the M-value (Student's t-test; $p<0.001$) (Figure 6.3A,B), with the highest stability for ERE *hatn10*. In each of the 6 experiments, *hatn10* had an M-value below

0.5 and this ERE was found to be the most stably expressed reference target in 4 out of 6 experiments, indicating that *hatn10* is an interesting candidate for inclusion as a reference target in a broad range of experiments.

Assessment of the validity of ERE reference targets versus common reference genes to normalize genes of interest

To test the accuracy of qPCR results after normalization with either frequently used reference genes (*gapdh*, *bactin2* and *elfa*) or ERE reference targets (*hatn10*, *dna15ta1* and *loopern4*), the expression of known differentially expressed genes was measured in a diverse set of experimental conditions (developmental time series, different organs, morpholino and compound treatments).

According to earlier reports, *zorba* transcripts are only present in zebrafish embryos until the mid-blastula transition (MBT) at about 3.5 hpf, after which zygotic transcription is initiated[28,29]. This means that *zorba* transcripts are strictly maternally derived with almost no zygotic transcription. This was validated by microarray data reported by Yang *et al.* (2013)[30], where transcriptomes were compared between different developmental stages in zebrafish embryos. We looked at *zorba* expression in a developmental time series using RT-qPCR and normalized the data either with frequently used reference genes or with ERE reference targets. When using the ERE's as reference targets, a more than 20 fold expression difference was noted between the 0 hpf (maternal) and 8 hpf (zygotic) time points, confirming that *zorba* transcripts are almost exclusively maternally derived (Figure 6.4A). When applying the classic reference genes for normalization, only a threefold expression difference was observed, falsely indicating a relatively small expression difference for *zorba* between maternal and zygotic transcription stages.

During early embryogenesis, the *pax6a* gene is expressed in specific parts of the developing brain, although from larval stages on, expression gets more restricted to the eye[31]. Predominant eye expression of *pax6a* is further evidenced by microarray expression analysis (own data, not shown) revealing a 25% higher *pax6a* expression in the adult zebrafish eye compared to the brain. We looked at *pax6a* RT-qPCR expression levels in different organs from adult zebrafish. When expression levels were normalized to the ERE reference targets, the higher expression of *pax6a* in the eye versus the brain could be confirmed (Figure 6.4B).

In contrast, normalization to the common reference genes resulted in an unexpectedly higher expression of *pax6a* in the brain compared to the eye.

In zebrafish embryos, knockdown of *slc2a10* using MO injection affects the expression of a number of genes involved in cardiovascular development, as evidenced by microarray expression analysis[18]. One of these prototypical affected genes is *acta2*, showing a small upregulation upon *slc2a10* knockdown. We conducted RT-qPCR expression analysis for *acta2* and revealed that both common reference gene and ERE normalization resulted in a similar slight upregulation of the *acta2* gene after *slc2a10* MO injection (Figure 6.4C). The *acta2* gene is also known to be upregulated upon treatment with TGFBRI compound to a greater extent than after *slc2a10* MO injections[18]. We confirmed a threefold overexpression of *acta2* upon administration of TGFBRI compound, both after common reference gene and ERE normalization (Figure 6.4D).

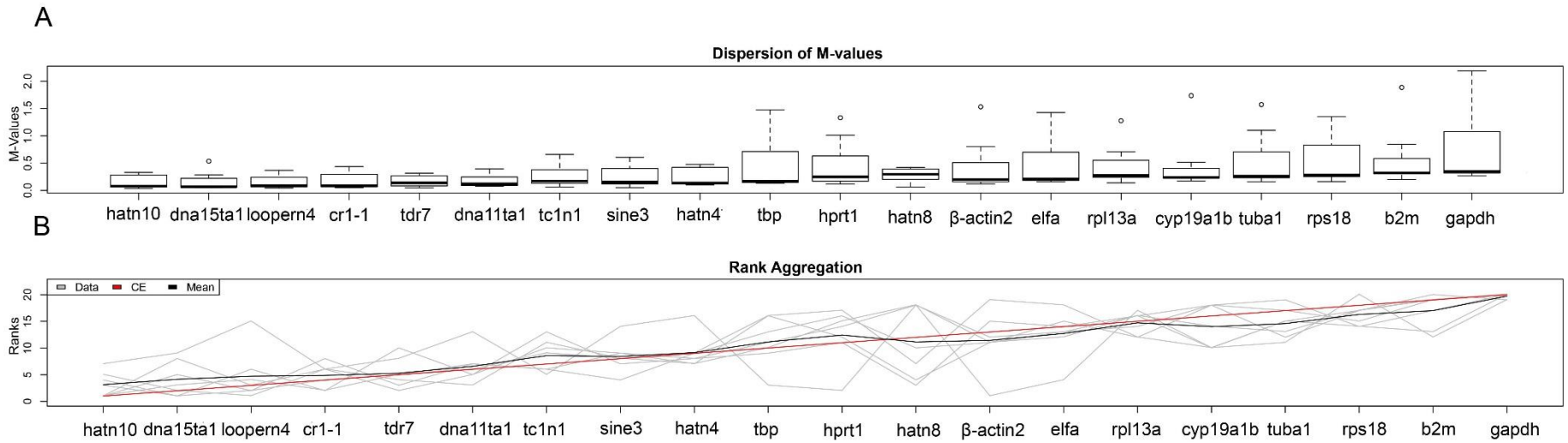

Figure 6.3. Rank aggregation analysis.

A: Box plot representation of dispersion of the M-value. Boxes depict first and third quartile and the median is indicated with a line in the middle of the box, outliers are drawn as circles. Reference targets are ranked according to rank aggregation outcome (most stable reference targets on the left). **B**:Rank aggregation analysis ordering the reference genes, based on their rank position according to each stability measurement (grey lines), from the most stable (left) to the least stable (right). Mean rank position of each gene is shown in black, as well the model computed by the Monte Carlo algorithm (red line). All EREs, except for *sine3*, are ranked better than the commonly used reference genes. .

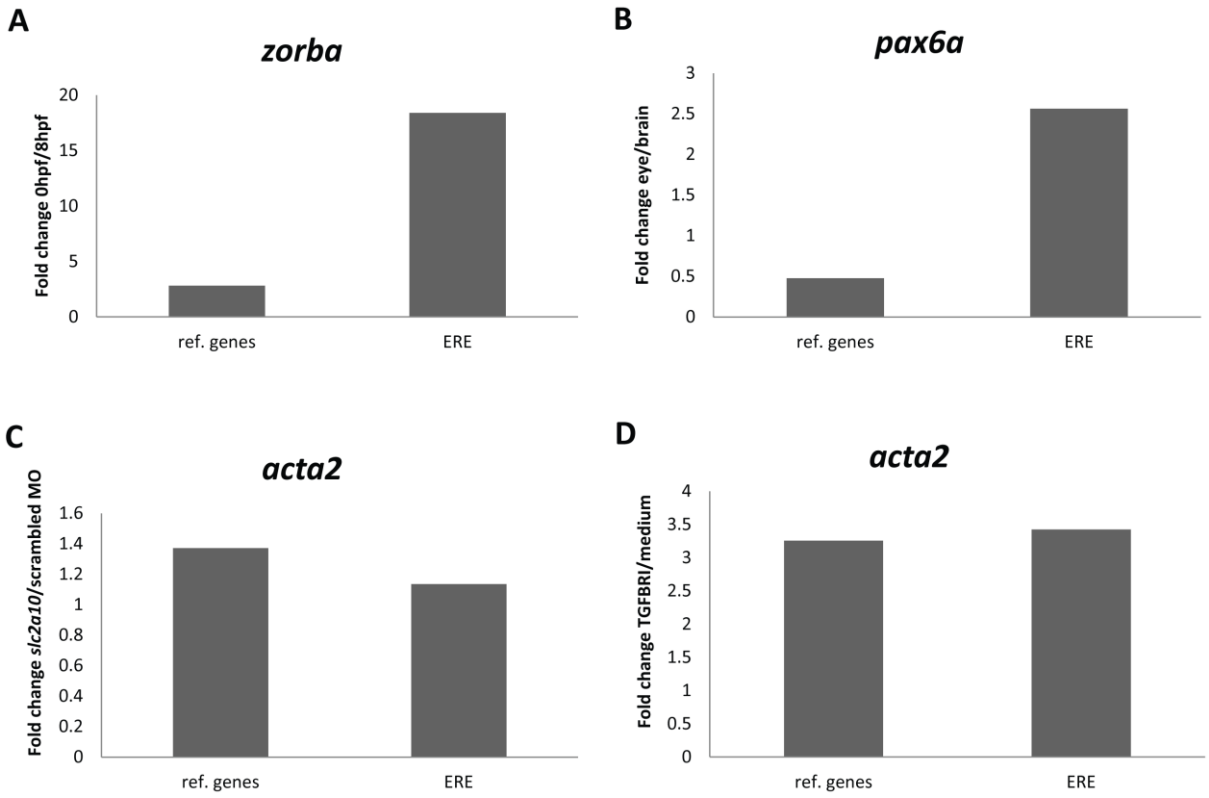

Figure 6.4. Fold change expression of selected genes of interest after normalization with common reference genes (ref. genes) and with ERE reference targets (ERE).

A: Fold change expression of *zorba* between 0 hpf and 8 hpf. **B:** Fold change expression of *pax6a* between adult zebrafish eye and brain tissues. **C:** Fold change expression of *acta2* between slc2a10 MO and scrambled MO injections. **D:** Fold change expression of *acta2* between TGFBRI compound and screening medium treatment.

Discussion

Several reports indicate that, even within a species, no single gene can be regarded as an ideal reference gene for the normalization of qPCR data across diverse sample types and experimental situations[8,10,32]. This is due to variations in expression levels of these genes across different experimental conditions, developmental stages or across different tissues or cells. In this study, we specifically aimed to identify a set of reference targets that are stably expressed over a diverse set of samples obtained from the zebrafish, a model organism which is becoming increasingly popular in disease modeling, developmental studies and toxicology. Our strategy was based on the identification of specific types of repetitive elements that have spread throughout the zebrafish genome during evolution and that are also present in genomic sequences that are transcribed to RNA. With a single pair of RT-qPCR primers, one specific expressed repetitive element (ERE) can be amplified, thereby simultaneously detecting numerous different transcripts in which the specific ERE is present. The underlying assumption is that by measuring many transcripts at the same time, differential expression of a few of them will not drastically alter the total level of ERE expression. Therefore, expression of this set of repeats is expected to be highly stable throughout different experimental situations, as it serves as an estimation of the general mRNA fraction abundance. The use of expressed repeat elements was first presented by Vandesompele *et al.* (2nd International qPCR Symposium, Freising-Weihenstephan, Germany, September 6, 2005) and subsequently confirmed by Marullo *et al.* (2010)[13] where primate specific Alu repeats were used for normalization of biomarkers in human blood. Recently, it has been reported that expressed Alu repeats can be successfully used as a normalization factor in RT-qPCR experiments where human cancer cells were subjected to various perturbations[14] or in human embryonic stem cell differentiation experiments[15].

In this study, 10 different zebrafish EREs were selected as candidate normalization targets based on a minimal number of expressed copies and conservation score. Subsequently, expression stability of these EREs and 10 commonly used reference mRNAs for zebrafish studies were compared. The standard reference genes are involved in different cellular processes and structures such as metabolism (*hprt1, gapdh*), transcription (*tbp*), translation (*elfa*), cytoskeletal structure (*bactin2, tuba1*), major histocompatibility complex (*b2m*) and steroid biosynthesis (*cyp19a1b*), thus avoiding co-regulation upon different

treatments[11,32,33]. We did not include the frequently used rRNA transcripts (e.g. 18S and 28S rRNA) into this study. Indeed, while rRNA represents more than 90% of total RNA, it has been shown that the rRNA to mRNA ratio can vary depending on the experimental condition[34-36]. Moreover, the high abundance of rRNA compared to mRNA may hamper the correction of the baseline fluorescence in qPCR data analysis[7,37]. Finally, rRNA is transcribed by a different endogenous RNA polymerase, is not polyadenylated, and has a different function compared to mRNA, making ribosomal RNA a non-representative form of RNA for normalization of mRNA. Therefore, the use of rRNA as a normalization factor in qPCR experiments is not recommended and could lead to false interpretation of the data.

Expression stabilities were tested in a diverse sample set, covering different experimental setups in zebrafish research, including morpholino and compound treated samples and samples from different developmental stages and from different adult tissues. Especially for the latter two sample types, good quality normalization factors are difficult to find[11], most likely because of dramatic changes in expression profiles during zebrafish development and major differences in expression between different matured organs[30,38]. Indeed, expression analysis in different developmental stages and tissues from zebrafish, revealed a poor expression stability of all commonly used reference mRNAs with M-values higher than 0.5, implying that these genes are not suitable for reliable normalization of expression data in these experimental conditions. Strikingly, the expression of one of the most frequently used reference genes, *gapdh*, is the least stable of all reference targets tested in this study. In keeping with this observation, previous studies in vertebrate tissues and cell lines have already reported on the poor performance of *gapdh* as an internal reference gene and on its expression variability[39-43]. Consequently, we would strongly discourage further use of *gapdh* as reference gene for normalization in zebrafish experiments. Remarkably, most of the zebrafish EREs performed very well, with in many cases M-values below 0.5, signifying a high expression stability, thus clearly marking EREs as the reference target of choice in these experimental conditions. The robustness of ERE normalization for expression analysis in different developmental stages and tissues from zebrafish was further evidenced by the validation of known differential expression levels for respectively the *zorba* and *pax6a* genes. Normalization with common reference genes resulted in completely different expression patterns, leading to false interpretation of the data. The performance of EREs in terms of stability is less pronounced in perturbation experiments such as compound

treatments or morpholino injections. While almost all reference targets scored relatively well, again expression stability of the EREs was generally better than for the common reference genes. The relatively good performance of all reference targets, regardless of their nature, in compound and morpholino experiments reflects the more subtle impact of these treatments on the general expression profile in zebrafish embryos. Indeed, validation of known differential expression levels for the *acta2* gene in these conditions revealed no major difference between both normalization strategies.

To identify the most stably expressed reference targets throughout all different experiments performed, we conducted a rank aggregation analysis. This analysis indicates that the expression stability of the EREs was better than for the common reference genes. ERE *hatn10*, *dna15ta1* and *loopern4* represent the most stable reference targets with M-values ≤ 0.5 in all 6 experiments. We recommend including at least these 3 genes in zebrafish gene expression studies for evaluation of their suitability as normalization targets.

The MIQE guidelines from 2009 emphasize the need for accurate normalization of RT-qPCR data in order to obtain reliable expression data. However, a recent paper in Nature Methods that surveyed 1700 publications with qPCR-based data from 2009 to 2013 reported the poor application of these guidelines including inadequate normalization procedures with widespread use of single, unvalidated reference genes[44]. It has long been recognized that this can lead to unreliable results, in particular for measuring subtle differences in expression levels. Our study fully complies with the MIQE guidelines and tackles the issue of proper normalization in zebrafish expression studies, by providing for the first time a set of robust candidate reference targets to normalize RT-qPCR data in a wide range of zebrafish experiments. EREs have the potential to dramatically facilitate and improve gene expression studies in zebrafish. In addition, the bio-informatics strategy outlined for identification and validation of such EREs in this study can be applied to other organisms. As such, we expect similar ERE qPCR assays to be developed and used in other model organisms for normalization purposes.

Acknowledgments

We are indebted to Petra Vermassen for expert technical assistance.

References

1. Bustin SA, Benes V, Garson JA, et al: The MIQE guidelines: minimum information for publication of quantitative real-time PCR experiments. Clin Chem 55:611-22, 2009
2. Derveaux S, Vandesompele J, Hellemans J: How to do successful gene expression analysis using real-time PCR. Methods 50:227-30, 2010
3. Dheda K, Huggett JF, Chang JS, et al: The implications of using an inappropriate reference gene for real-time reverse transcription PCR data normalization. Anal Biochem 344:141-3, 2005
4. Goossens K, Van Poucke M, Van Soom A, et al: Selection of reference genes for quantitative real-time PCR in bovine preimplantation embryos. BMC Dev Biol 5:27, 2005
5. Kim BS, Rha SY, Cho GB, et al: Spearman's footrule as a measure of cDNA microarray reproducibility. Genomics 84:441-8, 2004
6. Tricarico C, Pinzani P, Bianchi S, et al: Quantitative real-time reverse transcription polymerase chain reaction: normalization to rRNA or single housekeeping genes is inappropriate for human tissue biopsies. Anal Biochem 309:293-300, 2002
7. Vandesompele J, De Preter K, Pattyn F, et al: Accurate normalization of real-time quantitative RT-PCR data by geometric averaging of multiple internal control genes. Genome Biol 3:RESEARCH0034, 2002
8. Dhorne-Pollet S, Thelie A, Pollet N: Validation of novel reference genes for RT-qPCR studies of gene expression in Xenopus tropicalis during embryonic and post-embryonic development. Dev Dyn 242:709-17, 2013
9. Jacob F, Guertler R, Naim S, et al: Careful selection of reference genes is required for reliable performance of RT-qPCR in human normal and cancer cell lines. PLoS One 8:e59180, 2013
10. Ledderose C, Heyn J, Limbeck E, et al: Selection of reliable reference genes for quantitative real-time PCR in human T cells and neutrophils. BMC Res Notes 4:427, 2011
11. McCurley AT, Callard GV: Characterization of housekeeping genes in zebrafish: male-female differences and effects of tissue type, developmental stage and chemical treatment. BMC Mol Biol 9:102, 2008
12. Hellemans J, Mortier G, De Paepe A, et al: qBase relative quantification framework and software for management and automated analysis of real-time quantitative PCR data. Genome Biol 8:R19, 2007
13. Marullo M, Zuccato C, Mariotti C, et al: Expressed Alu repeats as a novel, reliable tool for normalization of real-time quantitative RT-PCR data. Genome Biol 11:R9, 2010
14. Rihani A, Van Maerken T, Pattyn F, et al: Effective Alu repeat based RT-Qpcr normalization in cancer cell perturbation experiments. PLoS One 8:e71776, 2013
15. Vossaert L, O'Leary T, Van Neste C, et al: Reference loci for RT-qPCR analysis of differentiating human embryonic stem cells. BMC Mol Biol 14:21, 2013
16. Nasevicius A, Ekker SC: Effective targeted gene 'knockdown' in zebrafish. Nat Genet 26:216-20, 2000

17. Coucke PJ, Willaert A, Wessels MW, et al: Mutations in the facilitative glucose transporter GLUT10 alter angiogenesis and cause arterial tortuosity syndrome. Nat Genet 38:452-7, 2006

18. Willaert A, Khatri S, Callewaert BL, et al: GLUT10 is required for the development of the cardiovascular system and the notochord and connects mitochondrial function to TGFbeta signaling. Hum Mol Genet 21:1248-59, 2012

19. Rojas JC, Aguilar B, Rodriguez-Maldonado E, et al: Pharmacogenetics of oral anticoagulants. Blood Coagul Fibrinolysis 16:389-98, 2005

20. Weigt S, Huebler N, Strecker R, et al: Developmental effects of coumarin and the anticoagulant coumarin derivative warfarin on zebrafish (Danio rerio) embryos. Reprod Toxicol 33:133-41, 2012

21. Murphey RD, Zon LI: Small molecule screening in the zebrafish. Methods 39:255-61, 2006

22. Gupta T, Mullins MC: Dissection of organs from the adult zebrafish. J Vis Exp, 2010

23. Vermeulen J, Derveaux S, Lefever S, et al: RNA pre-amplification enables large-scale RT-qPCR gene-expression studies on limiting sample amounts. BMC Res Notes 2:235, 2009

24. Untergasser A, Cutcutache I, Koressaar T, et al: Primer3--new capabilities and interfaces. Nucleic Acids Res 40:e115, 2012

25. Ruijter JM, Ramakers C, Hoogaars WM, et al: Amplification efficiency: linking baseline and bias in the analysis of quantitative PCR data. Nucleic Acids Res 37:e45, 2009

26. Pihur V, Datta S, Datta S: RankAggreg, an R package for weighted rank aggregation. BMC Bioinformatics 10:62, 2009

27. Jurka J, Kapitonov VV, Pavlicek A, et al: Repbase Update, a database of eukaryotic repetitive elements. Cytogenet Genome Res 110:462-7, 2005

28. Bally-Cuif L, Schatz WJ, Ho RK: Characterization of the zebrafish Orb/CPEB-related RNA binding protein and localization of maternal components in the zebrafish oocyte. Mech Dev 77:31-47, 1998

29. Kimmel CB, Ballard WW, Kimmel SR, et al: Stages of embryonic development of the zebrafish. Dev Dyn 203:253-310, 1995

30. Yang H, Zhou Y, Gu J, et al: Deep mRNA sequencing analysis to capture the transcriptome landscape of zebrafish embryos and larvae. PLoS One 8:e64058, 2013

31. Lakowski J, Majumder A, Lauderdale JD: Mechanisms controlling Pax6 isoform expression in the retina have been conserved between teleosts and mammals. Dev Biol 307:498-520, 2007

32. Casadei R, Pelleri MC, Vitale L, et al: Identification of housekeeping genes suitable for gene expression analysis in the zebrafish. Gene Expr Patterns 11:271-6, 2011

33. Tang R, Dodd A, Lai D, et al: Validation of zebrafish (Danio rerio) reference genes for quantitative real-time RT-PCR normalization. Acta Biochim Biophys Sin (Shanghai) 39:384-90, 2007

34. Hansen MC, Nielsen AK, Molin S, et al: Changes in rRNA levels during stress invalidates results from mRNA blotting: fluorescence in situ rRNA hybridization permits renormalization for estimation of cellular mRNA levels. J Bacteriol 183:4747-51, 2001

35. Huggett J, Dheda K, Bustin S, et al: Real-time RT-PCR normalisation; strategies and considerations. Genes Immun 6:279-84, 2005

36. Solanas M, Moral R, Escrich E: Unsuitability of using ribosomal RNA as loading control for Northern blot analyses related to the imbalance between messenger and ribosomal RNA content in rat mammary tumors. Anal Biochem 288:99-102, 2001

37. Hendriks-Balk MC, Michel MC, Alewijnse AE: Pitfalls in the normalization of real-time polymerase chain reaction data. Basic Res Cardiol 102:195-7, 2007

38. Abramsson A, Westman-Brinkmalm A, Pannee J, et al: Proteomics profiling of single organs from individual adult zebrafish. Zebrafish 7:161-8, 2010

39. Barber RD, Harmer DW, Coleman RA, et al: GAPDH as a housekeeping gene: analysis of GAPDH mRNA expression in a panel of 72 human tissues. Physiol Genomics 21:389-95, 2005

40. Bustin SA: Absolute quantification of mRNA using real-time reverse transcription polymerase chain reaction assays. J Mol Endocrinol 25:169-93, 2000

41. Bustin SA: Quantification of mRNA using real-time reverse transcription PCR (RT-PCR): trends and problems. J Mol Endocrinol 29:23-39, 2002

42. Dheda K, Huggett JF, Bustin SA, et al: Validation of housekeeping genes for normalizing RNA expression in real-time PCR. Biotechniques 37:112-4, 116, 118-9, 2004

43. Lin J, Redies C: Histological evidence: housekeeping genes beta-actin and GAPDH are of limited value for normalization of gene expression. Dev Genes Evol 222:369-76, 2012

44. Bustin SA, Benes V, Garson J, et al: The need for transparency and good practices in the qPCR literature. Nat Methods 10:1063-7, 2013

Supplementary Figures

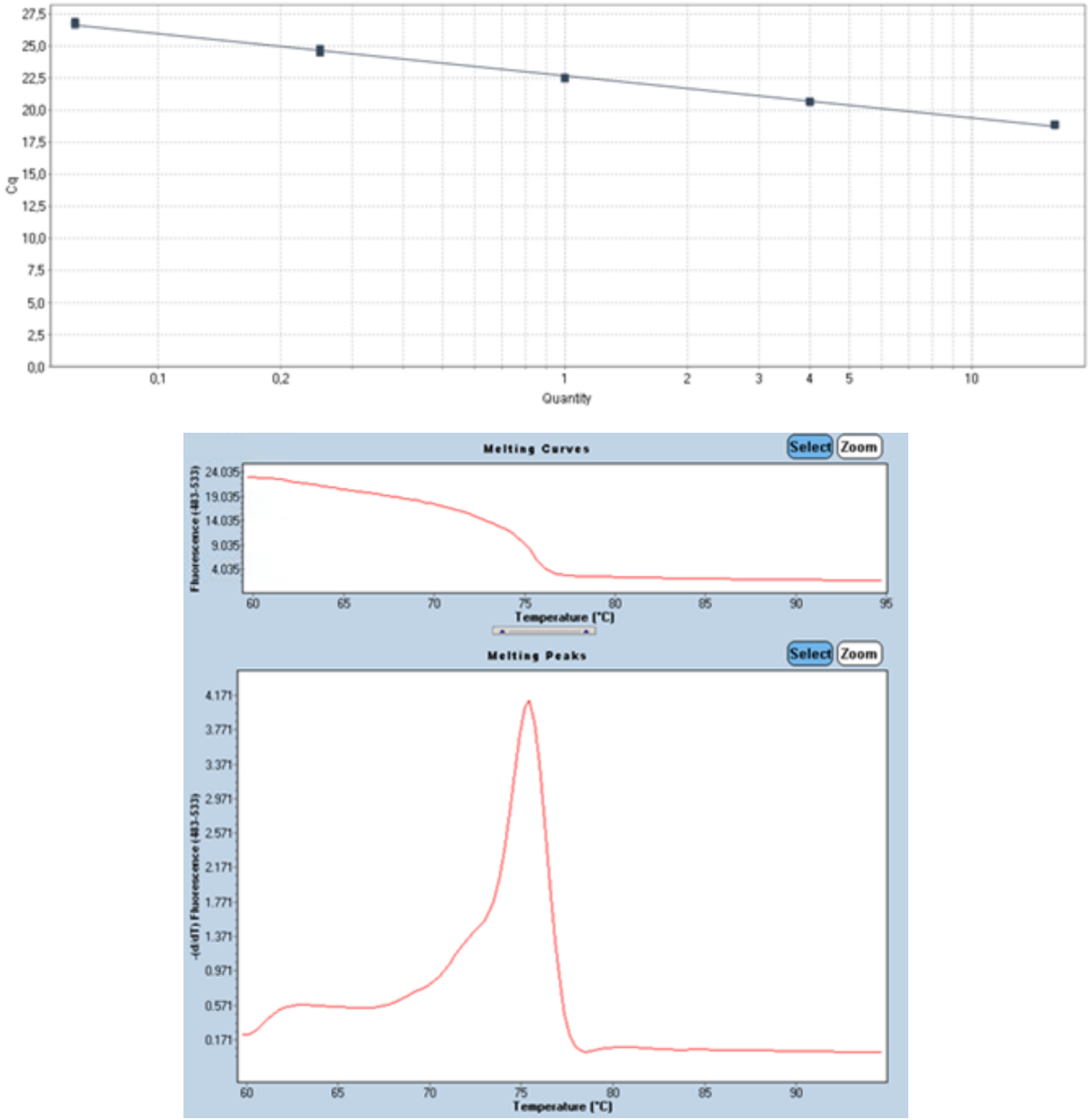

Supplemental Figure 6.1. Representative example of an ERE standard dilution and melting curve.

A: Standard dilution curve, used to determine the primer amplification efficiency of the *dna15ta1* primer set. In this example Cq values obtained for the *dna15ta1* primer set are plotted against the cDNA quantity (ng) (exported from qbase+ software). For each quantity two technical replicates are included. **B:** Melting curve analysis for the *dna15ta1* primer set (exported from LightCycler 480 software). On top, the sample fluorescence is plotted against temperature. Below, the first negative derivative of the sample fluorescence is plotted against temperature, displaying the melting temperature as a peak. In this example, there is a single sharp peak from an amplicon having a Tm of 76 °C, indicating the specificity of the *dna15ta1* primer set.

Supplemental Figure 6.2. Schematic representation of ERE primer design (hypothetical example).

The full-length repeat element (dark grey line, top) and a number of aligned repeat element containing fragments obtained from a combined RefSeq/non-RefSeq blastn search are depicted. In a first step we determine the part of the ERE sequence that is most frequently expressed. To delineate this area, all RefSeq and non-RefSeq blast results are aligned with the consensus repeat sequence and sequences that are commonly present in most of the fragments are used as a template for primer design using primer 3 with default settings.

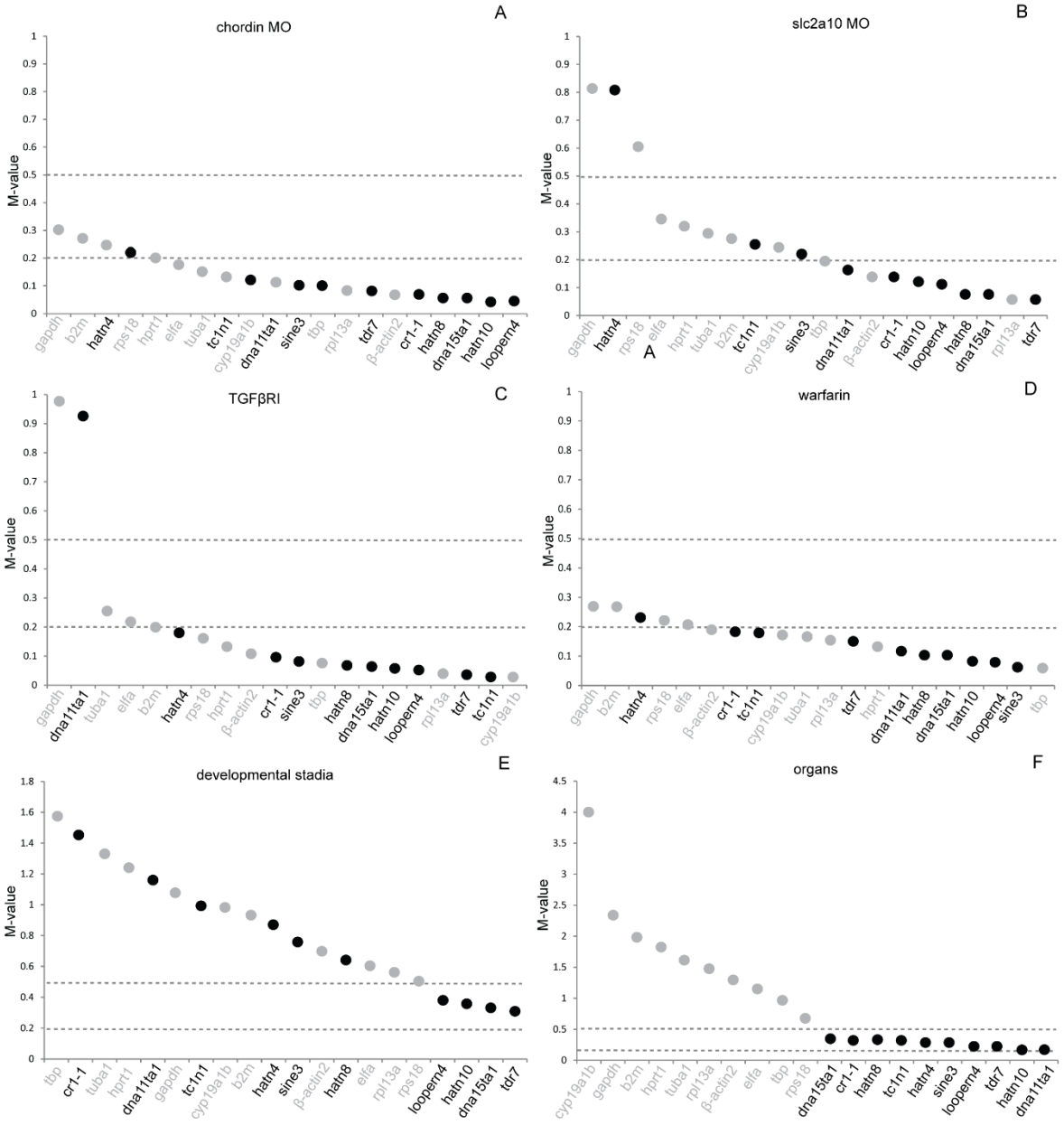

Supplemental Figure 6.3. Average expression stability of common reference genes and expressed repeat elements (based on LinRegPCR corrected Cq values).

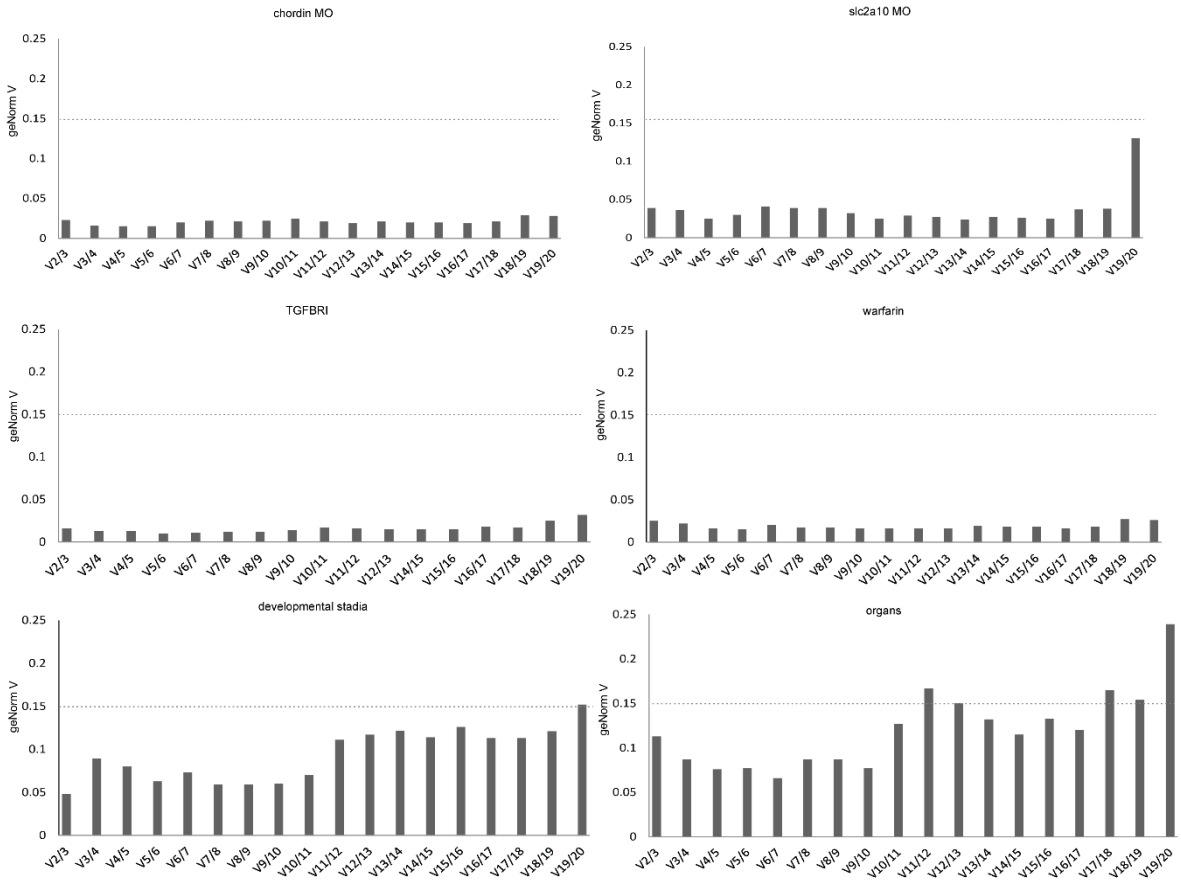

Supplemental Figure 6.4. GeNorm calculated pairwise variation $V_{n/n+1}$ values for the different experimental conditions.

The optimal number of reference targets (n) is reached, when the inclusion of the next reference target (n+1) reduces the $V_{n/n+1}$ value below 0.15. For every experiment the $V_{2/3}$ value is lower than 0.15, indicating that the inclusion of only two reference targets, the ones with the lowest M-value, is sufficient for adequate normalization.

Supplemental Table 6.1. Target specific amplification efficiency parameters.

Reference target	E computed	E (SE) computed	R^2 computed	Slope computed	Efficiency (%)	Efficiency LinRegPCR
cr1-1	2.012	0.018	0.999	-3.293	101.22	1.85
dna11ta1	2.076	0.04	0.994	-3.153	107.57	1.89
dna15ta1	2.012	0.027	0.997	-3.295	101.14	1.94
hatn10	2.043	0.013	1	-3.224	104.25	1.88
hatn4	2.05	0.02	0.999	-3.208	104.98	1.87
hatn8	2.025	0.027	0.997	-3.265	102.43	1.84
loopern4	2.095	0.035	0.996	-3.114	109.47	1.87
sine3	2.014	0.036	0.996	-3.288	101.44	1.86
tc1n1	2.034	0.049	0.993	-3.242	103.45	1.88
tdr7	2.022	0.036	0.996	-3.271	102.17	1.87
b2m	1.946	0.057	0.992	-3.459	94.6	1.86
bactin2	1.993	0.054	0.991	-3.340	99.3	1.86
cyp19a1b	2.015	0.045	0.994	-3.288	101.5	1.84
elfa	2.060	0.049	0.993	-3.187	106.0	1.88
hprt1	1.957	0.042	0.994	-3.430	95.7	1.86
rpl13a	1.912	0.040	0.994	-3.553	91.2	1.87
rps18	1.987	0.042	0.994	-3.352	98.7	1.86
tbp	1.954	0.055	0.990	-3.438	95.4	1.85
tuba1	2.077	0.024	0.998	-3.150	107.7	1.89
gapdh	2.025	0.07	0.976	-3.263	102.5	1.89

PART IV: Discussion

They stumble that run fast

~William Shakespeare's Romeo and Juliet~

Discussion and future perspectives

NB is an embryonal tumor of the autonomic nervous system, emerging from neural crest derived precursor cells committed to the sympathetic neuronal lineage[1]. As a typical embryonal tumor, NB occurs mainly in very young children with the median age at diagnosis of 17 months[2] and presents with low mutational burden. The *ALK* gene is the only major mutational target occurring in 8 to 10 percent of NB patients at diagnosis[3,4]. In contrast to the low mutation rates, recurrent DNA copy number alterations (CNAs) including *MYCN* and *ALK* amplifications and recurrent large and focal DNA partial gains and losses as well as whole chromosome imbalances are observed with a very high frequency[5]. Hence, NB has been coined a DNA copy number disease. One of the most prominent CNAs is gain of a large segment of the long arm of chromosome 17, with breakpoints being located within chromosome band 17q23 or distal thereof. Partial gains occur both in high risk NBs with and without MYCN amplification and are associated with poor patient outcome[6]. While mutations are rare and thus offering limited options for precision oncology, a better understanding of the molecular perturbations installed through these large CNAs can offer novel therapeutic targets and options for design of novel therapies. The search for these genes however is difficult: while it can be logically assumed that genes on 17q contribute to the tumor phenotype through dosage effects as has been described recently in ependymoma[7], thus far, the size of the commonly gained region, estimated to be around 25 Mb, has precluded the identification of these culprit genes.

BRIP1 as a new cooperative oncogene in NB oncogenesis

Through previous bio-informatic analysis using the CONEXIC algorithm, BRIP1 was selected as a strong 17q candidate cooperative driver oncogene (Fieuw A., thesis id 4390537). While the latter study was conducted on a relative small number of high stage tumors (with and without *MYCN* amplification), a further integrated and cross species genomics bio-informatic analysis described in this thesis confirmed *BRIP1* (located on chromosome 17q23) as top candidate. This stimulated further research towards providing functional and mechanistic

support for this hypothesis as described in **paper 1**. Our data convincingly show that *BRIP1* acts through a gain of function mechanism, with tumor cells relying on high levels of *BRIP1* for survival and *in vivo* modeling in zebrafish demonstrating that elevated *BRIP1* levels accelerate MYCN driven tumor formation thus in keeping with a cooperative oncogene function.

The attribution of an oncogenic gain of function to *BRIP1* in NB may be, at first glance, confusing given the well-established role of *BRIP1* as tumor suppressor gene and its known role as Fanconi anemia gene. Indeed, BRIP1 is known to interact with BRCA1 and plays a crucial role in several DNA repair processes. This places BRIP1 in a growing list of genes that now have been recognized to act both as oncogenes and tumor suppressors depending on a given cellular or temporal context with best examples being *NOTCH1* and *EZH2*[8,9]. Interestingly, in familial breast cancer, in addition to inactivating BRIP1 mutations also a rare M299I variant was detected shown to result in a more robust repair of DNA interstrand crosslinks than wild type BRIP1[10], thus also pinpointing to an oncogenic role. In further support, BRIP1 expression levels are often elevated in breast cancer and infer a poor prognosis. While intriguing, further in depth mechanistic and functional studies, as done in this thesis for NB, are needed to better understand the possible opposing oncogenic functions of BRIP1 in breast cancer.

BRIP1 protects NB cells from replicative stress

As pointed out in detail in the introduction, replicative stress is the process characterized by the slowing or stalling of the replication fork[11]. Several causes for replicative stress have been described including shortage of nucleotides and replication factors, G-quadruplex structures, covalent protein-DNA adducts, R-loops, heterochromatin and DNA damage. Also, several oncogenes, including MYC and RAS,[12] have been shown to cause replicative stress. Interestingly, while MYC is typically known as transcription factor controlling a broad range of genes driving cell cycle (amongst others)[13,14], it has also been shown to directly interfere with control of initiation of replication through binding to origins of replication[15]. As such, MYC will boost overall replication speed which may render developing cancer cells particularly vulnerable to the above describes triggers for replicative stress. Of further importance in understanding the complex yin and yang like interaction of DNA repair and

replicative stress versus oncogenesis, MYC also promotes the expression of DNA damage response proteins such as *CHK1* and *WRN* helicase, both of which are required for MYC dependent cancer cell proliferation and survival[16,17]. Surprisingly, abolished ATR levels in mice with ATR seckel syndrome, completely prevented the development of MYC induced lymphomas[16] indicating that replication stress resistance is necessary for MYC driven oncogenesis and that MYC is intrinsically boosting this process. In keeping with these findings, using a SHEP Tet 21/n inducible MYCN system, it was also shown that MYCN induces replication stress in NB cells. MYCN induction resulted in the phosphorylation of RPA, a marker for replication stress[18,19], suggesting similar replicative stress control by both MYC and MYCN. Petroni *et al*. could show that overexpression of MYCN induces the DNA damage response and leads to the stabilization of p53[19] and interestingly similar mechanisms were also described in zebrafish [20]. In this MYCN driven model for NB, also used in this thesis, tumor penetrance was 20%, with evidence of dramatic loss of initiating tumor cells at week 5.5 and formation of full blown tumors at week 9. In *tg(dβh:EGFP-MYCN; dβh:ALK ^{F1174L})* double transgenic fish, penetrance increases above 50%. More detailed analysis showed that *MYCN* overexpression induced adrenal sympathetic neuroblast hyperplasia, blocked chromaffin cell differentiation and ultimately triggered a developmentally timed apoptotic response[20]. It has been assumed that co-expression of activated *ALK* with *MYCN* provides pro-survival signals that block this apoptotic response and allowing continued expansion and oncogenic transformation of hyperplastic neuroblasts, thus promoting progression to NB[20]. We could show that overexpression of *dβh:BRIP1* into the *tg(dβh:EGFP-MYCN)* transgenic background also enhanced the penetrance three-fold. My current working hypothesis is that increased *BRIP1* expression will repress replicative stress induced DNA damage during the early phase of neuroblast hyperplasia. To investigate this we will perform more in depth DNA damage and replicative stress assays on the different stages of tumor formation in zebrafish and monitor how elevated *BRIP1* levels impact on DNA damage levels.

BRIP1, one protein, many functions

While multiple functions have already been assigned to BRIP1 in relation to DNA damage signaling, DNA repair and protecting cells from replicative stress, it is assumed that further roles of BRIP1 in these and possibly also other processes are still to be uncovered. Of further

notice, although BRIP1 was initially found to be implicated in homologous recombinant (HR) pathway through binding with BRCA1, several other functions are assumed to act independent of BRCA1. At present, based on the work presented in this thesis, it is difficult to assign involvement of any of these functions in the BRIP1 mediated tumor acceleration process and possibly most or all functions could indeed be implicated. Here below I will discuss some of the BRIP1 functions in further detail and how they could impact on the observed accelerated tumor formations process.

As an established Fanconi anemia gene, BRIP1 is implicated in the two major processes that are perturbed in the affected cells: interstrand crosslink (ICL) DNA repair and replication stability and integrity. ICLs represent a major challenge for DNA replication and transcription as they preclude DNA strand separation. It has been shown that cells depleted for BRIP1 are more sensitive for DNA cross-linking agents (mitomycin C, cisplatin)[21,22], indicative for an involvement of BRIP1 in unraveling of ICLs. Indeed, processing of ICLs requires activation of the Fanconi anemia pathway and ubiquitination of FANCI and FANCD2[23]. Subsequently, BRIP1 will be recruited to the ICL and will resolve this through binding with MLH1[22,24]. In relation to replication fork stability, several recent proteomics studies have shown direct interaction of BRIP1 in stalled and/or collapsed forks[25].

BRIP1 has a DNA helicase domain and this function has been extensively studied in relation to unwinding and resolving so-called G-quadruplex DNA structures. As explained in more detail above, such G-quadruplexes are extremely stable structures sterically impeding DNA replication and thus posing a potential threat when not removed timely[26]. As such, one can imagine that depletion of BRIP1 protein in highly challenged initiating tumor cells can lead to increased unresolved G-quadruplexes thus leading to increased replication fork stalling and thus replicative stress. In addition, BRIP1 is also important to dissociate DNA:RNA hybrids (R-loops) known to occur due to replication transcription conflicts[27,28]. Interestingly, even in the absence of agents that exogenously induce replication stress, BRIP1 helicase activity is important to maintain genome integrity. BRIP1 is involved in intra-S phase checkpoint signaling through interaction with TopBP1, allowing phosphorylation of CHK1 and RPA following replication stress[29,30]. Taken together, it is clear that unraveling the exact contribution of BRIP1 to the NB oncogenic phenotype will require dedicated further research using the appropriate assays. Also, I plan on a follow up study to demonstrate not only BRIP1

driven tumor acceleration but also tumor dependency using a new generation inducible dβ(i)BRIP1 overexpression transgenic zebrafish. In a first step, the *BRIP1* overexpression construct will be switched on in a MYCN background leading to a high NB tumor penetrance. In a second step when full blown tumors are observed, the overexpression (i)BRIP1 will be switched off and I hypothesize that upon loss of (i)BRIP1 in MYCN/BRIP1 double transgenic tumors, a regression of the already established NB tumors will be observed

In relation to the interaction of BRIP1 with BRCA1, it is of interest that in this thesis we also show that *BRCA1* is highly expressed in NB tumors. In addition to the well-established role of BRCA1 in DNA double strand break repair, recent studies indicate that this protein is also implicated in many other processes including replication stress and activation of the ATR/CHK1 pathway, control of R-loop mediated DNA damage[31], facilitating phosphorylation of CHK1 upon sensing of ssDNA[32]and even acting as transcription factor amongst other controlling levels of the ribonucleotide reductase component RRM2 essential for DNA replication and DNA repair[33]. These findings, like for BRIP1, suggest that BRCA1 also acts as a cooperative oncogene in NB. Preliminary data from our lab and data from the Molenaar lab (personal communication) indeed support this hypothesis by *in vitro* data showing that NB cells depend on high *BRCA1* levels for survival. To study this *in vivo* we overexpressed *BRCA1* in the MYCN zebrafish model but observed no tumor acceleration. However, as *BRCA1* is not conserved in the zebrafish genome, the relevant functional context for BRCA1 operation may be lacking explaining the observed results. Further modeling therefore should be done in a mouse model or the newly described mouse neural crest derived NB model (Olsen *et al.* Oncogene, accepted).

Finally, it has been reported that *BRIP1* is a downstream target of *FOXM1*[34] and thus forms part of a broad DNA damage response network regulated by *FOXM1*. Indeed, upon lentiviral knockdown of FOXM1 in IMR-32 NB cells, we clearly observed an enrichment for DNA repair by gene set enrichment analysis (GSEA) and we could also confirm *BRIP1* as a downstream target of *FOXM1.* In the second part of my thesis, I described the major impact of FOXM1 driven DREAM complex targets on an embryonal stem cell derived gene signature and

hypothesize that this controls stem cells characteristics of aggressive NB cells by keeping the cell cycle and DNA repair mechanisms in check (**paper 2**).

FOXM1 as master regulator of the DNA damage response

The main function of the DREAM complex is to repress gene expression during quiescence (G0). When cells exit the G0 phase, FOXM1 and MYBL2 are recruited to promote mitotic gene expression thereby controlling proper DNA replication and avoiding excessive DNA damage[35,36]. Besides being a member of the DREAM complex, FOXM1 is also an integral component of the DNA damage checkpoint signaling network, driving the transcription of a diverse range of genes encoding for DNA damage sensors, signaling mediators and effectors for cell cycle checkpoints, cell death and senescence[37]. Using Chip-seq data, we could show that *FOXM1* is a downstream target of *MYCN,* thus illustrating one mechanism through which MYCN can restrain replication stress and control the DNA repair pathway. Using the MYCN zebrafish NB model, I recently initiated *FOXM1* targeted overexpression in order to monitor effects on accelerated tumor formation as a prelude to gain further insights into how FOXM1 and MYCN cooperate in NB oncogenesis.

Sumoylation is an important posttranslational modification for the FOXM1 protein. Importantly, recent evidence showed that increased sumoylation of FOXM1 by SUMO2 during M-phase specifically inhibits the negative regulatory domain of FOXM1, leading to an enhanced FOXM1 transcriptional activity. In response to treatment with DNA damaging agents such as epirubicin, or mitotic inhibitors, FOXM1 sumoylation was enhanced in MCF-7 breast cancer cells[38]. In this respect, it has also been shown that sumoylation plays a critical role in the DNA damage response, as it has been linked to DNA repair through studies on the base excision repair pathway. Moreover, it was shown that SUMO2 (and SUMO1/3) accumulate at sites of double stranded breaks or replication fork stalling[39,40]. The close coordination between the processes of DNA repair and sumoylation has recently been confirmed by demonstrating that FOXM1 and many of its direct and indirect target genes, including BRCA1, BARD1 and RRM2, are posttranslationally regaled through so called sumo-waves or group protein modifications.[41]. Interestingly, I modelled overexpression of

dβh:SUMO2 into *tg(dβh:MYCN*-EGFP) zebrafish and indeed showed acceleration of NB onset (preliminary results), suggesting that sumoylation is an important process in NB development.

Targeting BRIP1, FOXM1 and the DNA damage response as entry point for precision oncology for children suffering from high risk NB: towards a durable cure with fewer side effects

Finding a new cure or strategy for the treatment of cancer patients, is probably the holy grail for every cancer researcher. Both *BRIP1* and *FOXM1* are promising therapeutical targets since drastic phenotypic effects are observed in NB cells upon knock down (**paper 1** and **paper 2**). Currently, chemotherapy in combination with additional treatment (including bone marrow transplantation and immunotherapy) are still failing in roughly half of the high risk cases. Moreover, follow up studies of long term survivors are now showing increasingly the dramatic impact of the aggressive therapy schemes on their quality of life, not in the least through significant increase in the risk for therapy induced cancers later in life. Clearly, to cope with these urgent clinical needs, more potent, durable and targeted strategies are needed.

Despite intensive screening, no specific compound targeting BRIP1 could be identified so far (Brosh lab, personal communication). Although direct inactivation of BRIP1 is therefore currently not possible, several indirect approaches can be pursued. In breast cancer, it was shown that *BRIP1* is controlled by the E2F/retinoblastoma (RB1) pathway through a conserved E2F responsive site in the *BRIP1* promotor and that *BRIP1* could be repressed using dihydroxyvitamin D_3 binding on this site[42]. Also other therapeutic options targeting the E2F/RB1 pathway, such as the CDK4/6 inhibitor palbociclib, have been described. Interestingly, it has been shown in the past that NB cells are sensitive for this inhibitor[43]. Another option is through the stabilization of G-quadruplex structures. BRIP1 is indispensable for the unraveling of G4 structures[26], and stabilizing these structures would induce replication stress in the cancer cells. Several G4 stabilizers have been described (telomestatin, TMPYP4 tosylate, pyridostatin, BRACO-19) and some of them, amongst others BRACO-19, are well tolerated in mice opening perspectives for clinical use[44]. Importantly,

since G4 structures are mainly formed at the telomeres, using these compounds would also affect hTERT, which was recently identified as an important oncogene in NB development[45,46]. Stabilizing quadruplex structures could also be a strategy in the NB patient subgroup with ATRX deletions[47], since *ATRX* null neuroprogenitor cells are hypersensitive to the G4 stabilizing ligand telomestatin[48]. Finally, as BRIP1, WRN and BLM function together in a complex for the unraveling of G-quadruplex structures[26], an alternative approach for targeting BRIP1, would be through the use of the WRN helicase inhibitor (NSC 617145). As such, inhibiting WRN would indirectly also affect BRIP1 function.

In contrast to BRIP1, several compounds have been described targeting FOXM1. Siomycin A and thiostreptin inhibit the transcriptional activity and the expression of FOXM1 through acting as proteasome inhibitors[49]. Indeed, we could observe a downregulation of FOXM1 upon addition of Siomycin A in the NB cell line N206, however only starting 72h after addition (**paper 3**). In gastroenteropancreatic neuroendocrine tumors slightly synergistic effects were observed upon addition of Siomycin A and cisplatin, however, we could not confirm this synergistic effect in NB cells[50]. Siomycin A is a promiscuous molecule with potent off-target effects, most notably inhibition of the 20S proteasome, therefore also targeting several other proteins, possibly explaining our results.

By performing a library screen of 54211 small molecules, a small molecule inhibitor of FOXM1 (FDI-6) was discovered in the group of Balasubramanian[51]. FDI-6 binds directly to FOXM1 and displaces FOXM1 from its genomic targets. The authors performed transcriptome profiling after 0, 3, 6 and 9 hours of FDI-6 treatment and could clearly demonstrate downregulation of FOXM1 target genes[51]. Upon addition of FDI-6 to IMR-32 NB cells, we could indeed confirm downregulation of FOXM1 target genes 6h after administration. However, 24h after administration, to our surprise we consistently observed upregulation of the FOXM1 target genes. To exclude that this loss off FDI-6 efficacy is due to compound degradation, we administrated the drug every 12h to the cells, however, this did not result in a sustained downregulation of FOXM1 activity, indicating that compound degradation is not the reason for the observed phenotype (data not shown). These results precluded further studies using this compound. The reason for the short lived response of the cells to the drug are unclear. One could imagine that the cells respond through classical drug resistance mechanisms such as activation of drug efflux pumps or the sequestering of

the drug into cellular vesicles that are then eliminated by exocytosis[52] but one would think that such mechanism requires more time to be installed. Alternatively, cells may be strongly dependent on FOXM1 activity and undergo fast pathway rewiring that leads to reactivation of FOXM1 activity through an as yet unknown mechanism. In any case, given the strong focus of the research community on FOXM1[53] and the drug being available for several years it is indeed disturbing that no follow up studies have been reported, neither by the Balasubramanian lab nor by other labs.

Fortunately, the activity of FOXM1 is fine-tuned by several post-translational modifications, thus offering alternative opportunities for drugging. Phosphorylation of FOXM1 by phospho-like kinase 1 (PLK1) at the G2/M phase results in the activation of FOXM1 activity and the expression of key mitotic regulators[54]. PLK1 is only expressed in dividing cells and to a much lesser extent than cancer cells thus offering a therapeutic window. Several compounds targeting PLK1 have been described and many of them compete with ATP for the substrate binding site[55] including volasertib (BI6727). Several preclinical experiments have demonstrated that volasertib is potent in inducing tumor regression. Therefore, this agent has recently been awarded the "Breakthrough Therapy Status" by the FDA for its significant benefit in treating AML patients[55]. Interestingly, recently it was shown that PLK1 inhibitors induce reduced proliferation, cell cycle arrest and cell death in NB cells[56], indicating that this is an important pathway. Another indirect FOXM1 drugging approach is through targeting maternal embryonic leucine zipper kinase (MELK). FOXM1 forms a protein complex with MELK and resulting in the phosphorylation and activation of FOXM1[57]. While several studies have been conducted with the MELK inhibitor OTS167[58], experts in the field strongly doubt the on target specificity of OTS167 (Bollen lab, personal communication) precluding the use of this drug for pre-clinical studies. Interestingly, through a large kinase inhibitor screen, a novel MELK inhibitor, MELK-T1 was recently identified[59], opening new perspectives for specific inhibition of MELK dependent FOXM1 activation. The posttranslational sumoylation of FOXM1 offers yet another therapeutic opportunity. A compound library screen resulted in the identification of compound 21 that decreases sumoylation with 85%[60].

Besides targeting BRIP1 and FOXM1, further therapeutic approaches can also be pursued. In this thesis we show that NB cells experience replication stress and that ATR/CHK1 signaling for sensing of ssDNA is (highly) activated. Therefore, other compounds and mechanisms that

enhance replication stress and that target the ATR/CHK1 axis could also be of great interest for treating NB patients. Several novel drugs targeting CHK1 (LY2606368, CCT245737) and ATR (ATR-101, VX-970) already entered clinical trials, opening perspectives for treatment of NB patients. Of interest, an alternative approach to inhibit CHK1 is to target WEE1 (MK-1775), a kinase that phosphorylates cell cycle regulators CDK1 and CDK2. Inhibition of WEE-1 leads to enhanced CDK1/2 activity causing cells in S phase to enter mitosis prematurely before DNA replication is complete[61] causing mitotic catastrophy. Interestingly, the combination of WEE1 and CHK1 inhibitors has been tested in NB cells and indeed resulted in a synergistic effect[61,62].

In this thesis we show that *FOXM1* is a downstream target of MYCN, presenting yet another therapeutic option. Given the impact of MYCN in NB biology, *MYCN* is amplified in around 20% of the tumors[63], an enormous effort has already been invested in the identification of compounds that target MYCN. Hence, direct inhibition of MYCN *in vivo* is cumbersome, since MYC proteins are composed of two extended alpha-helices with no obvious surfaces for small molecule binding. However, several indirect approaches can be pursued, BET family adaptor proteins localize to MYC promotors , and therefore targeting BET also indirectly influences *MYCN* activity. Several BET inhibitors have been described, amongst others JQ1 and OTX015. In NB cell lines, responses to JQ1 inhibition varied from highly sensitive to resistant[64], with amplification of *MYCN* as a top predictive marker of response to JQ1 treatment. Also OTX015 has been shown to have therapeutic effects against preclinical MYCN driven NB models[65].

Proteins that prevent dephosphorylation at T58 stabilize MYCN, which may be the case with AURKA in NB[66]. Interestingly, increased expression of *AURKA* is found in *MYCN* amplified NB, mediated potentially by MYCN itself[67]. Therefore, promoting dissociation of the AURKA-MYCN complex, which results in rapid proteosomal degradation of MYCN, represent another strategy to target oncogenic stabilization of MYCN. Certain AURKA inhibitors, such as MLN8237, induce a particular conformational change in the kinase that actively reinitiates MYCN degradation through this mechanism[68]. MLN8237 was identified as a promising agent

for NB but has not displayed robust antitumor activity in early-phase pediatric studies, warranting the development of improved inhibitors[69,70].

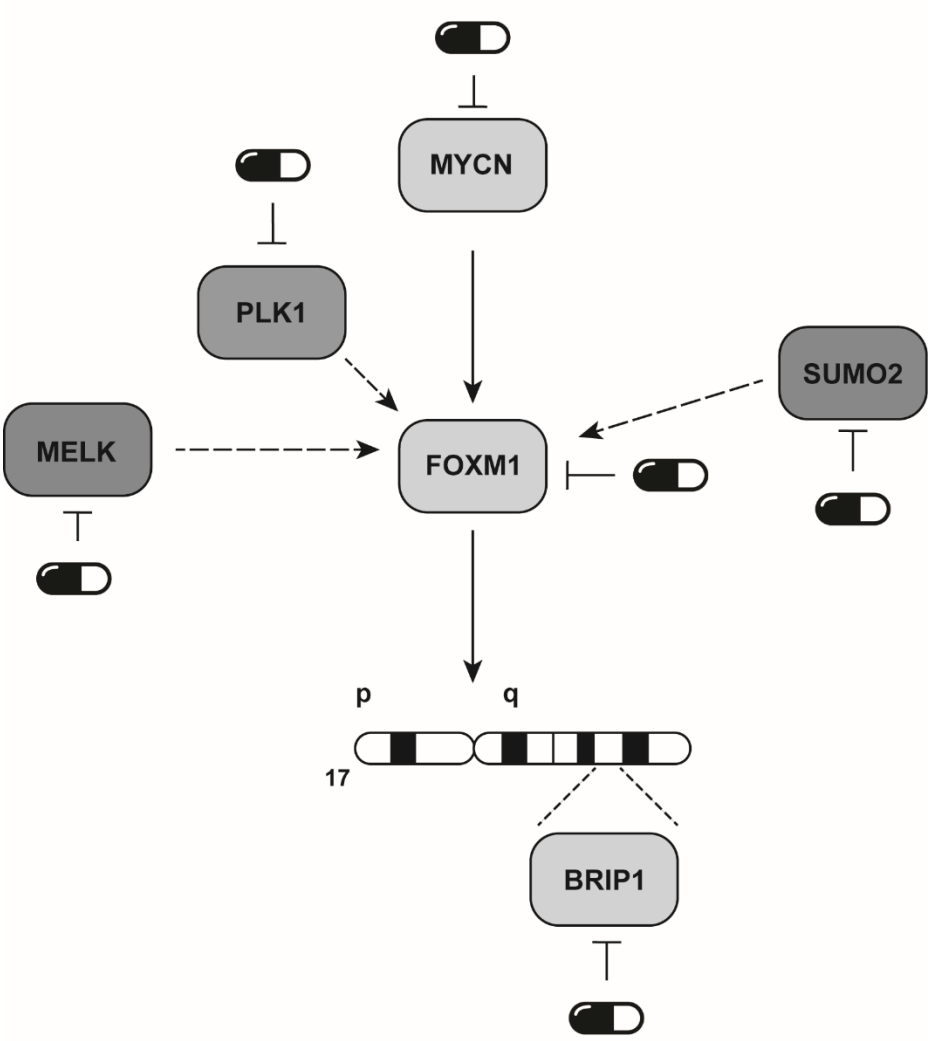

Figure 7.1: Schematic overview of the MYCN-FOXM1-BRIP1(17q) axis and possible therapeutic interventions.

BRIP1 and 17q gain: one done, more to go?

I consider the identification of *BRIP1* as a cooperative oncogene for MYCN driven tumor formation as a major novel finding in NB biology offering novel unexpected opportunities for drugging. While my data convincingly show the importance of BRIP1 as putative effector of the dosage effects caused by chromosome 17q gain, I believe that further genes on 17q are

important in NB. Which would explain the apparent tremendous high selective pressure towards retaining chromosome 17 imbalances causing 17q gain as an almost invariable feature of the high risk NB genome. Most notably, in a MYCN driven NB mouse model, gain of chromosome 11 (which is syntenic to chromosome 17q in human) is also observed in about 25% of the tumors[71], showing that this process is conserved. A further search for dosage sensitive genes on 17q is certainly warranted. First, the involved large segment (17q23-qter) is large, suggesting that in addition to BRIP1 at least one additional gene, possibly located much more distal towards the 17q telomere could be implicated. Second, based on a time course analysis of gene expression (1,2 and 6 weeks after birth) in the superior cervical ganglia and the celiac ganglia of Th-MYCN and wild type mice during several stages of NB development [72], several downstream targets of FOXM1 (TOP2A, BIRC5, TLK1…) were found amongst the top upregulated genes and in keeping with being FOXM1 targets involved in DNA metabolism and DNA repair (Durinck et al, in preparation). These data are in keeping with the presently proposed hypothesis in the host lab that gain of chromosome 17q, through combined dosage effects of multiple genes, drives a cellular state characterized by replicative stress resistance and highly efficient DNA repair. Recent work from the Gilbertson team indeed demonstrated such a phenomenon to be active in the brain tumor ependymoma. Genome wide copy number alterations are also frequently observed in these tumors and to sift through the many putative candidates the team used a large *in vivo* screen of 84 candidate oncogenes and 39 candidate tumor suppressor genes (TSG) located in 28 copy number aberrations. As such, they identified eight new oncogenes and ten new tumor suppressor genes, all involved in similar cell functions[7]. This study thus indeed illustrates that multiple dosage sensitive genes residing in the commonly affected chromosome regions can be actively involved in tumor initiation and/or progression through installing a so-called cellular state driven through one or more altered cellular functions[7].

Zebrafish as a model to study NB tumor acceleration and validation of candidate cooperative oncogenes

The MYCN driven zebrafish NB model was demonstrated to be useful for testing the effect of cooperative oncogenes on tumor acceleration as illustrated by the pioneering work of the Look lab for mutant ALK and confirming earlier observations in mouse. More recently, NF1 loss-of-function mutations were also shown to accelerate MYCN driven tumor formation in

zebrafish[73]. My study adds yet another gene to the list of those impacting on MYCN driven tumor onset and penetrance and thus further reinforces the relevance of this animal model for these experiments. Indeed, many additional genes are now under study in the host lab for leukemia and NB, all in the slip stream of my initial *BRIP1* work. Further, the zebrafish cancer core of the host lab is rapidly expanding and exploring further novel paths including genomic profiling methods of tumor cells (including single cells) as well as using zebrafish for drug testing, amongst others.

Optimizing of RT-qPCR normalization in zebrafish studies

Much of my early PhD work was focused on introducing modeling of cancer in zebrafish in the Ghent zebrafish lab, following my stay in the Look lab at the Dana Farber Cancer Institute (Boston, USA). Given the worldwide recognized expertise of the Center for Medical Genetics in Ghent in normalization strategies for qPCR based gene expression studies[74,75], I decided to exploit this know how in the context of the zebrafish model system. Indeed, gene expression analysis is increasingly important in many fields of biological research and RT-qPCR is currently frequently used given its practical simplicity and processing speed. However, different critical factors can influence the outcome of the RT-qPCR studies and these have to be applied properly to obtain biologically meaningful results. Since under specific biological conditions the frequently used reference genes in zebrafish did not perform up to standard, we applied a new normalization strategy based on expressed repeat elements (**paper 4**). Starting from a database encompassing all repetitive elements expressed in zebrafish, we selected 10 EREs for further validation. Comparing the 10 most frequently used reference genes in zebrafish with the 10 selected EREs, we could convincingly show that in almost every situation the EREs perform much better than the standard reference genes. Especially in challenging situations (such as time series or comparing different tissues) the EREs were more stably expressed resulting in biologically more reliable and robust results. This work has broader application possibilities as we suggest that this strategy can be applied to other model organisms as well. Indeed, using a similar workflow we could identify and validate EREs for the usage in mice (Renard, Vanhauwaert *et al*. Scientific Reports, under minor revision).

General conclusions and perspectives

When I started on the BRIP1 modeling in NB, ALK was the only gene known to drive accelerated tumor formation in the MYCN targeted overexpressing zebrafish NB model (see above). Selecting zebrafish at the start of this work therefore was a major challenge but fortunately, in the end, turned out to be successful. My pioneering work in the lab has now evolved into a fully equipped and operational zebrafish cancer modeling unit currently actively exploring the mode of action for many novel candidate genes. Despite these successes important challenges remain. Most notably, MYCN amplification only represents about half of all high risk NBs. Most of the remaining half carry a large 11q deletion and 17q gain with no subset specific associated mutations. This currently precludes the modeling of this important group of tumors with poor prognosis. Recent work in the host lab has led to the identification of several 11q candidates following the same bioinformatics approach applied here. Therefore, yet another major breakthrough may be ahead of us as modeling the high risk NB without MCYN amplification is considered as one of the major aims for ongoing NB research.

Further, as indicated, BRIP1 function in relation to NB tumor formation needs further investigation and also direct drugging of BRIP1 would possibly add yet another drug to the currently rapidly growing repertoire of compounds for precision treatment for NB. Further, also the additional 17q candidate cooperative genes need further modeling and investigation as they themselves can also represent novel drug targets. Then, a further challenge is to test the optimal combination therapies as single compound treatment invariably leads to resistance.

References:

1. Marshall GM, Carter DR, Cheung BB, et al: The prenatal origins of cancer. Nat Rev Cancer 14:277-89, 2014
2. Maris JM: Recent advances in neuroblastoma. N Engl J Med 362:2202-11, 2010
3. George RE, Sanda T, Hanna M, et al: Activating mutations in ALK provide a therapeutic target in neuroblastoma. Nature 455:975-8, 2008
4. Chen Y, Takita J, Choi YL, et al: Oncogenic mutations of ALK kinase in neuroblastoma. Nature 455:971-4, 2008
5. Kumps C, Fieuw A, Mestdagh P, et al: Focal DNA copy number changes in neuroblastoma target MYCN regulated genes. PLoS One 8:e52321, 2013
6. Bown N, Cotterill S, Lastowska M, et al: Gain of chromosome arm 17q and adverse outcome in patients with neuroblastoma. N Engl J Med 340:1954-61, 1999
7. Mohankumar KM, Currle DS, White E, et al: An in vivo screen identifies ependymoma oncogenes and tumor-suppressor genes. Nature Genetics 47:878-+, 2015
8. Radtke F, Raj K: The role of Notch in tumorigenesis: Oncogene or tumour suppressor? Nature Reviews Cancer 3:756-767, 2003
9. Hock H: A complex Polycomb issue: the two faces of EZH2 in cancer. Genes Dev 26:751-5, 2012
10. Cantor SB, Bell DW, Ganesan S, et al: BACH1, a novel helicase-like protein, interacts directly with BRCA1 and contributes to its DNA repair function. Cell 105:149-160, 2001
11. Zeman MK, Cimprich KA: Causes and consequences of replication stress. Nat Cell Biol 16:2-9, 2014
12. Hills SA, Diffley JFX: DNA Replication and Oncogene-Induced Replicative Stress. Current Biology 24:R435-R444, 2014
13. Bouchard C, Dittrich O, Kiermaier A, et al: Regulation of cyclin D2 gene expression by the Myc/Max/Mad network: Myc-dependent TRRAP recruitment and histone acetylation at the cyclin D2 promoter. Genes Dev 15:2042-7, 2001
14. Dominguez-Sola D, Gautier J: MYC and the control of DNA replication. Cold Spring Harb Perspect Med 4, 2014
15. Dominguez-Sola D, Ying CY, Grandori C, et al: Non-transcriptional control of DNA replication by c-Myc. Nature 448:445-51, 2007
16. Murga M, Campaner S, Lopez-Contreras AJ, et al: Exploiting oncogene-induced replicative stress for the selective killing of Myc-driven tumors. Nat Struct Mol Biol 18:1331-5, 2011
17. Moser R, Toyoshima M, Robinson K, et al: MYC-Driven Tumorigenesis Is Inhibited by WRN Syndrome Gene Deficiency. Molecular Cancer Research 10:535-545, 2012
18. Petroni M, Sardina F, Heil C, et al: The MRN complex is transcriptionally regulated by MYCN during neural cell proliferation to control replication stress. Cell Death Differ 23:197-206, 2016
19. Petroni M, Veschi V, Prodosmo A, et al: MYCN Sensitizes Human Neuroblastoma to Apoptosis by HIPK2 Activation through a DNA Damage Response. Molecular Cancer Research 9:67-77, 2011
20. Zhu S, Lee JS, Guo F, et al: Activated ALK collaborates with MYCN in neuroblastoma pathogenesis. Cancer Cell 21:362-73, 2012

21. Litman R, Peng M, Jin Z, et al: BACH1 is critical for homologous recombination and appears to be the Fanconi anemia gene product FANCJ. Cancer Cell 8:255-265, 2005

22. Peng M, Litman R, Xie J, et al: The FANCJ/MutL alpha interaction is required for correction of the cross-link response in FA-J cells. Embo Journal 26:3238-3249, 2007

23. Moldovan GL, D'Andrea AD: How the Fanconi Anemia Pathway Guards the Genome. Annual Review of Genetics 43:223-249, 2009

24. Cantor SB, Xie J: Assessing the link between BACH1/FANCJ and MLH1 in DNA crosslink repair. Environ Mol Mutagen 51:500-7, 2010

25. Sirbu BM, McDonald WH, Dungrawala H, et al: Identification of Proteins at Active, Stalled, and Collapsed Replication Forks Using Isolation of Proteins on Nascent DNA (iPOND) Coupled with Mass Spectrometry. Journal of Biological Chemistry 288:31458-31467, 2013

26. Bharti SK, Awate S, Banerjee T, et al: Getting Ready for the Dance: FANCJ Irons Out DNA Wrinkles. Genes 7, 2016

27. Hamperl S, Cimprich KA: Conflict Resolution in the Genome: How Transcription and Replication Make It Work. Cell 167:1455-1467, 2016

28. Cantor S, Drapkin R, Zhang F, et al: The BRCA1-associated protein BACH1 is a DNA helicase targeted by clinically relevant inactivating mutations. Proc Natl Acad Sci U S A 101:2357-62, 2004

29. Gong ZH, Kim JE, Leung CCY, et al: BACH1/FANCJ Acts with TopBP1 and Participates Early in DNA Replication Checkpoint Control. Molecular Cell 37:438-446, 2010

30. Gupta R, Sharma S, Sommers JA, et al: FANCJ (BACH1) helicase forms DNA damage inducible foci with replication protein A and interacts physically and functionally with the single-stranded DNA-binding protein. Blood 110:2390-8, 2007

31. Hatchi E, Skourti-Stathaki K, Ventz S, et al: BRCA1 Recruitment to Transcriptional Pause Sites Is Required for R-Loop-Driven DNA Damage Repair. Molecular Cell 57:636-647, 2015

32. Yarden RI, Metsuyanim S, Pickholtz I, et al: BRCA1-dependent Chk1 phosphorylation triggers partial chromatin disassociation of phosphorylated Chk1 and facilitates S-phase cell cycle arrest. International Journal of Biochemistry & Cell Biology 44:1761-1769, 2012

33. Rasmussen RD, Gajjar MK, Tuckova L, et al: BRCA1-regulated RRM2 expression protects glioblastoma cells from endogenous replication stress and promotes tumorigenicity. Nature Communications 7, 2016

34. Monteiro LJ, Khongkow P, Kongsema M, et al: The Forkhead Box M1 protein regulates BRIP1 expression and DNA damage repair in epirubicin treatment. Oncogene 32:4634-45, 2013

35. Sadasivam S, Duan S, DeCaprio JA: The MuvB complex sequentially recruits B-Myb and FoxM1 to promote mitotic gene expression. Genes Dev 26:474-89, 2012

36. Zhan M, Riordon DR, Yan B, et al: The B-MYB transcriptional network guides cell cycle progression and fate decisions to sustain self-renewal and the identity of pluripotent stem cells. PLoS One 7:e42350, 2012

37. Zona S, Bella L, Burton MJ, et al: FOXM1: An emerging master regulator of DNA damage response and genotoxic agent resistance. Biochimica Et Biophysica Acta-Gene Regulatory Mechanisms 1839:1316-1322, 2014

38. Myatt SS, Kongsema M, Man CWY, et al: SUMOylation inhibits FOXM1 activity and delays mitotic transition. Oncogene 33:4316-4329, 2014

39. Jackson SP, Durocher D: Regulation of DNA Damage Responses by Ubiquitin and SUMO. Molecular Cell 49:795-807, 2013

40. Hendriks IA, Treffers LW, Verlaan-de Vries M, et al: SUMO-2 Orchestrates Chromatin Modifiers in Response to DNA Damage. Cell Reports 10:1778-1791, 2015

41. Xiao Z, Chang JG, Hendriks IA, et al: System-wide Analysis of SUMOylation Dynamics in Response to Replication Stress Reveals Novel Small Ubiquitin-like Modified Target Proteins and Acceptor Lysines Relevant for Genome Stability. Mol Cell Proteomics 14:1419-34, 2015

42. Eelen G, Bempt IV, Verlinden L, et al: Expression of the BRCA1-interacting protein Brip1/BACH1/FANCJ is driven by E2F and correlates with human breast cancer malignancy. Oncogene 27:4233-4241, 2008

43. Rihani A, Vandesompele J, Speleman F, et al: Inhibition of CDK4/6 as a novel therapeutic option for neuroblastoma. Cancer Cell International 15, 2015

44. Burger AM, Dai FP, Schultes CM, et al: The G-quadruplex-interactive molecule BRACO-19 inhibits tumor growth, consistent with telomere targeting and interference with telomerase function. Cancer Research 65:1489-1496, 2005

45. Peifer M, Hertwig F, Roels F, et al: Telomerase activation by genomic rearrangements in high-risk neuroblastoma. Nature 526:700-4, 2015

46. Valentijn LJ, Koster J, Zwijnenburg DA, et al: TERT rearrangements are frequent in neuroblastoma and identify aggressive tumors. Nat Genet 47:1411-4, 2015

47. Cheung NK, Zhang J, Lu C, et al: Association of age at diagnosis and genetic mutations in patients with neuroblastoma. JAMA 307:1062-71, 2012

48. Watson LA, Solomon LA, Li JR, et al: Atrx deficiency induces telomere dysfunction, endocrine defects, and reduced life span. J Clin Invest 123:2049-63, 2013

49. Halasi M, Gartel AL: Targeting FOXM1 in cancer. Biochemical Pharmacology 85:644-652, 2013

50. Briest F, Berg E, Grass I, et al: FOXM1: A novel drug target in gastroenteropancreatic neuroendocrine tumors. Oncotarget 6:8185-99, 2015

51. Gormally MV, Dexheimer TS, Marsico G, et al: Suppression of the FOXM1 transcriptional programme via novel small molecule inhibition. Nat Commun 5:5165, 2014

52. Baguley BC: Multiple drug resistance mechanisms in cancer. Mol Biotechnol 46:308-16, 2010

53. Gentles AJ, Newman AM, Liu CL, et al: The prognostic landscape of genes and infiltrating immune cells across human cancers. Nature Medicine 21:938-945, 2015

54. Fu Z, Malureanu L, Huang J, et al: Plk1-dependent phosphorylation of FoxM1 regulates a transcriptional programme required for mitotic progression. Nature Cell Biology 10:1076-1082, 2008

55. Liu Z, Sun Q, Wang X: PLK1, A Potential Target for Cancer Therapy. Transl Oncol 10:22-32, 2016

56. Ackermann S, Goeser F, Schulte JH, et al: Polo-Like Kinase 1 is a Therapeutic Target in High-Risk Neuroblastoma. Clinical Cancer Research 17:731-741, 2011

57. Joshi K, Banasavadi-Siddegowda Y, Mo XK, et al: MELK-Dependent FOXM1 Phosphorylation is Essential for Proliferation of Glioma Stem Cells. Stem Cells 31:1051-1063, 2013

58. Alachkar H, Mutonga M, Chung SY, et al: Preclinical efficacy of maternal embryonic leucine-zipper kinase (MELK) inhibition in acute myeloid leukemia. Cancer Research 74, 2014

59. Beke L, Kig C, Linders JTM, et al: MELK-T1, a small-molecule inhibitor of protein kinase MELK, decreases DNA-damage tolerance in proliferating cancer cells. Bioscience Reports 35, 2015

60. Kumar A, Ito A, Hirohama M, et al: Identification of Sumoylation Activating Enzyme 1 Inhibitors by Structure-Based Virtual Screening. Journal of Chemical Information and Modeling 53:809-820, 2013

61. Aarts M, Sharpe R, Garcia-Murillas I, et al: Forced Mitotic Entry of S-Phase Cells as a Therapeutic Strategy Induced by Inhibition of WEE1. Cancer Discovery 2:524-539, 2012

62. Dobbelstein M, Sorensen CS: Exploiting replicative stress to treat cancer. Nat Rev Drug Discov 14:405-23, 2015

63. Liu ZH, Thiele CJ: ALK and MYCN: When Two Oncogenes Are Better than One. Cancer Cell 21:325-326, 2012

64. Puissant A, Frumm SM, Alexe G, et al: Targeting MYCN in Neuroblastoma by BET Bromodomain Inhibition. Cancer Research 73, 2013

65. Henssen A, Althoff K, Odersky A, et al: Targeting MYCN-Driven Transcription By BET-Bromodomain Inhibition. Clinical Cancer Research 22:2470-2481, 2016

66. Otto T, Horn S, Brockmann M, et al: Stabilization of N-Myc Is a Critical Function of Aurora A in Human Neuroblastoma. Cancer Cell 15:67-78, 2009

67. Shang XY, Burlingame SM, Okcu MF, et al: Aurora A is a negative prognostic factor and a new therapeutic target in human neuroblastoma. Molecular Cancer Therapeutics 8:2461-2469, 2009

68. Brockmann M, Poon E, Berry T, et al: Small Molecule Inhibitors of Aurora-A Induce Proteasomal Degradation of N-Myc in Childhood Neuroblastoma. Cancer Cell 24:75-89, 2013

69. Mosse YP, Lipsitz E, Fox E, et al: Pediatric phase I trial and pharmacokinetic study of MLN8237, an investigational oral selective small-molecule inhibitor of Aurora kinase A: a Children's Oncology Group Phase I Consortium study. Clin Cancer Res 18:6058-64, 2012

70. Maris JM, Morton CL, Gorlick R, et al: Initial testing of the aurora kinase A inhibitor MLN8237 by the Pediatric Preclinical Testing Program (PPTP). Pediatr Blood Cancer 55:26-34, 2010

71. Althoff K, Beckers A, Bell E, et al: A Cre-conditional MYCN-driven neuroblastoma mouse model as an improved tool for preclinical studies. Oncogene 34:3357-3368, 2015

72. Beckers A, Van Peer G, Carter DR, et al: MYCN-targeting miRNAs are predominantly downregulated during MYCN-driven neuroblastoma tumor formation. Oncotarget 6:5204-5216, 2015

73. He SN, Mansour MR, Zimmerman MW, et al: Synergy between loss of NF1 and overexpression of MYCN in neuroblastoma is mediated by the GAP-related domain. Elife 5, 2016

74. Bustin SA, Benes V, Garson JA, et al: The MIQE guidelines: minimum information for publication of quantitative real-time PCR experiments. Clin Chem 55:611-22, 2009

75. Vandesompele J, De Preter K, Pattyn F, et al: Accurate normalization of real-time quantitative RT-PCR data by geometric averaging of multiple internal control genes. Genome Biol 3:RESEARCH0034, 2002

PART V: Summary, Samenvatting, CV

Science may set limits to knowledge,

but should not set limits to imagination

~Bertrand Russell ~

Summary:

Neuroblastoma is a neural crest derived childhood tumor. The majority of these tumors arise in the adrenal gland and the sympathetic ganglia of infants and young children. These tumors display a broad spectrum of clinical heterogeneity ranging from spontaneous regression to aggressive metastatic disease. Especially for the latter group of patients, no adequate therapy is available yet and survival chances remain very poor. Advanced targeted treatment strategies may provide solutions for this problem, however, in order to benefit from these personalized treatments, it is of utmost importance to identify molecular targets. So far, only a limited number of genes have been identified that play a role in neuroblastoma oncogenesis, with mutations in *ALK* being the most prevalent and only occurring in 10% of the cases. In contrast to the paucity of mutations, copy number aberrations are frequently observed in neuroblastoma tumors, with gain of chromosome 17q being the most common abnormality detected and correlated with poor patient outcome. A better knowledge of which genes on 17q are important in neuroblastoma development can offer novel therapeutic targets and options for design of novel therapies.

The first goal of my thesis was to follow-up on an initial bio-informatics approach intended to identify candidate 17q oncogenes. With this strategy, *BRIP1* located on chromosome 17q23 was identified as a cooperative oncogene in neuroblastoma development. High expression of *BRIP1* correlated with poor patient outcome and stable BRIP1 knock-down in neuroblastoma cell lines significantly reduced cell viability and colony forming capacity. Moreover, overexpression of *dβh-BRIP1* into the transgenic *tg(dβh-EGFP-MYCN)* zebrafish resulted in acceleration of neuroblastoma onset and tripled the penetrance compared to transgenic *tg(dβh-EGFP-MYCN)* zebrafish. Finally, we could show that overexpression of BRIP1 is indispensable to control replicative stress experienced by the neuroblastoma tumor genome and that BRIP1 creates a cellular state what we call “replication stress resistance”.

In the second part, we wanted to explore whether an ESC derived expression signature could capture a stemness phenotype in neuroblastoma cells that is associated with therapy

resistance. An ESC miRNA signature could be identified that allows to discriminate patients with worse survival in the global cohort of neuroblastoma patients, but most interestingly also in a subset of high-risk tumors, i.e. stage 4 tumors without *MYCN* amplification. Analysis of the protein coding genes that are correlated with the ESC miRNA signature score in neuroblastoma patients, pointed at a *FOXM1* driven cell cycle and DNA repair activation in therapy resistant tumors. Interestingly, these findings can reveal new therapeutic approaches for tumors where current treatment regimens fail.

In the last part of this thesis, we identified new reference genes for the normalization of RT-qPCR experiments in zebrafish. Proper selection of reference genes is a critical step to obtain biologically meaningful results. Starting from a database encompassing all repetitive elements expressed in zebrafish, we selected 10 expressed repeat elements (ERE's) for further validation. Comparing the 10 most frequently used reference genes in zebrafish with the 10 selected EREs, we could convincingly show that in almost every situation, our identified expressed repeat elements perform much better than the standard reference genes.

Samenvatting:

Neuroblastoom is een kinderkanker met een neuronale oorsprong die voornamelijk optreedt in de bijnieren en de sympathische ganglia van baby's en jonge kinderen. Deze tumoren vertonen een zeer gevarieerd klinisch beeld dat kan gaan van spontane regressie tot zeer agressieve tumoren die uitzaaien. Vooral voor die laatste groep van patiënten zijn er tot op heden geen efficiënte therapieën beschikbaar en blijven de overlevingskansen laag. Geavanceerde gerichte therapeutische strategieën kunnen mogelijks een oplossing bieden voor dit probleem. Om van deze gepersonaliseerde therapieën gebruik te kunnen maken is het echter een vereiste dat er moleculaire doelwitten geïdentificeerd worden. Tot op vandaag is er slechts een beperkt aantal genen geïdentificeerd met een rol in neuroblastoom ontwikkeling, waarbij mutaties in het *ALK* gen het meest worden waargenomen en dat in slechts 10% van de neuroblastoom patiënten. In tegenstelling tot het beperkt aantal mutaties worden in neuroblastoom zeer frequent copynumbervariaties waargenomen, waarbij winst van chromosoom 17q, dat gecorreleerd is met een slechte overleving voor de patiënten, de frequentste kopie nummer afwijking is. Een beter inzicht in welke genen op 17q belangrijk zijn voor de ontwikkeling van neuroblastoom kan helpen voor de identificatie van nieuwe doelwitgenen en therapieën.

Het eerste doel van mijn thesis was het verder onderzoeken van 17q oncogenen die in een eerdere bio-informatica analyse waren geïdentificeerd als potentieel kandidaat genen. *BRIP1*, gelokaliseerd op chromosoom 17q23, werd geïdentificeerd als een belangrijk coöperatief oncogen in de ontwikkeling van neuroblastoom. Hoge expressie van BRIP1 is gecorreleerd met een slechte overleving van neuroblastoom patiënten en stabiele neerregulatie van BRIP1 in neuroblastoom cellijnen resulteerde in een verminderde cel viabiliteit en kolonie vormende capaciteit. Daarnaast resulteerde overexpressie van *dβh-BRIP1* in de transgene zebravislijn *tg(dβh:*EGFP-MYCN*)* in een versnelling van neuroblastoom ontwikkeling en werd ook de penetrantie voor tumorvorming verdrievoudigd. Finaal konden we aantonen dat *BRIP1* noodzakelijk is voor het controleren van replicatie stress in het neuroblastoom tumor genoom en dat *BRIP1* een cellulaire toestand induceert die wij beschrijven als 'replicatie stress resistentie'.

In het tweede deel werd nagaan of een signatuur afkomstig van embryonale stamcellen een stamcel fenotype kan bepalen in neuroblastoom cellen die resistent zijn aan therapie. We konden een ESC miRNA signatuur bepalen die in staat was om neuroblastoom patiënten met een slechte prognose te identificeren. Bovendien, kon deze signatuur ook gebruikt worden voor het bepalen van ultra hoog risico patiënten in de hoog risico neuroblastoom subgroep, namelijk de stadium 4 patiënten zonder *MYCN* amplificatie. Analyse van de eiwit coderende genen gecorreleerd met de ESC miRNA signatuur toonden aan dat *FOXM1* belangrijk was voor het aansturen van deze signatuur. Deze bevindingen kunnen leiden tot nieuwe therapeutische strategieën voor tumoren waar de huidige behandelingsschema's falen.

In het laatste deel van deze thesis werden nieuwe referentie genen voor de normalisatie van RT-qPCR experimenten in zebravis geïdentificeerd. Correcte selectie van referentie genen is belangrijk om biologisch relevante resultaten te verkrijgen. Hiervoor zijn we gestart van een databank waarin alle repetitieve elementen die in zebravis tot expressie worden gebracht zijn gebundeld en vervolgens werden uit deze databank 10 repeat element geselecteerd voor verdere validatie. Wanneer we de 10 meest gebruikte referentie genen gebruikt in zebravis, vergeleken met onze repeat elementen, konden we zeer overtuigend aantonen dat in bijna iedere situatie onze repeat elementen veel beter presteerden dan de standaard referentie genen.

Curriculum Vitae

Personalia:

- Surname: Vanhauwaert
- First name: Suzanne
- Address: Gullegemsesteenweg 197
  8501 Bissegem
- Telephone: +32479255543
- Email: suzannevanhauwaert@hotmail.com
- Place of birth: Kortrijk
- Date of birth: March 15th 1988

Experience:

- 2011-now: PhD researcher at Centrum for Medical Genetics, Ghent, Belgium. Supervisor: Prof.dr. Frank Speleman

- August 2013-March 2014: Visiting researcher at Dana Farber Cancer Institute, Harvard Medical School, Boston, USA. Lab of Prof. A. Thomas Look

Education:

- October 2006-June 2009: Bachelor Biochemistry-Biotechnology at KU Leuven (cum laude)

- October 2009-Juni 2011: Master Biochemistry-Biotechnology at KU Leuven (magna cum laude)
- Master thesis: Identification of the platelet specific function of DCBLD2 (laboratory for thrombosis research, directed by Prof. dr. Hans Deckmyn, Kortrijk)

Prizes:

- Prize for the best oral presentation, ANR 2016, Cairns Australia
- PDL prize for the best master student 2010-2011

Courses:

- 4th course in integration of cytogenetics, microarrays and massive sequencing in biomedical and clinical research, 25-28 October 2011, Ronzano, Italy.
- FELASA B attest (laboratory animal science)

Languages:

- Dutch: Native speaker
- English: Good
- French: Reasonable
- German: Basic

A1 Publications:

- Vanhauwaert S, Van Peer G, Rihani A, Janssens E, Rondou P, Lefever S, De Paepe A, Coucke PJ, Speleman F, Vandesompele J, Willaert A. Expressed repeat elements improve RT-qPCR normalization across a wide range of zebrafish gene expression studies. *PLoS One.* 2014 Oct 13;9(10):e109091.

- Vanhauwaert S, De Brouwer S, Decaesteker B, Leonelli C, Mestdagh P, Jo Vandesompele, Karen Sermon, Geertrui Denecker, Christophe Vanneste, Frank Speleman, De Preter K. A MYCN activated FOXM1 driven embryonal pathway defines therapy resistant neuroblastoma patients and marks FOXM1 as target for future drug screening. (*submitted to clinical cancer research*)

- Vanhauwaert S, Leonelli C, Durinck K, Decaesteker B, Vanneste C, Fieuw A, Dewyn G, Janssens E, Loontiens S, He S, Cantor S, Freeman K, Van Roy N, Denecker G, De Vos W, Look AT, De Preter K, Speleman F. BRIP1 overexpression accelerates MYCN driven neuroblastoma formation and is part of a FOXM1 driven gene signature providing protection to excessive replicative stress. *In preparation*

- Renard M, Vanhauwaert S, Vanhomwegen M, Rihani A, Vandamme N, Goossens S, Berx G, Van Vlierberghe P, Haigh JJ, Van Laere J, Lambertz I, Bracke KR, Brusselle GG, Speleman F, Vandesompele J, Willaert A. Expressed repetitive elements outperform classical reference genes for normalization of reverse transcription qPCR data in mice. *Scientific Reports, under minor revision*

- Van Deun J, Mestdagh P, Agostinis P, Akay Ö, Anand S, Anckaert J, Martinez Z[7], Baetens T, Beghein E, Bertier L, Berx G, Boere J, Boukouris S, Bremer M, Buschmann D, Byrd J, Casert C, Cheng L, Cmoch A, Daveloose D, De Smedt E, Demirsoy S, Depoorter V, Dhondt B, Driedonks T, Dudek A, Elsharawy A, Floris I, Foers A, Gärtner

K, Garg A, Geeurickx E, GettemLeans J, Ghazavi F, Giebel B, Groot Kormelink T, Hancock G, Helsmoortel H, Hill A, Hyenne V, Kalra H, Kim D, Kowal, Kraemer S, Leidinger P, Leonelli C, Liang Y[24], Lippens L, Liu S, Lo Cicero A, Martin S, Mathivanan S, Mathiyalagan P, Matusek T, Milani G, Monguió-Tortajada M, Mus L, Muth D, Németh A, Nolte-'t Hoen E, O'Driscoll L, Palmull R, Pfaffl MW, Primdal-Bengtson B, Romano E, Rousseau Q, Sahoo S, Sampaio N, Samuel M, Scicluna B, Soen B, Steels A, Swinnen JV, Takatalo M, Thaminy S, Théry C, Tulkens J, Van Audenhove I, van der Grein S, Van Goethem A, van Herwijnen M, Van Niel G, Van Roy N, Van Vliet A, Vandamme N, Vanhauwaert S, Vergauwen G, Verweij F, Wallaert A, Wauben M, Witwer KW, Zonneveld M, De Wever O, Vandesompele J, Hendrix A. EV-TRACK: transparent reporting and centralizing knowledge in extracellular vesicle research *Nature methods, accepted*

- De Rocker N, Vergult S, Koolen D, Jacobs E, Hoischen A, Zeesman S, Bang B, Béna F, Bockaert N, Bongers EM, de Ravel T, Devriendt K, Giglio S, Faivre L, Joss S, Maas S, Marle N, Novara F, Nowaczyk MJ, Peeters H, Polstra A, Roelens F, Rosenberg C, Thevenon J, Tümer Z, Vanhauwaert S, Varvagiannis K, Willaert A, Willemsen M, Willems M, Zuffardi O, Coucke P, Speleman F, Eichler EE, Kleefstra T, Menten B. Refinement of the critical 2p25.3 deletion region: the role of MYT1L in intellectual disability and obesity. *Genetics in Medicine 2013*, 2015 Jun;17(6):460-6.

- Durinck K, Wallaert A, Van de Walle I, Van Loocke W, Volders PJ, Vanhauwaert S, Geerdens E, Benoit Y, Van Roy N, Poppe B, Soulier J, Cools J, Mestdagh P, Vandesompele J, Rondou P, Van Vlierberghe P, Taghon T, Speleman F. The Notch driven long non-coding RNA repertoire in T-cell acute lymphoblastic leukemia. *Haematologica,* 2014 Dec;99(12):1808-16.

- Malfait F, Kariminijad A, Van Damme T, Gauce C, Syx D, Mehri-Soussi F, Symoens S, Vanhauwaert S, Bozorgmehr B, Kariminejad M.H, Ebrahimiadib N, Hausser I, Huysseune A, Fournel-Gigleux S, De Paepe A. Defective initation of glycosaminoglycan synthesis due to mutation in B3GALT6 causes a pleiotropic

connective tissue disorder with severe alteration in proteoglycan assembly and collagen fibrillogenesis. *American Journal of Human Genetics*, 2013 Jun 6;92(6):935-45

Book chapters:

- Vanhauwaert S, Lefever S, Coucke P, Speleman F, De Paepe A, Vandesompele J, Willaert A. RT-qPCR gene expression analysis in zebrafish: Preanalytical precautions and use of expressed repetitive elements for normalization. *Methods in cell biology* March 2016

Oral Presentations:

- Vanhauwaert S, Fieuw A, Leonelli C, Janssens E, De Wyn J, Depuydt P, De Brouwer S, Neuroblastoma Research Consortium, Van Roy N, He S, Look AT, De Preter K, Speleman F. The *BRIP1/FANCJ* DNA helicase is a druggable 17q driver oncogene involved in G-quadruplex induced replicative stress resistance in neuroblastoma. BeSHG, January 24th 2016, Leuven, Belgium

- Vanhauwaert S, Fieuw A, Leonelli C, Janssens E, De Wyn J, Depuydt P, De Brouwer S, Neuroblastoma Research Consortium, Van Roy N, He S, Look AT, De Preter K, Speleman F. The *BRIP1/FANCJ* DNA helicase is a druggable 17q driver oncogene involved in G-quadruplex induced replicative stress resistance in neuroblastoma. wetenschapsdag, March 16th 2016, Gent, Belgium

- Vanhauwaert S, Fieuw A, Leonelli C, Janssens E, De Wyn J, Depuydt P, De Brouwer S, Neuroblastoma Research Consortium, Van Roy N, He S, Look AT, De Preter K, Speleman F. The *BRIP1/FANCJ* DNA helicase is a druggable 17q driver oncogene involved in G-quadruplex induced replicative stress resistance in neuroblastoma. IUAP, June 8th 2016, Brussel, Belgium

- Vanhauwaert S, Fieuw A, Leonelli C, Janssens E, De Wyn J, Depuydt P, De Brouwer S, Neuroblastoma Research Consortium, Van Roy N, He S, Look AT, De Preter K, Speleman F. The *BRIP1/FANCJ* DNA helicase is a druggable 17q driver oncogene involved in G-quadruplex induced replicative stress resistance in neuroblastoma. Advances in Neuroblastoma research (ANR2016); June 23rd 2016, Cairns, Australia

- Vanhauwaert S, Fieuw A, Leonelli C, Janssens E, De Wyn J, Depuydt P, De Brouwer S, Neuroblastoma Research Consortium, Van Roy N, He S, Look AT, De Preter K, Speleman F. The *BRIP1/FANCJ* DNA helicase is a druggable 17q driver oncogene involved in G-quadruplex induced replicative stress resistance in neuroblastoma. Zebrafish disease modeling meeting 9 (ZDM9), October 1st 2016, Singapore

Poster Presentations:

- Vanhauwaert S, Van Peer G, Rihani A, Janssens E, Rondou P, Lefever S, De Paepe A, Coucke P, Speleman F, Vandesompele* J, Willaert A*: Expressed repeat elements improve RT-qPCR normalization across a wide range of zebrafish gene expression studies. Zebrafish genetics meeting, Madison, USA, June 24-28 2014.

- Vanhauwaert S.*, Beckers A.*, Leonelli C., Wallaert A., Fieuw A., Carter D.R., Cheung B.B., Schulte J., Marschall G.M., De Preter K., Speleman F. The MYCN-MYBL2-FOXM1 regulatory axis and DNA damage response in neuroblastoma. Genetic instability and DNA repair, Whistler, Canada, 1-6 March 2015

- Vanhauwaert S., Fieuw A., Leonelli C., Janssens E., De Brouwer S., He S., Look A. T., De Preter K., Speleman F. : The *BRIP1/FANCJ* DNA helicase as novel 17q driver oncogene

in Neuroblastoma. Zebrafish Disease Models Conference (ZDM8), Boston, USA, 24-27 August 2015

- Vanhauwaert S., Fieuw A., Leonelli C., Janssens E., De Wyn J., Depuydt P., De Brouwer S., Neuroblastoma Research Consortium, Van Roy N., He S., Look A. T., De Preter K., Speleman F. : The *BRIP1/FANCJ* DNA helicase is a 17q driver oncogene protecting neuroblastoma cells from MYCN induced replicative stress at G-quadruplexes. 4th Neuroblastoma Research Symposium, Newcastle, UK. 26-27 November 2015

Dankje wel...

Een dankwoord, tja hoe begin je eraan? Er zijn immers zoveel mensen die de voorbije 5 jaar hun steentje hebben bijgedragen en ervoor gezorgd hebben dat dit doctoraat tot een goed einde kwam. Want een doctoraat, dat doe je niet alleen, dat is nu wel duidelijk, aan al deze mensen, BEDANKT!

Uiteraard is de ene persoon al meer betrokken geweest dan de andere. Mijn doctoraat ging nooit tot stand gekomen zijn zonder mijn promotor Frank Speleman, bedankt om mij op sleeptouw te nemen en mij het vertrouwen te geven om zebravis kanker modellen te introduceren in het labo. Ook Andy verdient een extra woordje van dank, je hebt mij als volledig groentje geïntroduceerd in de wondere wereld van de visjes en ik kon altijd terecht met mijn vragen bij jou. Nu ik het zelf al een stuk drukker heb in het labo dan in het begin, besef ik des te meer dat dit voor jou niet altijd evident was. Ook Pieter Rondou, mijn oorspronkelijke co-promotor verdient een extra dankwoordje, jouw eeuwige enthousiasme werkte echt aanstekelijk en zorgde er voor dat ik vol goede moed aan een nieuw experiment startte. Katleen, uiteraard ben ik jou niet vergeten, het laatste jaar zijn we steeds meer gaan samenwerken en ik kijk er naar uit om in de toekomst samen nog meer data te genereren (en wie weet waag ik mij ook wel voorzichtig in de uitdagende wereld van het data-minen).

I would also like to thank Tom Look, thanks for giving me the opportunity to come and visit your lab. My stay in your lab made me a more mature scientist and my zebrafish skills have definitely been risen to another level. Shuning, thanks for being such a nice friend and making my stay in Boston so wonderful. Mark, I couldn't wish for a nicer person to share my bench with, thanks for all the help and nice chats. To all the Look members (Dong, Shuning, Mark, Marc, Koshi, Julia, Evisa, Ting, Tian Tian, Cherry and Ashley), even though I was a lot younger and much less experienced, you were always willing to help me and I'm really grateful for that. Marc, thanks for being such a nice roomie, because of you I had a lovely and warm home in Boston.

Oorspronkelijk was ik helemaal in mijn eentje in de wondere wereld van het zebravis kankeronderzoek. Gelukkig kreeg ik na een tijdje toch versterking van team VIS! Els, Siebe en Givani, zonder jullie was ik nooit zover geraakt, ik ben jullie ongelooflijk dankbaar voor al jullie hulp en enthousiasme. Daarnaast heb ik ook heel goeie herinneringen aan onze leuke babbels. Ik heb de eer gehad om met zeer veel mensen de bureau te kunnen delen: Nadine, Joni, Evelien, Kaat, Pieter, Tim, Farzaneh, Hetty, Gloria, Sofia, Annelynn, Filip, Aline, Els, Siebe, Givani en Charlotte. Bedankt voor de vele wetenschappelijke input maar ook voor de vele gezellige babbels en om mij op te peppen wanneer ik het eventjes niet meer zag zitten. Ook alle CMGG collega's wil ik bedanken voor de vele ontspannende en leuke activiteiten samen!

Carina en Givani onder jullie vleugels nam het BRIP1 project een vliegende (of is het een vissende?) start. Ik ben jullie ongelooflijk dankbaar voor jullie inzet en jullie eeuwige geduld met mij. Jolien, bedankt om mij te helpen met het compound werk.

Tante Petra en Nonkel Simon, bedankt om mij in extremis te helpen met het ontwerpen van de cover van mijn boekje. Zonder jullie had ik nu een gewone saaie witte kaft...

Wie ik ook zeker niet mag vergeten zijn mijn vrienden. Bedankt om voor de nodige afleiding te zorgen wanneer ik daar nood aan had en altijd vol interesse te vragen of mijn visjes ondertussen al kanker hebben.

Mama, soms heb ik wel eens nood aan een directe telefoonlijn naar hierboven. Bedankt om mij te maken tot de persoon die ik nu ben en jouw onvoorwaardelijke steun.

Papa, Andreas en Barbara, we hebben een moeilijke periode achter de rug, maar het heeft ons gezin wel sterker gemaakt en we hangen nu nog meer aan elkaar. Ik vind het ontzettend lief van jullie dat jullie altijd vol enthousiasme vroegen hoe het nog met mijn visjes gaat, ook al was het niet altijd helemaal duidelijk wat ik eigenlijk aan het doen was. Ik hoop dat mijn presentatie op mijn verdediging toch een en ander duidelijk maakt.

Marianne, Johan, Idril en Melian, bedankt om mij zo goed op te nemen in de familie en jullie interesse in mijn werk.

Lieve Olorin, bedankt voor je steun, je luisterend oor, je liefde...